INTERIM REPORT

INITIAL CAL/APT PROGRAM: SITE INFORMATION, TEST PAVEMENTS CONSTRUCTION, PAVEMENT MATERIALS CHARACTERIZATIONS, INITIAL CAL/HVS TEST RESULTS, AND PERFORMANCE ESTIMATES

Report Prepared for

CALIFORNIA DEPARTMENT OF TRANSPORTATION

by

John Harvey, Louw Du Plessis, Fenella Long, Shakir Shatnawi, Clark Scheffy, Bor-Wen Tsai, Irwin Guada, David Hung, Nick Coetzee, Michael Riemer, and C.L. Monismith

June, 1996

INSTITUTE OF TRANSPORTATION STUDIES
UNIVERSITY OF CALIFORNIA, BERKELEY

Technical Report Documentation Page

1. Report No. RTA-65W485-3	2. Government Accession No.	3. Recipient's Catalog No.	
4. Title and Subtitle Initial CAL/APT Program: Site Information, Test Pavements Construction, Pavement Materials Characterizations, Initial CAL/HVS Test Results, and Performance Estimates		5. Report Date April 1996	
		6. Performing Organization Code	
7. Authors John T. Harvey, Louw Du Plessis, Fenella Long, Shakir Shatnawi, Clark Scheffy, Bor-Wen Tsai, Irwin Guada, David Hung, Nick Coetzee, Michael Riemer, and Carl L. Monismith		8. Performing Organization Report No.	
9. Performing Organization Name and Address Asphalt Research Program: CAL/APT Program Institute of Transportation Studies University of California at Berkeley Berkeley, CA 94720		10. Work Unit No.	
		11. Contract or Grant No. RTA-65W485	
12. Sponsoring Agency Name and Address Division of New Technology and Research California Department of Transportation Sacramento, CA 94273-0001		13. Type of Report and Period Covered Interim Report, June 94-July 95	
		14. Sponsoring Agency Code	
15. Supplementary Notes This 5 year project is being performed in cooperation with the U.S. Department of Transportation, Federal Highway Administration.			

16. Abstract. This report, an interim report covering the work completed on the CAL/APT Project during the period June 1994 through July 1995 presents the results of laboratory tests on the pavement materials, and evaluates a number of different pavement-materials-characterization and pavement-performance-prediction procedures. This information as well as additional data to be acquired subsequently will be used for complete analyses of response of the first two pavement sections (four test sections) to accelerated loading with the Heavy Vehicle Simulator (HVS). Experience gained from test-section construction suggests that the following guidelines might be of use for the construction of highway pavements by Caltrans:
Reduce the length of mix that can be laid down prior to beginning compaction,
Increase the minimum compaction thickness, especially for placement over cold existing surfaces and during night construction,
Require simultaneous construction of adjoining lanes where feasible and,
Install lateral confinement such as curbs or other similar devices prior to mix compaction where possible and economically feasible.

Extensive analyses of the fatigue performance and resulting influences on subgrade strain of both the drained (ATPB) and undrained sections have been conducted. These analyses assumed the pavement to be represented as a multi-layer elastic solid and utilized a series of models for both fatigue and rutting. The predicted fatigue life is larger for the drained pavement than for the undrained pavement. This is due primarily to the increased stiffness of the ATPB compared to that of the aggregate base it replaces. However, the relative performance of drained and undrained pavements may be different under field conditions especially if severe moisture conditions reduce the effectiveness of the asphalt treatment. An increase in load from 40 to 100 kN (9,000 to 22,500 lb) causes a much larger reduction in the subgrade rutting life than predicted for the fatigue life.

17. Key Words Heavy Vehicle Simulator (HVS), asphalt concrete pavement, asphalt-treated permeable base, pavement construction, asphalt concrete, unbound materials, pavement instrumentation and monitoring, fatigue		18. Distribution Statement No restrictions. This document is available to the public.	
19. Security Classif. (of this report) Unclassified	20. Security Classif. (of this page) Unclassified	21. No. of Pages	22. Price

DISCLAIMER

The contents of this report reflect the views of the authors who are responsible for the information and the accuracy of the data presented herein. The contents do not necessarily reflect the official views or policies of the California Department of Transportation or the Federal Highway Administration. The report does not constitute a standard, specification, or regulation.

FINANCIAL DISCLOSURE STATEMENT

This research has been funded by the Division of New Technology and Research of the State of California Department of Transportation (contract No. RTA-65W485). The total contract amount for the five year period (1 July 1994 through 30 June 1999) is $5,751,159. This report, which should be considered as an interim report, describes the work completed during the period June 1994 through July 1995. The information contained herein as well as additional data to be acquired subsequently will be used for complete analyses of the first test program which includes four pavement test sections subjected to accelerated pavement testing with the Heavy Vehicle Simulator (HVS).

IMPLEMENTATION STATEMENT

While this report is considered as an interim report, the results obtained during the construction of the test pavements do provide some guidelines which should be considered for pavement construction, namely:

- Reduce the length of mix that can be laid down prior to beginning compaction,
- Increase the minimum compaction thickness, especially for placement over cold existing surfaces and during night construction,
- Require simultaneous construction of adjoining lanes where feasible and,
- Install lateral confinement such as curbs or other similar devices prior to mix compaction where possible and economically feasible.

ACKNOWLEDGMENTS

Financial support for this project was provided by the State of California Department of Transportation as part of the CAL/APT Project. Mr. Wesley Lum of the Division of New Technology and Research is the CAL/APT Project Manager and Mr. William Nokes, Office of Project Planning and Design, is the Contract Monitor for the University of California, Berkeley contract.

TABLE OF CONTENTS

LIST OF FIGURES

LIST OF TABLES

EXECUTIVE SUMMARY

This report, which should be considered as an interim report, includes the work completed on the CAL/APT Project at the University of California, Berkeley during the period June 1994 through July 1995. Its purpose is: 1) to present the results of laboratory tests on the pavement materials, results of post-construction pavement tests, and pavement performance predictions, and 2) to evaluate different pavement-materials-characterization and pavement-performance-prediction procedures. This information as well as additional data to be acquired subsequently will be used for complete analyses of response of the first two pavement sections (four test sections) to accelerated loading with the Heavy Vehicle Simulator (HVS).

Chapter 1 provides a summary of the overall objectives of the CAL/APT program, a summary of potential benefits which can accrue from the program, a brief summary of the pilot study (termed Phase I), work completed to July 1995, together with the objectives of the first test plan for this project which started in June 1994 and termed Phase II.

The first test plan includes two objectives: 1) to verify existing design methodologies for Asphalt Treated Permeable Base (ATPB) pavements and conventional Aggregate Base (AB) pavements based on considerations of fatigue cracking when subjected to trafficking at moderate temperatures; and 2) to compare the fatigue performance of structural overlays on the cracked pavements, the overlays consisting of Asphalt Rubber Hot Mix Gap-Graded (ARHM-GG) using type 2 asphalt rubber binder and conventional Dense Graded Asphalt Concrete (DGAC) mixes.

Chapter 2 describes the design and construction of the two pavement sections together with the basis for selection of the four test sections within the limits of the two pavement sections.

The test pavements were constructed in accordance with standard Caltrans procedures within a building at the Richmond Field Station termed the "Fog Chamber." The building had been used in the 1960's to study runway lighting patterns for landings under foggy conditions.

The two pavement sections, designed for a Traffic Index of 9, consisted of: 1) 137 mm (0.45 ft)-asphalt concrete, 274 mm (0.90 ft)-class two aggregate base, 229 mm (0.75 ft)-class 1 aggregate subbase for the undrained pavement; and 2) 137 mm (0.45 ft)-asphalt concrete, 76 mm (0.25 ft)-ATPB, 182 mm (0.60 ft)-class 2 aggregate base, 229 mm (0.75 ft)-class 1 aggregate subbase for the drained pavement. Both sections were placed on a subgrade consisting of clay (CH in the United Soil Classification System) and a design R value of 10 was used for thickness selection.

Results of construction control tests on the pavement sections are summarized. Inspection during construction was provided by Contra Costa County, Caltrans District 4, and UCB staff. In general, the pavement sections conformed to the Caltrans requirements.

Chapter 3 describes the instrumentation installed in the test sections as well as that used to make periodic surface measurements and presents results obtained from the first test through August 1995.

Each pavement test section contains 2 Multi-Depth Deflectometers (MDDs) and thermocouples throughout the depth of the asphalt-treated portion of the pavement. The MDDs

provide a continuous record of the accumulation of permanent deformation with trafficking in each of the pavement components as well as transient response under moving wheel loads. The thermocouples provided a continuous recording of pavement temperatures with depth.

Two additional pieces of equipment have been utilized to measure pavement response. The Road Surface Deflectometer (RSD) and the Laser Profilometer. The RSD is similar to a Benkelman Beam and provides a measure of the surface deflection of the structure under a moving load. The Laser Profilometer is used to measure the permanently deformed transverse profile of the test section surface.

Results of the measurements from the MDDs, thermocouples, RSD, and Laser Profilometer through July 1995 on the first test section are presented.

Chapter 4 describes the materials characterization procedures used to define the stiffness characteristics of the subgrade, subbase, and untreated base materials together with the test results. The stiffness or modulus tests included the following: resilient modulus from triaxial compression (subgrade, subbase, and base), bender element (subgrade), K-mold (subgrade and subbase), Dynamic Cone Penetrometer (DCP), (subgrade, subbase, and base), and Heavy Weight Deflectometer (HWD) (subgrade and subbase/base).

Results of the triaxial compression repeated load tests on the subgrade soil indicate that the stiffness of this subgrade material is stress dependent with stiffness decreasing with an increase in applied stress. In addition the results indicate that the stiffness after soaking may be only 50 to 75 percent of that at the time of construction. Moduli determined from the bender element tests on the subgrade indicate the same sensitivity to changes in water content as the

triaxial compression repeated load tests. Moreover, the test results provide modulus degradation (reduction) curves (modulus decrease with increase in shear strain) which are characteristics of fine-grained soils.

Results of triaxial compression repeated load tests on the base and subbase materials can be plotted in the conventional manner and the moduli defined by the following expression:

$$M_R=A*SPS^B$$

Where M_R is the resilient modulus, SPS is the sum of the principal stresses in the triaxial test, and A and B are experimentally determined coefficients. Moduli in the saturated condition for both the base and subbase were less than in the in-situ dried-out condition.

Modulus values for these materials were also determined using a K-mold test (developed by the CSIR), by means of a Dynamic Cone Penetrometer (also developed by the CSIR), by estimation from R measured values and from the Heavy Weight Deflectometer (HWD) tests conducted at various times during the construction process and subsequent thereto. Generally, the HWD, K-mold, and M_R test values were in the same range while the DCP and estimated exhibited higher values.

Chapter 5 contains results of tests on the asphalt concrete mix including Stabilometer "S" values (average S=46), shear strain characteristics in repetitive simple shear tests at constant height, controlled-strain flexural fatigue data, and the results of the SHRP Superpave Level I mix evaluation. While the mix met Caltrans requirements it did not meet all of the Superpave Level I design criteria.

Stiffness determinations as well as the flexural fatigue and repetitive simple shear tests were performed on both laboratory compacted and field compacted specimens. Shear stiffness

and repetitive simple shear tests were performed on similar specimens by both the Caltrans and UCB laboratories to compare test results using the SHRP developed equipment. In general, the tests on the field compacted specimens provided lower test values which could be attributed to asphalt stiffening resulting from the reheating of the mix required to prepare the laboratory compacted specimens of the field mixed material.

Some repeated load triaxial compression test results for the asphalt-treated permeable are also included to provide a measure of the stiffness characteristics of this layer as well.

Chapter 6 contains preliminary estimates of the propensity for fatigue cracking in the pavement sections. The structures have been idealized as layered elastic systems and the computer programs for analysis of multi-layered elastic systems, ELSYM5 and CIRCLY have been utilized. The CIRCLY program was used because it permits consideration of frictionless as well as full friction interface conditions.

Material characteristics (moduli) for the pavement layers were selected from the information presented earlier. Fatigue characteristics are based on the fatigue test results reported herein as well as on fatigue criteria suggested by the Asphalt Institute, Shell, and the CSIR. Considerations of surface rutting were limited to use of subgrade strain models including those used by the Asphalt Institute, Shell, Nottingham, and the CSIR. These models attempt to control surface rutting by limiting the vertical compressive (elastic) strain at the surface of the subgrade and are independent of the permanent deformation characteristics of the asphalt concrete.

The critical strain for fatigue was taken as the maximum principal tensile strain on the

underside of the asphalt concrete layer. From cores which had been taken soon after construction there was evidence of a lack of bond between the layers of the asphalt concrete (which had been placed in two lifts). Accordingly, the CIRCLY program was used to examine the tensile strain occurring at the underside of the first lift as well as at the bottom of the entire layer.

In general, the predicted fatigue lives exceed the design life (approximately 1,000,000 ESALS) for which the sections were designed according to the Caltrans procedure. This has been attributed, at least in part, to the good construction-especially of the asphalt concrete.

Chapter 7 provides a summary of the test results together with recommendations for guidelines which might be used for construction of highway pavements by Caltrans.

A high degree of compaction was achieved in the asphalt concrete surface mix. Better compaction nearly always results in improved fatigue performance and less rutting (if air-void contents are not below approximately 2.5 percent for dense graded mixes).

Experience gained from test-section construction suggests that the following guidelines might be of use for the construction of highway pavements by Caltrans:

- Reduce the length of mix that can be laid down prior to beginning compaction,
- Increase the minimum compaction thickness, especially for placement over cold existing surfaces and during night construction,
- Require simultaneous construction of adjoining lanes where feasible and,
- Install lateral confinement such as curbs or other similar devices prior to mix compaction where possible and economically feasible.

Extensive analyses of the fatigue performance and resulting influences on subgrade strain

of both the drained (ATPB) and undrained sections have been conducted. These analyses assumed the pavement to be represented as a multi-layer elastic solid and utilized a series of models for both fatigue and rutting as noted in chapter 6.

The predicted fatigue life is larger for the drained pavement than for the undrained pavement. This is due primarily to the increased stiffness of the ATPB compared to that of the aggregate base it replaces. However, the relative performance of drained and undrained pavements may be different under field conditions especially if severe moisture conditions reduce the effectiveness of the asphalt treatment. A companion laboratory study is underway to evaluate the effect of the environment on the performance of ATPB. These effects may be evaluated in future HVS test sections as well.

When the first HVS test and analyses are completed, the actual fatigue life will be compared to predicted fatigue lives to validate the models. The SHRP surrogate model simulates a larger fatigue life than the Asphalt Institute, SHRP A-003A (laboratory), and the Shell models. The relative effectiveness of these models will be compared in the final report.

The moduli of the unbound layers and the thickness of the subbase have little effect on the fatigue life of the HVS pavement. Changes in the asphalt concrete moduli have much greater effect. Increasing the dual-tire load from 40 to 100 kN (9,000 to 22,500 lb) results in a decrease in fatigue life: however, the resulting damage is not as large as normally predicted using conventional load equivalency factors. These results provide the first link between laboratory and in-situ performance simulated by the HVS that will be validated after all four sections have been tested by the HVS.

The predicted subgrade rutting life is in the same range for both the drained and undrained pavement structures. The CSIR model is the most susceptible to changes in the modulus, especially the subgrade modulus. The Asphalt Institute, Shell, and Nottingham models predicted subgrade rutting lives within a one-order-of-magnitude range. Increases in moduli in any pavement layer result in increases in the predicted subgrade rutting life. However, the degree of the effect varies from layer to layer. An increase in aggregate subbase thickness results in large increases in the subgrade rutting life. Therefore, HVS test section 500RF, which has the thinnest aggregate subbase should, according to predictions, have a smaller rutting life than the other sections to be tested later.

An increase in load from 40 to 100 kN (9,000 to 22,500 lb) causes a much larger reduction in the subgrade rutting life than predicted for the fatigue life.

CHAPTER 1

INTRODUCTION

1.1 PROJECT OBJECTIVES

The overall objective of the Caltrans Accelerated Pavement Testing (Cal/APT) Program is to provide Caltrans with complete operational Accelerated Pavement Testing (APT) capability using the Heavy Vehicle Simulator (HVS) system technology, both in a controlled experimental setting at the University of California, Berkeley (UCB) Richmond Field Station (RFS) and on selected field sites throughout California. APT capability includes the HVS equipment,[1] associated measuring and monitoring systems, APT expertise developed in South Africa over more than 25 years (including an extensive data base), and trained UCB and Caltrans personnel.

A partial list of potential benefits which can accrue from the Cal/APT program includes:

- Rapid evaluation of current and new construction procedures as a part of pavement construction, rehabilitation, or reconstruction;
- Rapid evaluation of construction quality control measures;
- Improvement of pavement structural and material design methodologies, including those for both new construction and rehabilitation;

[1]Appendix A contains a description of the equipment.

- Greater knowledge and understanding of pavement and material behavior;
- Rapid evaluation and comparison of alternative rehabilitation measures for both flexible and rigid pavements;
- Assessment of materials which are at present not standard road building materials; for example, mixes containing waste materials and those containing modified binders;
- Reduction of pavement costs by reducing unnecessary pavement thickness or by improving the structural balance of the design; for example, development of layer equivalencies for new materials such as mixes containing asphalt-rubber;
- Avoidance of failure caused by implementation of unproven designs or extrapolation of current designs beyond their empirical data base; and
- Provision of validation information for laboratory tests and for performance prediction procedures (e.g. those developed during the SHRP research program) to both Caltrans and contractor groups as Caltrans moves to implement the performance specification initiative (PSI).

It must be emphasized that this is only a partial listing of potential benefits. As the work develops and a more detailed strategic plan is formulated, other benefits are expected to accrue as well.

1.2 BACKGROUND

Nokes et al. *(1996)* described in detail the establishment of the Caltrans Accelerated Pavement Testing Program. Recognizing the benefits of APT, Caltrans decided in 1992 to thoroughly evaluate HVS equipment developed in South Africa. This decision was supported by

productive HVS operations by the Council for Scientific and Industrial Research (CSIR) of South Africa, by substantial improvements in South African pavement technology resulting from the HVS program, and by demonstrated expertise by CSIR engineers in full-scale pavement testing based on approximately 25 years of experience and an extensive data base of pavement performance from about 400 HVS test sections. Before committing the substantial financial resources required to purchase the equipment and services, a pilot study was undertaken to demonstrate the efficacy of the South African HVS technology.

The importance of complementing full-scale accelerated load testing with laboratory testing had also been demonstrated *(Nokes et al., 1996)*. Results of the Strategic Highway Research Program (SHRP) Project A-003A conducted at the University of California, Berkeley were also becoming available at about the same time. These results included equipment and procedures for evaluating the fatigue and permanent deformation characteristics of asphalt-aggregate mixes including the effects of aging and moisture *(Monismith, Hicks, and Finn, 1994)*. It was thus logical to combine these developments with accelerated pavement testing in order to develop and implement improved pavement technology. A simplified framework within which this could be accomplished is shown in Figure 1.1.

The pilot study (termed Phase I), combining HVS testing and laboratory testing within the framework of Figure 1.1, was successfully completed in early 1994. Results of that study have previously been described *(Harvey and Monismith, 1994a and 1994b; Rust et al., 1993; and Weissman, 1993)*. As a result of the pilot study, Caltrans staff successfully pursued funds to implement an APT program using HVS testing, SHRP-developed laboratory tests, and the data base and experience of the CSIR staff.

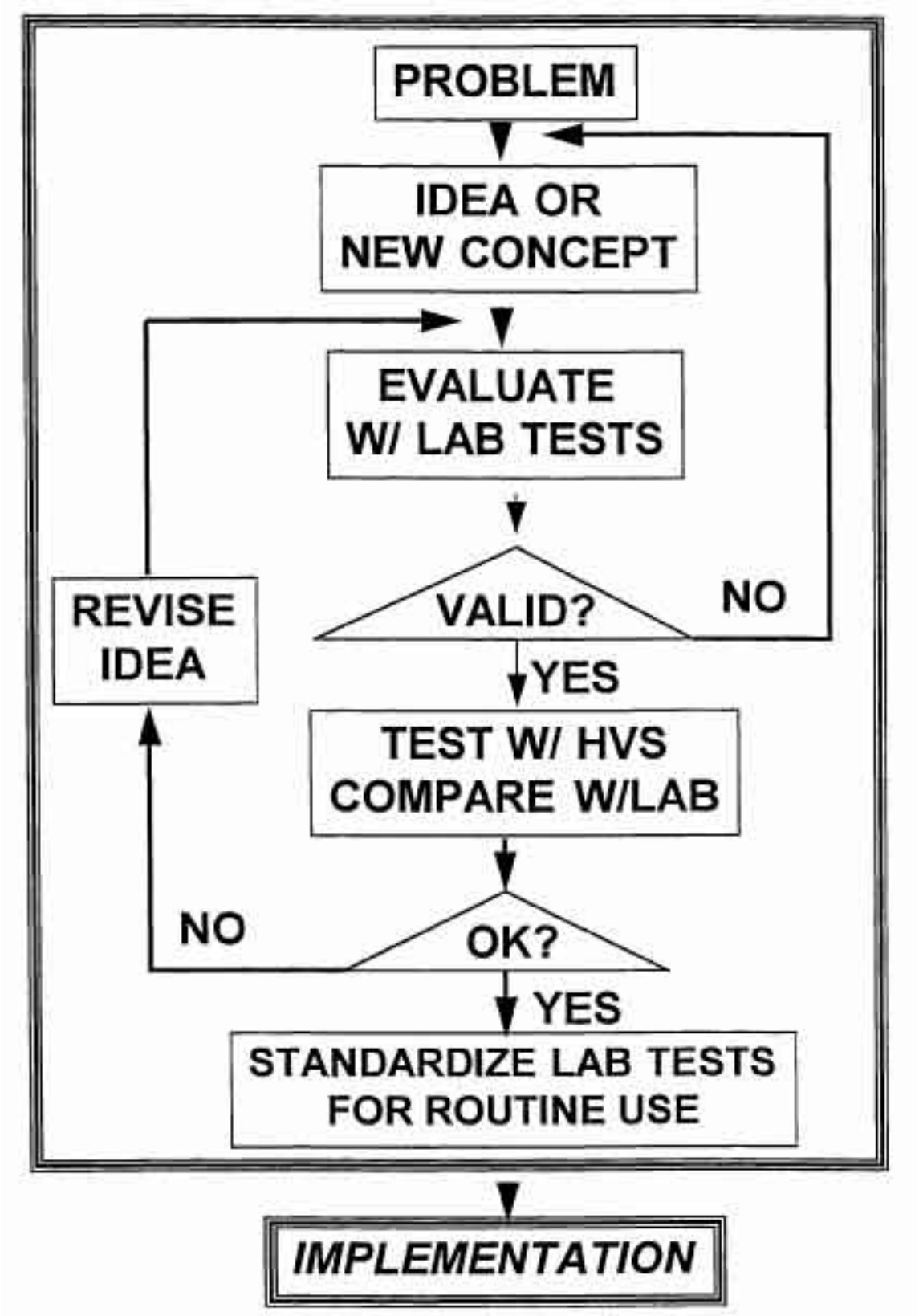

Figure 1.1 Role of the HVS and Laboratory Testing in Pavement Technology Development and Implementation

The current program, Phase II, was approved by Caltrans management in February 1994 and was initiated the following June. It has involved the purchase of two (2) refurbished HVSs and related services, the purchase of SHRP laboratory test equipment for the Caltrans laboratory in Sacramento, and the implementation of a five-year research and development program totaling more than $9 million. This major program is a joint effort between Caltrans, the University of California, Berkeley, the Division of Roads and Transport Technology of the CSIR, and Dynatest Consultants Inc. of Ojai, California.

This interim report describes work completed during the first year of the Phase II effort.

1.3 WORK COMPLETED TO DATE

Since the start of the project in June 1994, the following broad technical objectives have been realized:

- Delivery and Acceptance of Two HVS Units by Caltrans; HVS No. 1 (CALHVS1) accepted in March 1995 and HVS No. 2 (CALHVS2) accepted in June 1995.
- Development of Short-Term Strategic Plan; approved by Caltrans management in May 1995 enabling construction of the first two pavement test sections at the UCB Richmond Field Station.
- Development of First Experimental Test Plan for HVS No. 1 (Appendix A); completed in May 1995, the plan details the test program for both HVS No.1 and the associated laboratory program at UCB and at Caltrans' laboratory in Sacramento.
- Design and Construction of Two Pavement Test Sections at UCB Richmond Field

Station; accomplished through a cooperative effort of UCB, Caltrans Headquarters and District 4, CSIR, Dynatest Consultants, and Contra Costa County.

- Laboratory and Field Testing of Materials and Pavement Structures in First Two APT Sections; following the Test Plan for CALHVS1, again as a cooperative effort between the four participating organizations.
- Commencement of HVS Testing of First APT Sections at RFS; which began on May 3, 1995 using UCB staff and CALHVS1.

1.4 FIRST EXPERIMENTAL TEST PLAN

The first Test Plan, in addition to describing the overall objectives of the project, provides a detailed description of the initial program and identifies the following objectives:

- Objective One

  The first objective is to develop data to verify existing design methodologies for Asphalt Treated Permeable Base (ATPB) pavements and conventional Aggregate Base (AB) pavements with regard to failure under trafficking at moderate temperatures, while preparing a uniform platform on which the overlays required for Objective Two will be constructed. This objective completes part of the work under Goal 1 of the CAL/APT Strategic Plan.

  This objective includes:

  - quantification of the effective elastic moduli of the various pavement layers, based on an ad-hoc use of layered elastic analysis;
  - quantification of the stress dependence of the pavement layers;

- determination of the failure mechanisms of the various layers; and
- determination of the fatigue lives of the two main pavement structures (the scope of this test does not allow for the development of transfer functions for fatigue of the pavement layers).

- Objective Two

  The second objective of this series of HVS tests is to compare the fatigue performance of structural overlays of Asphalt Rubber Hot Mix Gap-Graded (ARHM-GG) mixes using type 2 asphalt rubber binder with that of conventional Dense Graded Asphalt Concrete (DGAC) mixes. This study is in essence a repeat of the Phase I study conducted in South Africa in 1993 for Caltrans and serves, therefore, to validate the findings of the tests performed in South Africa *(Harvey and Monismith, 1994a, and Rust et al., 1993)*. This objective is part of Goal 3 of the CAL/APT Strategic Plan.

The schedule in the Test Plan (included as Appendix A of this report) calls for an initial sequence of four HVS tests: drained ATPB site, undrained AB site, drained ATPB site, and undrained AB site. Two alternatives (Alternatives 1 and 3) for overlaying the sections with different thicknesses of the two materials recommend that the underlying pavements be tested in a dry state. Alternative 2 recommends saturating the pavements prior to testing the second two sites. This is not a preferred alternative since saturation could result in large differences in support for the overlays between the drained and undrained pavements. In the future, the test plan team and the CAL/APT Steering Committee will decide which alternative will be selected for Goal 3.

1.5 PURPOSE AND SCOPE OF INTERIM REPORT

The purpose of this interim report is 1) to present the results of laboratory tests on the pavement materials, results of post-construction pavement tests, and pavement performance predictions, and 2) to evaluate different pavement-materials-characterization and pavement-performance-prediction procedures. Ultimately, this information and data from future work will be used for complete analysis of the first two pavements (four test sections) after HVS testing to failure. Conclusions and recommendations from the first experiment will be presented in a future report after testing is completed. The work included herein is that which had been largely completed during the first year of the project, June 1994 through July 1995.

CHAPTER 2

INITIAL HVS TEST PAVEMENTS:

DESIGN, CONSTRUCTION, AND TEST SECTION SELECTION

2.1 INTRODUCTION

The HVS test pavements were constructed in the fog chamber (Building 280) at the University of California's Richmond Field Station. This building was originally constructed to study aircraft landing and runway lighting patterns under fog conditions *(Finch, Horonjeff, and Paula, 1966)*. It provides an excellent location to do controlled tests with the CALHVS1 because it is enclosed and is sufficiently large to permit nearly full-scale pavement sections to be constructed. Moreover, conducting tests within the building eliminates potential noise problems which may arise because of the proximity of the Marina Bay residential section in Richmond, California. The covered portion of the building available for test sections is approximately 9.5 m (30 ft) wide by 300 m (1,000 ft) long. The building has a suite of offices and storage space for equipment, permitting data reduction on-site.

The drained and undrained pavement sections, constructed within the building, were designed according to the Caltrans procedures described in its Highway Design Manual *(California Department of Transportation, 1987)*. Construction of the sections followed Caltrans procedures and specifications. Construction was inspected by UCB and Contra Costa County (CCCo) with intermittent monitoring by Caltrans District 4 staff. Selection of the HVS test sites followed procedures developed by CSIR based on their 25+ years of experience in such activities.

This chapter provides a summary of the pavement designs, materials characterization for the design process, and results of construction-control procedures.

2.2 EXISTING SUBBASE AND SUBGRADE CONDITIONS

Within Building 280 there was an existing pavement section which had been utilized during the fog chamber studies. The thin asphalt concrete layer and a portion of the underlying untreated aggregate, classed as subbase, were removed prior to construction.

To define existing subsurface conditions, four boreholes were drilled. Two were located in each of the areas where the drained and undrained pavement sections were to be constructed. All of the boreholes were excavated to groundwater with a hand auger. The interface between the subgrade and subbase was somewhat poorly defined, consisting of a zone approximately 50 to 100 mm (2 to 4 in) thick of a mix of subbase and subgrade material. Once past the subbase, subgrade samples were collected for later testing, and water contents were measured at various depths.

Soil profiles from all boreholes were similar. As can be seen in the borehole analyses (Appendix B), the uppermost layer of the subgrade is a stiff, high plasticity, black or gray clay. Below the upper layer are repeated layers of stiff brown clay and softer green clay, with inclusions of small white stones approximately 2 to 9 mm in diameter. Once the groundwater table was encountered, at depths between 3.5 and 4.8 m (11.5 and 15.7 ft), excavation was stopped. The boreholes were left open for several days to confirm the location of the groundwater table.

Observations made at the four boreholes are consistent with a line of much deeper boreholes (30 m [100 ft]) in a well field placed by Lawrence Berkeley Laboratory (LBL) parallel

to and approximately 100 m (350 ft) east of the HVS test sections. In their report *(Pouch, 1986)*, UCB geologists described the area as an alluvial fan/delta on top of older Bay Mud deposits, through which have passed meandering streams. The fluvial deposits consist of alternating layers dominated by clays, with some sands and gravels most likely correlated with wet season flows. The sands and gravels occur as lenses in the clay matrix.

2.2.1 Soil Classification

Three methods were used to classify subgrade and subbase materials including the Unified Soil Classification System (USCS) *(American Society for Testing and Materials, 1989)*; the AASHTO (sometimes referred to as the Highway Research Board) system *(American Association of State Highway and Transportation Officials, 1990)*; and the Caltrans specification system *(California Department of Transportation, 1992a)*.

The subgrade consists mostly of high plasticity clays, with some strata containing small quantities (less than 25 percent) of small white stones. The Atterberg Limits are as follows:

	Plasticity Index	Liquid Limit
max	41	55
min	27	39

The Atterberg Limits indicate that the subgrade can be separated into two layers at a depth of about 1.5 to 2.0 m. The upper layer is classified as a CH (USCS system) while the plasticity index (PI) of the lower layer was sufficiently low to change the classification to CL. According to the AASHTO system the subgrade is classed as an A-7-6 soil regardless of depth.

The existing granular (subbase) material overlying the clay subgrade varied in depth from 0.40 to 1.00 m. Tests were performed on this material by UCB and Contra Costa County

(CCCo) staff. Gradation curves for the material are shown in Figure 2.1 and resulting classifications are as follows:

Agency	USCS	AASHTO	Caltrans
UCB	GW	A-1-a	Class 2
CCCo	GW-GM	A-1-a	Class 2

For contract purposes, the in-place material was considered a Class 5 aggregate subbase; however, based on gradation and quality tests it meets the Class 2 requirements of Caltrans *(California Department of Transportation, 1992a)*.

2.2.2 R-values

Stabilometer R-value tests were performed on both subgrade and in-place granular subbase materials by CCCo staff according to Caltrans Method 301. Results of the tests are summarized in Table 2.1.

For the subgrade, five samples were obtained from various excavations within the planned pavement area. Results of the tests indicate an R-value range of 4 to 30. For pavement design purposes, a subgrade R-value of 10 was selected.

For the subbase, five R-values tests were performed, three from specific locations inside the proposed test pavement area. The results show some variation, ranging between 55 and 82. These R-values are all above 50, the minimum required for Class 2 aggregate subbase, and all but one test result is above 60, the minimum required for Class 1 aggregate subbase.

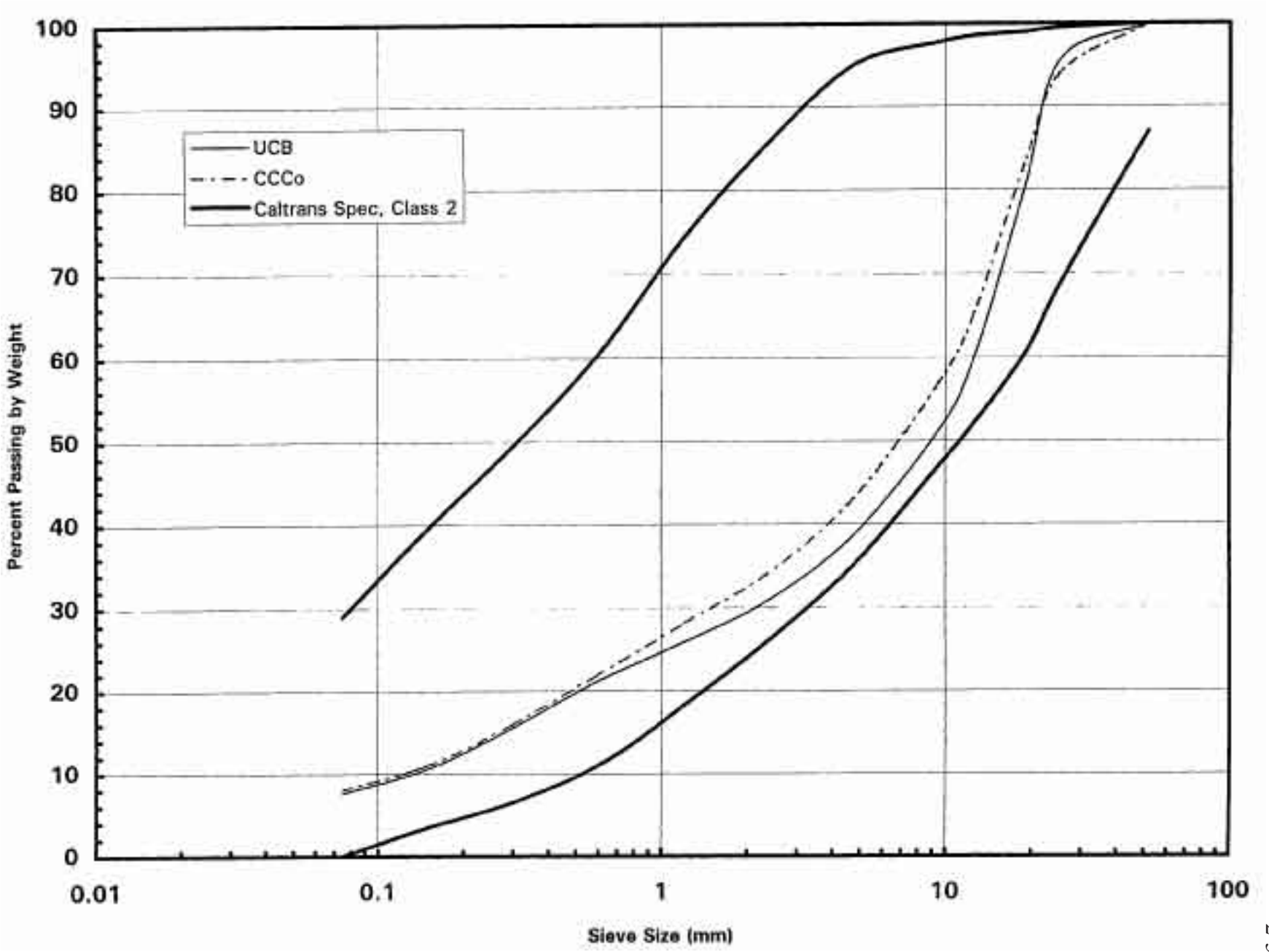

Figure 2-1. Gradient of Aggregate Subbase.

Table 2.1 R-value Test Results, Subgrade and In-Place Subbase

Sample	-Value			
	Subgrade	Location (ft)	Subbase	Location (ft)
1	28	1+11, 19	75	1+11, 19
2	4	2+42, 1	72	2+42, 1
3	7 *	0+85, 4	82	composite
4	30	1+90, 10	55	1+60, 20
5	16	0+40, 20	67	0+40, 20
Average	17		70	
Standard Deviation	12		10	

*1.5 m depth

Some difficulty was experienced in preparing samples of the subbase material for R-value testing because approximately 5 to 10 percent of the material consists of aggregate between the 25 mm (1 in) and 75 mm (3 in) sieve sizes. The oversize material (greater than 25 mm) was removed and replaced with smaller material, following standard Caltrans procedures.

2.2.3 Sand Equivalent Test Results

Sand Equivalent (SE) Tests (Caltrans Method 217) were performed on the samples of the subbase material by CCCo and UCB staff. The average of three samples tested by the CCCo staff was 30. A total of 8 samples were tested by the UCB staff; for samples taken in the vicinity of Station 1+11, the average of 4 tests produced a SE of 21 while the average of 4 tests in the vicinity of Station 2+42 resulted in a SE of 30. For the Class 2 aggregate subbase the minimum requirement for this parameter is 21.

2.3 STRUCTURAL DESIGN AND LAYOUT

Pavement thicknesses were selected according to Caltrans procedures using the computer program NEWCON90 *(California Department of Transportation, 1991)*. Final thickness designs for the drained and undrained sections were based on a subgrade R-value of 10 and a traffic index of 9. Design thicknesses are shown in Table 2.2.

These designs reflect field conditions where high quality subbase material is available at the construction site. During construction of the test sections, this subbase layer was graded to provide a 2.0 percent downward transverse cross-slope to the east and a 0.75 percent downward longitudinal slope to the south (Figure 2.2).

The untreated aggregate base was specified as a Caltrans Class 2 aggregate base, and the asphalt concrete was a Caltrans Type A 19 mm 3/4 in. coarse mix. The asphalt treated permeable base (ATPB) was also specified following Caltrans Standard Specifications *(California Department of Transportation, 1992a)*.

Because a pavement at least 7.5 m (24 ft) wide was desired, the limited width of Building 280 (9.5 m [30 ft]) prevented use of shoulders. Accordingly, K barriers were selected to provide the requisite lateral support to the pavement. As a result each test section was 7.8 m (25.6 ft) wide by 30 m (100 ft) long.

An edge drain, provided with a standard clean-out, was placed along the east side of the pavement sections following Caltrans Standard Plans *(California Department of Transportation, 1992b)*. Ramps were included at both ends for construction and access

Table 2.2 Pavement Structures and Design Layer Thicknesses

Undrained Pavement *aggregate base only*			Drained Pavement *aggregate base and asphalt treated permeable base*		
Material		**Layer Thickness**	**Material**		**Layer Thickness**
Asphalt Concrete	411mm (1.35 ft)	137mm (0.45 ft)	Asphalt Concrete	395mm (1.30 ft)	137mm (0.45 ft)
Aggregate Base		274mm (0.90 ft)	Asphalt Treated Permeable Base		76mm (0.25 ft)
			Aggregate Base		182mm (0.60 ft)
Aggregate Subbase		design 229mm (0.75 ft)*	Aggregate Subbase		design 229mm (0.75 ft)*
Subgrade		semi-infinite	Subgrade		semi-infinite

* actual subbase thickness varies due to cross-slope and slope in subgrade:
at site 500 about 137mm (0.45 ft), at site 501 about 215mm (0.7 ft), at site 502 about 215mm (0.7 ft), at site 503 about 305mm (1.0 ft)

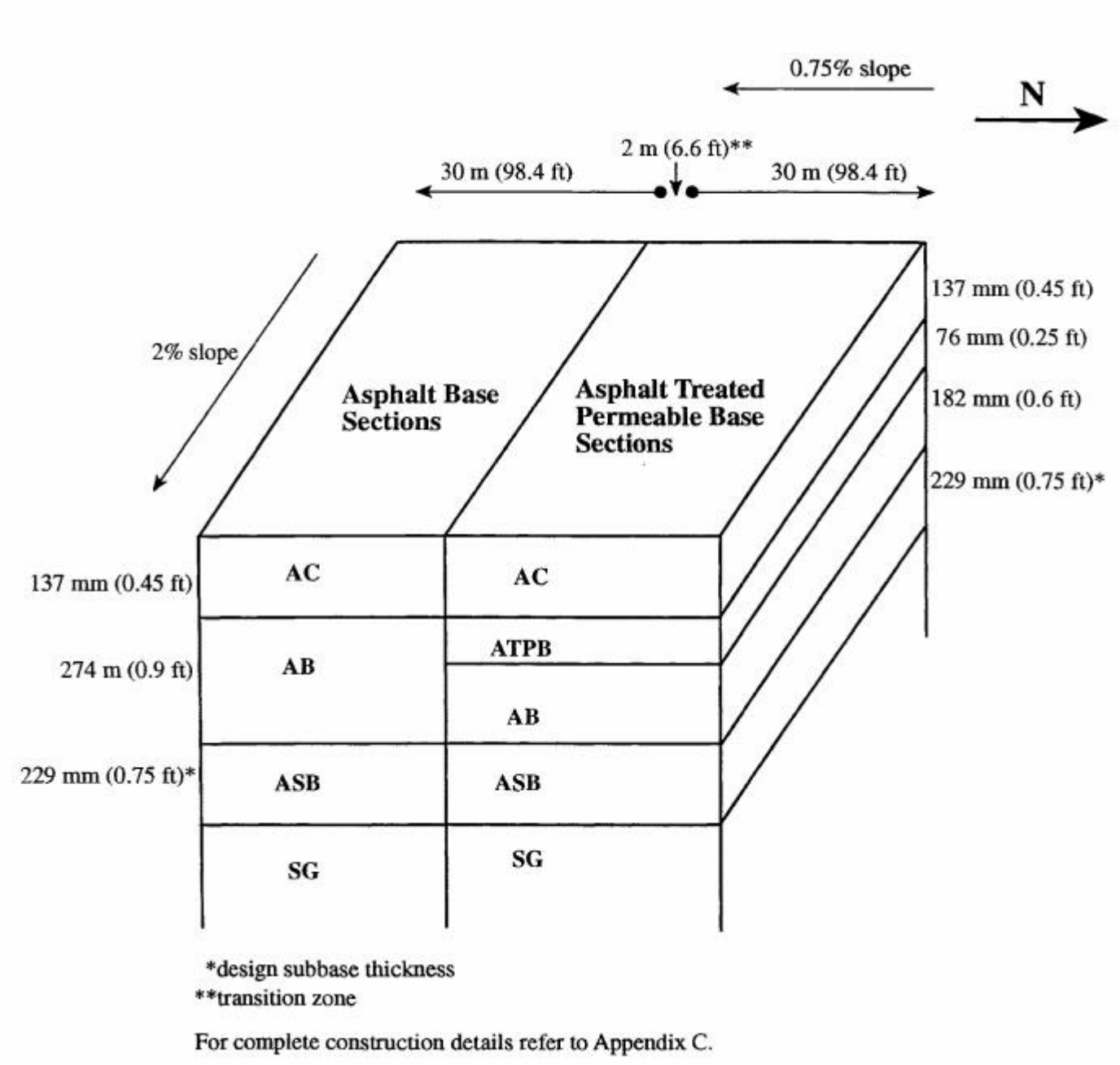

Figure 2.2 Construction of First Test Pavements

purposes, and a 2 m (6.6 ft) transition zone was placed between the drained and undrained test sections.

2.4 TEST SECTION CONSTRUCTION

Construction was performed by Ghilotti Brothers of San Rafael, California, the low bidder for the contract. Special provisions for the contract are included as Appendix C of this report. Construction inspection, sample collection, and quality assurance testing were performed by Contra Costa County, Caltrans District 4, and UCB. The imported aggregate base and existing aggregate subbase were compacted to meet Caltrans standard specifications using Test Method 231 (nuclear density gage). The asphalt concrete and ATPB layers were compacted in accordance with method specifications *(California Department of Transportation, 1992a)* but were checked for density for research purposes using Test Method 375 (nuclear density gage).

2.4.1 Subgrade

The subgrade was not reworked. Its in-place relative compaction was measured using Caltrans Test 231 which requires an in-place wet density determination and laboratory compaction at the in-situ water content. Three relative compaction tests were performed on subgrade samples from each of the two sections. Relative compactions in the drained section were 95 percent, 91 percent, and 98 percent, while those for the undrained sections were 96 percent, 94 percent, and 98 percent. These resulted in averages of 95 percent and 96 percent, respectively, meeting the minimum of 95 percent required by the Caltrans Standard Specifications *(California Department of Transportation, 1992a)*.

2.4.2 Unbound Subbase and Base

The existing subbase was reworked, graded, and compacted to the specified layer elevation and density. To insure a uniform platform for placement of the base and surface layers, level measurements (referenced to benchmarks outside the sections) were made at 4.3 m (14 ft) longitudinal and 1.6 m (5.1 ft) transverse intervals. The actual thickness of the subbase varied somewhat across the pavements because of the transverse and longitudinal cross-slopes and some variation in the cross-slope of the subgrate. The resulting thicknesses are shown in Figure 2.2.

Nuclear density tests were performed on the compacted aggregate subbase on two occasions. At the time of construction, two test measurements yielded relative densities of 95 percent and 97 percent. Four tests conducted 28 days later yielded larger relative densities of 99 percent, 98 percent, 100 percent, and 99 percent.

The base layer was constructed using imported aggregate. Gradation and other classification tests were performed on this material by CCCo, Caltrans, and UCB. Results of the grading analyses are shown in Figure 2.3 and the resulting classifications for the data from the three agencies are as follows:

Agency	USCS	AASHTO	Caltrans Specification
UCB	GW	A-1-a	Class 2 AB
CCCo	GW-GM	A-1-a	Class 2 AB
Caltrans	GW-GM	A-1-a	Class 3 AB

Three R-values tests were performed on the aggregate base material, one on a sample from the plant before construction, one on a sample from the plant during construction, and one on a composite sample collected from the in-situ layer. The results are consistent, ranging between 78 and 83, and meet the minimum R-value requirement of 78 for a Class 2 aggregate base.

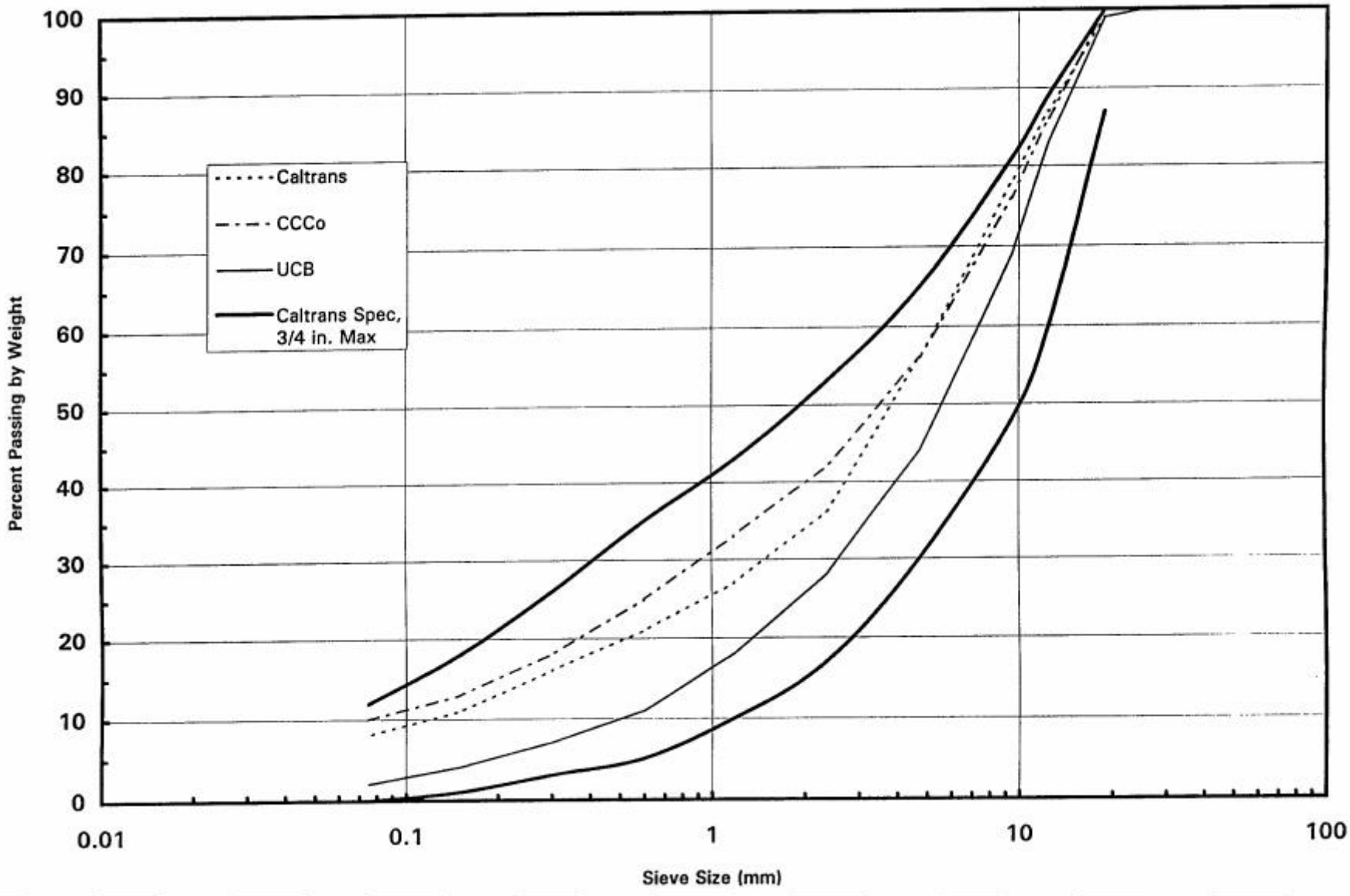

Figure 2.3 Gradations of Aggregate Base

Density tests were performed immediately after compaction according to Caltrans Test Method 231. Three tests were performed within each section based on a random site selection pattern. In addition, three more tests were performed on each section at locations away from the first three to obtain data for the entire section. All tests were performed at a depth of 150 mm (6 in). Results are shown in Table 2.3. As seen in the table, the relative compaction exceeds the minimum requirement of 95 percent.

Table 2.3 Relative Compaction and Water Contents - Aggregate Base [150 mm depth]

Density Test Location	Relative Density (%)	In-Situ Water Content (%)	Optimum Water Content (%)
Undrained section for record (random)	100, 100, 100	6.0	6.0
Undrained section additional	103, 102, 101	5.9	7.4
Drained section for record (random)	101, 100, 101	5.0	7.3
Drained section additional	100, 99, 99	5.7	6.7

During construction, deflection tests using the heavy weight deflectometer (HWD) were performed at the surface of the subbase, at the surface of the untreated base, and at the surface of the asphalt concrete. Looseness of the base surface immediately following construction, as evidenced by scuffing and footprints, was of some concern. To check if there was a density gradient in the base layer, a series of nuclear density tests were performed, at the surface (in the backscatter mode), at a depth of 50 mm (2 in.), and at 100 mm (4 in.). Results are shown in Table 2.4.

Although the densities measured in the backscatter mode were lower than those measured at 50 and 100 mm depths, the measurements did not indicate a deep penetration of loose material. From visual observation, it appeared to have only been about 3 to 8 mm thick.

After the base had dried for 17 days, the surface was dry and very hard. Walking produced neither scuffing nor footprints. At that time, HWD deflection testing was again performed.

In addition to the HWD tests, Dynamic Cone Penetrometer (DCP) tests were performed just after construction and again 17 days later. Results of the analysis of the DCP tests as well as of the HWD tests are reported subsequently.

2.4.3 Water Content of Unbound Materials

Water contents of the subgrade, subbase, and base layers were determined at various stages prior to and during construction. Table 2.5 provides a summary of the water contents determined by CCCo, UCB, and Caltrans District 4 laboratories. These water contents serve as one of the bases for selecting conditions for laboratory specimen preparation.

It should be noted that the subgrade water content determinations are based on measurements using soil from various areas throughout the site. The range provides an indication of the site specific variability of the sub-surface water content. In addition, it is important to note that the location and depths of the samples tested by the three agencies were not identical, a factor that could partially explain observed differences.

Table 2.4 Aggregate Base Density Tests at Surface and at 50 mm and 100 mm Depths

Method 231 Density Test Location	% Relative Density Backscatter	% Relative Density 50 mm (2 in.)	% Relative Density 100 mm (4 in.)
Undrained section Station 0+30.40 8' to west K-rail	99	103	103
Undrained section Station 0+30.40 18' to west K-rail	98	102	101
Undrained section Station 0+73.25 9' to west K-rail	98	103	103
Undrained section Station 0+73.25 20' to west K-rail	99	103	103
Undrained section Station 1+01.85 6' to west K-rail	97	103	102
Undrained section Station 1+01.85 15' to west K-rail	95	100	102
Drained section Station 1+44.75 6' to west K-rail	99	103	103
Drained section Station 1+44.75 19' to west K-rail	96	100	99
Drained section Station 1+73.35 3' to west K-rail	97	103	103
Drained section Station 1+73.35 13' to west K-rail	97	102	101
Drained section Station 2+01.90 9' to west K-rail	95	100	101
Drained section Station 2+01.90 17' to west K-rail	98	103	101
Average	97.3	102.1	101.8

Table 2.5 Water Contents of Unbound Materials - Summary by Date and Agency

Materials	Agency	Sampling Dates (Month/Year)	Water Content Range (Percent)
Subgrade	CCCo	11/94; 2/95	13.6 - 20.6
	UCB	3/95; 4/95	16.4 - 23.9
	Caltrans	3/95	15.7
Subbase	CCCo	11/94; 2/95	4.0 - 7.3
	UCB	3/95	4.6 - 7.3
	Caltrans	3/95	5.4 - 7.9
Base	CCCo	4/95	4.2
	UCB	4/95	5.5
	Caltrans	4/95	5.0 - 6.0

2.4.4 Asphalt Concrete Materials and Mix Design

The surface mix was a Caltrans Type A, 19 mm (3/4 in.) maximum size coarse graded asphalt concrete. It was produced at the Gallagher and Burke drier drum plant in Oakland, California. Materials for the mix included Shell AR-4000 asphalt cement and an aggregate combination from the Kaiser Sand and Gravel Radum Plant (1/4 in. x No. 10 and Rodmill Sand sizes) and the Lonestar Eliot Plant (3/8 in. x dust, 1/2 in. x 1/4 in., and 3/4 in. x 1/2 in. sizes). Results of specification tests performed during mix design and on samples taken during construction at the plant and at the site show that the mix met Caltrans standards. Table 2.6 contains a summary of the initial test results on the AR-4000 asphalt cement as well as a summary of viscosity determinations performed on samples taken at the time of construction.

Table 2.6 Test Data Shell AR-4000 Asphalt Cement

Test	Initial[a]	During Construction	Specification Limit
Original Asphalt			
Absolute Viscosity @ 60°C (140°F), poise	2600	--------	
Kinematic Viscosity @ 135°C (275°F), csf	273	--------	
Brookfield Viscosity @ 135°C (275°F), cp	262[b]	--------	
Brookfield Viscosity @ 170°C (347°F), cp	50[b]	--------	
Penetration at 25°C (77°F), dmm	40	--------	
Specific Gravity @ 15.5°C (60°F)	1.0237	--------	
RTFO Residue			
Absolute Viscosity @ 60°C (140°F), poise	4604	3906[c]	3000-5000
Kinematic Viscosity @ 135°C (275°F), cst	345	--------	275, min
Penetration @ 25°C (77°F), dmm	29	--------	25, min
Percent of Original Penetration	72.5	--------	45, min

[a] Test performed 1/17/95.
[b] Tests performed 3/95; approximately 2 months after the other tests had been performed.
[c] Average of three samples.

Conformance of the aggregate gradation to specifications is shown in Table 2.7, for both the mix design and for samples collected at the plant and construction site. Table 2.7 indicates that aggregate gradations from the plant and site samples were close to the mix design values and were clearly within the Caltrans operating range.

Table 2.7 Design and Quality Assurance Testing of Asphalt Concrete Aggregate

Asphalt Concrete: 3/4 in. maximum size, Type A, Coarse gradation

Sieve Size (mm)	(US)	Specification Limits to Proposed Gradation (X)	Mix Design *Caltrans District 4 Lab*	Specification Operating Range	Plant Sample Bottom Lift *Caltrans Richmond Lab*	Extracted Top Lift *CC County Materials Lab*	Extracted Top Lift *Caltrans TransLab*	Extracted Bottom Lift *Caltrans TransLab*	Plant Aggregate Combined *Caltrans TransLab*
25.4	1 in.		100	100	100	100	100	100	100
19	3/4 in.		99	90-100	92	97	87	94	96
12.5	1/2 in.		80		75	82	70	74	76
9.5	3/8 in.		67	60-75	66	69	62	62	66
4.75	No. 4	45-50	49	45-55	51	52	45	47	49
2.36	No. 8	32-36	33	29-39	35	36	31	32	34
1.18	No. 16		22		24	25	22	22	23
0.6	No. 30	15-18	14	10-20	17	18	16	15	15
0.3	No. 50		9		12	14	12	11	10
0.15	No. 100		6		8	9	8	8	6
0.075	No. 200		3	3-7	4	5	5.1	4.8	3

The suggested asphalt content range from the mix design was 4.6 to 4.9 percent, by weight of aggregate. Extraction data from site samples is included in Table 2.8. A study of the variability of extracted asphalt contents has indicated that the standard deviation is approximately 0.21 percent (internal Caltrans study by S. Shatnawi). Test results indicate that the asphalt contents were generally in the range 4.7 to 5.3 percent and may have been somewhat high in portions of the top lift.

Table 2.8 Mix Design and Extracted Asphalt Contents

Mix Design Caltrans District 4 Recommended	Top Lift Site Sample Caltrans TransLab Sta 1+75 east	Bottom Lift Site Sample Caltrans TransLab 0+30 east side	Site Sample Top Lift Contra Costa County Mat Lab	Plant Production Bottom Lift Caltrans Richmond Lab
4.6-4.9	5.1-5.4	4.7-4.8	4.8	4.8
	5.25 (average)	4.8 (average)		

The Hveem stabilometer value was 47 at the design asphalt content of 4.9 percent, well above the minimum specification requirement of 37. Laboratory compacted specimens from the field mix showed nearly the same value as can be seen in Table 2.9. These results indicate that the mix should have a low probability of rutting, according to California experience, when used in a typical highway application.

Table 2.9 Hveem Stabilometer Values from Mix Design and Laboratory Compacted Site Samples

Mix Design Caltrans District 4 Lab, 4.9% Bitumen Content	Site Sample Top Lift Contra Costa County Materials Lab	Caltrans TransLab Top Lift	Caltrans TransLab Bottom Lift
47	48 (average of 5)	46 (average of 3)	46 (average of 3)

Sand equivalent and LA Rattler tests were performed on the mix aggregate by the Caltrans District 4 laboratory. The sand equivalent value was 70, well above the specification minimum of 50. The LA Rattler test results were 4 percent loss at 100 revolutions and 21 percent loss at 500 revolutions, which are less than the specification maximum limits of 10 and 45 percent loss, respectively.

The mix contained 100 percent crushed particles and exhibited a stabilometer value after moisture vapor susceptibility conditioning of 36, both exceeding Caltrans specification requirements.

2.4.5 Asphalt Concrete Construction

Caltrans Standard Specification (Section 39-6.03), a method specification, was used in compacting the asphalt concrete. Several factors must be considered during construction using a method specification, including compaction equipment, temperature, lift thickness, and coverages.

Compaction equipment. The specification includes provisions for alternative compaction equipment, approved by the engineer in accordance with California Test 113. This specification allowed the contractor to use only two rollers. Alternative compacting equipment may be used for the initial or breakdown compaction if operated according to the procedures and under the conditions designated in the approval. For the breakdown roller, Ghilotti Brothers Construction used a 7-ton Dynapac CC21A vibratory compactor.

Using the alternative method also eliminated the need for pneumatic-tired rollers since the construction did not require compacted thicknesses of less than 61 mm (0.20 ft). A 10-ton Caterpillar CB534 roller was used for the finish compaction. Although this roller is normally

used primarily for breakdown compaction, it qualifies for finish compaction when the vibrating unit is off.

Temperature. Standard Specifications Section 39-6.01 states that all mixtures, except open graded asphalt concrete, shall be spread, and the first coverage of breakdown compaction shall be applied when the temperature of the mixture is not less than 121°C (250°F), and all breakdown compaction shall be completed before the temperature of the mixture drops below 93° C (200°F). The contractor met the temperature requirements on the first coverage of breakdown, with the average breakdown temperature being 135° C (275°F). All breakdown compaction was completed before the mixture temperature dropped below the specified minimum.

Another temperature requirement limits construction of Type A asphalt concrete to periods when the atmospheric temperature is above 10°C (50°F). At the time of placement, the atmospheric temperature ranged between 16°and 21°C (60°F and 69°F).

Lift thickness. Finally, a succeeding lift shall not be placed over a previous lift exceeding 76 mm (0.25 ft) in compacted thickness until the temperature of the lower lift is less than 71°C (160°F) at mid-depth. This criterion was easily achieved on the east side of the sections. However, on the west side, placement of the second lift had to be delayed until the lower lift had cooled to the specified temperature. The need to wait was due to the fact that, unlike typical paving construction, the RFS site was enclosed, eliminating the cooling effects of surface winds.

Caltrans standard specifications require asphalt concrete to be spread and compacted in a certain number of lifts, depending on the overall thickness shown on the plan. For both the

drained and undrained sections, the total AC thickness of 137 mm (0.45 ft) required at least two lifts.

A bottom lift of 76 mm (0.25 ft) and a top lift of 61 mm (0.20 ft) were used. The specifications require that layer thickness be within ± 15 mm (0.05 ft) of the design thickness. Cores taken from the site after construction showed the lift thicknesses were nearly all within specification, although a few from the west side had thicknesses in the bottom lift exceeding the maximum by about 3 mm (0.01 ft).

Coverages. Caltrans standard specifications state that a coverage shall be as many passes as necessary to cover the entire width being paved. A pass shall be one movement of a roller in either direction. The east side was compacted before the west side and, in order for the roller to compact the west side, the rollers had to roll over the east side several more times before getting to the west side. Although the east side thereby received more passes, an average of five coverages were applied to each side.

2.4.6 Air-Void Content

Maximum Specific Gravities. The Rice Maximum Specific Gravity (MSG), ASTM Test D 2041, is used in the calculation of mix air-void contents. The Rice MSG was measured by three laboratories, Contra Costa County, UCB, and TransLab. Contra Costa County reported a value of 2.530. The value reported by UCB was 2.513 based on two tests. The TransLab results were based on the average of two tests from each lift; from the bottom lift: 2.542 and 2.539, with an average of 2.541, and from the top lift: 2.524 and 2.531, with an average of 2.528.

Using the specific gravities of the asphalt and aggregate and the percent by weight of asphalt and aggregate, the theoretical maximum specific gravity of the bottom lift was 2.501 and that of the top lift was 2.487.

Measurements. Contra Costa County (CCCo) staff measured in-place densities during construction using the nuclear density gage (Caltrans Test Method 375). This test is applied to individual layers of asphalt concrete which have compacted thickness of at least 46 mm (0.15 ft), or to the combination of two thinner layers of AC produced from the same source which have an accumulated thickness of 46 mm (0.15 ft) or more. The count ratio is calculated from the one-minute density count using the nuclear gage in the backscatter mode. Finally, the in-place density is determined by using a count ratio/density table that is established for each gage. The density measurements were used with the maximum specific gravity from ASTM D 2041 to calculate air-void contents and, with the specific gravity from standard laboratory compaction, to calculate relative densities. The nuclear density gage measurements were distributed across the entire paved area. Table 2.10 contains a summary of the density, air void, and relative compaction data obtained by CCCo.

Table 2.10 Density, Air-Void Contents, and Relative Compaction Obtained from CCCo Using the Nuclear Density Gage

Density, Air-Void Contents, and Relative Compaction Obtained From CCCo Using the Nuclear Density Gage

Test Maximum Density = 2.43 g/cc

Undrained, East Side, Bottom Lift

Station	Density (g/cc)	Air-Void (%)	Relative Compaction
0+30.40	2.37	5.69	97.5
0+44.60	2.30	8.48	94.7
0+58.90	2.40	4.50	98.8
0+73.25	2.37	5.69	97.5
0+87.65	2.37	5.69	97.5
1+01.85	2.36	6.09	97.1
AVERAGE	***2.36***	***6.02***	***97.2***

Drained, East Side, Bottom Lift

1+30.70	2.36	6.09	97.1
1+44.75	2.35	6.49	96.7
1+59.15	2.32	7.68	95.5
1+73.35	2.34	6.88	96.3
1+87.60	2.37	5.69	97.5
2+01.90	2.37	5.69	97.5
AVERAGE	***2.35***	***6.42***	***96.8***

Undrained, West Side, Bottom Lift

Station	Density (g/cc)	Air-Void (%)	Relative Compaction
0+30.40	2.36	6.09	97.1
0+44.60	2.38	5.29	97.9
0+61	2.40	4.50	98.8
0+73.25	2.40	4.50	98.8
0+87.65	2.32	7.68	95.5
1+01.85	2.37	5.69	97.5
AVERAGE	***2.37***	***5.62***	***97.6***

Drained, West Side, Bottom Lift

1+30.70	2.33	7.28	95.9
1+44.75	2.37	5.69	97.5
1+59.15	2.36	6.09	97.1
1+73.35	2.36	6.09	97.1
1+87.60	2.34	6.88	96.3
2+01.90	2.37	5.69	97.5
AVERAGE	***2.36***	***6.29***	***96.9***

Undrained, East Side, Top Lift

Station	Density (g/cc)	Air-Void (%)	Relative Compaction
0+30.40	2.32	7.68	95.5
0+44.60	2.32	7.68	95.5
0+58.90	2.32	7.68	95.5
0+73.25	2.35	6.49	96.7
0+87.65	2.34	6.88	96.3
1+01.85	2.27	9.67	93.4
AVERAGE	***2.32***	***7.68***	***95.5***

Drained, East Side, Top Lift

1+30.70	2.42	3.70	99.6
1+44.75	2.35	6.49	96.7
1+59.15	2.31	8.08	95.1
1+73.35	2.32	7.68	95.5
1+87.60	2.30	8.48	94.7
2+01.90	2.28	9.27	93.8
AVERAGE	***2.33***	***7.28***	***95.9***

Undrained, West Side, Top Lift

Station	Density (g/cc)	Air-Void (%)	Relative Compaction
1+01.85	2.27	9.67	93.4
0+87.65	2.27	9.67	93.4
0+73.25	2.32	7.68	95.5
0+58.90	2.27	9.67	93.4
0+44.60	2.33	7.28	95.9
0+30.40	2.36	6.09	97.1
AVERAGE	***2.30***	***8.34***	***94.8***

Drained, West Side, Top Lift

2+01.90	2.32	7.68	95.5
1+87.60	2.32	7.68	95.5
1+73.35	2.33	7.28	95.9
1+59.15	2.30	8.48	94.7
1+44.75	2.34	6.88	96.3
1+30.70	2.33	7.28	95.9
AVERAGE	***2.32***	***7.55***	***95.6***

After construction, cores were taken in the transition zone between the drained and undrained sections for air-void content measurement and later testing in the simple shear tester. The UCB laboratory used parafilm^{TM} with ASTM Method D 1188 to measure bulk specific gravity, which was then used with the maximum specific gravity from the UCB Rice Test to calculate air-void content.

The bulk specific gravity (B.S.G.) is computed as follows:

$$B.S.G. = \frac{A}{(D - E) - \left(\frac{D - A}{F}\right)} \tag{2-1}$$

where A = weight of dry uncoated specimen in grams, D = weight of dry specimen plus Parafilm^{TM} coating in grams, E = weight of the dry specimen plus Parafilm^{TM} coating in water in grams, and F = specific gravity of the Parafilm^{TM} at 25°C (a value of 0.9 was assumed). Finally, the air-void content (AV) is calculated by using the Rice and the bulk specific gravity as follows:

$$Air\text{-}Void\ \ Content\ \ (\%) = \left(1 - \frac{Bulk\ \ Specific\ \ Gravity}{Rice\ \ MSG}\right) \bullet 100 \tag{2-2}$$

These data are included in Table 2.11.

Table 2.11 UCB Calculated Density, Air-Void Contents, and Relative Compaction of Site Cores from Transition Zone

Density, Air-Void Contents, and Relative Compaction Of Site Cores Calculated at UCB Lab at Station 1+18

Transition Area, East Side, Bottom Lift @sta 1+18

Specimen	Density (g/cc)	Air-Void (%)	Rel Comp (%)
SAC-1B	2.43	3.39	99.9
SAC-2B	2.42	3.66	99.6
SAC-3B	2.43	3.37	99.9
SAC-4B	2.43	3.33	100.0
SAC-5B	2.43	3.27	100.0
SAC-6B	2.42	3.84	99.4
SAC-7B	2.41	4.07	99.2
SAC-8B	2.41	4.23	99.0
SAC-9B	2.41	3.91	99.4
SAC-10B	2.40	4.34	98.9
SAC-11B	2.38	5.21	98.0
SAC-12B	2.41	4.05	99.2
AVERAGE	***2.42***	***3.89***	***99.4***

Transition Area, West Side, Bottom Lift @sta 1+18

Specimen	Density (g/cc)	Air-Voids(%)	Rel Comp (%)
SAC-13B	2.40	4.56	98.7
SAC-14B	2.44	3.06	100.3
SAC-15B	2.41	4.29	99.0
SAC-16B	2.41	4.20	99.1
SAC-17B	2.43	3.20	100.1
SAC-18B	2.43	3.30	100.0
SAC-19B	2.44	3.10	100.2
SAC-20B	2.41	4.00	99.3
SAC-21B	2.40	4.40	98.9
SAC-23B	2.45	2.60	100.7
AVERAGE	***2.42***	***3.97***	***99.6***

Transition Area, East Side, Top Lift @sta 1+18

Specimen	Density (g/cc)	Air-Void (%)	Rel Comp (%)
SAC-1T	2.36	6.27	96.9
SAC-2T	2.35	6.48	96.7
SAC-3T	2.36	6.15	97.1
SAC-4T	2.35	6.32	96.9
SAC-5T	2.33	7.25	95.9
SAC-6T	2.37	5.64	97.6
SAC-7T	2.33	7.39	95.8
SAC-8T	2.32	7.53	95.6
SAC-9T	2.34	6.74	96.4
SAC-10T	2.36	6.17	97.0
SAC-11T	2.34	6.77	96.4
SAC-12T	2.37	5.78	97.4
AVERAGE	***2.35***	***6.54***	***96.7***

Transition Area, West Side, Top Lift @sta 1+18

Specimen	Density (g/cc)	Air-Void (%)	Rel Comp (%)
SAC-13T	2.35	6.64	96.5
SAC-14T	2.40	4.40	98.9
SAC-15T	2.37	5.56	97.7
SAC-16T	2.38	5.20	98.0
SAC-17T	2.40	4.40	98.9
SAC-18T	2.40	4.60	98.7
SAC-19T	2.38	5.40	97.8
SAC-20T	2.34	6.90	96.3
SAC-21T	2.31	7.90	95.2
SAC-23T	2.36	5.90	97.3
AVERAGE	***2.37***	***5.69***	***97.5***

Relative compaction requires the calculation of another value, the laboratory density under standard compaction (California Test 304). The test procedure requires acquisition of a representative sample of asphalt concrete from the paving operation and the compaction of five briquettes. The density of each briquette is then determined, and the average is reported as the laboratory compaction density. CCCo calculated the laboratory compaction density to be 2.43 g/cc.

Finally, the relative compaction (RC) is determined as follows:

$$RC\ (\%) = \frac{Average\ \ In\text{-}Place\ \ Density}{Laboratory\ \ Compaction\ \ Density} \bullet 100 \qquad (2\text{-}3)$$

These data are summarized in Table 2.10.

Air-void contents (AV) were calculated using in-place densities obtained by CCCo using the nuclear gage and the Rice value obtained by UCB as follows:

$$AV\ (\%) = \left(1 - \frac{In\text{-}Place\ \ Density}{Rice\ \ MSG}\right) \bullet 100 \qquad (2\text{-}4)$$

Air-void contents for the bottom lift obtained from the nuclear density gage (CCCo) were much larger than those of the transition-zone cores as shown in the following tabulation for the averages of Tables 2.10 and 2.11.

	Top lift	Bottom lift
CCCo (Nuclear Density Gage)	7.71	6.09
UCB (Parafilm^{TM} ASTM D 1188)	6.54	3.89

The reason for the differences between the sets of tests is that the CCCo tests on the bottom lift were made before placement of the top lift, while UCB cores were taken from the fully constructed AC. The bottom lift had been subjected to additional densification during compaction of the top lift.

Additional considerations. During construction, the contractor was able to obtain low air-void contents in much of the asphalt concrete layer, lower than is often obtained on typical Caltrans construction projects. Some of the primary factors in achieving good compaction were:

- Temperature, with compaction beginning as soon as it is possible to put equipment on the mat without causing it to shove and ending before the mix has cooled below approximately 82° to 93°C (180° to 200°F), and
- Number of passes, obtaining approximately 6 to 10 passes before the mix temperature has fallen below that at which further compaction effort is ineffective.

It is important to remember that the contractor did not use any special equipment or techniques and was given no special instructions except to follow Caltrans standard specifications (method specification for compaction). The following are observations of possible factors that assisted the contractor in achieving a high level of compaction.

Lift thickness. For this project the maximum allowable lift thicknesses were used, 76 mm (0.25 ft) for the bottom lift and 61 mm (0.20 ft) for the top lift. On many Caltrans paving projects the bottom lift is about 46 to 61 mm (0.15 to 0.20 ft) and the top lift is as thin as 37 to 46 mm (0.12 to 0.15 ft). When an overlay is being placed over an existing pavement having an uneven surface, lift thicknesses may be even thinner in high spots on the existing surface. Mix placed in thin lifts tends to cool more rapidly than mix placed in thicker lifts, especially when placed on a cold existing surface or when placed at night. Mix placed in thin lifts also has a greater tendency to develop slippage cracks, requiring that compaction be delayed for additional cooling. In combination, faster cooling rates and delays in beginning compaction result in fewer passes at lower temperatures, which will result in larger air-void contents. In addition, very thin

lifts with 19 mm (3/4 in.) aggregate may make it more difficult for the larger particles to become oriented under the roller, especially if there is any segregation in the mix.

Lateral confinement. The aggregate base, ATPB, and asphalt concrete layers were placed between concrete K-barriers. The K-barriers restricted lateral spreading of the mix during compaction. On a typical section without lateral confinement, a 3.9 m (12 ft) wide unrolled mat may spread to 4.0 to 4.1 m (12.3 to 12.5 ft) by the time compaction is completed. With the lateral confinement all compaction energy resulted in vertical displacement of the mix, which may have made each pass of the rollers more effective. Lateral confinement also allowed the roller operators to begin earlier and make more passes at the edge of the mat without fear of shoving.

Additional lateral confinement probably occurred because of the short distance of the test sections which resulted in the west lane of the pavement being placed while the east lane was still being compacted.

Limited laydown distance and indoor paving. The constructed length of the test sections was approximately 74 m (244 ft) including 58 m of test pavement, 2 m of transition, and about 14 m of ramps, which is very short compared to typical projects. Because of the short section lengths, the contractor was able to perform many passes while the mix was still hot. In addition, the building enclosure helped maintain the temperature of the mix by reducing the flow of air. On typical projects much larger quantities of mix may be placed before compaction begins, and wind and cool temperatures may more quickly cool the mix.

On typical projects adjoining lanes may not be spread and compacted at the same time. The short test sections resulted in the contractor placing and compacting both lanes while both were still at sufficiently high temperatures for compaction. For this reason compaction to pinch

the construction joint resulted in additional passes for both lanes while they were still compactable. The time between laydown of the two lanes was approximately 1 to 1.5 hours for the two lifts.

The short sections also resulted in the contractor placing the top lift while the bottom lift was still hot. On the west lane, laydown was delayed until the mix had cooled to the maximum allowable laydown temperature. From the data presented previously, it is apparent that the air-void content of the bottom lift was approximately 1 to 2 percent less than that of the top lift. If the bottom lift had been allowed to cool more, or especially if it had been compacted on a different day, it is likely that laydown of the top lift would not have heated the bottom lift sufficiently to obtain that additional compaction. The beneficial effects of additional compaction of the bottom lift are discussed in detail in Chapter 5 of this report.

2.4.7 Bonding Between Asphalt Concrete Lifts

Cores taken from the east lane at station 1+18 in the transition between the drained and undrained sections split at the interface between the two asphalt concrete lifts; some of the cores taken from the west lane did so as well. Large slabs, approximately 1 m square, taken from the east lane split with no force applied other than that required to extract them. Additional 38 mm (1.5 in.) cores taken in the east lane at approximately station 2+00 also split. Cores taken later using an air-cooled core had similar results.

No tack coat was applied between lifts. Temperatures taken at mid-depth of the first lift just before placement of the second lift ranged between 34°and 58°C (94°and 136°F) in the east lane and 40°and 71°C (104°and 160°F) in the west lane. In both lanes temperatures increased uniformly with the stationing. In the transition zone at station 1+18, the second lift was placed at

about 38°C (100°F) in the east lane and at about 71°C (160°F) in the west lane. Current Caltrans specifications require that a succeeding lift not be placed until the preceding lift has cooled to 71°C (160°F) or less.

It is unknown whether the poorer bonding in the east lane is due to cooler temperatures in the first lift. In any event, lack of bonding between the asphalt concrete layers may result in larger tensile strains at the bottom of each lift, which would be expected to result in somewhat earlier fatigue cracking. The actual amount of bonding between the layers in-situ under HVS trafficking is uncertain. The potential effects of lack of bonding between the layers on fatigue cracking is addressed in Chapter 6.

2.4.8 Asphalt Treated Permeable Base (ATPB)

The permeable base in the drained pavement test sections was specified to meet Caltrans standard specifications for asphalt treated permeable base (ATPB). The ATPB was composed of Shell AR-8000 asphalt cement and aggregate combined from the Kaiser Sand and Gravel Radum plant (1/4 in x No. 10 size) and the Lonestar Eliot plant (1/2 in x 1/4 in and 3/4 in x 1/2 in sizes).

Specification tests from the mix design and from samples taken at the plant and site during construction indicate that the ATPB met Caltrans specifications. The aggregate gradation was within specification (Table 2.12). The mix design bitumen content was 2.5 percent. The bitumen content obtained from extraction by the Contra Costa County Materials Laboratory was 2.9 percent. From plant production values measured by Caltrans Richmond Laboratory, the bitumen content was 2.8 percent.

Table 2.12 Design and Quality Assurance Testing of ATPB Aggregate

Sieve Size		Percentage Passing			
mm	US	Specification Limits	Mix Design (Caltrans District 4 Lab)	Site Sample (CC County Materials Lab)	Plant Sample (Caltrans Richmond Lab)
25.4	1 in.	100	100	100	100
19	3/4 in.	90-100	99	91	93
12.5	1/2 in.	35-65	56	51	54
9.5	3/8 in.	20-45	26	27	27
4.75	No. 4	0-10	7	8	6
2.36	No. 8	0-5	1	6	4
1.18	No. 16		0	6	3
0.6	No. 30		0	5	3
0.3	No. 50		0	5	2
0.15	No. 100		0	4	1
0.075	No. 200	0-2	0	3	1

Mix design results showed that the aggregate had 100 percent crushed materials, a cleanness value of 84, and LA Rattler test loss of 19 percent at 500 revolutions, all above the Caltrans specification requirements.

The Rice MSG for the ATPB was determined by Contra Costa County to be 2.621. The average of two tests performed by the UCB laboratory was also 2.621.

2.5 HVS TEST SECTION SELECTION

One of the most important factors in any HVS test is selecting a test section that is representative of the whole pavement. The importance of this prerequisite should not be underestimated, as all findings are based on testing of one 1 m by 8 m test section.

Apart from the engineering properties of the pavement, other factors which influence the selection of a particular HVS site include the ability to maneuver the HVS onto the site,

placement of the data acquisition trailer, access to the machine for servicing, and the ability for refueling equipment to reach the various fuel tanks on the HVS.

As noted earlier, the first series of HVS tests is designed to quantify and compare the structural performance of drained and undrained pavements designed according to the Caltrans methodology. For these tests four HVS test sites were required, two within each of the two pavement design sections.

In order to do comparative tests it is important that all four HVS test sites meet the necessary requirements for uniformity to the greatest degree possible. These include uniformity in:

- asphalt concrete
  - gradation
  - asphalt content
  - air-void content (compaction)
- unbound materials
  - aggregate type
  - compaction
- layer thickness
- subgrade structural behavior
- structural behavior of the whole pavement system, within each test section

Steps taken to ensure and to determine uniformity are discussed below.

2.5.1 Asphalt Concrete

During various stages of the paving process, samples of the hot-mix were evaluated in terms of the relevant characteristics mentioned above. All samples tested met Caltrans requirements. As noted earlier, nuclear density measurements were made across the entire test sections (at 4.3 m [14 ft] longitudinal and 2.6 m [8.5 ft] transverse intervals). In addition, cores were taken at several locations, primarily in the transition zone between the sections, to confirm

the nuclear density measurements. All tests indicated uniform compaction across the test sections. The difference in density between the two asphalt concrete lifts is perfectly acceptable because it occurs uniformly throughout the sections.

2.5.2 Unbound Materials

The existing subgrade met Caltrans density requirements without additional compaction. The existing subbase material was reworked, graded, and compacted to the specified layer thickness and density. The base layer was constructed using imported aggregate. All layers met Caltrans specifications for density. To ensure uniform layer thickness, levels were checked, as noted earlier, at 4.3 m (14 ft) longitudinal and 1.6 m (5.1 ft) transverse intervals.

The subbase does not have uniform thickness throughout the test sections, because the 0.75 percent transverse cross-slope was obtained by grading the subbase, and because of a somewhat thicker existing subbase at the south end of the fog chamber (undrained section). The effects of the non-uniform subbase thickness on predicted fatigue life have been analyzed (Chapter 6).

2.5.3 Structural Behavior

Elastic surface deflections were used to ensure uniformity in structural behavior of the pavement system as a whole for the paired test sites in each section. Surface deflections from Heavy Weight Deflectometer (HWD) loading were measured on all structural layers during all stages of construction.

Based on this information, four test sections were selected and marked. The CALHVS1 test plan (Appendix A) provides a full description of the individual tests, test sequence, and test

instrumentation. Graphical presentation of the final set of surface deflections (atop the AC layer), together with the selected four HVS test sites can be seen in Figure 2.4. A summary of the average deflections on the selected HVS test sites can be seen in Table 2.13. The general locations of the sections are shown in Figure 2.5.

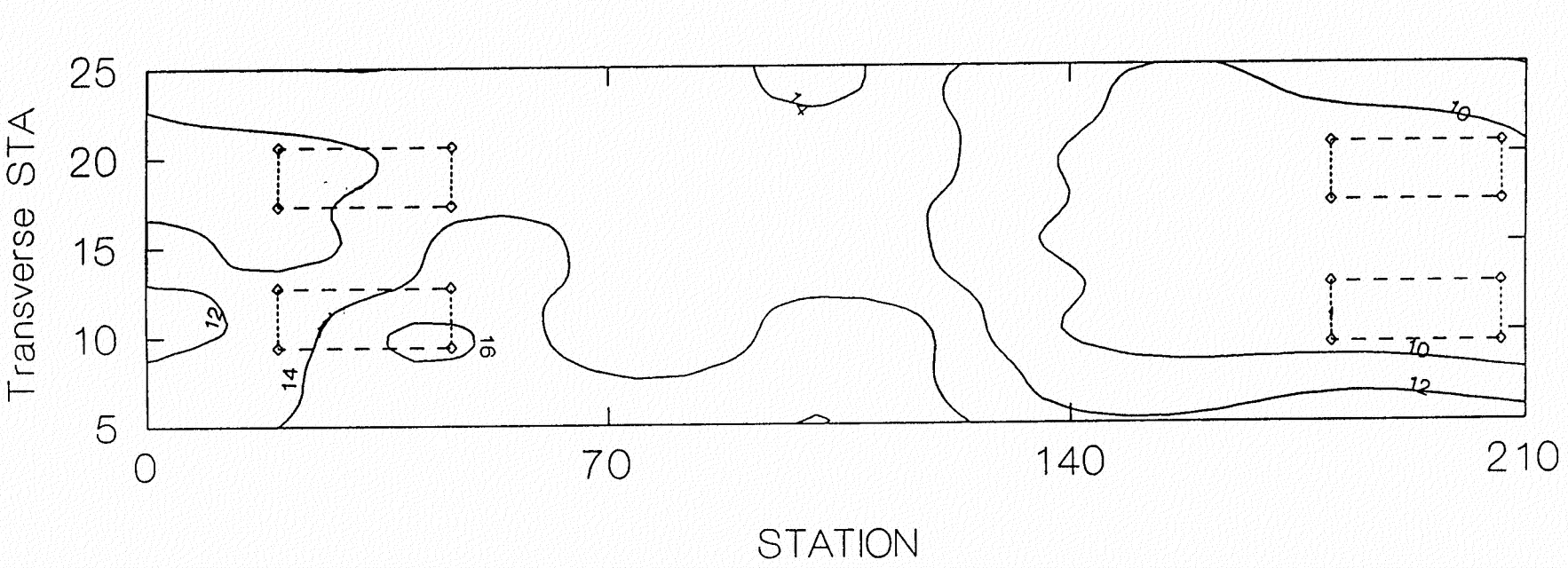

Figure 2.4 Location of Sites and Surface Deflections

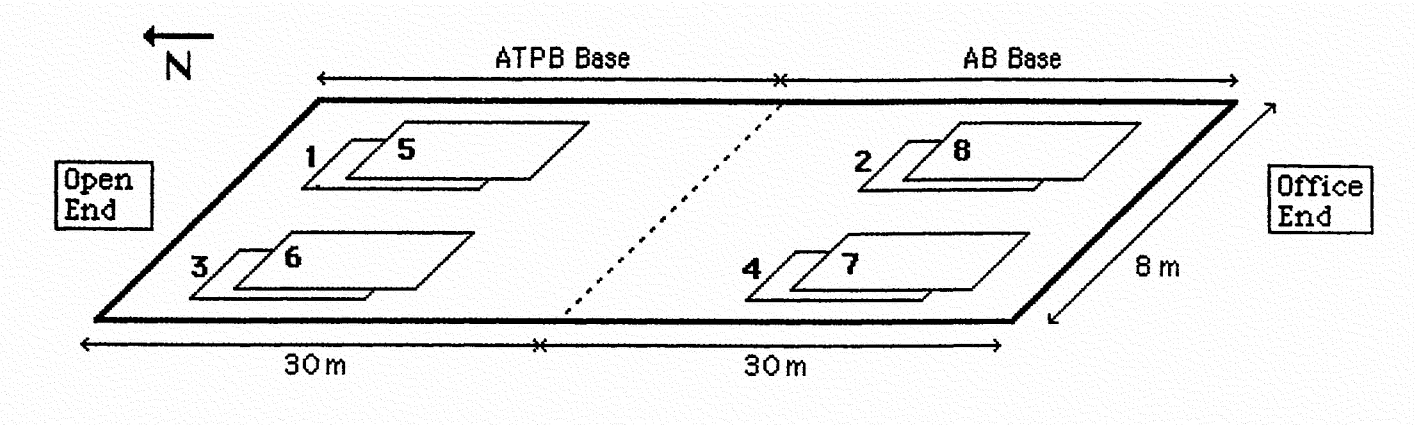

Figure 2.5 Layout of Test Sections

Table 2.13 Average HWD Deflections of the HVS Test Sections

Section Type:		ATPB Sections		AB Sections	
Test Number:		500RF	502RF	501RF	503RF
Deflection (mm)	Average	0.254	0.247	0.358	0.313
	80th Percentile	0.282	0.271	0.425	0.354

As was expected, the surface deflections on the undrained (AB) sections are larger that those measured on the drained (ATPB) sections.

CHAPTER 3

INSTRUMENTATION AND INTERIM RESULTS FOR CALHVS1 TEST 500RF

3.1 INTRODUCTION

The first test with CALHVS1, involving a drained pavement section (500RF), was initiated at the Richmond Field Station on May 3, 1995. This chapter presents some of the results obtained through August 1995. At that time, the test loading history included 150,000 repetitions of 40 kN (9,000 lb) loading, 50,000 repetitions of 80 kN (18,000 lb) loading, and 1,059,484 repetitions of 100 kN (22,500 lb) loading. Loading, simulating a half axle, is applied through a dual-tire assembly.

The purpose of this chapter is to:

- Describe each measurement instrument used during the first CALHVS1 test, including its purpose and the principles on which it relies,
- Show typical outputs, and
- Report the latest measurements.

Various instruments are used to monitor the behavior and performance of an HVS test pavement. Described in this chapter are instruments for monitoring both elastic and inelastic pavement response. The elastic response at the surface under various test loads is measured with the Road Surface Deflectometer (RSD), and the in-depth elastic deformations with the Multi-

Depth Deflectometer (MDD). The inelastic response (permanent deformation) is measured on the surface with the Laser Profilometer, and the in-depth permanent deformation of the various pavement layers is measured with the MDD.

Since temperature has a significant influence on the stiffness of the mix, thermocouples are used to monitor surface and in-depth pavement temperatures.

Although over 1.2 million load repetitions had been applied to the test pavement through August, the objective of this chapter is not to provide a full analysis of the results from the various instruments but only to show the type of data currently being collected. Analysis to date has been preliminary: complete analysis must wait until testing has been completed. Additional data, such as the changes in air-void content of the asphalt concrete layer and visual analysis of test-pit excavations, are necessary to provide complete understanding of the behavior of the test section.

A black deposit on the test section is currently being analyzed. Results will be included in a subsequent report.

3.2 INSTRUMENTATION AND MONITORING METHODS

The HVS test site consists of a 1 m by 8 m loading area. The test wheel travels the full length of the site and moves transversely on succeeding passes to eventually cover the full 1 m width. This action simulates the natural wandering effects of traffic within a road lane of normal width.

The 8 x 1 m site is divided longitudinally into 16 one-half meter intervals, and measurement locations or "points" are labeled from 0 to 16. Data are collected on the centerline and at 200 mm on either side of the centerline. This is illustrated in Figure 4 of Appendix A.

The instrumentation and monitoring methods used during CALHVS1 test 500RF are the following:

- Laser profilometer,
- Multi-depth deflectometer (MDD),
- Road surface deflectometer (RSD),
- Thermocouples, and
- Visual inspections and crack growth monitoring.

3.2.1 Laser Profilometer

The laser profilometer is used to measure the permanently deformed transverse profile of the test section surface. This output allows the determination of surface rut depth and its progression.

Description. The laser profilometer includes a 3 meter long frame which is positioned over the width of the test section at specific locations. A laser device, attached to the frame, moves transversely over the width as it scans the pavement surface. The surface profile is then generated by measuring the distance between the laser head and the road surface at 9 mm intervals. The accompanying data acquisition software applies the corrected offset value to ensure that the reported values are representative of actual rutting.

Results. Figure 3.1 illustrates the average rut depth and the average maximum rut depth as measured from 16 cross-sections along the test section. This figure shows that at the beginning of HVS traffic at 40 kN the rut depth increased quickly and then stabilized after about 50,000 load repetitions. The quick increase in the rut depth after the initial application of load is known as the imbedding phase. A similar imbedding phase can be seen when the load was increased to 80 kN and when it was increased again to 100 kN. The rut depth continued to increase after a million repetitions, and, at 1,259,484 repetitions (August 26, 1995), the average maximum rut depth was approximately 13 mm. At this time the average rut depth across the full 1 m cross-sections at the 16 locations exceeded 9 mm.

Figure 3.2 illustrates the transverse cross-section of the test section at the position of maximum rut depth, Point 15. The maximum rut depth along the cross-section at this location is approximately 17.5 mm. Changes in the transverse cross-section as the test progresses can be seen on the figure. Shaded areas represent locations outside the 1 m test section. The movement of material on the edges of the test section, due to lateral shoving, is clearly illustrated.

3.2.2 Multi-depth Deflectometer

Two MDDs were installed in the pavement to allow measurement of both elastic deflection and inelastic deformation at in-depth positions. The modules are normally placed at layer interfaces or at other critical depths in the pavement structure: Figure 3.3 shows their locations for test section 500RF.

Output from the MDDs reveals influence lines for elastic deflection and/or inelastic deformation at specific depths through time. The behavior of individual pavement layers can be determined through calculations. MDD measurements can be used to:

- characterize the behavior of the whole pavement system, in terms of the elastic and inelastic response of the various pavement layers;
- monitor changes in the stiffnesses of the various layers in the pavement with time;
- backcalculate effective elastic moduli (stiffnesses) of the various layers;
- determine stress dependency of pavement layers (non-linear elastic behavior); and
- determine the permanent deformation (compression) of all pavement layers.

Only the last use for the MDD measurements has been analyzed fully to date. The second use can be seen from the deflection data presented herein, but the data have not yet been fully analyzed.

Description. The MDD is installed inside a vertical hole drilled into the pavement. It consists of five Linear Variable Displacement Transformer (LVDT) modules, which are installed at critical depths in the pavement as shown in Figure 3.3. An anchor rod is fixed rigidly at a depth of 3 meters, and a slug which runs through the centers of the various MDD modules is connected to the anchor. Each MDD module records the movement (elastic and inelastic) of the pavement layer to which it is rigidly attached, relative to the anchor. MDD deflections under various wheel loads are collected periodically throughout an HVS test (as described in Appendix A).

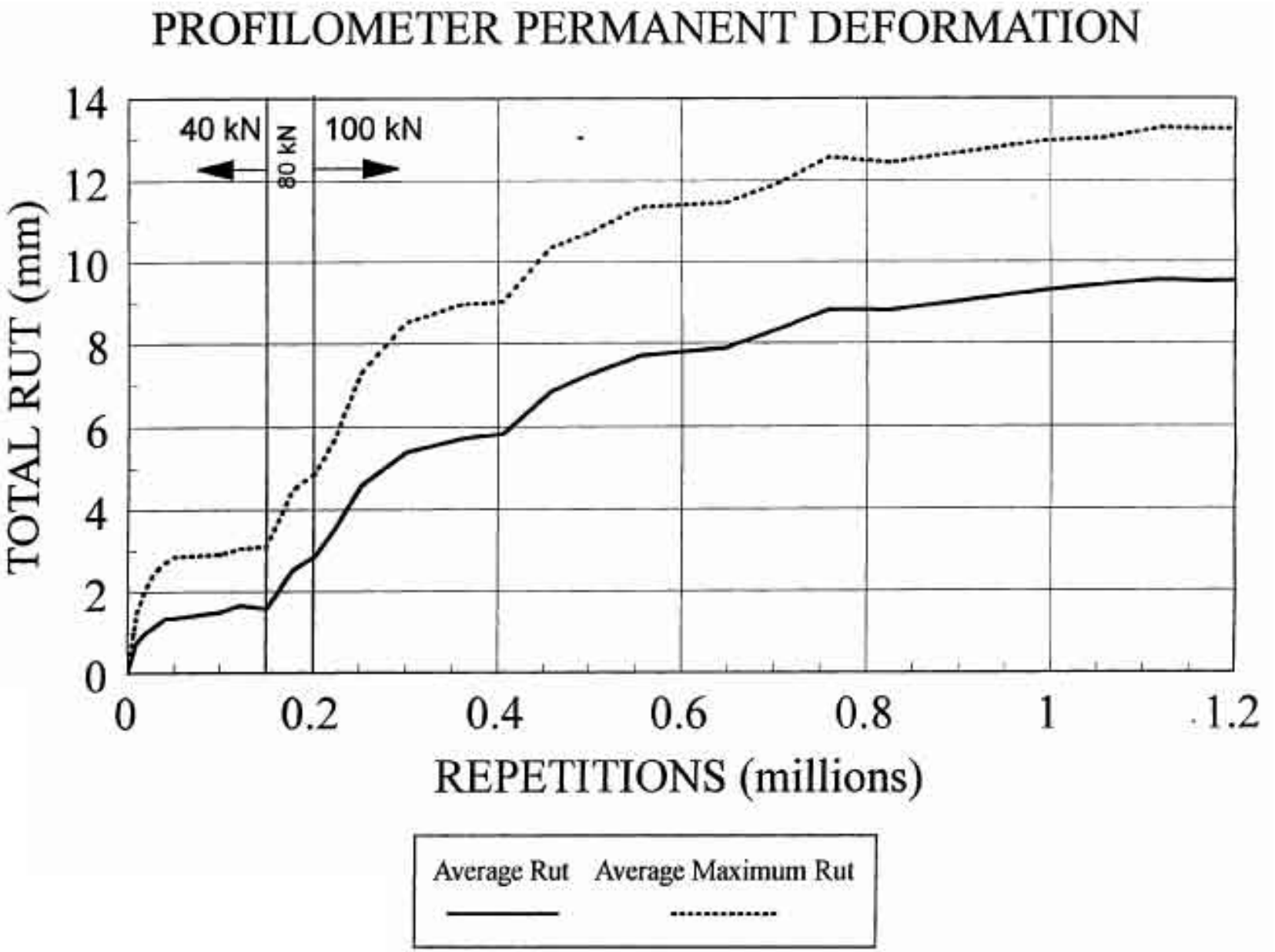

Figure 3.1 Average Rut Depth

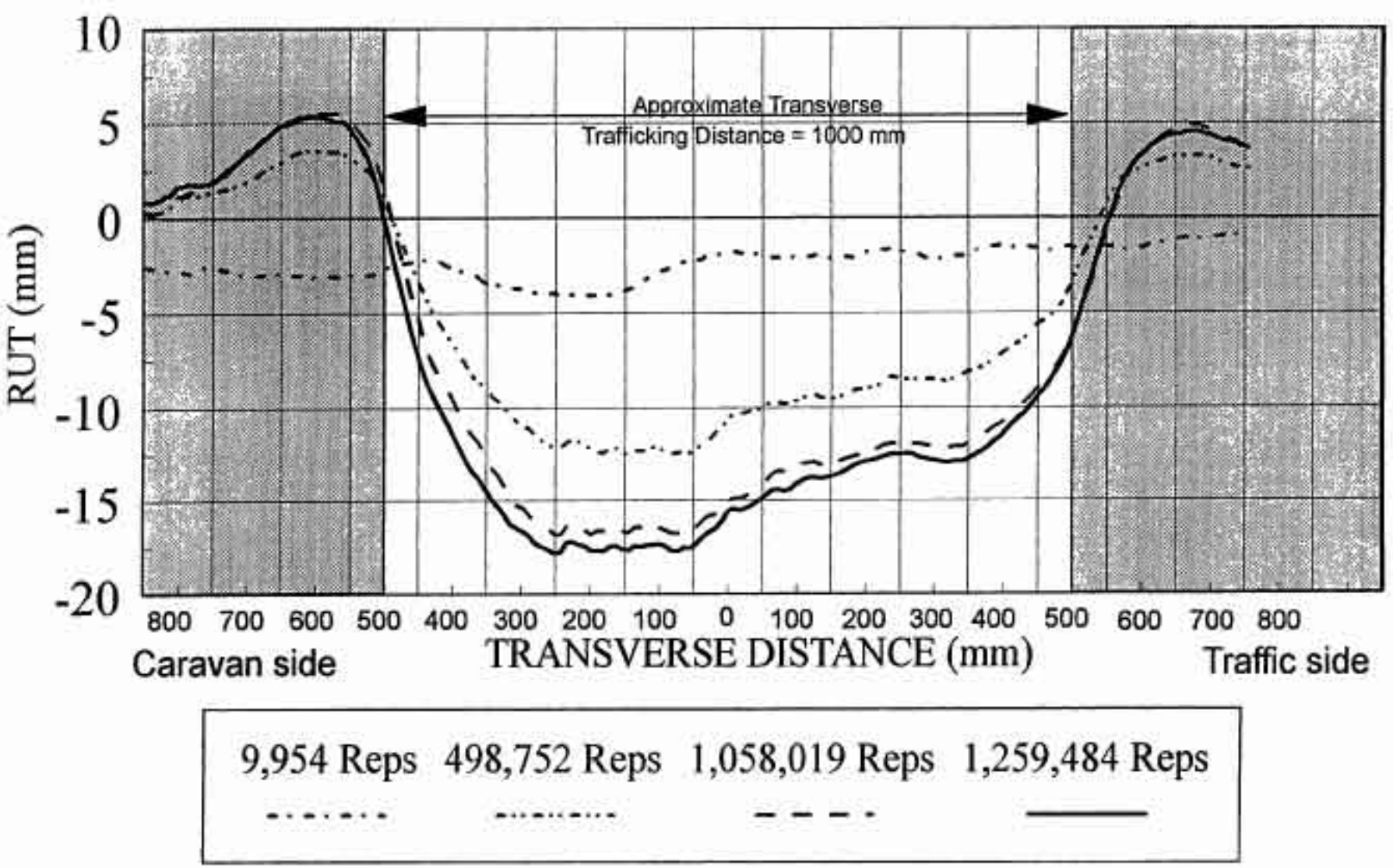

Figure 3.2 Transverse Cross Section at Point 15

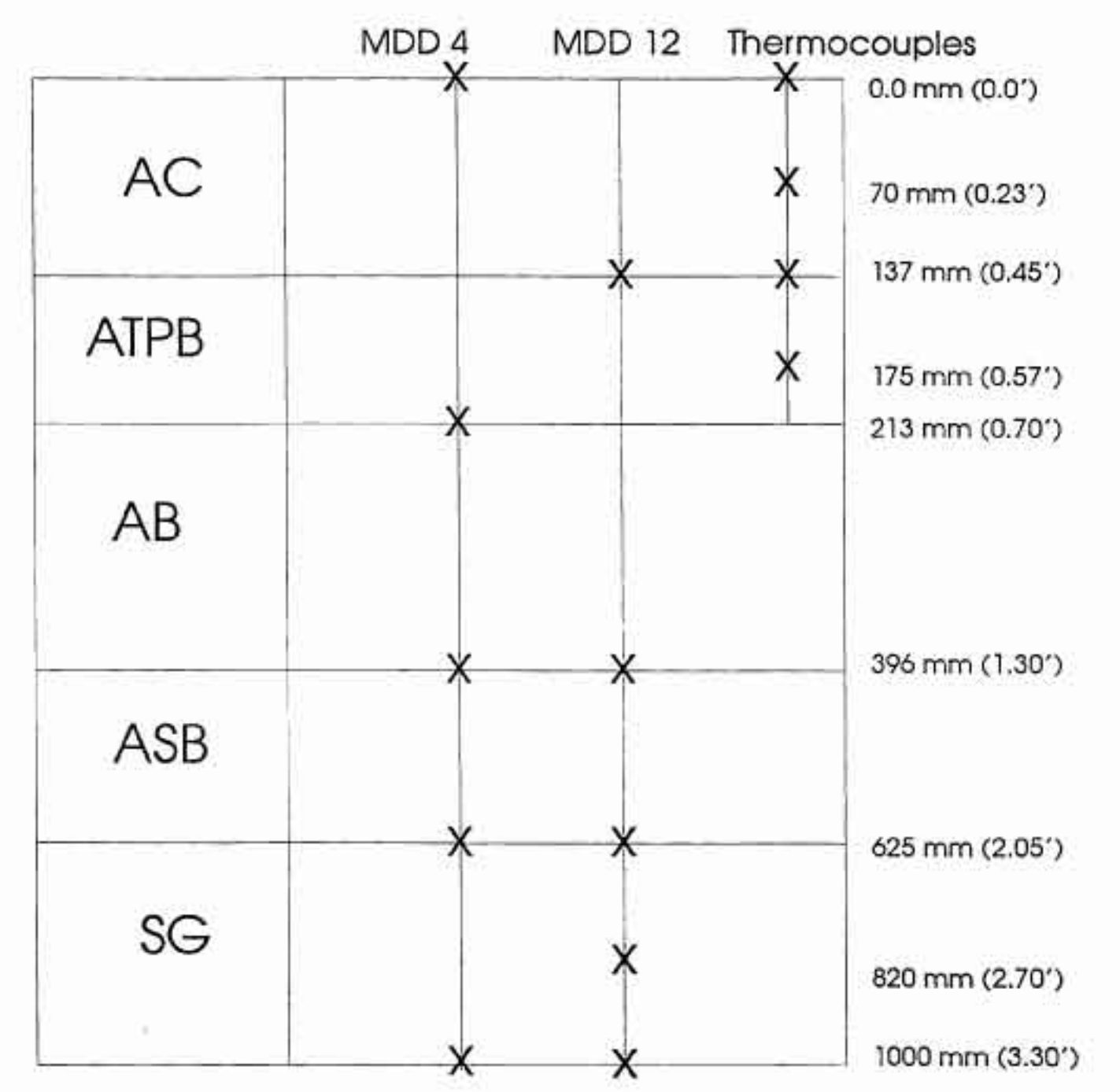

Figure 3.3 MDD and Thermocouple Positioning

Results. Only the elastic and inelastic responses of the various pavement layers are reported herein: further analysis of the MDD data will be included in a subsequent report. Figures 3.4 and 3.5 show how elastic deflections at MDD4 and MDD12 under measurement loads of 40 and 100 kN change with increasing repetitions of the 40 kN, 80 kN, and 100 kN test loading sequence. Data analysis is continuing and will be completed at the end of the HVS testing. However, these preliminary data show that the elastic deflection is increasing as the test progresses. The test load--it should be emphasized--was increased to 100 kN following 200,000 repetitions of 40 and 80 kN loads.

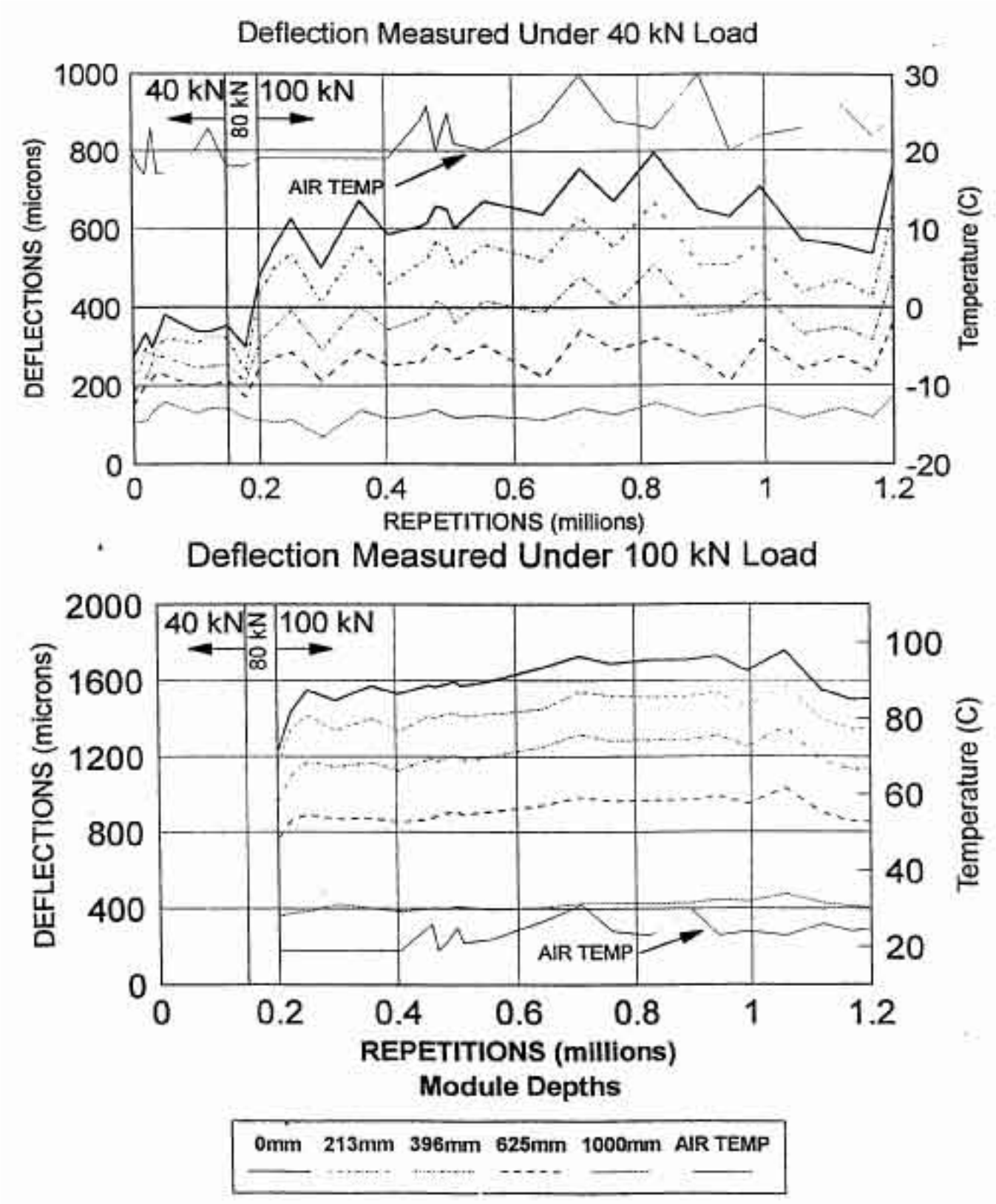

Figure 3.4 Elastic Deflections at MDD4 (40 kN and 100 kN Measurement Loads)

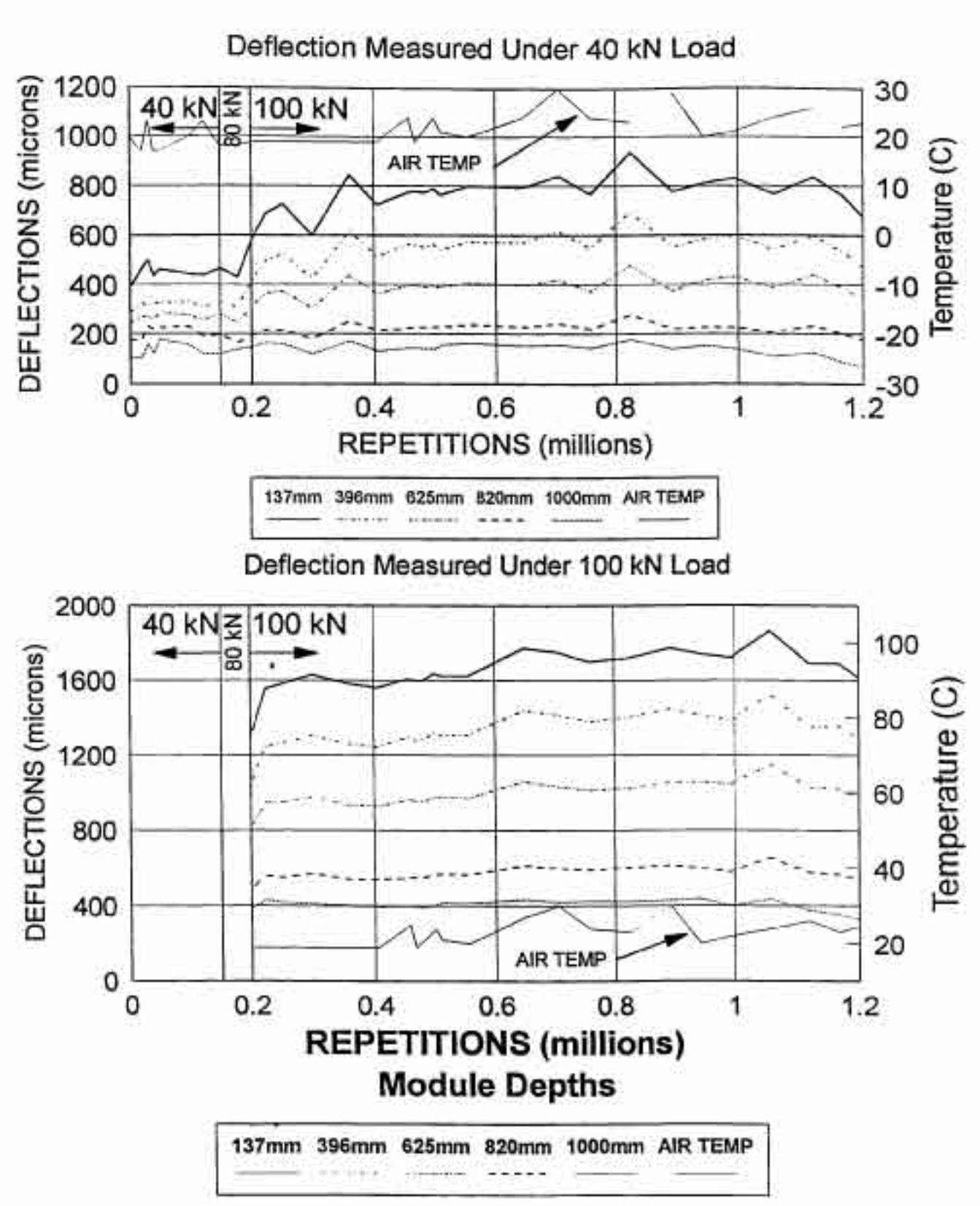

Figure 3.5 Elastic Deflections at MDD12 (40 kN and 100 kN Measurement Loads)

Figure 3.6 illustrates the permanent deformations recorded by the in-depth modules of MDD4 and MDD12. Due to technical difficulties, these permanent deformations were not recorded until after 200,000 load repetitions. The line plotted on Figure 3.6 for the surface module of MDD4 up until 200,000 repetitions was determined from the surface rutting measured by the laser profilometer.

From the data collected, the percentage of permanent deformation in each layer at MDD4 was calculated. These percentages, in addition to the total deformation found from the profilometer, were used to determine the permanent deformation of levels 2 to 5 at MDD4. The permanent deformation of MDD12 was determined using the data from MDD4 matching those levels that are the same in MDD4 and MDD12. It must be emphasized that the information presented here, estimated from available data, only gives an indication of the expected distribution of permanent deformation within each layer. The permanent deformation estimates have no effect on the elastic deflections, and all elastic deflection data were recorded as measured.

The permanent deformations of all layers are superimposed on Figure 3.7. From the data, estimates of the percentage of the total permanent deformation within each layer after 1,259,488 load repetitions (August 26, 1995) are shown in Table 3.1.

Table 3.1 Percentage Permanent Deformation in Each Layer

Layer	Asphalt Concrete	ATPB	Aggregate Base	Aggregate subbase	
% Deformation	42	30	15	8	5

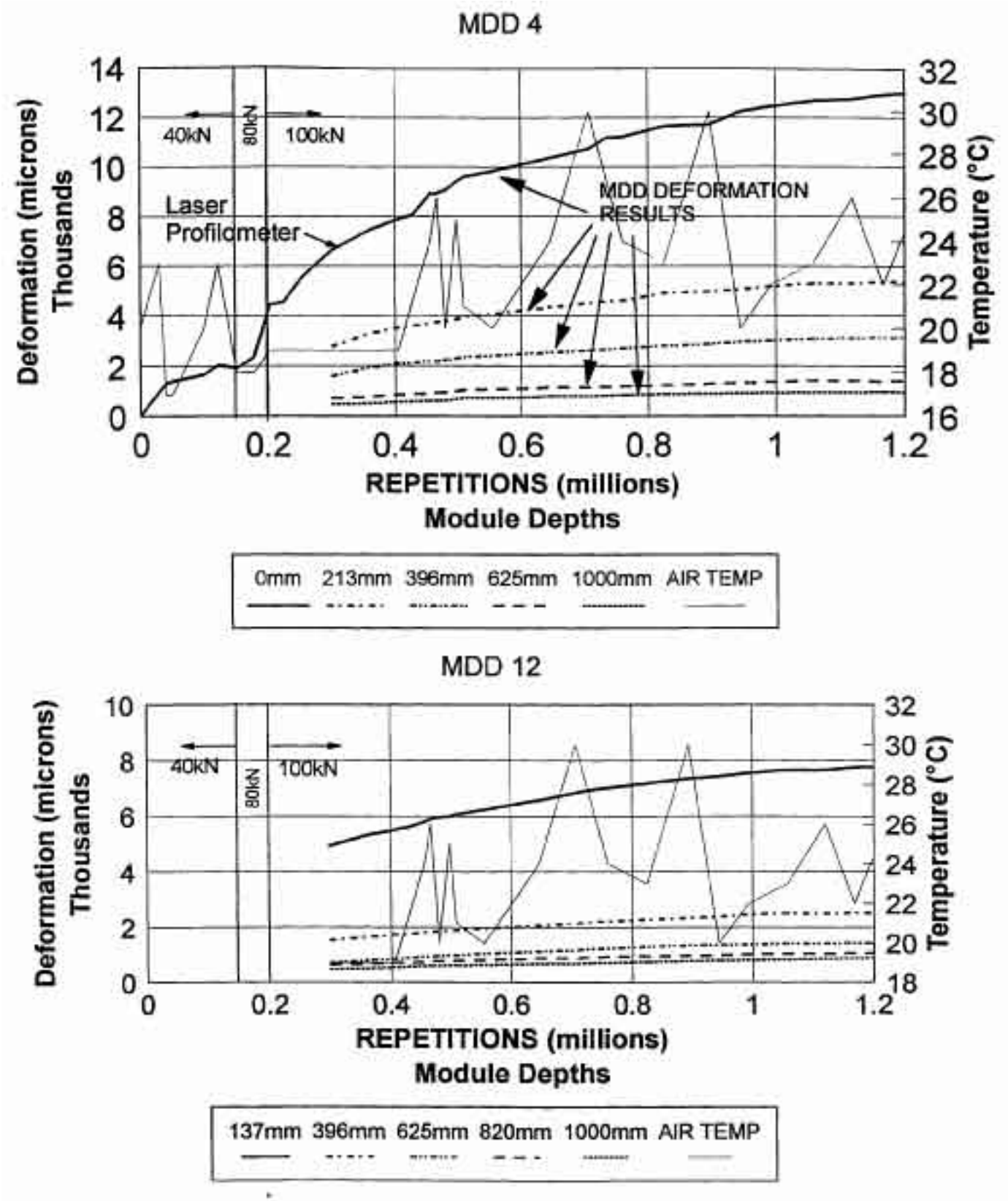

Figure 3.6 Permanent Deformation at MDD4 and MDD12

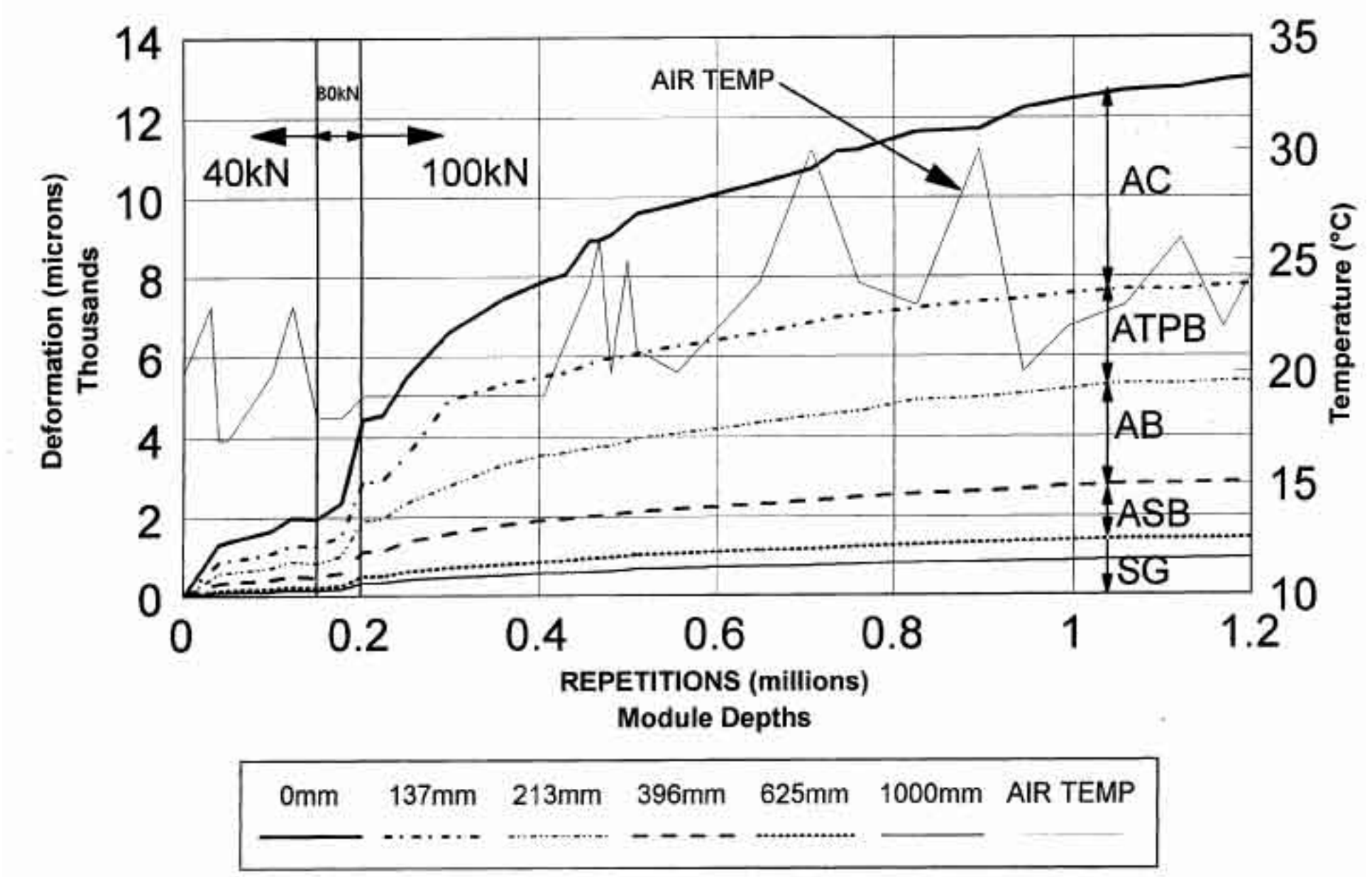

Figure 3.7 Average Layer Deformation

3.2.3 Road Surface Deflectometer

The road surface deflectometer (RSD), a modification of the Benkelman Beam, measures the elastic surface deflection of a pavement under the action of a wheel load. The output from the RSD can be used to:

- characterize pavement behavior in terms of its elastic surface deflections;
- backcalculate effective elastic moduli (stiffness);
- monitor changes in the stiffness of the pavement with time; and
- determine stress dependency of pavement layers (non-linear elastic behavior).

Description. The RSD consists of a 3 meter long beam, which is supported on two reference feet at one end. A measuring point is located on the other end. A LVDT is located between these two points. For measurement, the RSD is positioned in such a way that the reference feet stand outside the deflection bowl, and the deflection of the measuring point is measured by logging the movement of the LVDT at fixed intervals of wheel movement. An extensive number of data points (256) are recorded, defining the complete elastic deflection basin produced by the wheel load.

Results. Only the elastic surface deflection is reported at this stage; further analysis with RSD data will be included in a subsequent report. Elastic deflections as measured by the RSD are shown in Figures 3.8 and 3.9 for measurement loads of 40 kN and 100 kN, respectively. The deflections of the centerline when the load passes over the centerline at reference Points 4, 6, 8, 10 and 12 are illustrated. Because deflections are influenced by temperature, the ambient temperature at the time of deflection measurement is also plotted on the graphs. Figure 3.8 shows that the average elastic deflection, excluding Point 12, ranges from about 550 to 700

microns after 1 million repetitions. The elastic deflection at Point 12 exceeded 800 microns (0.8 mm) after 1 million repetitions. The large deflections recorded at Point 12 may indicate an area within the test section of relative weakness.

A similar trend is observed in Figure 3.9 for deflections under 100 kN loading. Under the 100 kN loading the deflections at Point 12 were not noticeably higher than at the other points. Recall that 100 kN loading was not applied as a test load until after 200,000 prior repetitions of 40 and 80 kN loads.

3.2.4 Thermocouples

Thermocouples are used in the HVS test to measure air temperature and pavement temperatures at various depths, including the surface. Because asphalt is a viscoelastic material, temperature has a significant influence on the stiffness of the asphalt concrete layer. Thus, for fatigue and rutting investigations temperature monitoring is vitally important.

Description. K-type copper constant thermocouple wire, together with a hand held monitor, are used to record the temperature data. By installing the wires at the desired depths, the complete temperature profile can be monitored.

Results. Depths of the thermocouples are shown in Figure 3.3. Their locations within the test site can be seen in Figure 4 of Appendix A. During the first test the temperature was recorded regularly. The variance between average daytime and nighttime temperatures is recorded. Figures 3.10 a-g show temperatures 50 mm (2 in) below the surface. Temperatures 137 mm (5.4 in) below the surface are shown in Figures 3.11 a-g. Figure 3.12 a-d shows plots of the temperature at 50 mm (2 in) below the surface during the warmest time of the day.

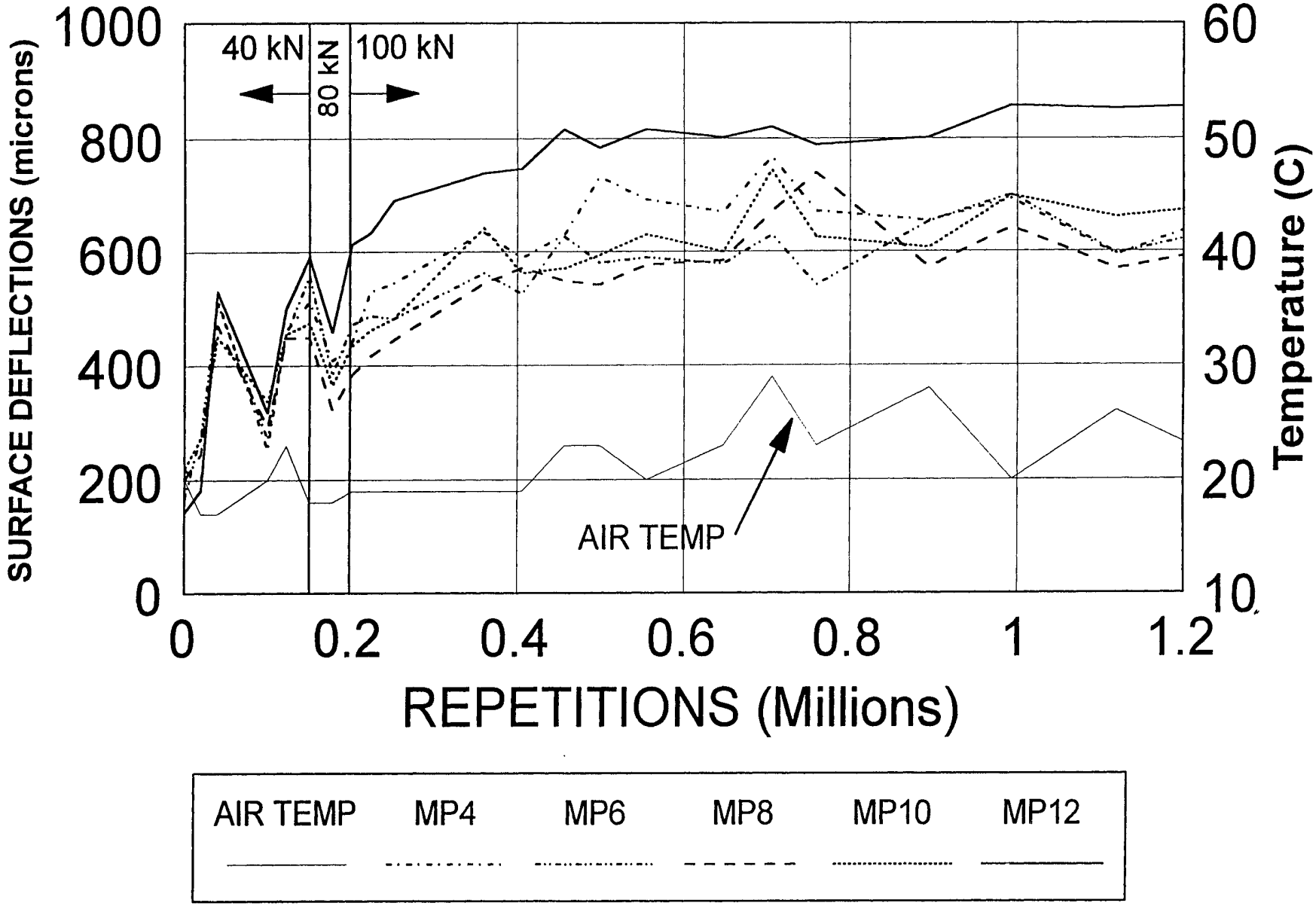

Figure 3.8 Elastic Surface Deflections by Road Surface Deflectometer (40 kN Measurement Load)

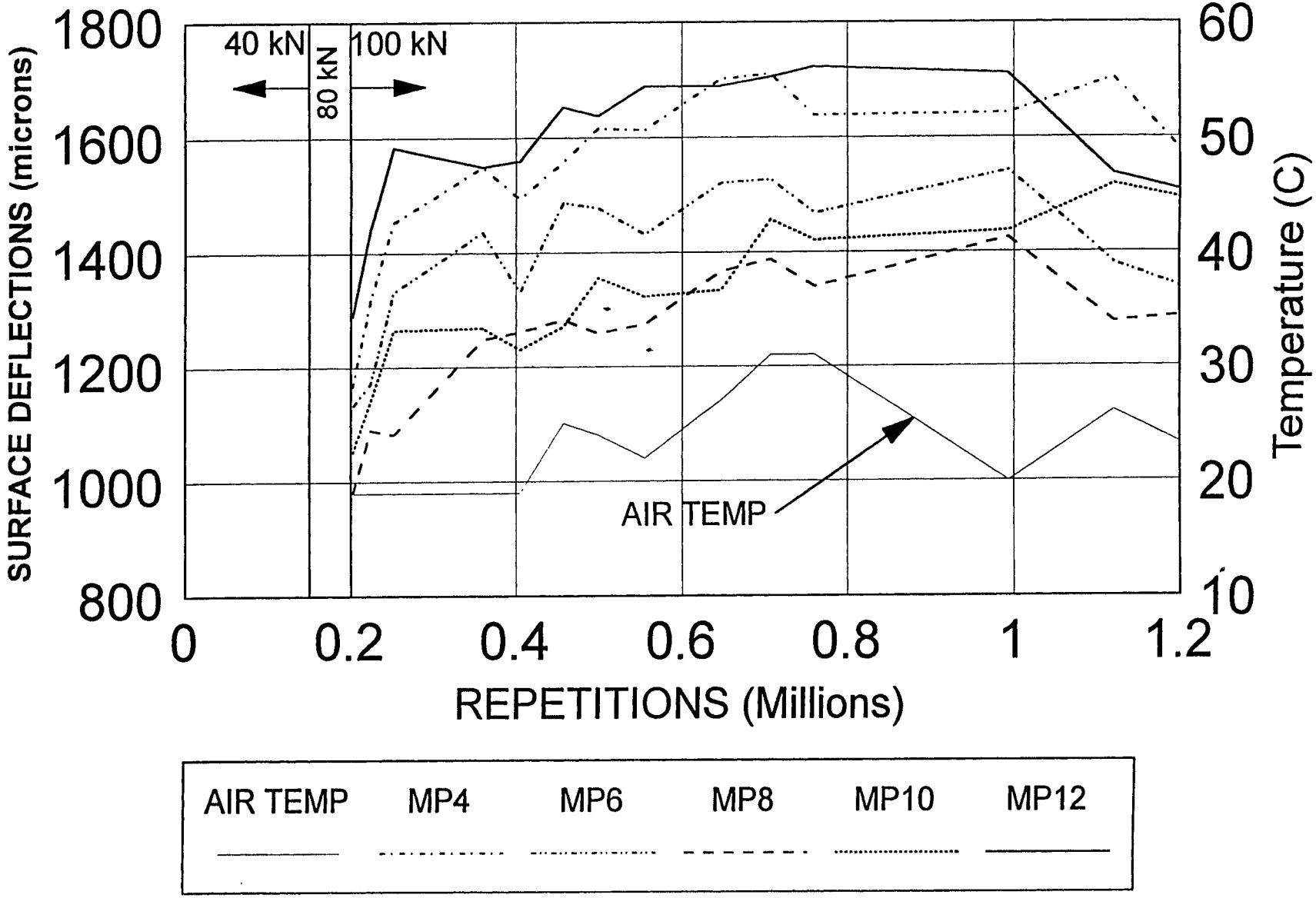

Figure 3.9 Elastic Surface Deflections by Road Surface Deflectometer (100 kN Measurement Load)

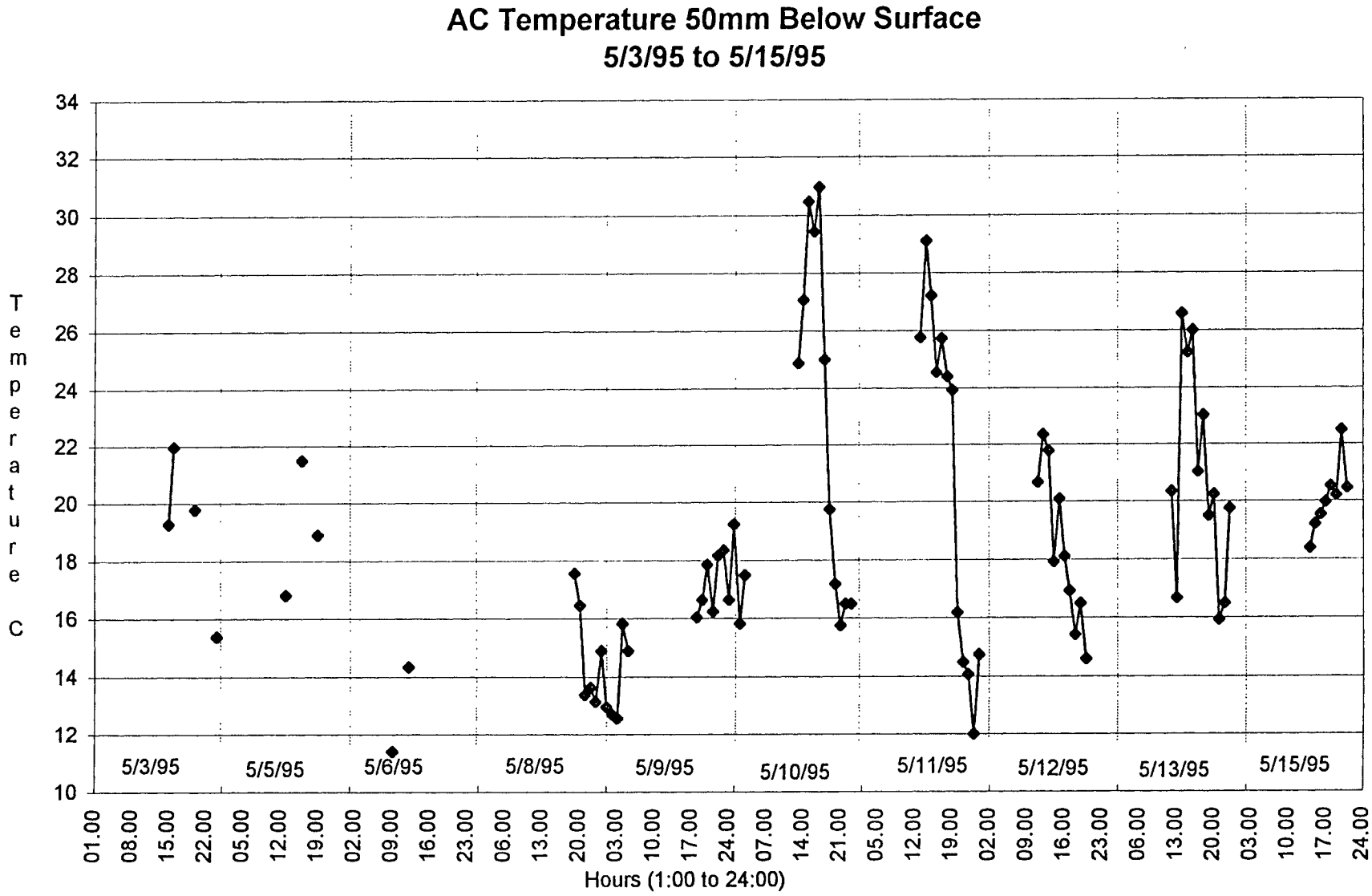

Figure 3.10a Asphalt Concrete Temperature at 50 mm Depth (May 3, 1995 - May 15, 1995)

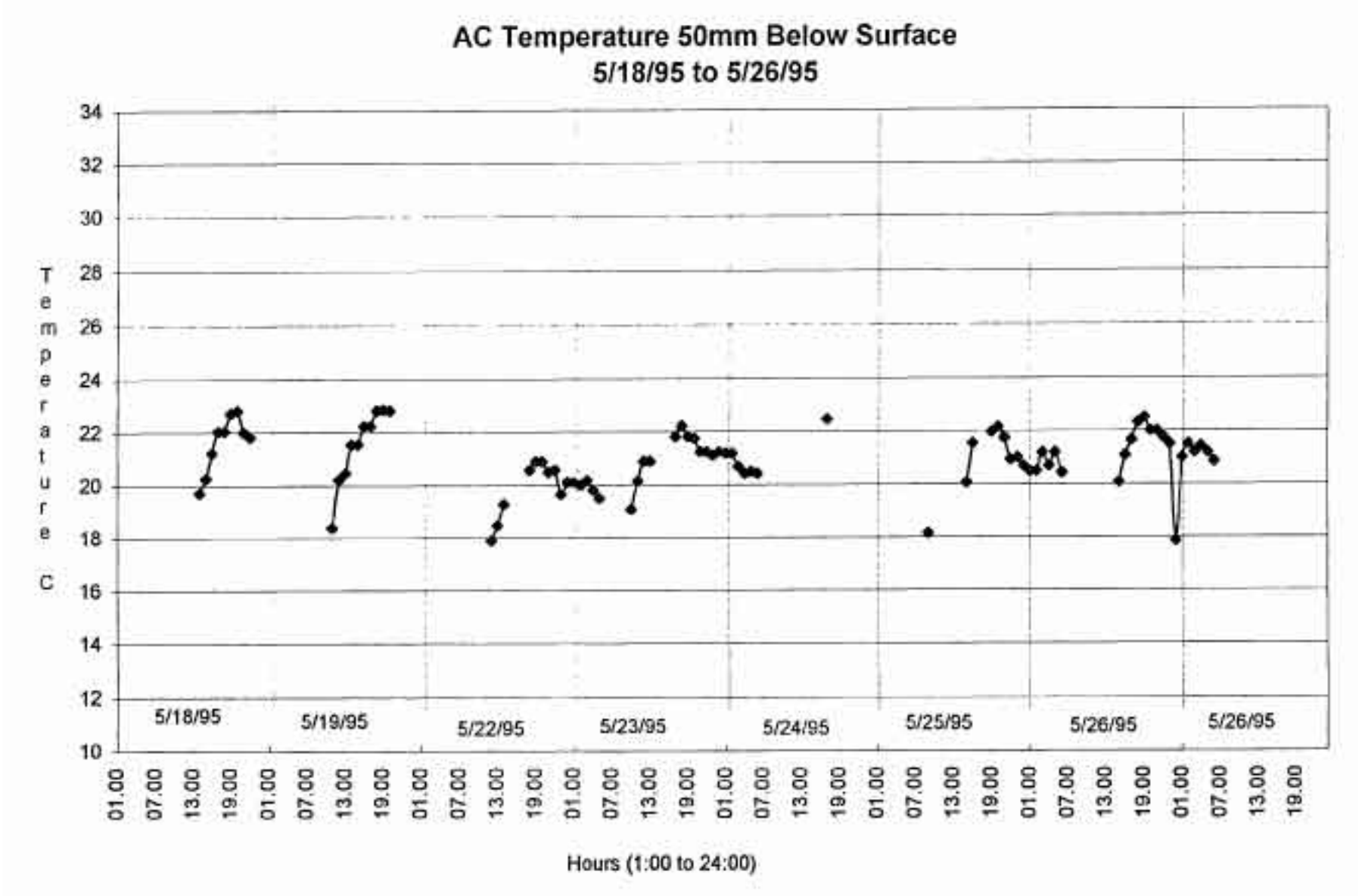

Figure 3.10b Asphalt Concrete Temperature at 50 mm Depth (May 18, 1995 - May 26, 1995)

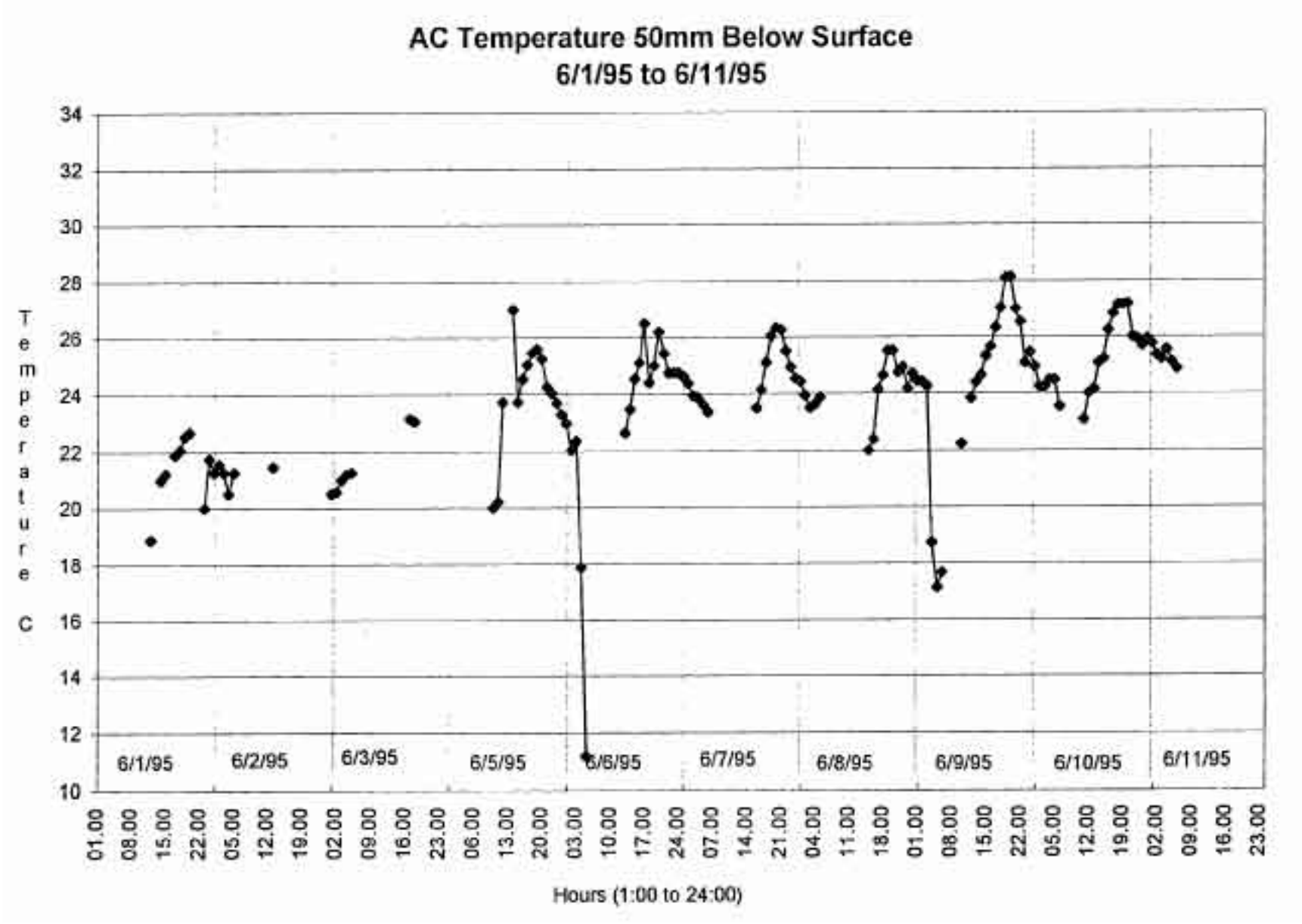

Figure 3.10c Asphalt Concrete Temperature at 50 mm Depth (June 1, 1995 - June 11, 1995)

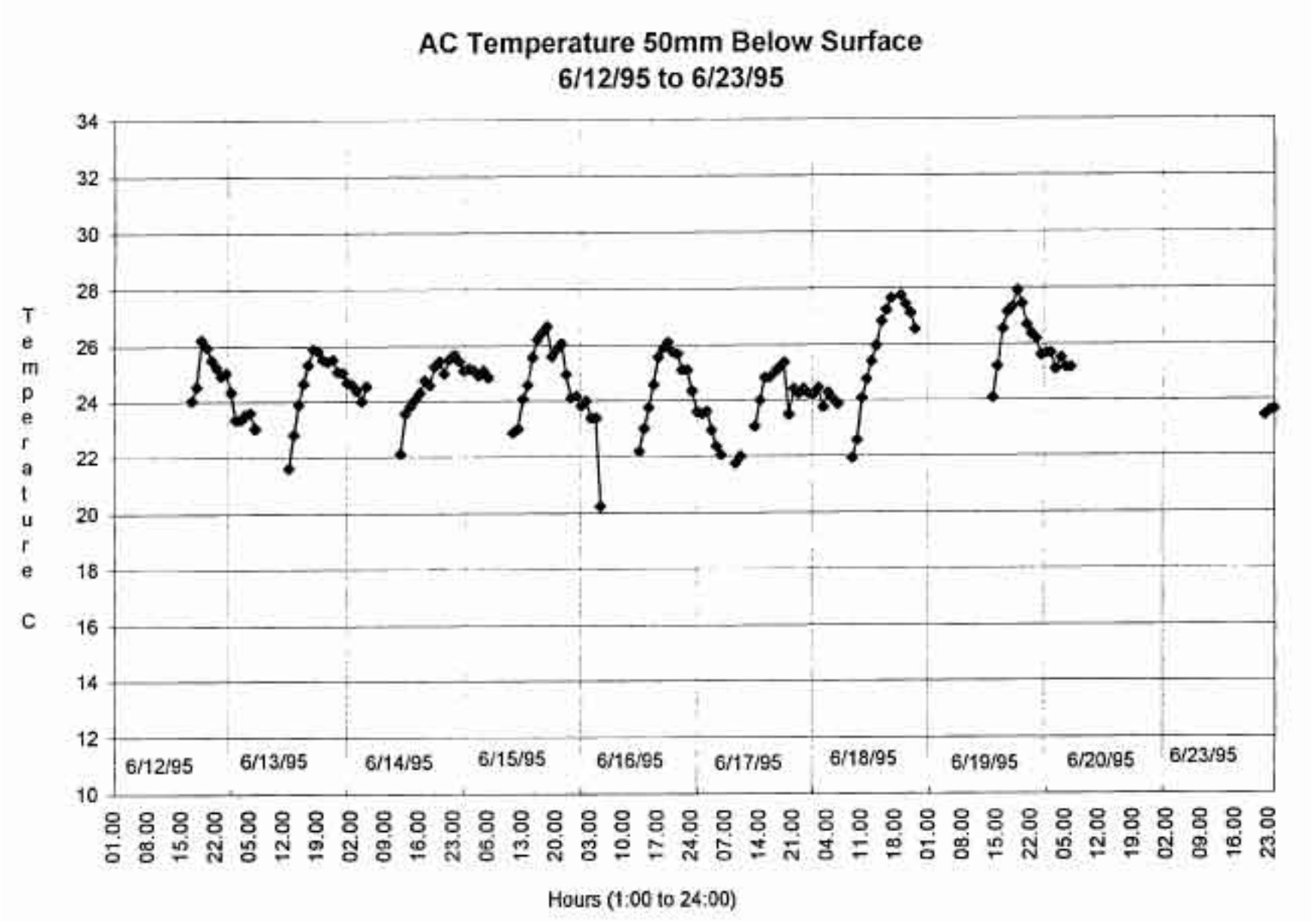

Figure 3.10d Asphalt Concrete Temperature at 50 mm Depth (June 12, 1995 - June 23, 1995)

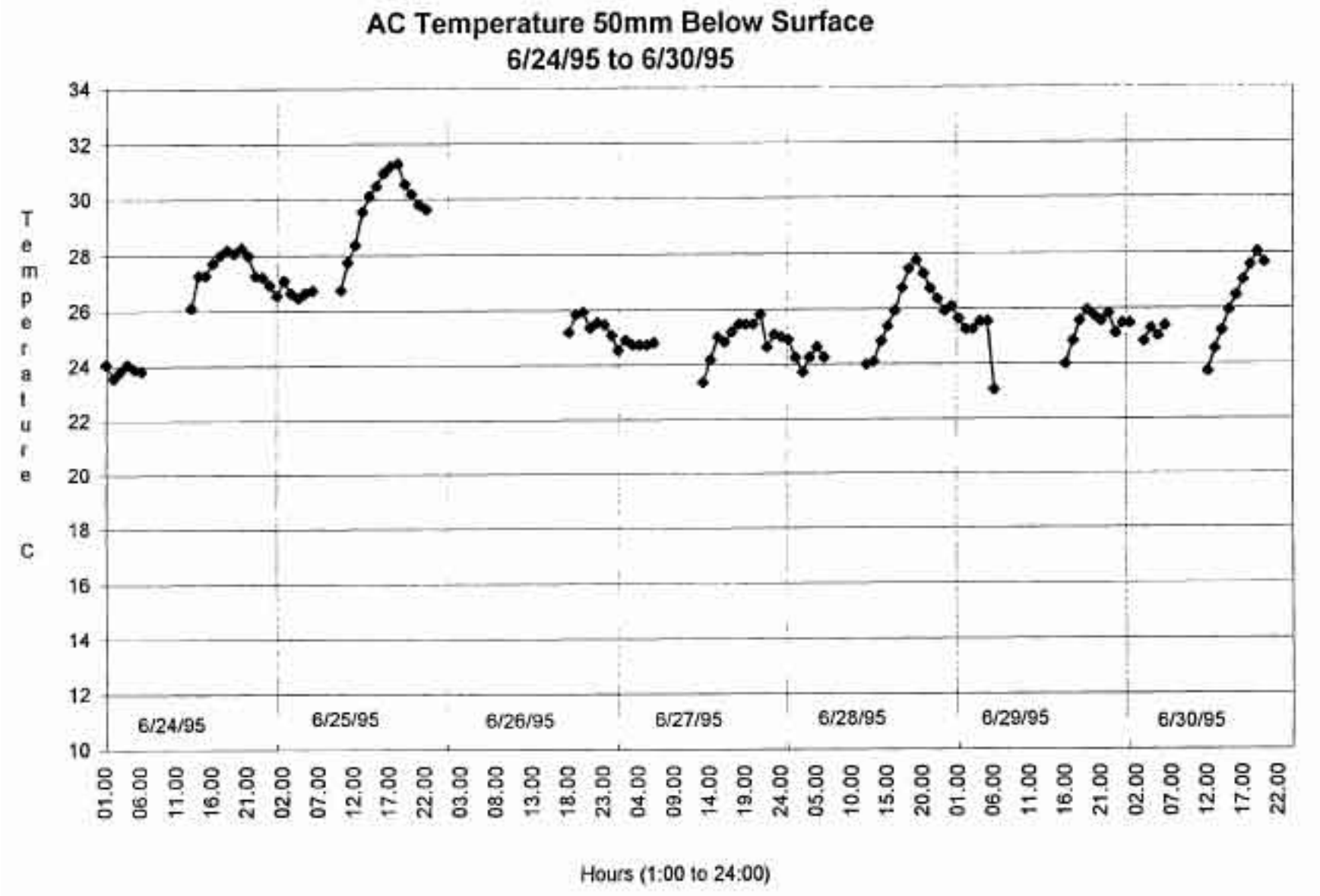

Figure 3.10e Asphalt Concrete Temperature at 50 mm Depth (June 24, 1995 - June 30, 1995)

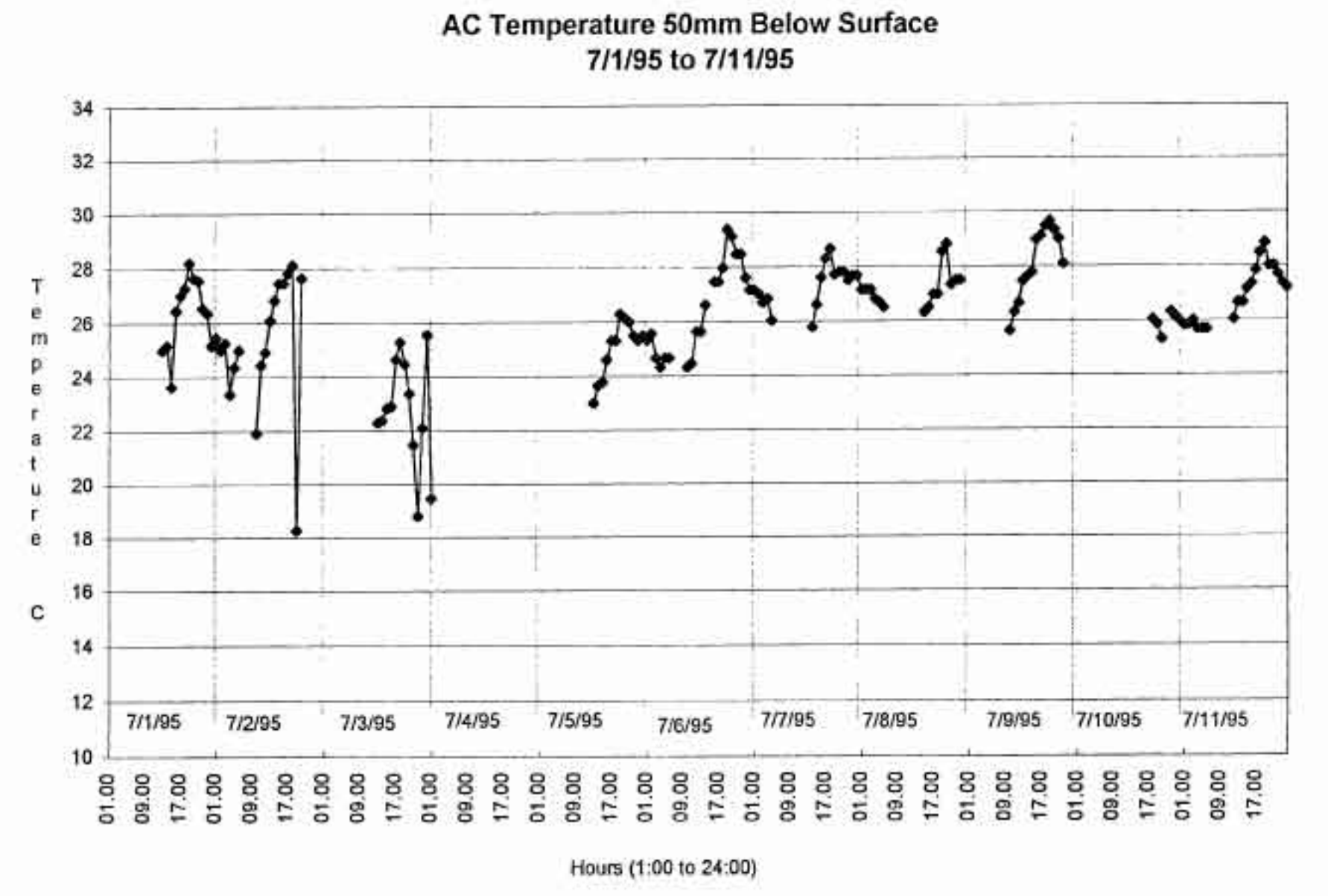

Figure 3.10f Asphalt Concrete Temperature at 50 mm Depth (July 1, 1995 - July 11, 1995)

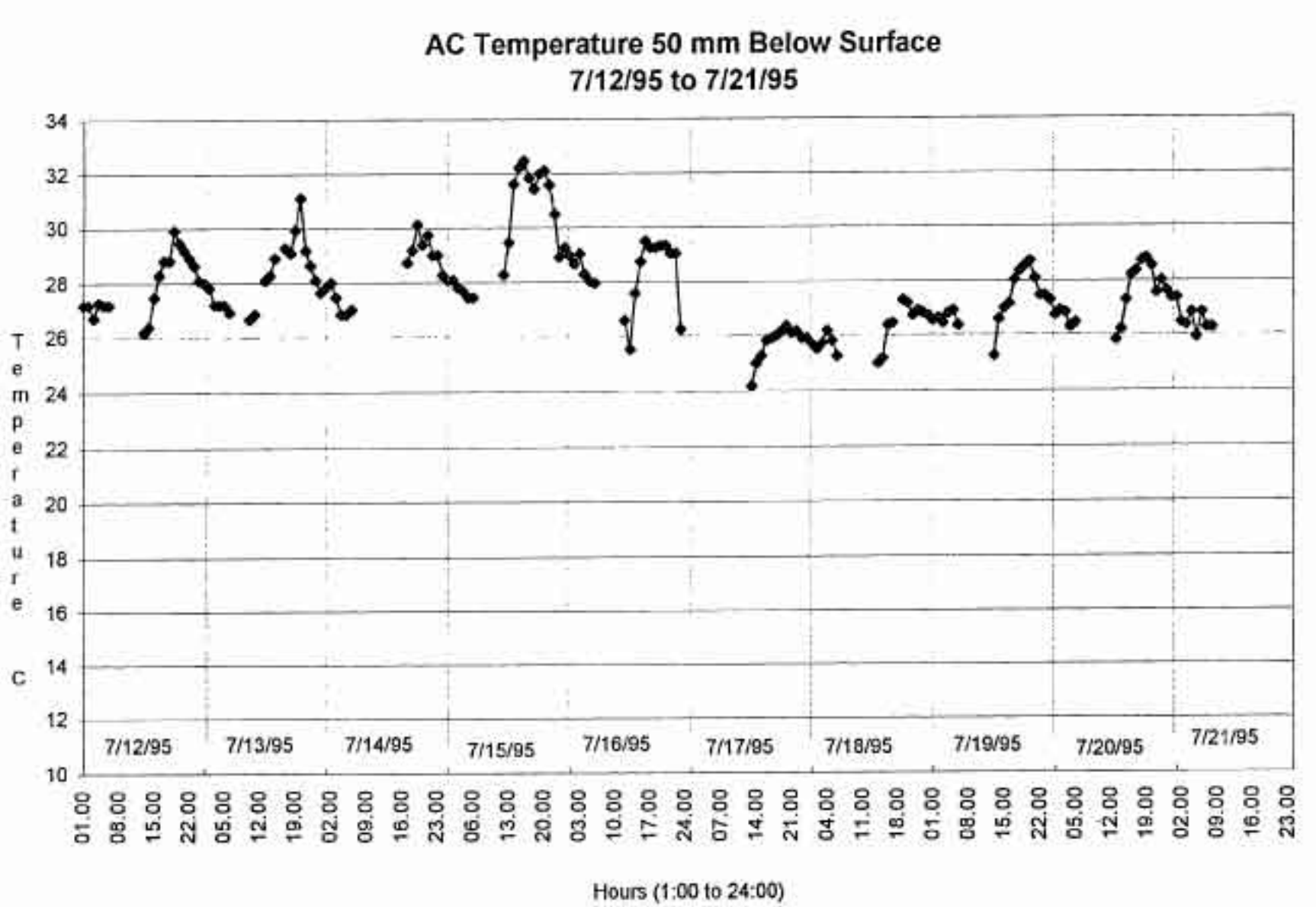

Figure 3.10g Asphalt Concrete Temperature at 50 mm Depth (July 12, 1995 - July 21, 1995)

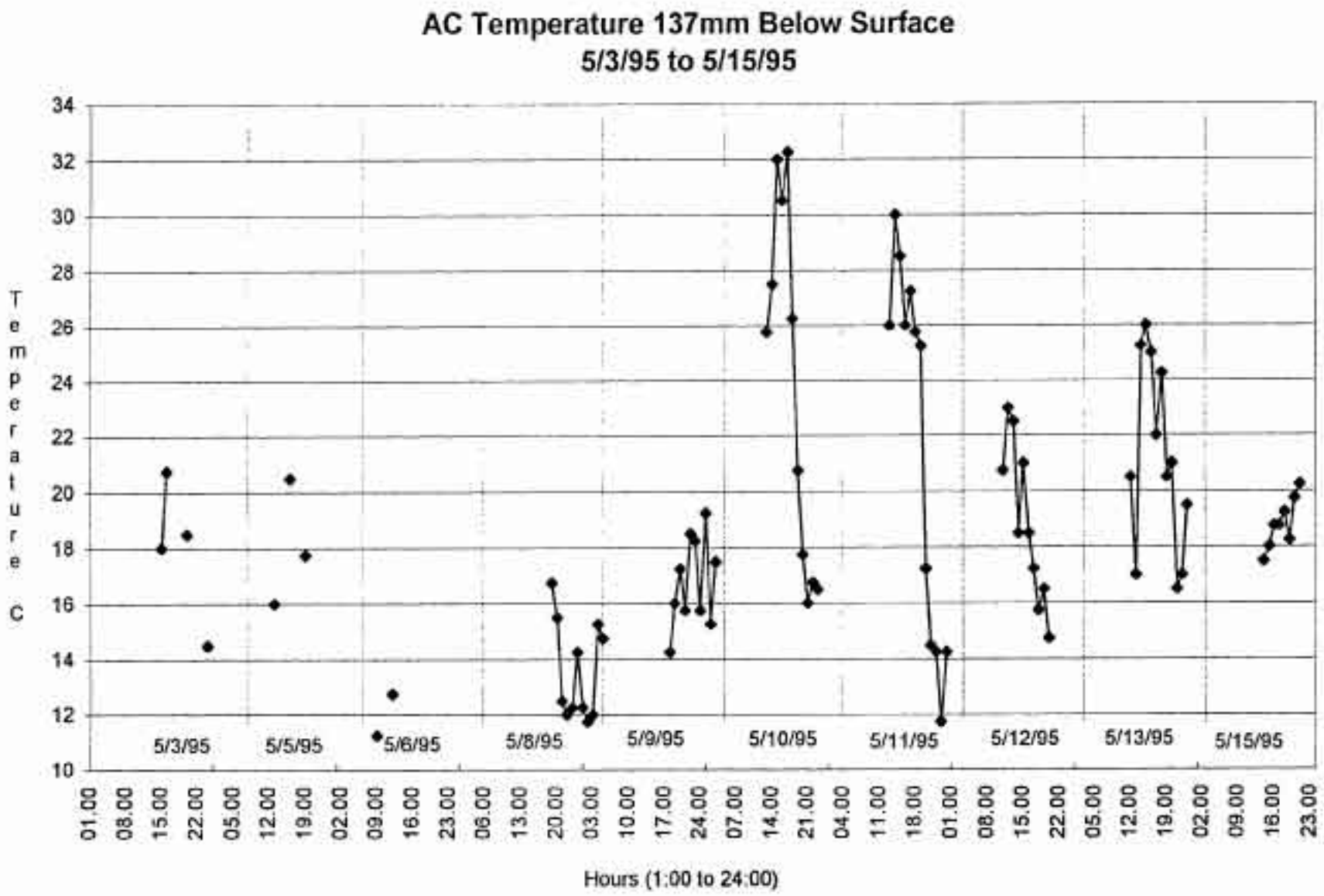

Figure 3.11a Asphalt Concrete Temperature at 137 mm Depth (May 3, 1995 - May 15, 1995)

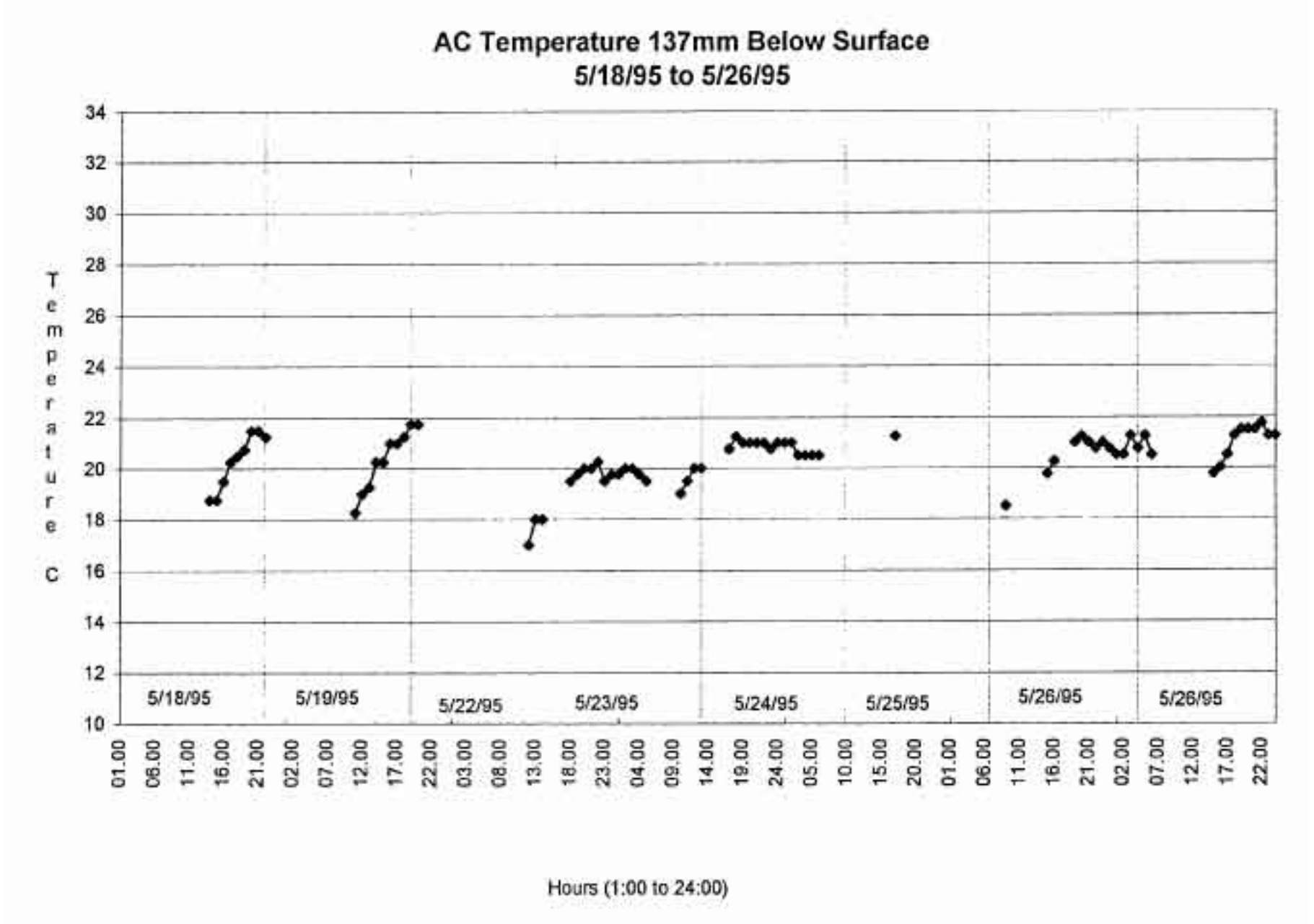

Figure 3.11b Asphalt Concrete Temperature at 137 mm Depth (May 18, 1995 - May 26, 1995)

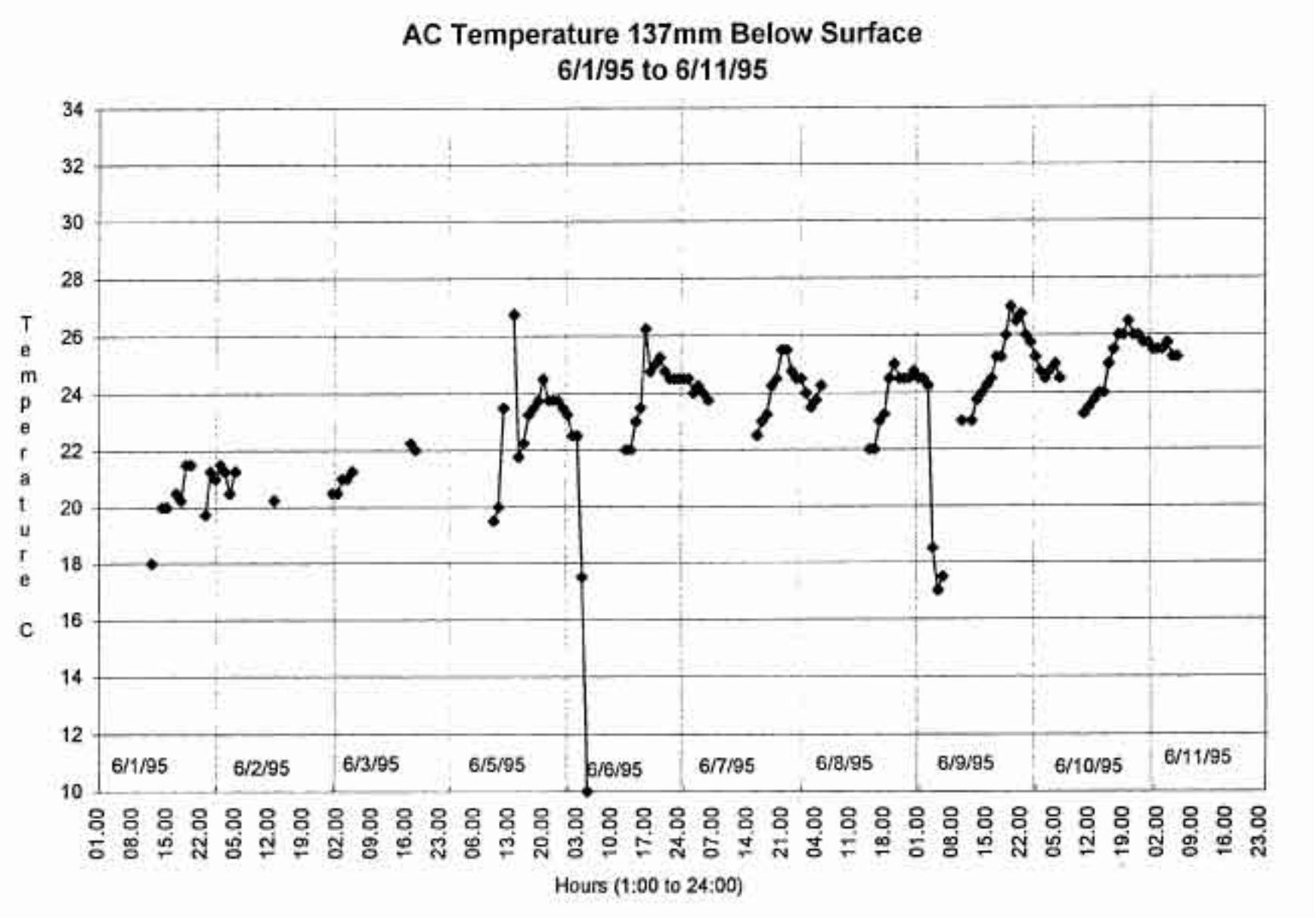

Figure 3.11c Asphalt Concrete Temperature at 137 mm Depth (June 1, 1995 - June 11, 1995)

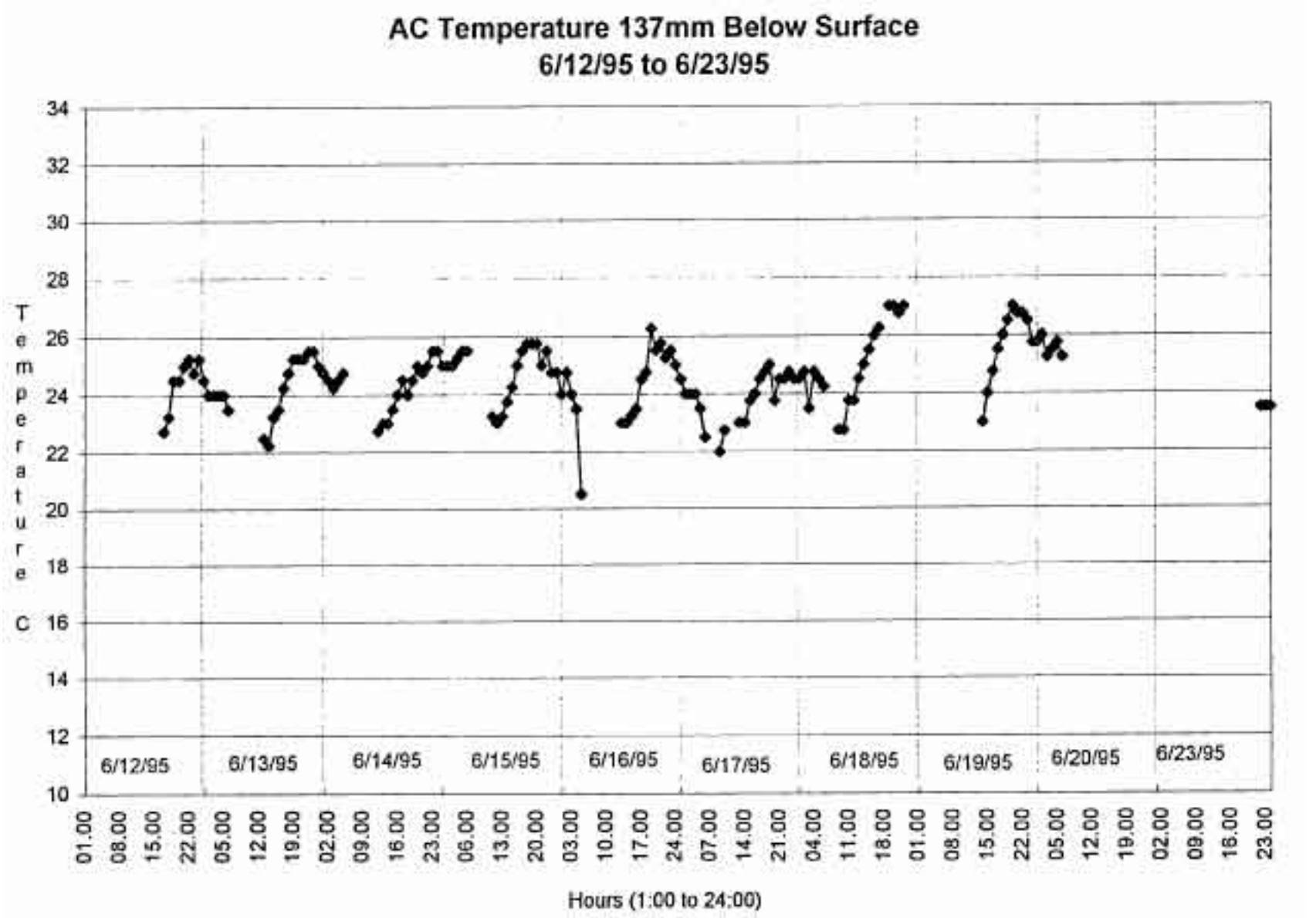

Figure 3.11d Asphalt Concrete Temperature at 137 mm Depth (June 12, 1995 - June 23, 1995)

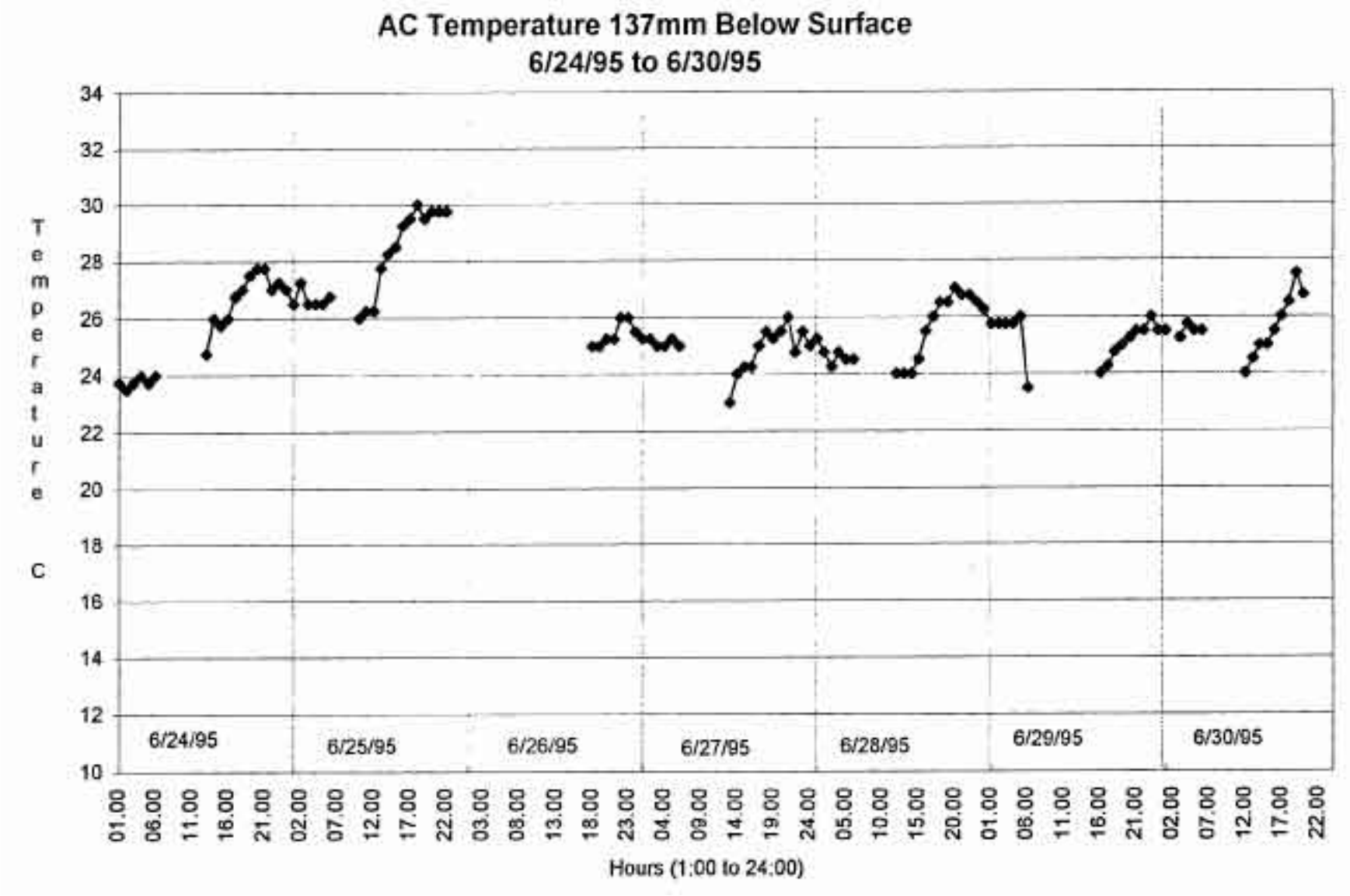

Figure 3.11e Asphalt Concrete Temperature at 137 mm Depth (June 24, 1995 - June 30, 1995)

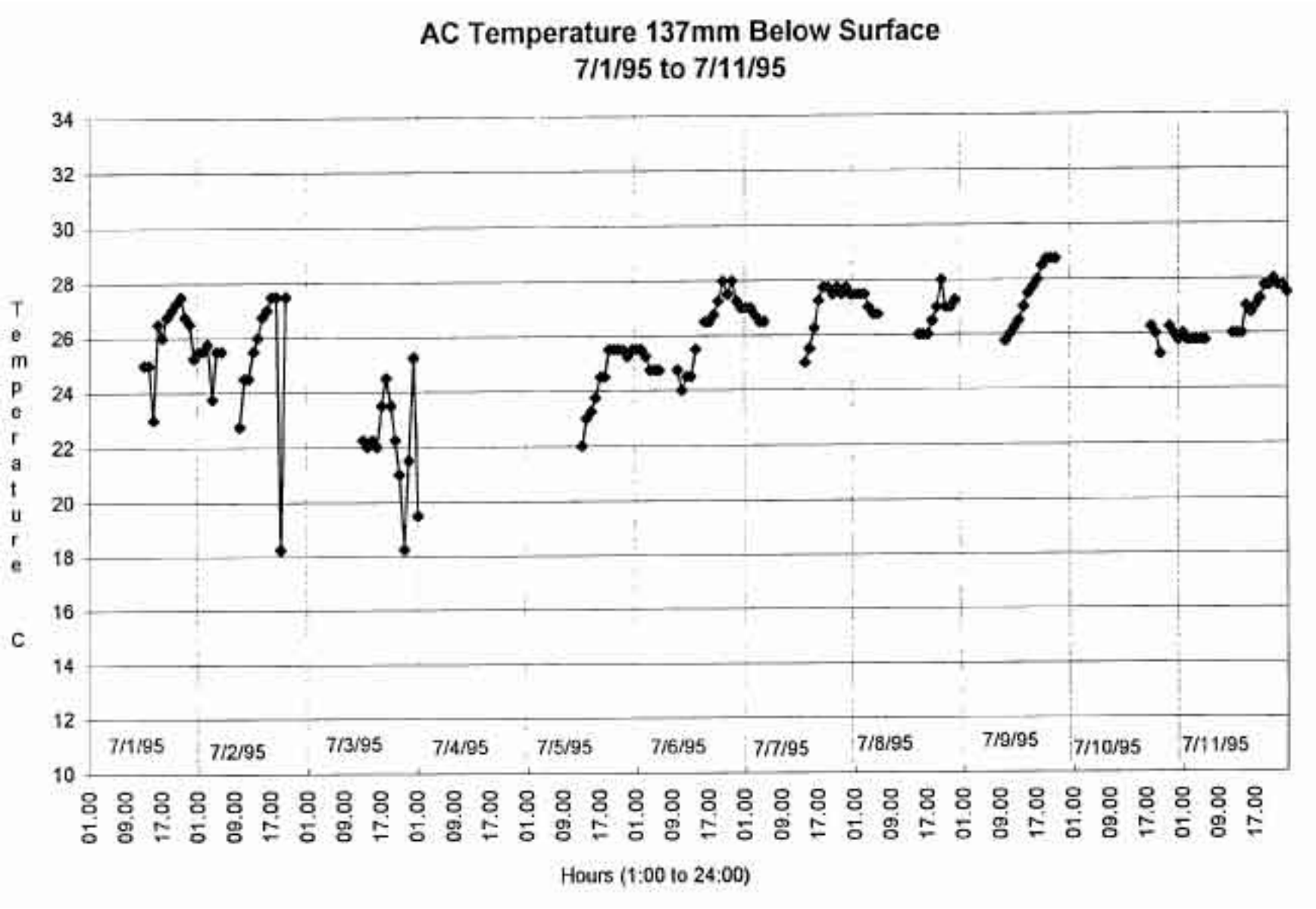

Figure 3.11f Asphalt Concrete Temperature at 137 mm Depth (July 1, 1995 - July 11, 1995)

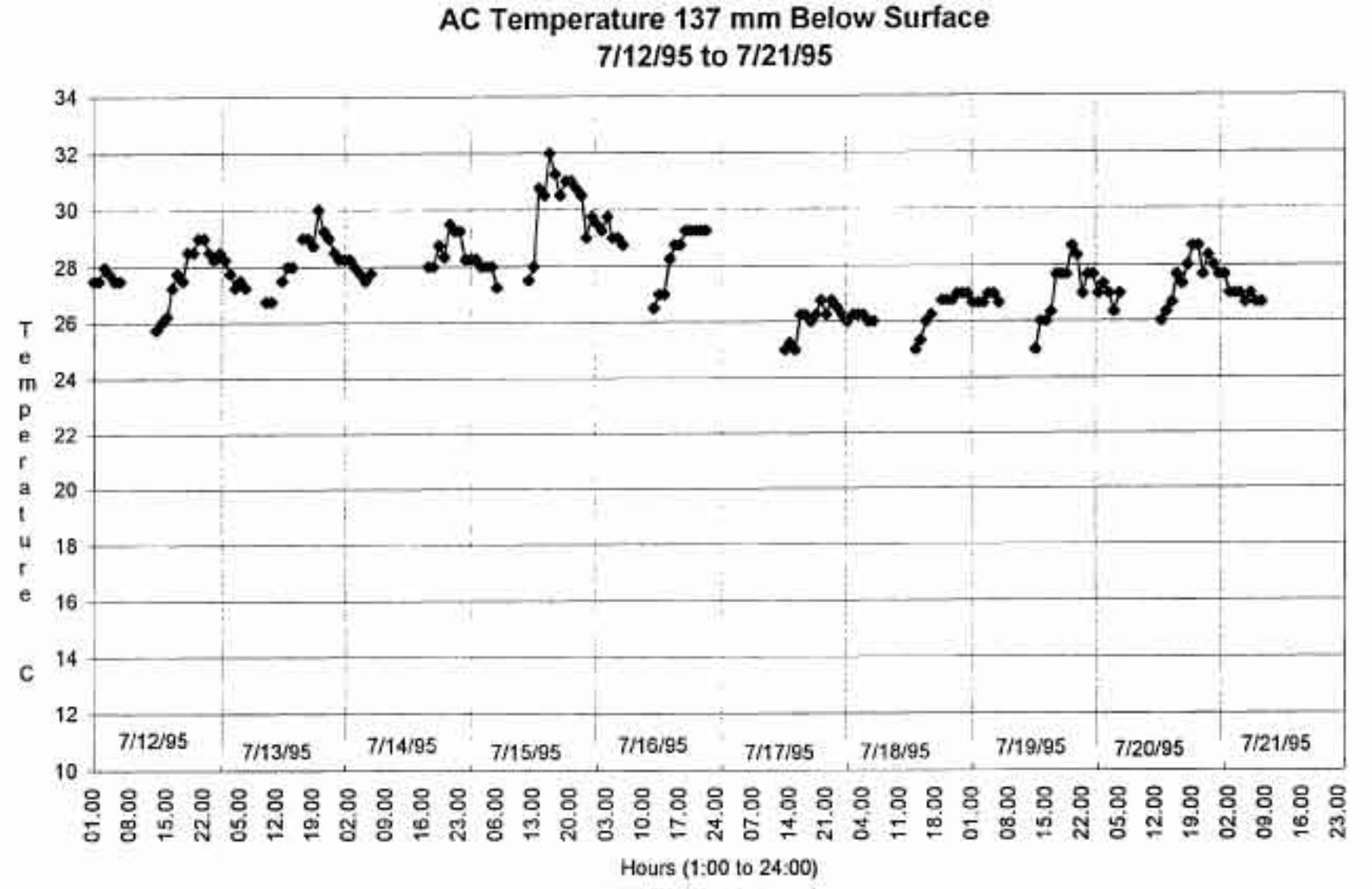

Figure 3.11g Asphalt Concrete Temperature at 137 mm Depth (July 12, 1995 - July 21, 1995)

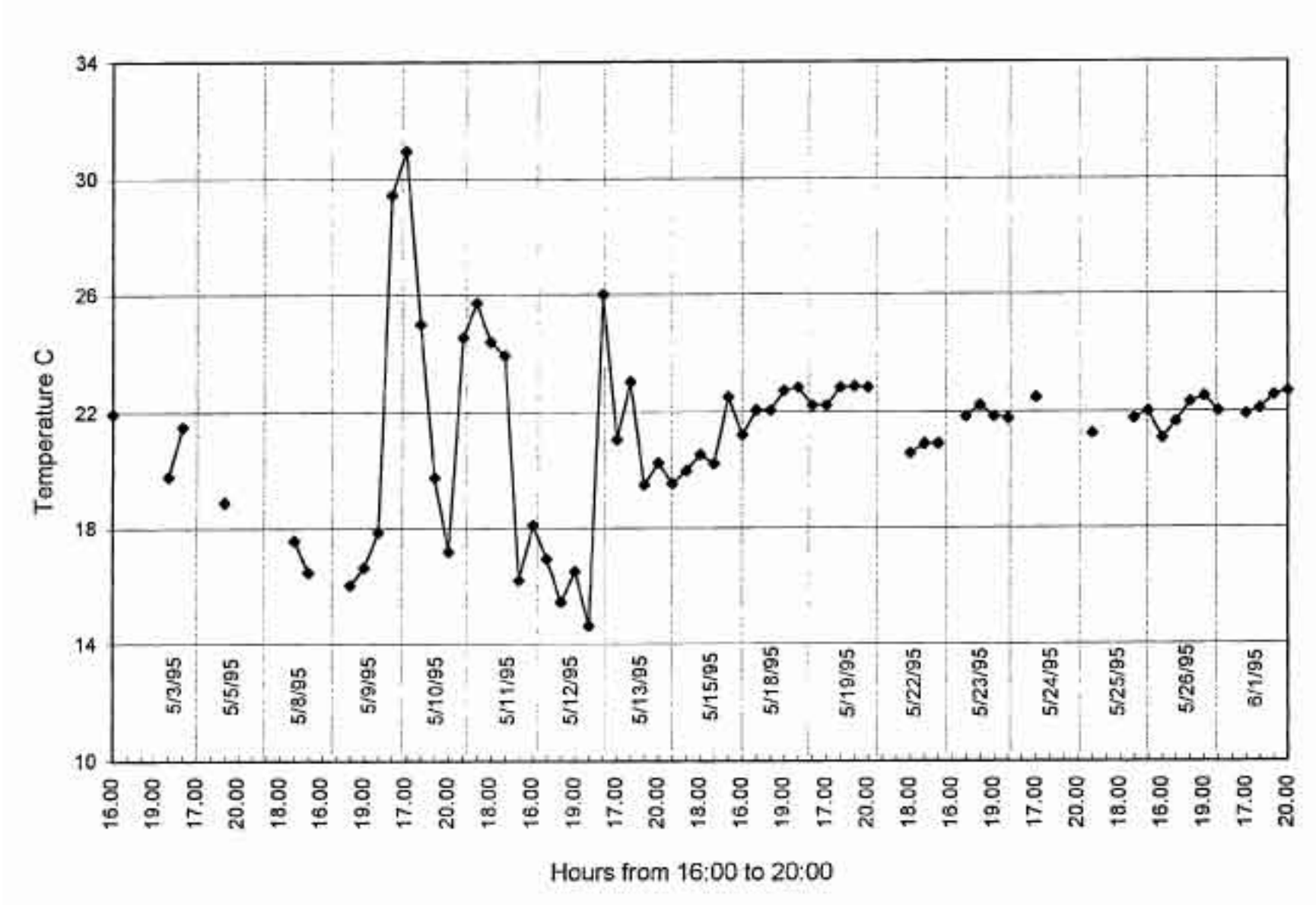

Figure 3.12a Asphalt Concrete Temperature at 50 mm Depth During Warmest Hours of Day (May 3, 1995 - June 1, 1995)

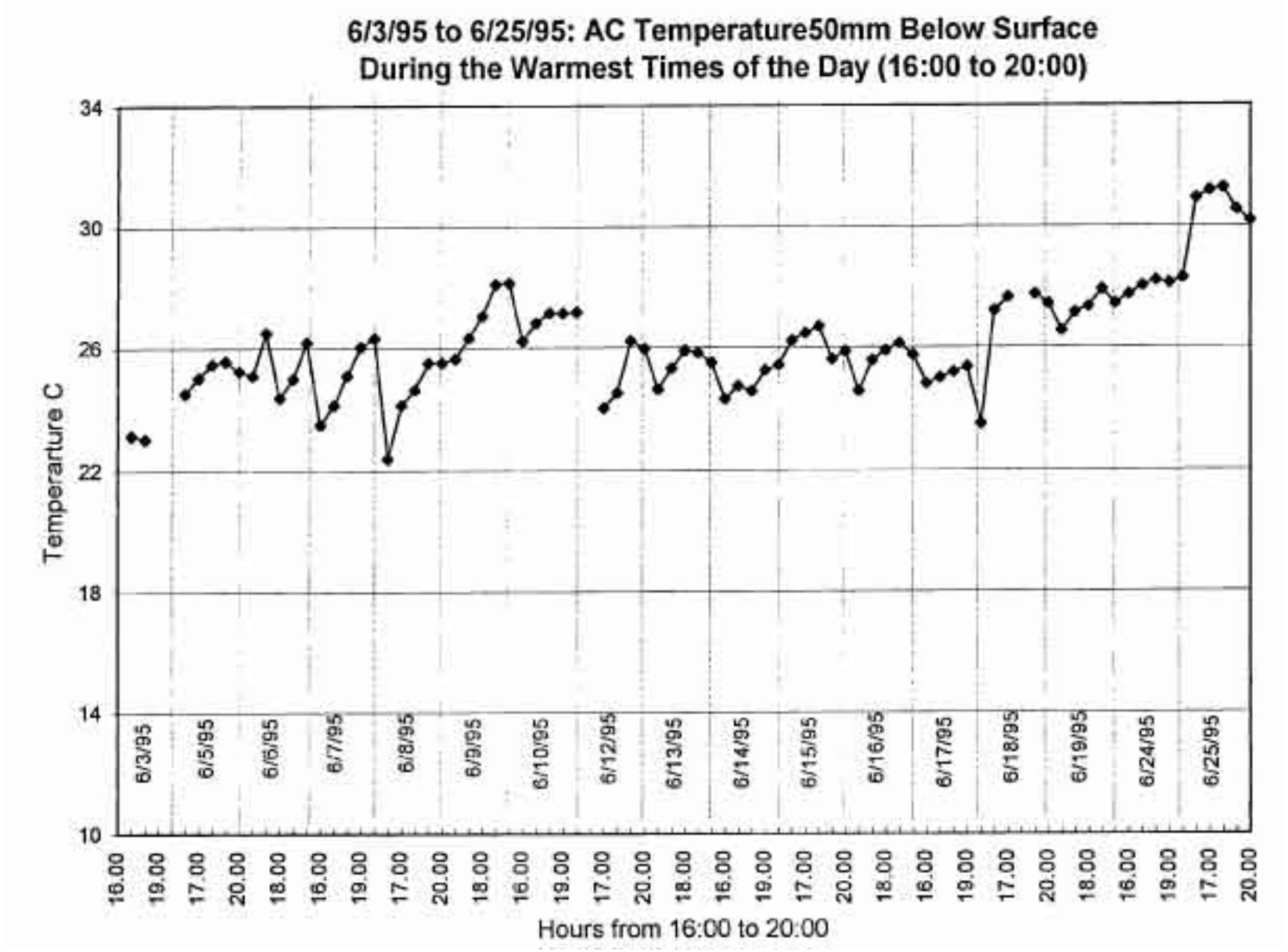

Figure 3.12b Asphalt Concrete Temperature at 50 mm Depth During Warmest Hours of Day (June 3, 1995 - June 25, 1995)

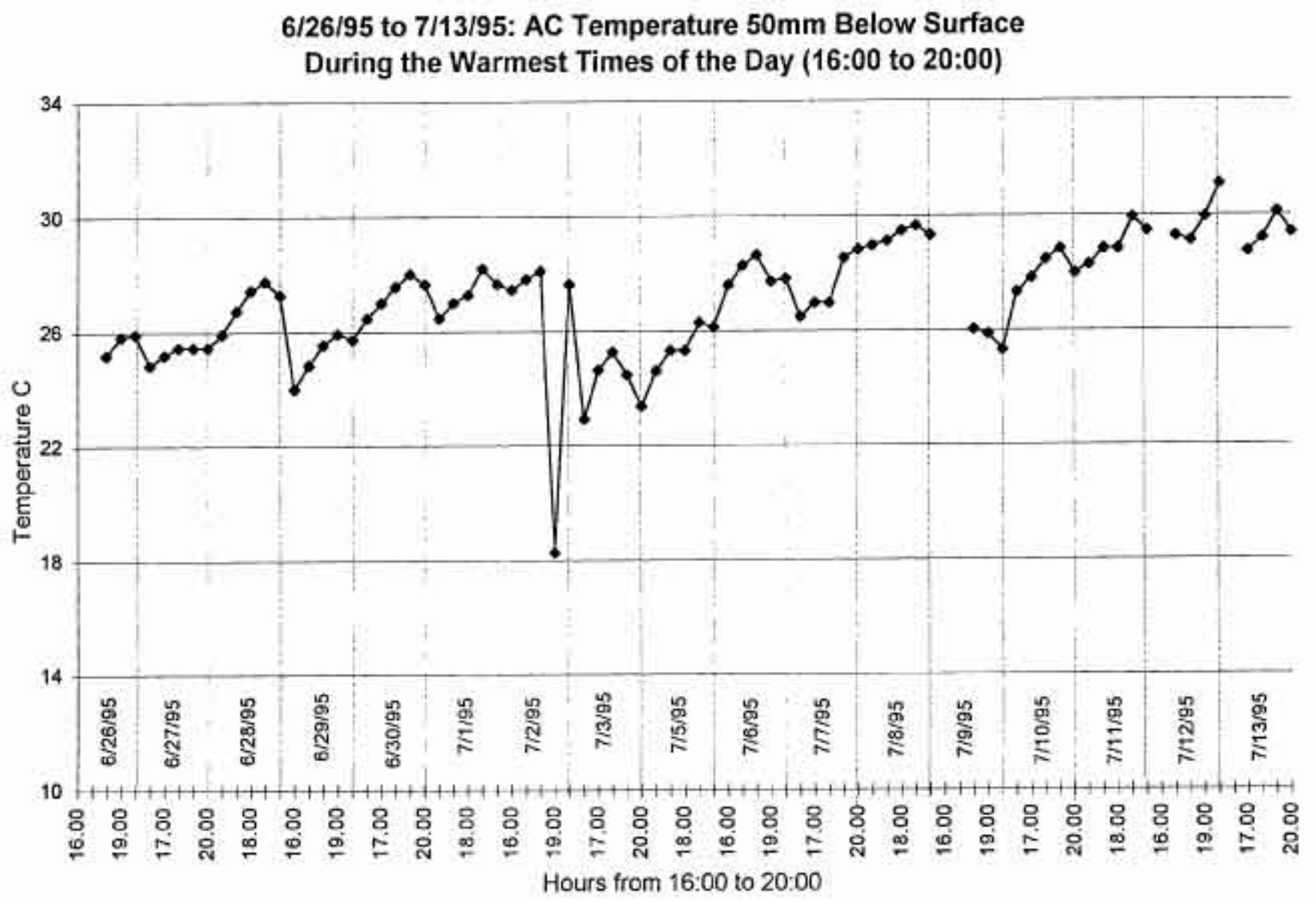

Figure 3.12c Asphalt Concrete Temperature at 50 mm Depth During Warmest Hours of Day (June 26, 1995 - July 13, 1995)

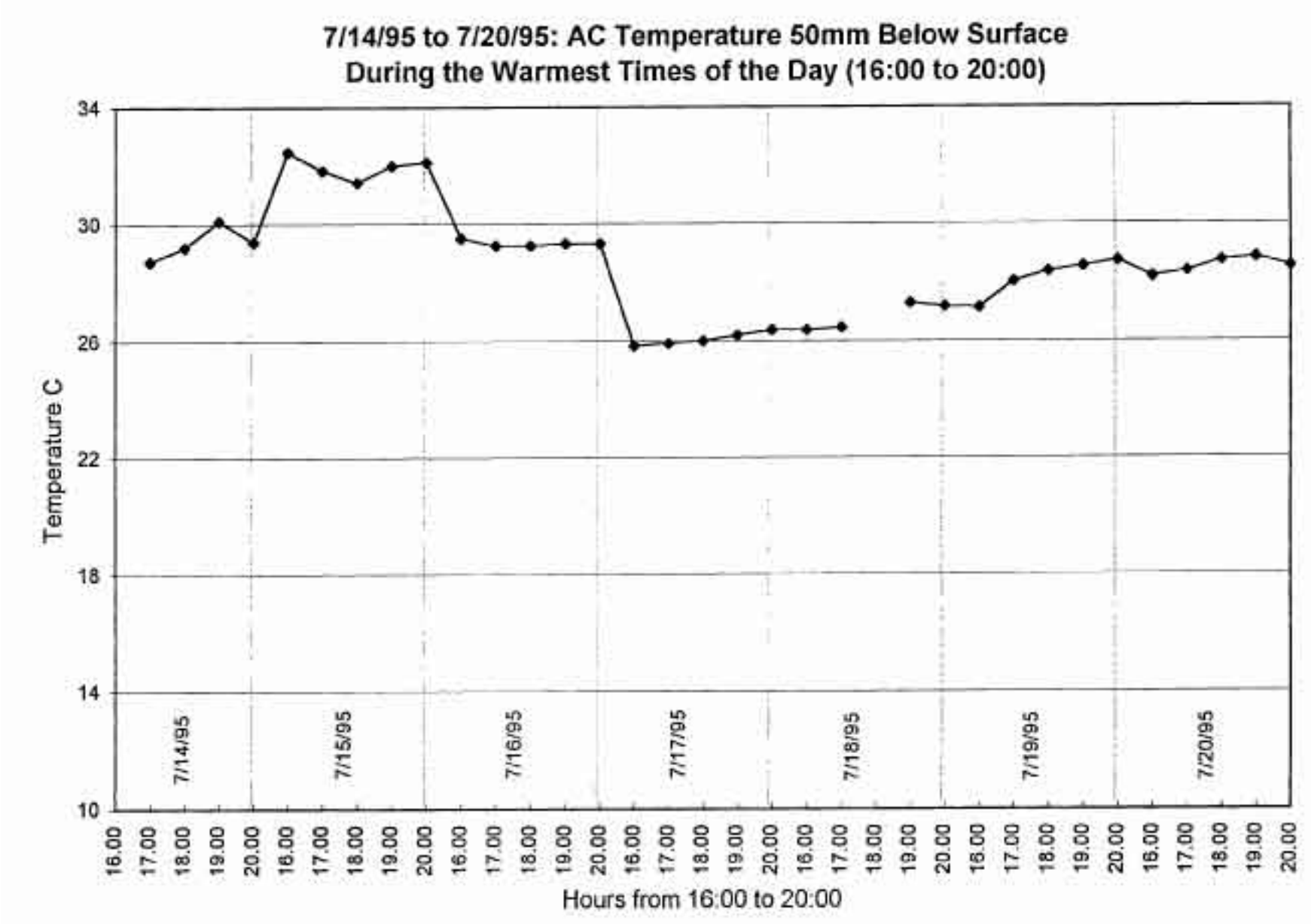

Figure 3.12d Asphalt Concrete Temperature at 50 mm Depth During Warmest Hours of Day (July 14, 1995 - July 20, 1995)

3.2.5 Crack Investigation

In order to evaluate fatigue performance, extensive regular visual monitoring is performed, and photographs are taken of the pavement surface after cracks have been highlighted with bright paint. Crack lengths are measured, and the cumulative crack length is plotted as a function of load repetitions.

The pavement appears to have thin cracks on its surface. These cracks are not consistent, however, and a crack observed one day may be unrecognizable the next. To better understand the nature of the cracking, small cores were extracted at two cracks in the turnaround area. The cracks were evident only at the surface and had not propagated through the asphalt concrete layer. It, therefore, appears that initial cracking was confined to the surface and did not extend more than about 0.5 mm below the surface which indicates that the pavement has not yet cracked in the typical fatigue failure mode, that is, from bottom-to-top. Possible causes for this surface cracking have not yet been investigated.

The results of the crack length monitoring continue to be analyzed as the HVS testing proceeds.

3.2.6 Trench

After completion of testing, a trench will be dug across each test section to gain an understanding of the in-situ profile of the pavement. This will aid in understanding the pavement behavior measured during the test. Samples for measuring material characteristics and moisture content will also be obtained from the trench. It is expected that trenching will occur after HVS testing of the overlays as described in Goal 3 of the CAL/APT Strategic Plan.

CHAPTER 4

MATERIALS CHARACTERIZATION:

SUBGRADE, SUBBASE, AND UNBOUND BASE

4.1 INTRODUCTION

Tests of the unbound materials (subgrade, subbase, and aggregate base) for design and for construction quality acceptance were performed using current Caltrans methods. Results from these tests have been described in Chapter 2: they are important in this investigation to insure that the test sections are similar to pavements Caltrans would produce in practice.

This chapter addresses measurements of the stiffness characteristics of the unbound materials. Stiffness or modulus tests, which were performed before, during, and just after construction, include the following; bender element, resilient modulus from triaxial compression, K-mold, Dynamic Cone Penetrometer, and Heavy Weight Deflectometer. The approximate locations of these tests (except the Heavy Weight Deflectometer) are identified in Figure 4.1. This broad range of test methods provides an opportunity to determine the efficacy of such tests as additions or replacements to current Caltrans procedures. Moreover, they provide essential data to support mechanistic pavement analyses. Test descriptions, results, and a comparison of elastic modulus predictions from each test are presented in this chapter.

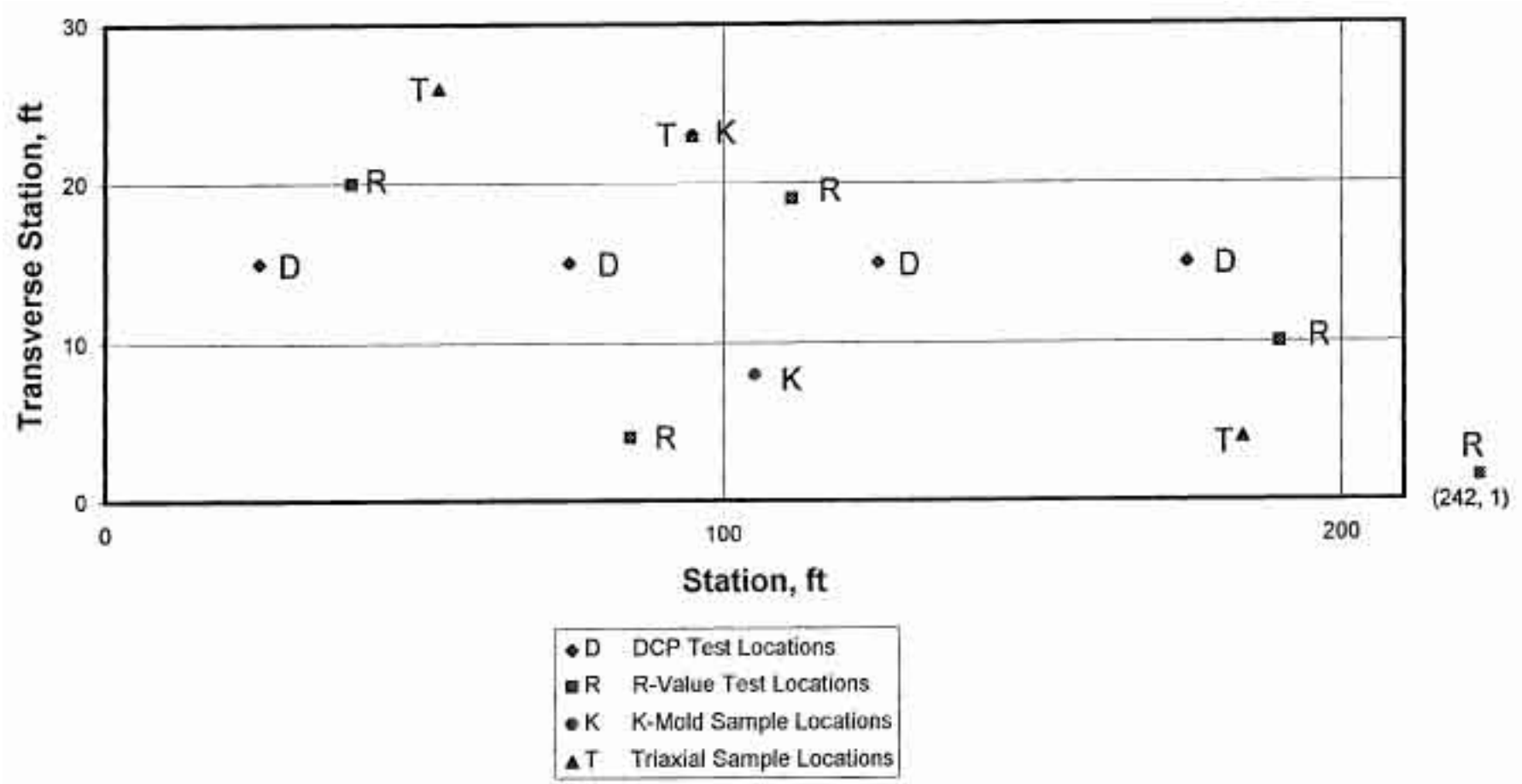

Figure 4.1 Unbound Soils Test Locations

4.2 TRIAXIAL AND BENDER ELEMENT TESTING OF SUBGRADE SOIL

The stiffness, or modulus, of the subgrade soil was measured using samples obtained from three different locations at the project site as shown in Figure 4.1: Station 0+54, 26 ft offset (16.4, 7.9 m) Specimen 1; Station 1+84, 4 ft offset (56.1, 1.2 m) Specimen 2; and Station 0+95, 23 ft offset (29.0, 7.0 m) Specimen 3. Bulk samples of the soil were retrieved from these locations during exploratory borings and density analysis. One specimen was prepared and tested using the soil from each location. Testing problems lead to the elimination of Specimen 1. In order to simulate the expected structure and density of the in-situ soil, which was a compacted fill, the specimens were compacted by kneading compaction using a Harvard Miniature Compactor to water contents and densities similar to those currently in the field, as measured using a nuclear gage at nearby locations in the fill. Those densities and water contents were:

	water content (% by weight)	compacted wet density (g/cm^3)
Specimen 2	22.4	2.06
Specimen 3	15.8	2.12

The specimens were compacted within a 75 mm (3 in.) diameter Shelby tube, to nominal dimensions of 72 mm (2.85 in.) in diameter and 140 to 150 mm (5.5 to 6 in.) in height. The specimens were then trimmed, extruded, weighed, and measured prior to testing. Based on reasonable estimates of the specific gravity of solids, all samples seem to be close to saturation at these densities and water contents, suggesting that the sample soils were located above the water table but within the capillary fringe. Since in-situ compaction is rarely carried out so close to the saturation curve unless required by specification (better compactive efficiency is typically obtained closer to the optimum water content), the fill was probably initially compacted at a

smaller water content and subsequently absorbed additional moisture. It seems likely, therefore, that specimens for the current testing may have been compacted at larger water contents than when the fill was originally placed.

The stiffness of clayey soil is typically much larger immediately following compaction, in the "as-compacted" state, than it is after the compacted soil is allowed free access to water during soaking. This is likely due to the additional binding strength between particles caused by the interfacial tension of water surrounding air bubbles within the voids. To investigate the importance of this effect, the modulus of each of the three specimens was investigated both in the as-compacted state and after soaking. To compare different measurement techniques, the specimens were tested both for resilient modulus in the triaxial apparatus and for shear modulus using shear wave velocity techniques. The procedures and results of these tests are discussed in the following sections.

4.2.1 Triaxial Compression Repeated Load Testing

Resilient moduli of the compacted subgrade soil were determined following the "AASHTO Standard Method of Test for Resilient Modulus of Subgrade Soils" *(American Association of State Highway and Transportation Officials, 1986)*. This method consists of performing a series of 20 cyclic triaxial tests on the soil specimen of interest, under various combinations of effective confining stress (s_3') and cyclic deviatoric stress ($s_d = s_1 - s_3$). Each cyclic test includes 200 cycles of loading, but only the stresses and strains in the final cycle are used to calculate the resilient modulus as follows:

$$M_r = \sigma_d / \varepsilon_r \quad (4\text{-}1)$$

where σ_d = the cyclic deviatoric stress and ε_r = the recoverable axial strain. The first five of the 20 cyclic tests, at low stress levels, are described as being for the "conditioning" of the specimen and thus are not included in the data presentation.

Cyclic triaxial testing was performed using the *CKC*^{TM} *e/p* pneumatic loader, under control of *Georobot* software (version 5.2). Due to the very small displacements, the standard triaxial apparatus was modified to accommodate two LVDTs on opposite sides of the loading rod, both of which were calibrated to a sensitivity of 0.5 mm/volt. This modification allowed more precise measurement of the average vertical displacements as well as provided a means of checking to see if imperfect alignment was producing any rocking of the upper specimen cap. All of the instrumentation and other components of the system were carefully calibrated prior to initiation of the testing program.

Small strain levels prompted the inclusion of an additional step in the data reduction process as well. Since the two LVDTs were externally mounted (as in a standard triaxial apparatus), the recorded deformations included compliance of the testing system resulting from deformations of the loading rod, the specimen caps, relative displacements between the rod and the threads in the caps, and deflections of the base of the cell, none of which should be attributed to the soil specimen when calculating strains. To account for the system compliance, a series of calibration tests were performed using the identical setup, but with a solid aluminum specimen in place of the soil. The magnitude of the system compliance at various loads was determined in this manner, and these superfluous deformations were subtracted from the measured deformations when calculating the resilient modulus of the soil specimens.

While the AASHTO resilient modulus test procedure is quite detailed in describing specific steps to be followed, there is one area in which there is considerable uncertainty: the procedure does not address the time intervals between tests. This is important for the testing of cohesive specimens, since even when the drainage valves are left open, it will take a considerable period of time for the pore pressures within a specimen to reach equilibrium after the effective stress is changed between testing increments. For example, if a cyclic test has just been completed at s_3' = 42 kPa (6.1 psi) and the next increment calls for s_3' = 21 kPa (3.0 psi), the center of the specimen will not immediately "feel" the change in confining stress once the pressure is changed, particularly if the specimen is not fully saturated.

To minimize the effects of such drainage difficulties, without unduly lengthening this already cumbersome testing process, two modifications were made to the testing procedure: 1) spiral strips of filter paper were wrapped around the specimen prior to placing the membrane, to shorten the drainage paths, and 2) the order of the 20 cyclic tests was rearranged (Table 4.1) to minimize the number of times the effective confining stress needed to be changed. The general trend of running the tests in order of increasing stress levels (larger s_d and smaller s_3') was preserved. In the interest of maintaining a uniform procedure, a standard waiting period of 30 minutes was adopted following any change of s_3' before running the next increment of testing. Table 4.1 also indicates an additional modification to the AASHTO procedure: the series of cyclic tests at the lowest confining stresses were performed at s_3'= 7 kPa (1.0 psi), rather than the specified 0 kPa. This alteration provided more stable (and realistic) stress conditions and prevented the specimens

Table 4.1 Modified Testing Sequence for a Single Resilient Modulus Test

Step	s_3 (kPa)	s_d (kPa)	Recorded*	Time Lag (min)
1	42	7	No	
2	42	14	No	10
3	42	28	No	10
4	42	56	No	10
5	42	70	No	10
6	42	7	Yes	30
7	42	14	Yes	10
8	42	28	Yes	10
9	21	7	Yes	30
10	21	14	Yes	10
11	21	28	Yes	10
12	7	7	Yes	30
13	7	14	Yes	10
14	7	28	Yes	10
15	42	56	Yes	30
16	42	70	Yes	10
17	21	56	Yes	30
18	21	70	Yes	10
19	7	56	Yes	30
20	7	70	Yes	10

*Record the recovered deformations at 200th repetition

from experiencing possible catastrophic failure during the most rigorous test increments, a drawback of the official procedure as noted by Zaman, Chen, and Laguros *(1994)*.

The results of a resilient modulus test on a single specimen are typically presented in the form of a graph of resilient modulus (M_r) versus deviatoric stress (s_d) for each of the 15 tests. The data points of the tests performed at each of the three levels of confining stress (s_3' = 7, 21, and 42 kPa [1.0, 3.0, and 6.1 psi]) form three lines on such a plot, with the upper line typically corresponding to the largest confining stress due to the stress-dependent nature of soils. As described earlier, each specimen was subjected to two or three test sequences to determine the effect of the specimen's condition (whether "as-compacted" or soaked) on its resilient modulus.

The resulting data for Specimen 2 are plotted in Figures 4.2a (as-compacted) and 4.2b (soaked). Three series of resilient modulus tests were performed on Specimen 3, under as-compacted, soaked, and fully saturated conditions. The soaked and fully saturated conditions were differentiated by the amount of time that the specimens were exposed to water prior to repeated load testing. Using the "B" value as a measure of saturation (when B is close to one a specimen is considered saturated), a value of about 0.75 represented the soaked condition while a value of 0.96 represented the fully saturated condition. The data from these series are plotted in Figures 4.3a, 4.3b, and 4.3c. It should be noted that the moduli recorded at the smallest loads are somewhat erratic, since the deformations of the stiffer materials at these low loads were close to the lower limit of reliable measurement with the current system.

The resilient modulus plots show a significant difference between the as-compacted stiffness and the soaked (or saturated) stiffness for all three of the specimens. Following

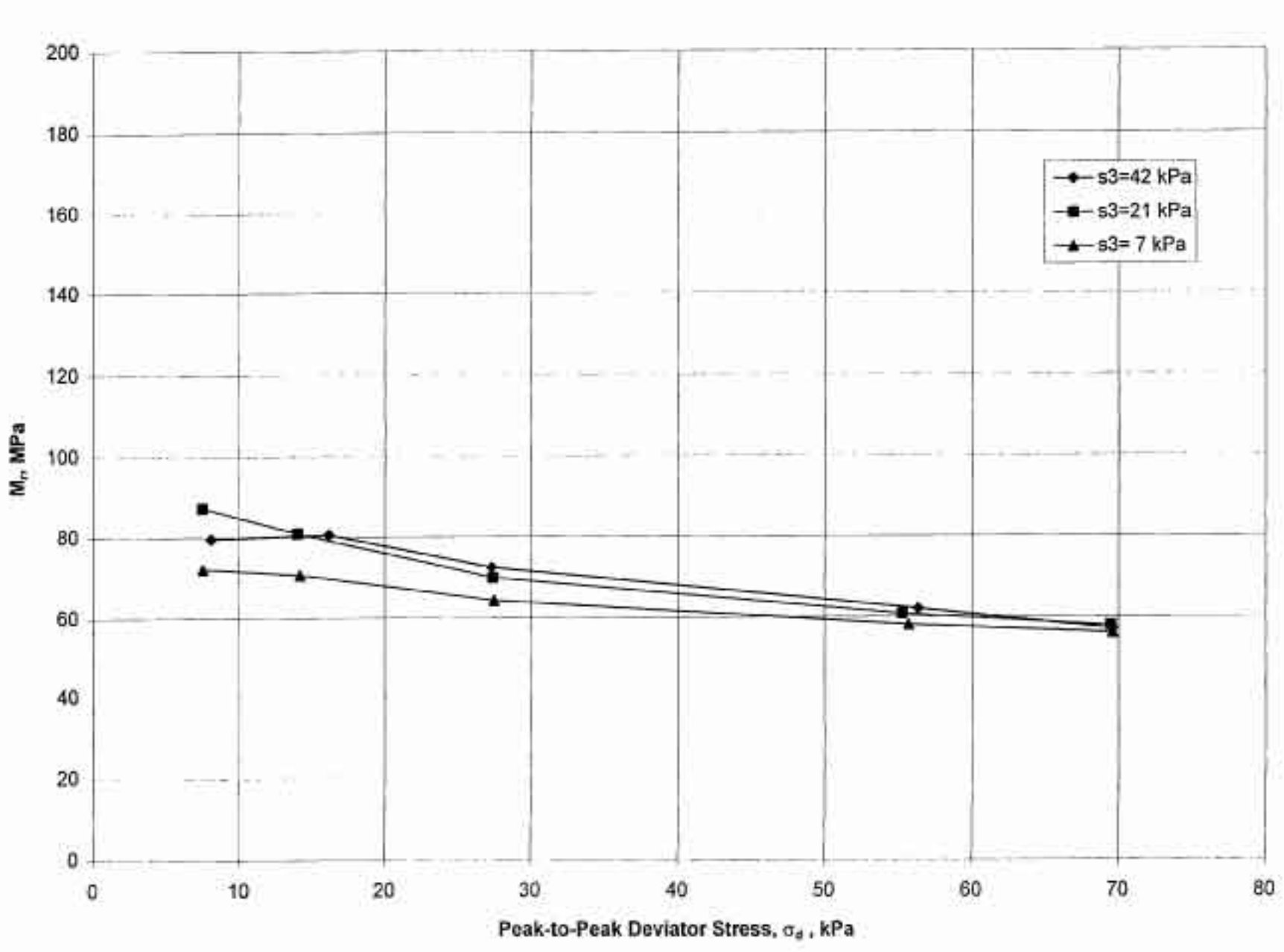

Figure 4.2a Resilient Modulus of Specimen 2 (As Compacted)

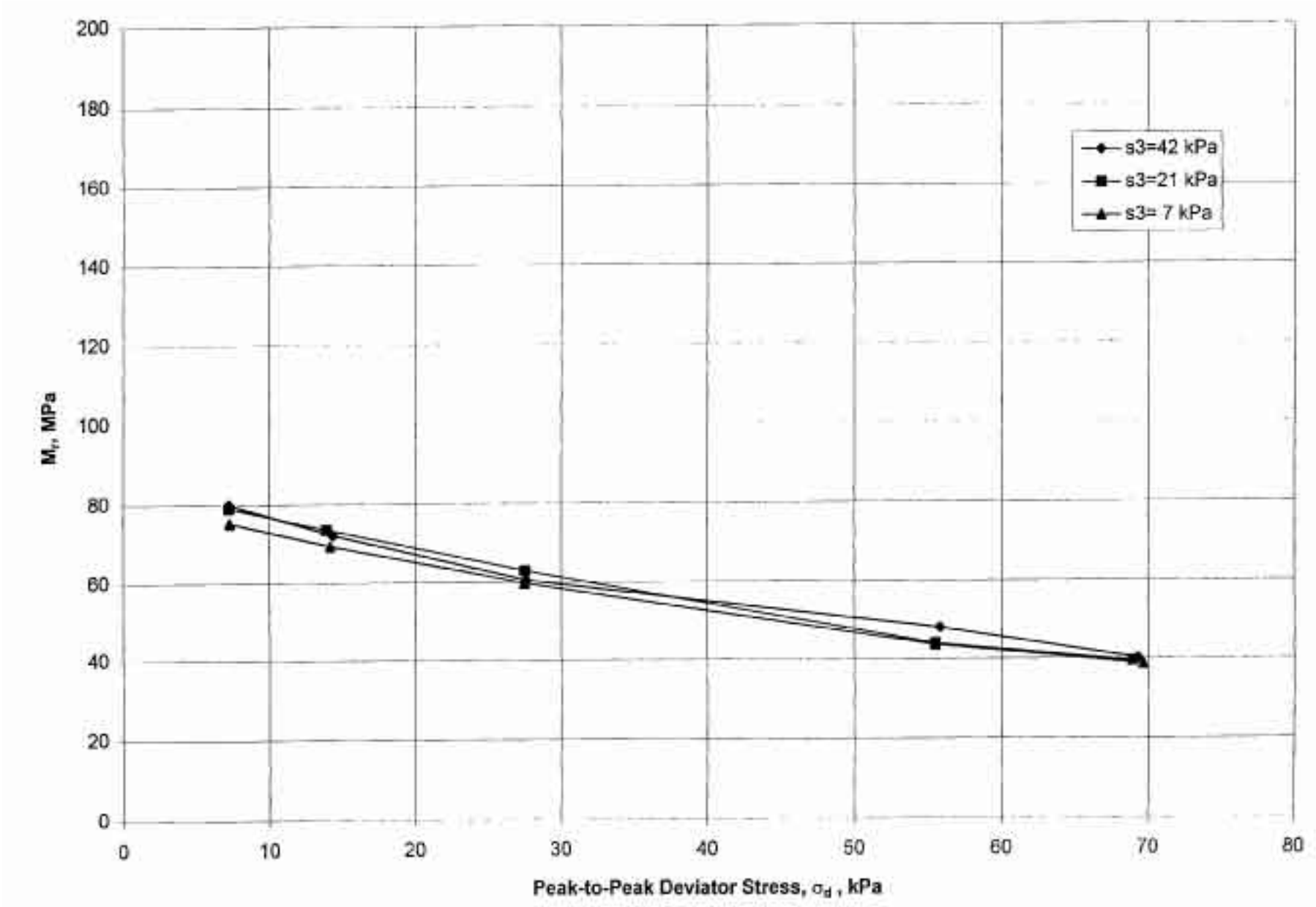

Figure 4.2b Resilient Modulus of Specimen 2 (Soaked)

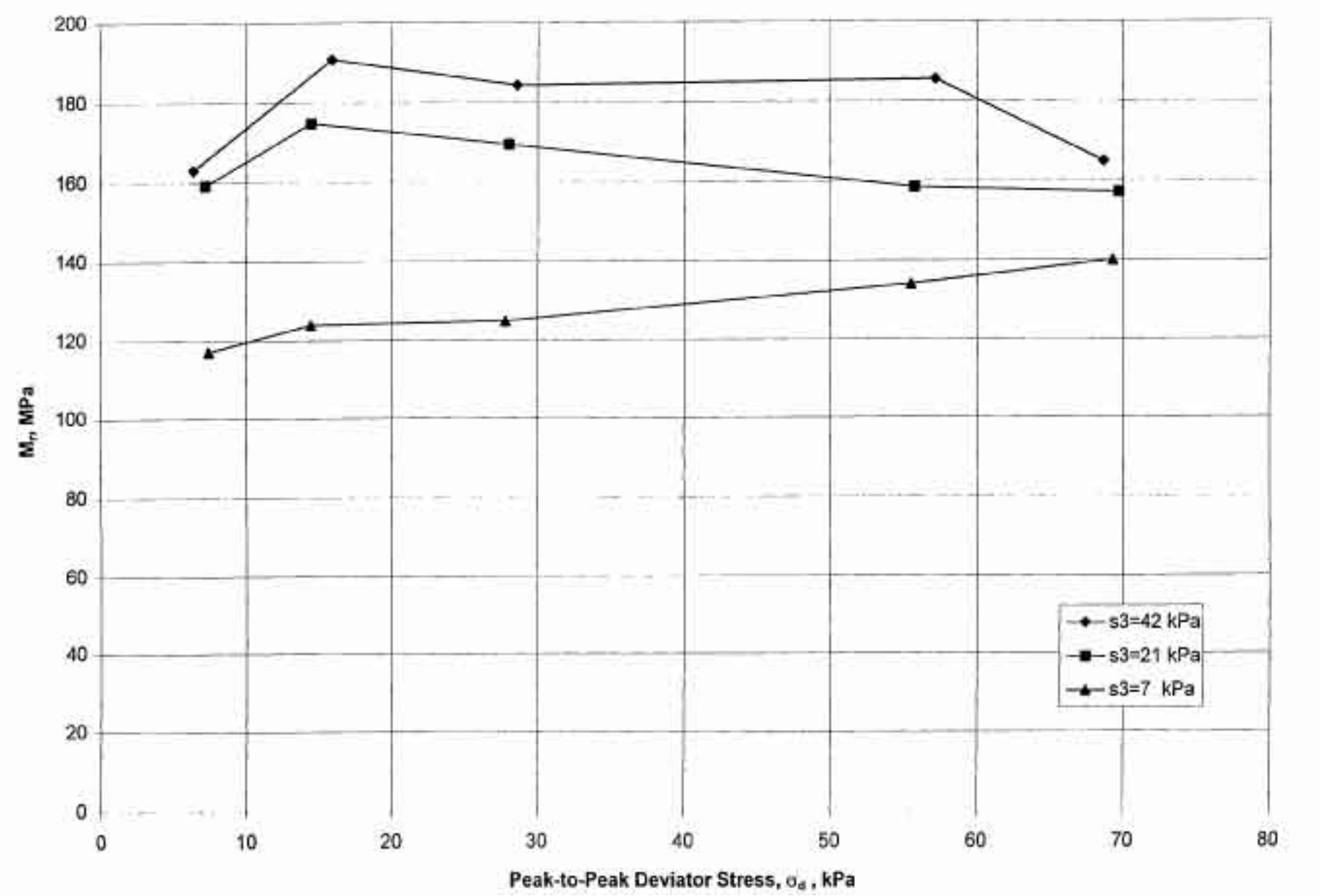

Figure 4.3a Resilient Modulus of Specimen 3 (As Compacted)

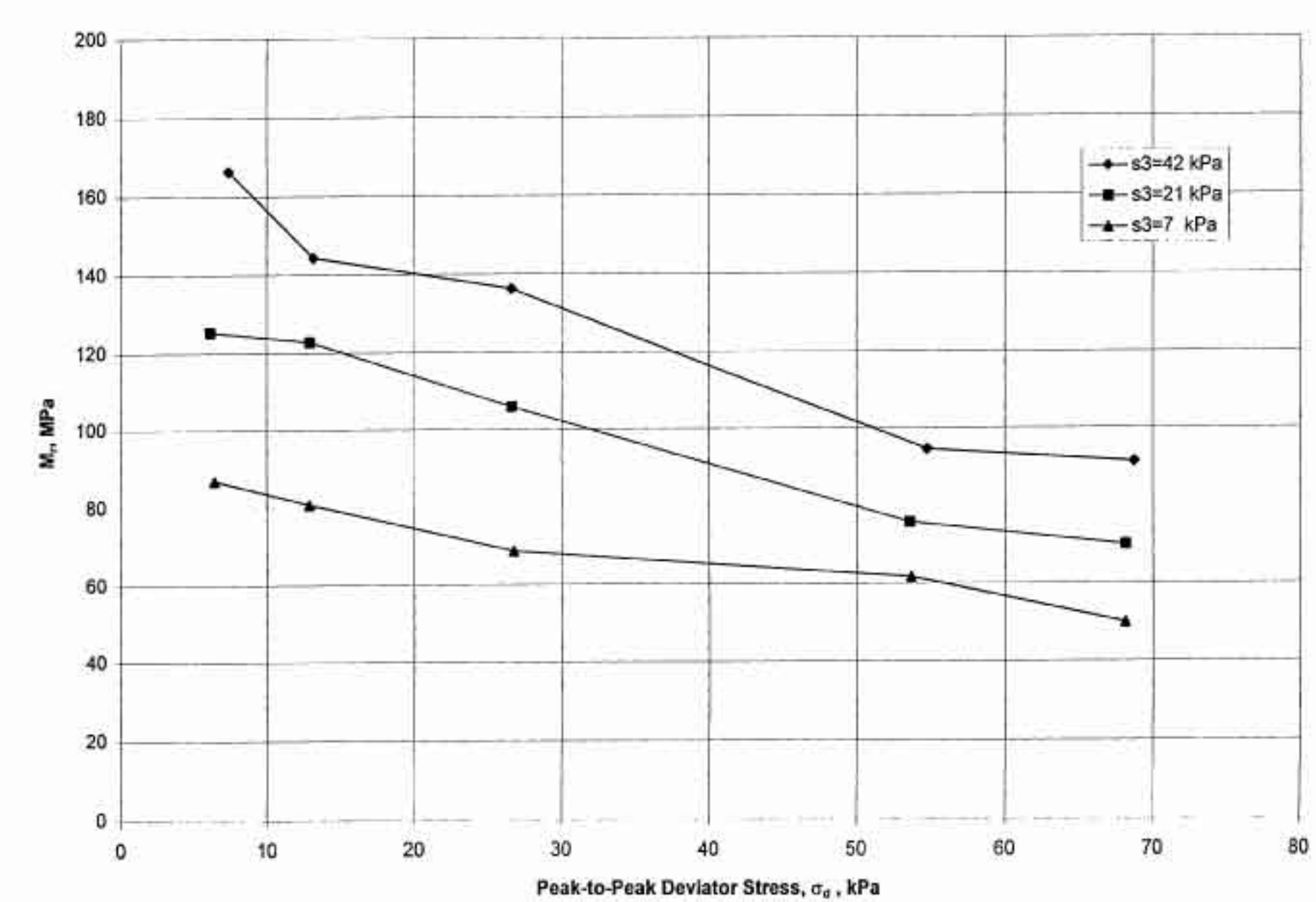

Figure 4.3b Resilient Modulus of Specimen 3 (Soaked)

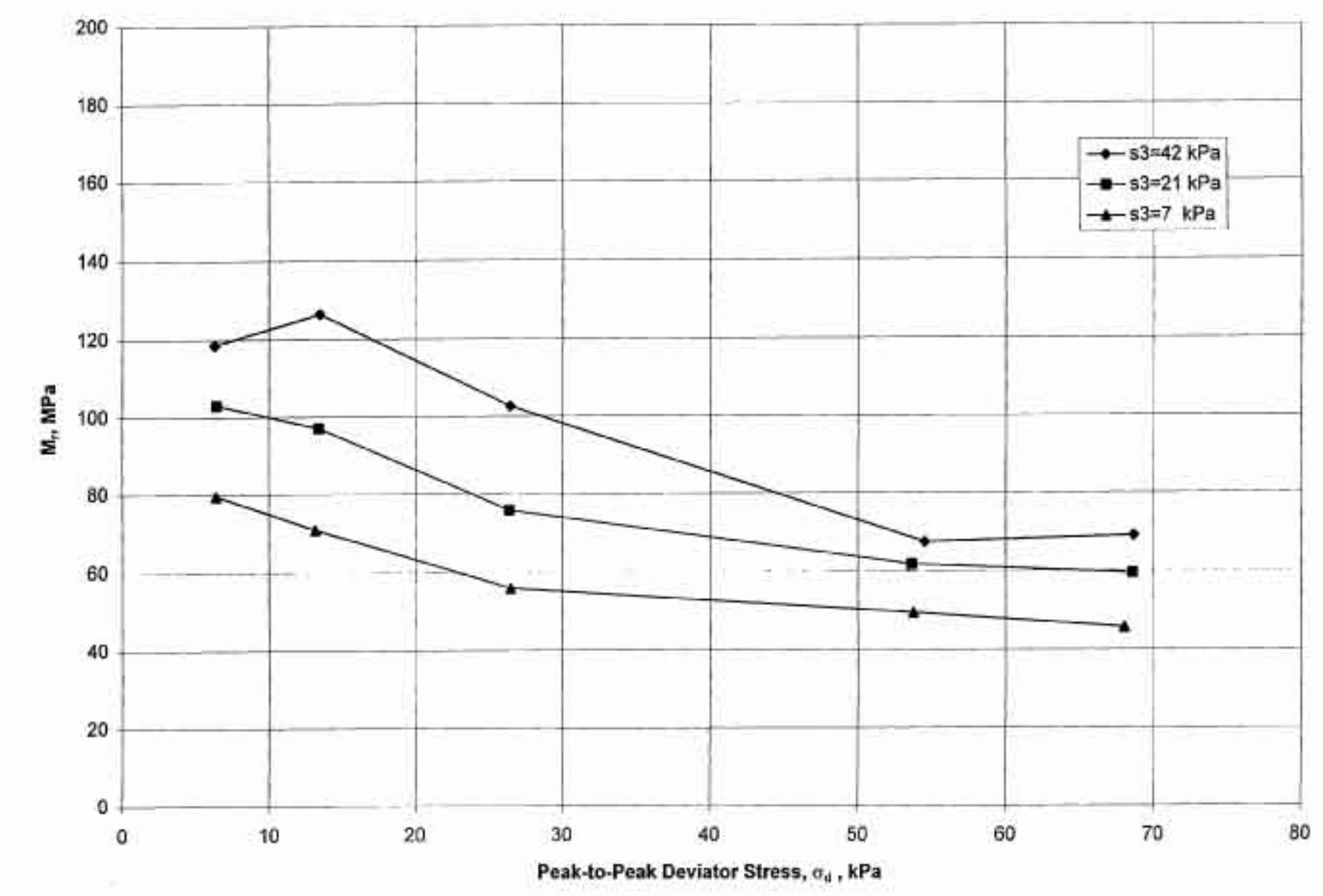

Figure 4.3c Resilient Modulus of Specimen 3 (Saturated)

access to water, the resilient modulus drops to between 40 and 80 percent of the original as-compacted value: the drop is particularly severe at larger stress and strain levels. It is also apparent that, as compacted, Specimen 3 did not experience a significant decline in modulus with increasing stress (deviatoric) or strain levels, as the modulus seems to remain essentially constant, or even increase slightly, as the loading level increases. This independence of modulus from strain is unusual for soil, which is typically strain-softening, and in this case may result from an increasing mobilization of the capillary forces when the soil structure is deformed, perhaps due to dilation. Once these capillary forces are relaxed by the saturation of the specimen, the resilient modulus does seem to decline with strain, as one would normally expect. Finally, it is apparent that the specimens show intrinsically different stiffnesses: Specimen 3 has nearly twice the stiffness of Specimen 2 under comparable loading conditions.

The smaller stiffness of Specimen 2 is most likely related to its larger compaction moisture content and slightly smaller density, which were selected based on field data as presented in Chapter 2. Assuming that the top portion of the subgrade is essentially uniform in composition throughout the test sections, which it appears to be from the boring logs, the test results demonstrate the effects of moisture content and density on subgrade stiffness.

A comparison of subgrade stiffness of this sort is not possible using the R-value test. A range of water contents would be expected under any pavement structure, which can also be evaluated using triaxial testing, as performed herein. The results indicate that the subgrade stiffness after soaking may be only 50 to 75 percent of that at the time of construction. The change in stiffness will depend on compaction, water content at time of compaction, and other factors.

4.2.2 Bender Element Testing: Shear Modulus at Small Strains

The bender element test was included in this project as a potential alternative to the repetitive axial load triaxial test for measuring subgrade stiffness. The test measures the shear modulus (G) at small strains by measuring the time required for a shear wave to travel from the bottom to the top of the specimen.

To make these measurements, each of the three compacted subgrade specimens was placed between specially adapted end caps, which were equipped with Bimorph Bender elements. As-compacted measurements of shear wave velocity were made prior to placing the specimens in the triaxial cell, and saturated values were taken immediately after removing the specimens from the cell.

Bender elements are small (approximately 1 cm square by 0.07 cm thick), wafer-shaped transducers consisting of alternating layers of polarized ceramic and metallic electrodes (Figure 4.4a). When an electrical current is applied across the electrodes, the bender element responds by "curling" slightly, as one ceramic layer shortens and the other lengthens (Figure 4.4b). When one end of the element is rigidly fixed, as in the caps of the triaxial specimen, the response appears as a deflection of the free end of the element.

Bender elements can also convert mechanical deflections to electrical signals, since deformations of the wafers produce small voltage differentials across the electrodes. By placing a wave-generating element at one end of a specimen and a receiving element at the other, one can measure the time required for the wave to travel through the specimen. Because the shear displacements caused by the travelling wave are very small (estimated to be about 10^{-4} percent),

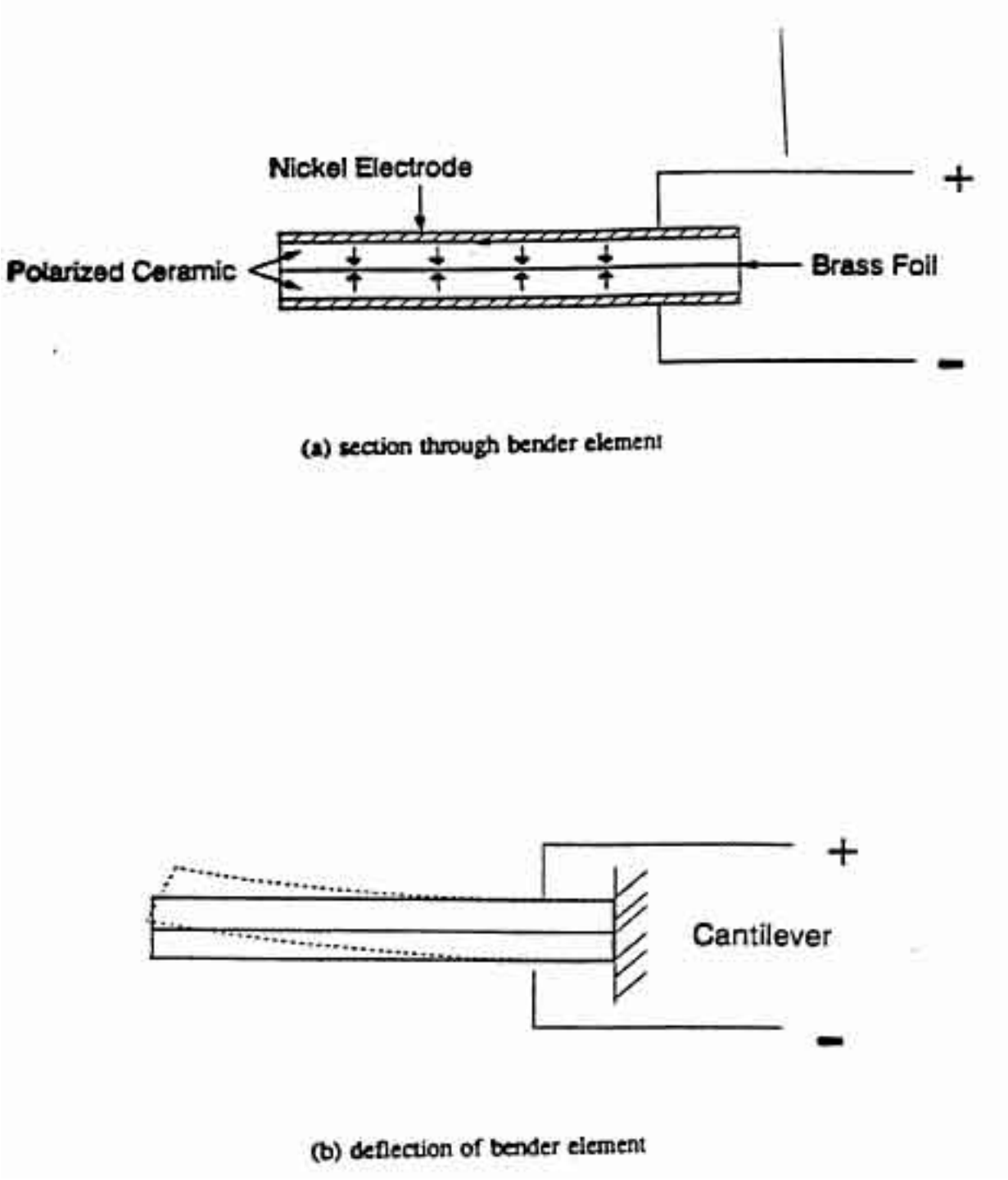

Figure 4.4 Schematic of Bimorph Bender Element (After Human, 1992)

the resulting modulus is often assumed to be the maximum shear modulus (G_{max}) associated with elastic deformations. Research by Dyvik and Madshus *(1985)*, who placed such a system in the caps of a resonant column device, showed that the two methods yielded very similar measures of G_{max}.

A schematic illustration of the components employed in measuring the maximum shear modulus is shown in Figure 4.5. A very brief (between 10 and 200 μsec duration) electrical signal, or "pulse," is produced by an electronic function generator and transmitted to the bender element in one end cap. The resulting movement of the element produces a shear displacement wave, which propagates vertically through the specimen. When the shear wave reaches the opposite end of the specimen, the receiving element is deformed and produces an electrical signal in response. Both the original pulse and the received signal are monitored by an oscilloscope, which displays the response of the receiving element over time (setting *time = 0* at the triggering of the output pulse). A typical record of the incoming wave (at the receiver), shown in Figure 4.6, consists of one or two major troughs over which numerous smaller waves are often superimposed. Numerical simulation of the bender element procedure has shown that these smaller waves, some of which usually precede the major troughs, are carried by compression (P) waves. In contrast, the shear waves are responsible for the larger, more stable troughs.

By sending pulses with a variety of durations (d), one observes that a consistent shear wave velocity is best achieved by characterizing the travel time (? t) as the elapsed time between the midpoint of the transmitted pulse and the center of the first shear wave trough (? t= t_a- d/2). Dyvik and Madshus *(1985)* showed that using the distance between the *tips* of the bender

elements as the travelling distance (L) of the shear wave gave the best agreement with the other measurements of modulus: this definition was used herein.

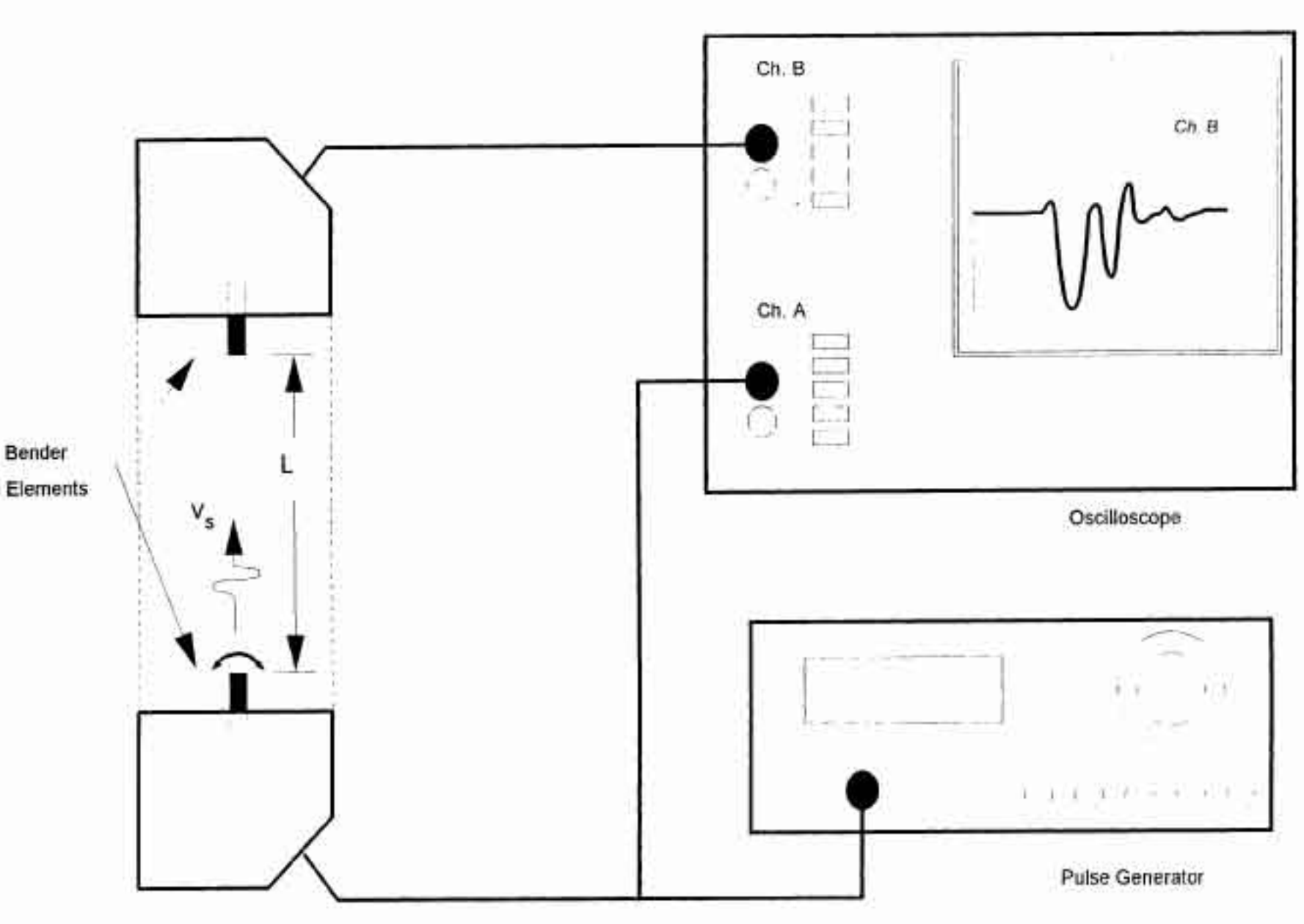

Figure 4.5 Schematic of Equipment Used To Measure G_{max}

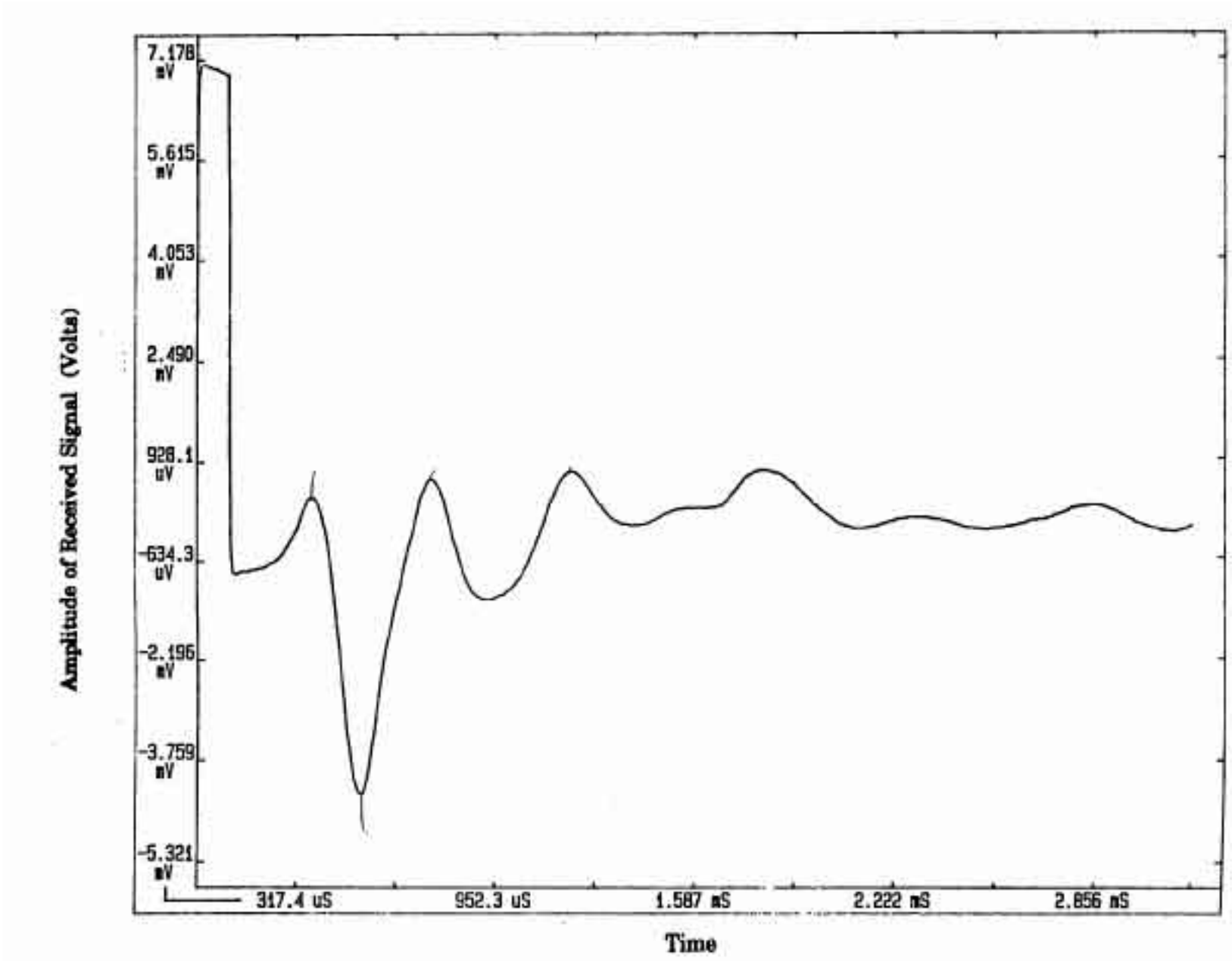

Figure 4.6 Typical Trace of Wave Arrival

Once the shear wave velocity (V_s) is known, the elastic shear modulus G_{max} is determined from:

$$G_{max} = \rho (V_s)^2 \quad (4\text{-}2)$$

where ? is the mass density of the medium through which the shear wave is transmitted. The various quantities required to calculate the shear modulus using bender elements are summarized for each specimen and each testing condition in Table 4.2. The resilient modulus can be estimated from G_{max} by assuming a Poisson's ratio (v) of 0.5 as follows:

$$M_R = G_{max} \bullet 2 (1 + \nu) \quad (4\text{-}3)$$

In examining the results, it is apparent that the specimen's condition, whether as-compacted or soaked, has a significant influence on the measured shear modulus. In the as-compacted condition, each specimen is two to three times stiffer than in the soaked condition. This is not surprising, since soaking (or saturation) allows additional water to enter the pores of the soil, and thereby relieves the capillary stresses caused by the air-water interfaces in the compacted soil. Table 4.2 shows a significant difference in modulus between the two specimens, with Specimen 3 being stiffer than Specimen 2. This agrees with the results of the resilient modulus testing described earlier and provides corroborating data on the reliability of both of these methods *(Viggiani and Atkinson, 1994)*. Further discussion will be provided in the final report on the current testing.

Table 4.2 Results of Shear Modulus Testing Performed Using Bender Elements

Specimen	Height (cm)	Density (g/cm^3)	L (cm)	Condition	Travel Time (x 10^{-6} sec)	V_g (m/sec)	G_{max} (x 10^4 kPa)	Estimated M_R (x 10^4 kPa)
2	15.37	2.06	14.10	As Compacted	984	143	4.2	12.6
				Soaked	1,339	105	2.3	6.9
3	15.41	2.12	14.14	As Compacted	667	212	9.5	28.5
				Soaked	1,195	118	3.0	9.0

4.2.3 Modulus Degradation

In geotechnical engineering, dynamic analyses of soil profiles to determine their response to seismic loading typically requires information on the relationship between the shear modulus (G) and the cyclic shear strain (?). The curves relating these two parameters for a given soil at different levels of confining stress are termed the modulus degradation curves of that soil. The relationship is typically assumed to normalize to a single curve for a given soil when the shear modulus is divided by the maximum, or elastic, shear modulus of the soil (G_{max}). During this project, measurements of both the small-strain shear modulus and the resilient modulus at larger strains were made. Accordingly, it may be instructive to combine this information to see if the combination reveals any glaring irregularities in the specimen's overall behavior.

To develop the modulus degradation curve, values of the resilient modulus must be converted to shear moduli, then divided by the G_{max} values determined using the bender elements. The normalized values are then plotted against the shear strain measured during the same test increment. A value of Poisson's ratio, v, must be assumed both for the conversion of resilient modulus and for the calculation of shear strain. For this analysis, v was taken to be 0.5, since the soil is essentially saturated and undrained during the cyclic loading. It is also important that the values of modulus being related are obtained at the same levels of confining stress. This is not typically a problem if the bender elements are embedded in the same caps used for cyclic testing, since the bender element tests can then be performed under controlled stress conditions. However, for this project alternate bender element caps were used, and the specimens were therefore under less controlled confining stresses. Since the shear wave tests on the saturated specimens were performed immediately following the removal of the specimen from the triaxial

cell, and since the effective stress following cyclic testing was held at 7 kPa (1.0 psi), it was assumed that the shear wave tests took place under confining stresses of approximately 7 kPa (1.0 psi), and therefore only the s'_3= 7 kPa (1.0 psi) resilient modulus tests under saturated conditions were used in developing the reduction curves.

The modulus reduction curves as determined by the procedures described above for Specimens 2 and 3 are presented in Figures 4.7 and 4.8, respectively. In addition to the data points from the five relevant cyclic test increments, each curve also shows the range of typical values found for cohesionless soils (after *Seed et al., 1984*). One would typically expect data for more cohesive soils, such as those tested in this project, to fall above or near the upper limit of this range, as do Specimens 2 and 3. While there is a larger variation in the locations of these curves than one might expect for relatively similar materials, given the uncertainties in confining stress both during shear wave propagation and during resilient modulus testing (due to equilibration issues discussed earlier), the data are sufficiently consistent to provide confidence in both testing techniques.

4.3 TRIAXIAL REPEATED LOAD TEST - GRANULAR MATERIALS

Repeated load triaxial compression tests were also performed on the granular base and subbase materials using specimens 100 mm (4 in) in diameter and 200 mm (8 in) in height. As with the tests on the subgrade materials, each specimen was subjected to a static confining pressure. Deviator stress and the resilient axial strain response of the specimen are used to compute a stress-dependent resilient modulus using Equation 4.1.

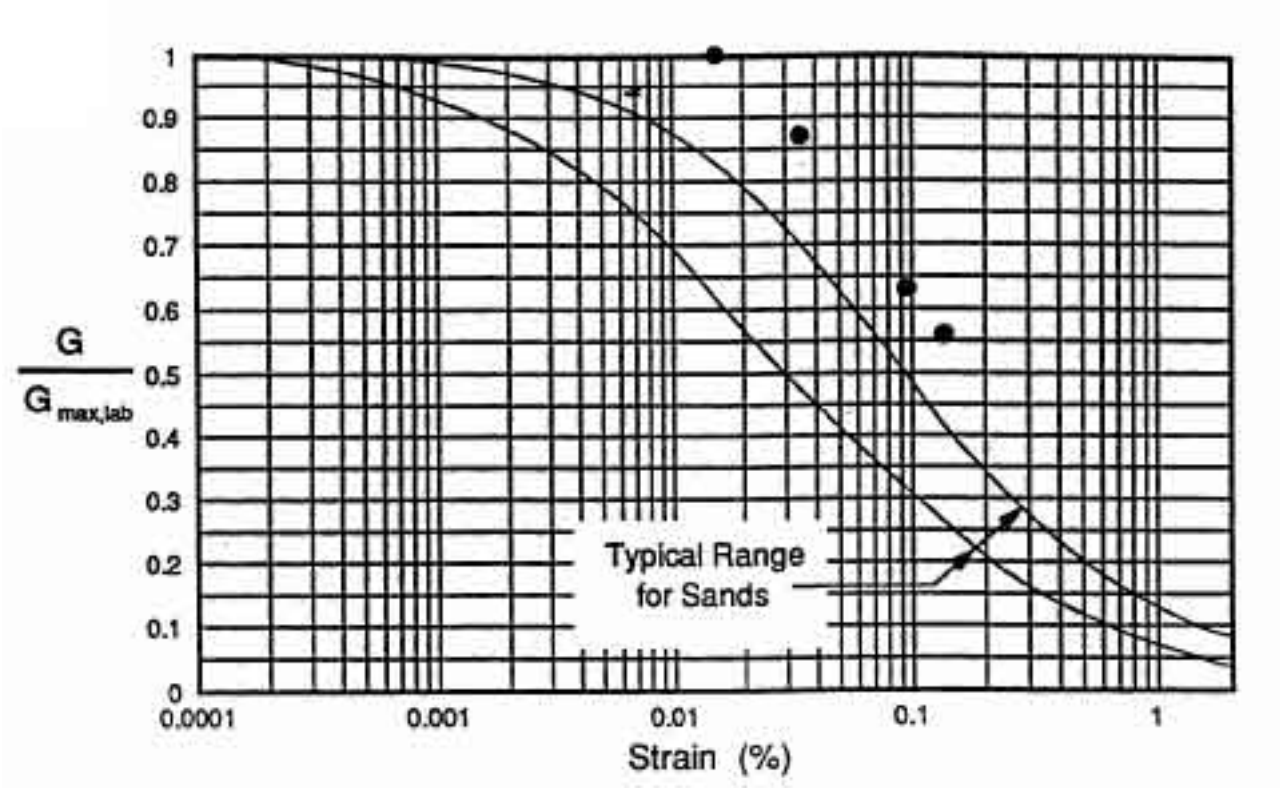

Figure 4.7 Modulus Degradation for Specimen 2 (Soaked)

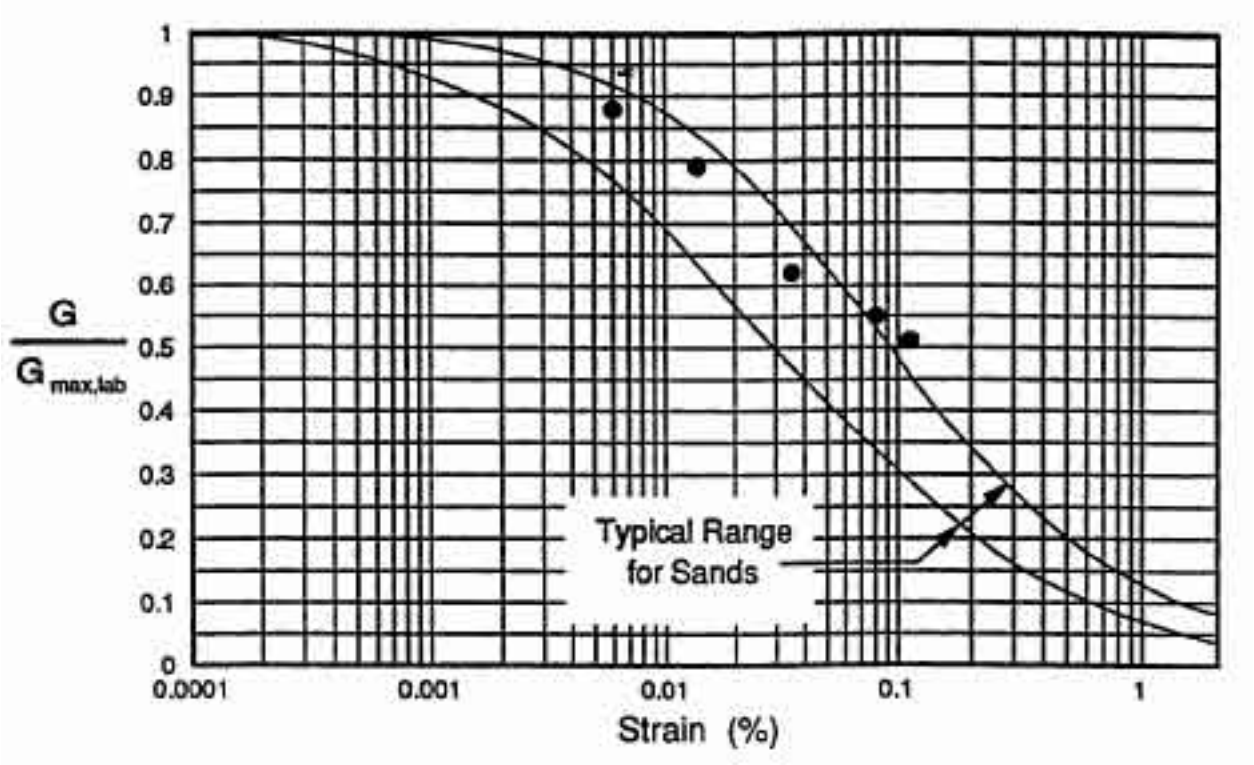

Figure 4.8 Modulus Degradation for Specimen 3 (Soaked)

4.3.1 Equipment, Specimen Preparation, and Test Procedures

The resilient modulus testing system is composed of the following components:

- Specimen preparation equipment: split mold and hand-held pneumatic hammer, membrane expander, ruler, and bottom plate.
- Loading frame and pressure cell: the pneumatic loading device consists of a double acting piston, load cell, and a loading shaft and operates at up to 759 kPa (110 psi) air pressure. The pressure cell contains a vacuum saturation line, bottom drainage line, cell pressure line, cell cover plate, cell base plate, and tie rods.
- Data collection elements: this subsystem contains an IBM 386 computer equipped with Automated Testing System (ATS) software *(Bronstein and Sousa, 1993)*, load cell, LVDTs, LVDT clamps, and pressure transducer.
- Other equipment: calipers, micrometer gage, membranes, vacuum source with bubble chamber and manometer, and porous stones.

Each specimen is compacted in a split mold using a hand-held vibrator. The amount of wet soil required for one layer is placed into the mold and compacted to the desired density; a total of five 40 mm (1.6 in) lifts are required to produce the 200 mm (8 in) high specimen. After the specimen is compacted, a 35 kPa (5 psi) vacuum pressure is applied to detect leakage via the bubble chamber. The LVDT clamps are then placed at the upper and lower quarter points of the specimen and the distance (center to center) between these two clamps is carefully measured: this serves as the input height of the specimen to ATS software which determines axial strain in the specimen. The ATS software uses digital, closed-loop load control and incorporates a data acquisition subsystem.

Once the triaxial chamber has been assembled, sample conditioning can be accomplished by applying various combinations of confining pressures and deviator stresses as follows:

Confining Pressure, s_3 kPa (psi)	Deviator Stress Sequence, s_d kPa (psi)	Number of Repetitions at Each s_d
35 (5)	35 (5), 69 (10)	200
69 (10)	69 (10), 104 (15)	200
104 (15)	104 (15), 138 (20)	200

After the specimen is conditioned, the following load sequence is used:

Confining Pressure, s_3 kPa (psi)	Deviator Stress Sequence, s_d kPa (psi)	Number of Repetitions at Each s_d
138 (20)	6.9, 14, 35, 69, 104, 138 (1, 2, 5, 10, 15, 20)	200
104 (15)	6.9, 14, 35, 69, 104, 138 (1, 2, 5, 10, 15, 20)	200
69 (10)	6.9, 14, 35, 69, 104 (1, 2, 5, 10, 15)	200
35 (5)	6.9, 14, 35, 69, 104 (1, 2, 5, 10, 15)	200
6.9 (1)	6.9, 14, 35, 69 (1, 2, 5, 10)	200

4.3.2 Test Results - Aggregate Base

Materials for aggregate base specimens were quartered from a composite of samples from across the test sections. Specimens of the aggregate base (AB) were prepared at two wet densities, 2.47 g/cc and 2.40 g/cc, both having the same water content, 5.5 percent. Two

specimens at the density of 2.47 g/cc, designated AB1 and AB2, were prepared. Similarly, two specimens, designated AB3 and AB4, were prepared at the smaller density. The temperature of the test was 20 ± 2°C. The relationship between the resilient modulus (M_R) and the sum of the principal stresses (SPS) was determined for each specimen as follows:

$$M_R = A \bullet SPS^B \quad (4\text{-}4)$$

where M_R is the resilient modulus in kPa, SPS is the sum of principal stresses in kPa, and A and B are experimentally determined coefficients. Each specimen was then saturated, and the relationship between M_R and SPS was determined for the saturated state. The test and saturation procedure was based on the AASHTO designation: T274-82 (1986): Resilient Modulus of Subgrade Soils *(American Association of State Highway and Transportation Officials, 1986)*.

Specimen AB5 was prepared to a wet density of 2.47 g/cc at a 5.5 percent water content. Only a saturated resilient modulus test was conducted on this specimen to evaluate any effects of the testing procedure in which the saturated resilient modulus test follows the as-compacted resilient modulus test.

Specimen AB6 was prepared to simulate the in-situ dried-out condition. The specimen was first compacted to a wet density of 2.47 g/cc at a water content of 5.5 percent: it was then wrapped with a membrane and placed at room temperature for 10 days with the top end open. After this drying period, a resilient modulus test was conducted followed by saturation, and a resilient modulus test was again performed.

Appendix D summarizes he test data, and Table 4.3 summarizes the test conditions.

Table 4.3 Summary of Conditions for Repeated Load Tests, Aggregate Base and Subbase

Material	Specimen Designation	Water Content at Compaction (percent)	Wet Density g/cc (lb/ft^3)	Test Conditions
Base	AB1	5.5	2.47 (154)	Tested as-compacted and after saturation
	AB2	5.5	2.47 (154)	Same as AB1
	AB3	5.5	2.40 (150)	Same as AB1
	AB4	5.5	2.40 (150)	Same as AB1
	AB5	5.5	2.47 (154)	Tested only in saturated condition
	AB6	5.5	2.47 (154)	After compaction, allowed to dry-out for 10 days; testing of "dry" condition and again after saturation
Subbase	SB1	7.5	2.44 (152)	Tested as-compacted and after saturation
	SB2	7.5	2.44 (152)	Saturated condition only

For this interim report, only the results for tests in the saturated condition for Specimens AB2, AB3, AB4, and AB5 are briefly considered (Figures 4.9 through 4.12). Specimen AB1 failed during modulus testing. As-compacted results are not available due to an error in the testing. Results of the tests for AB6, after drying and in the saturated condition, are shown in Figure 4.13.

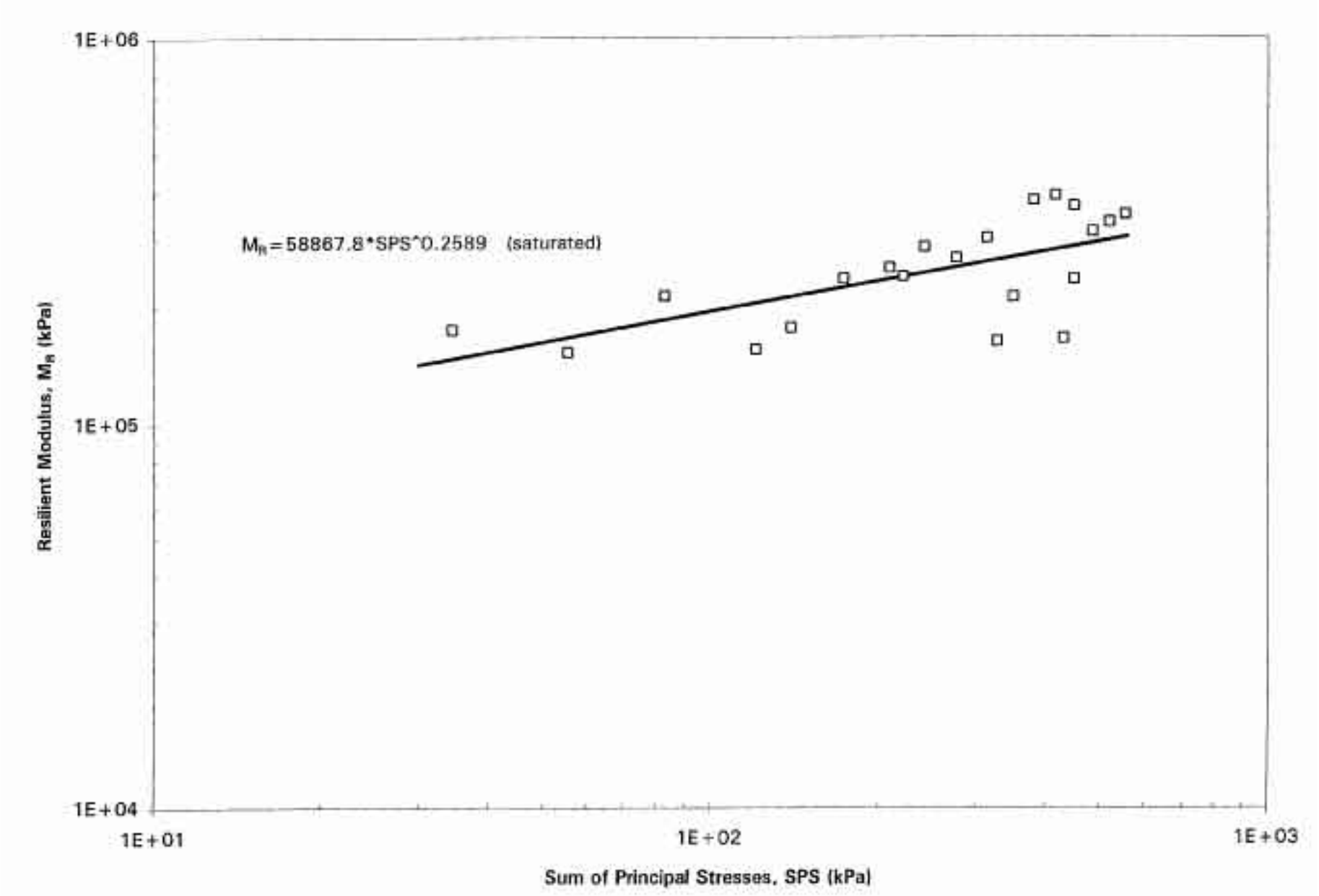

Figure 4.9 Resilient Modulus Test Results of AB2 Specimen (Saturated)

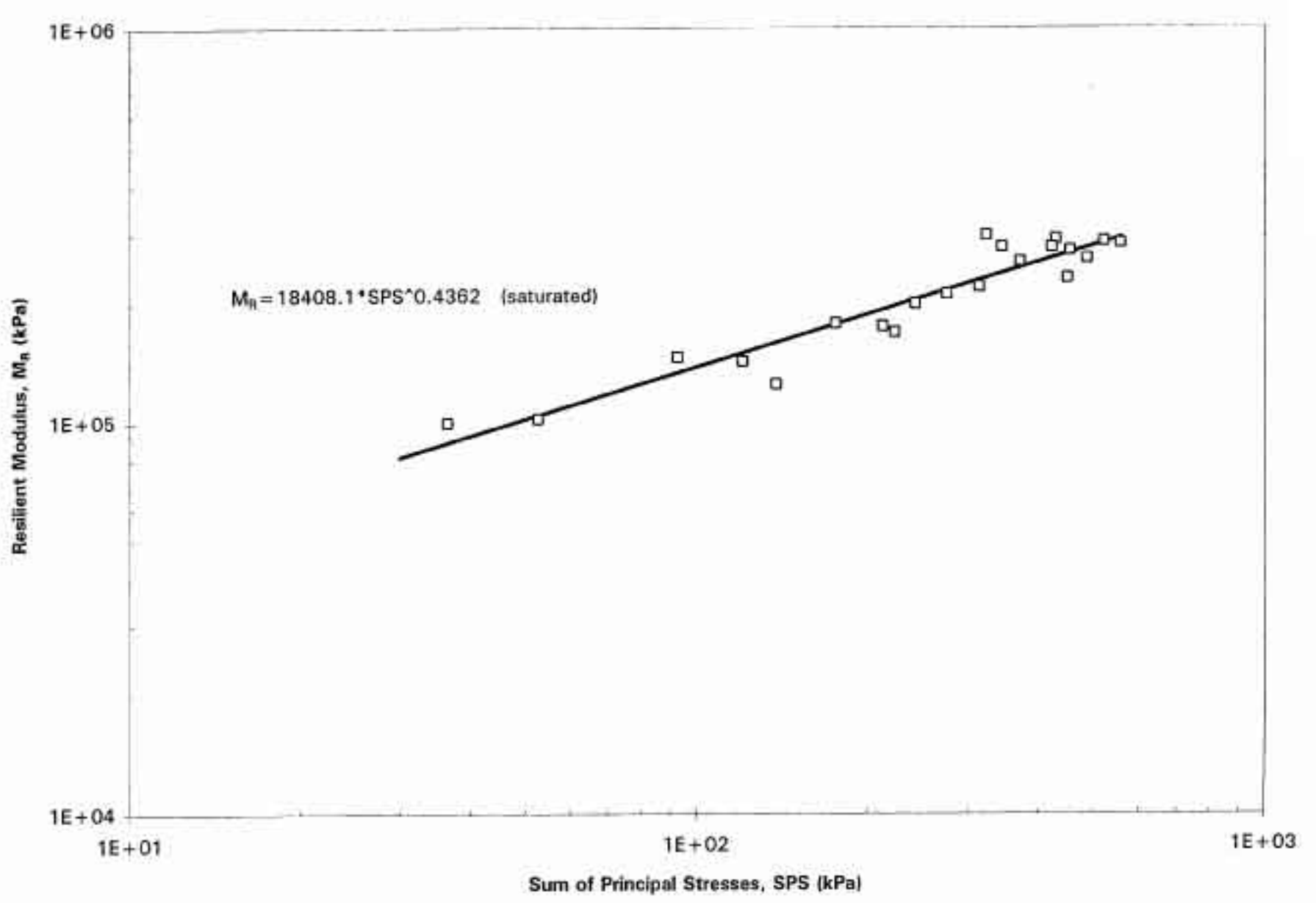

Figure 4.10 Resilient Modulus Test Results of AB3 Specimen (Saturated)

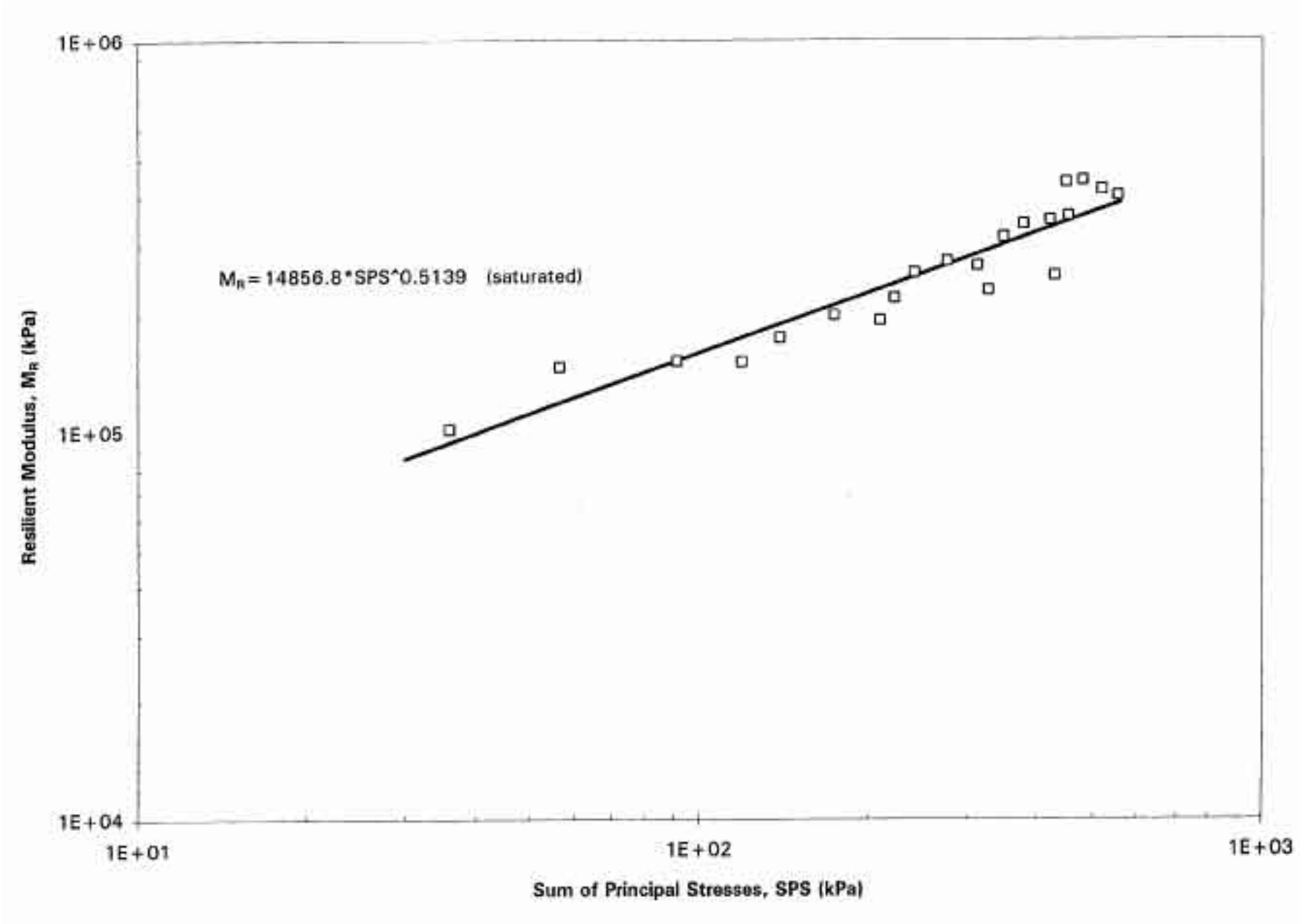

Figure 4.11 Resilient Modulus Test Results of AB4 Specimen (Saturated)

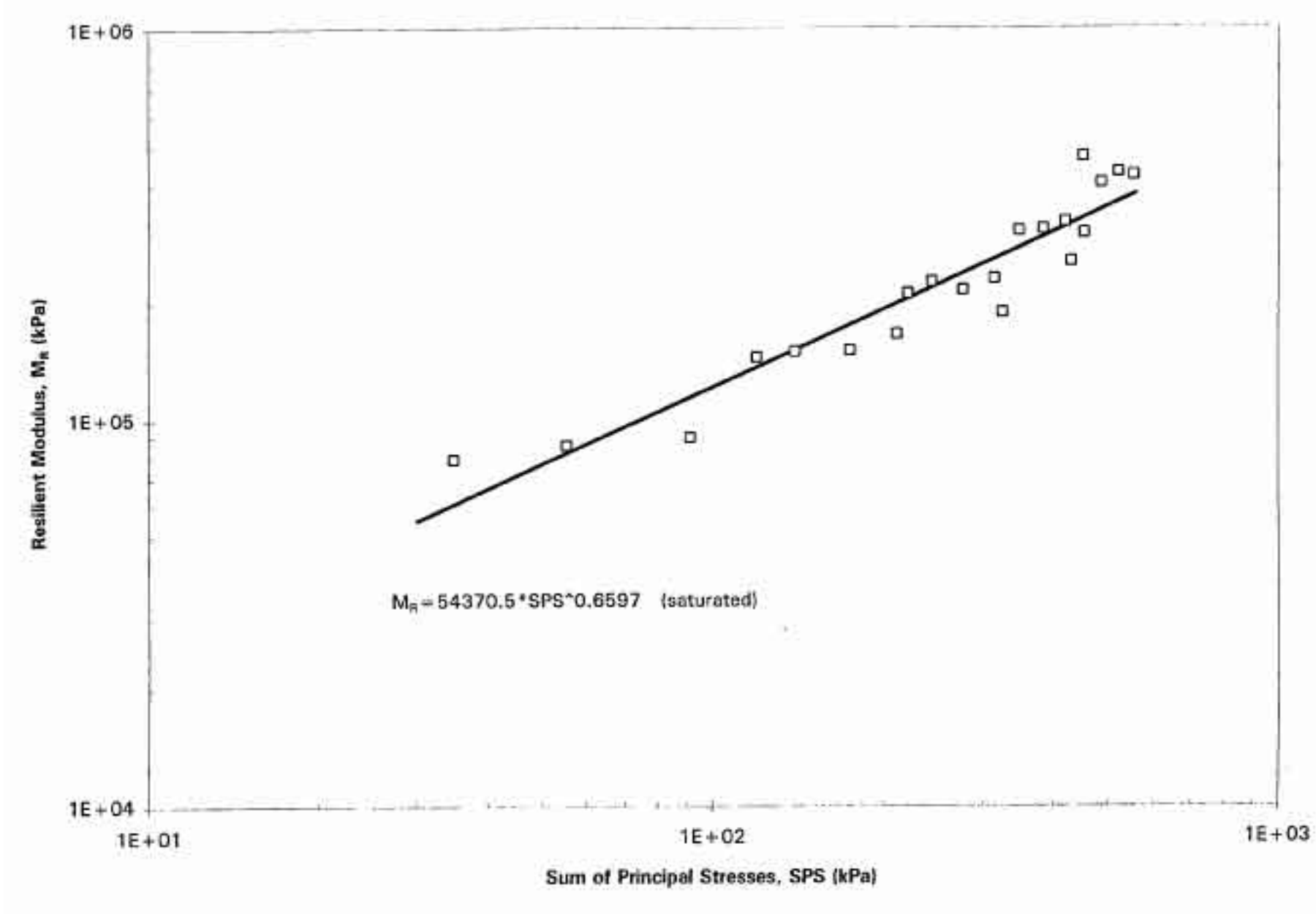

Figure 4.12 Resilient Modulus Test Results of AB5 Specimen (Saturated)

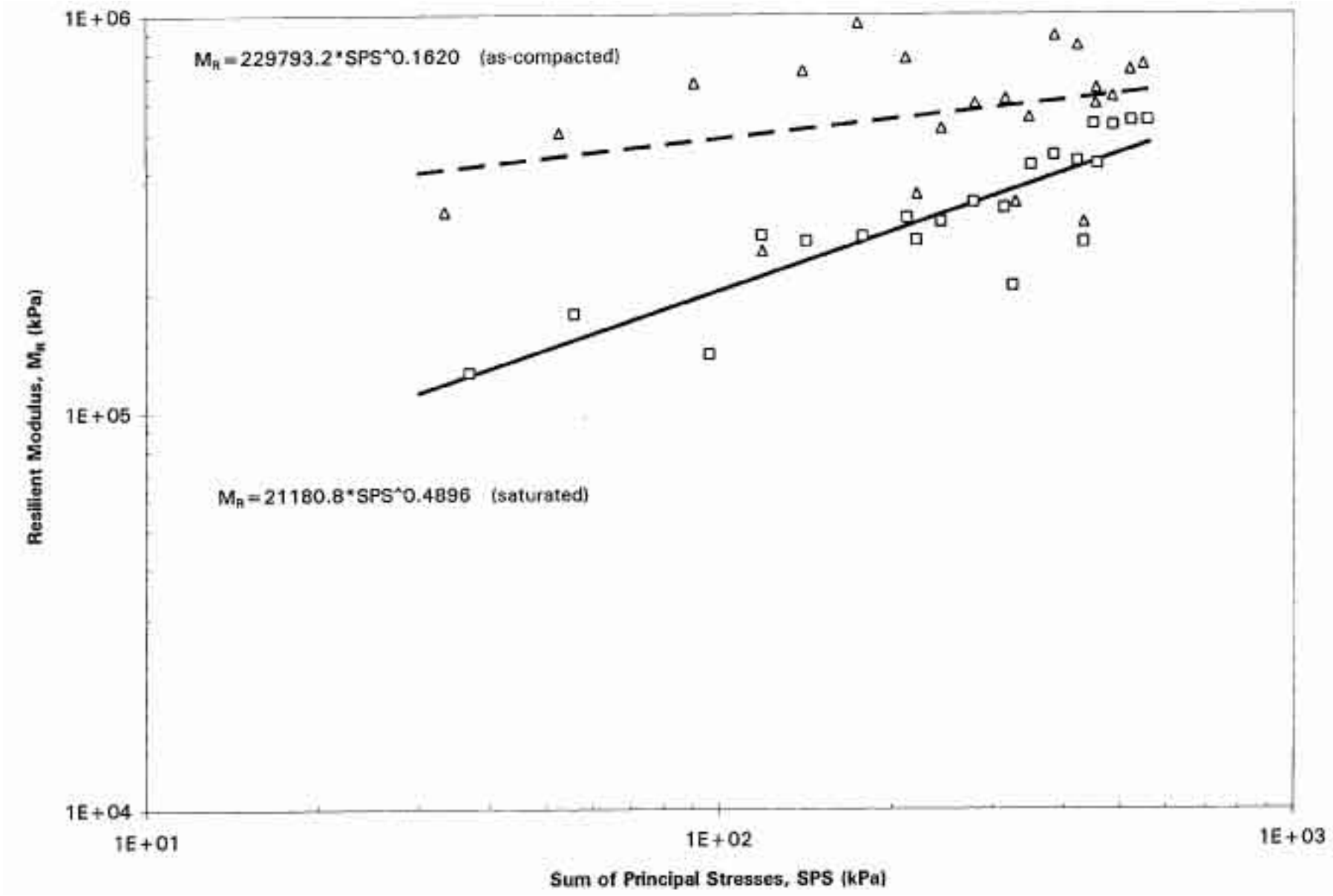

Figure 4.13 Resilient Modulus Test Results of AB6 Specimen

Possibly as a result of its larger density, moduli of Specimen AB2, over the range of stress conditions used, are larger than those for specimens AB3 and AB4, which are reasonably similar to each other. The moduli of Specimen AB5, tested only in the saturated condition, are similar to those for specimens AB3 and AB4 even though the initial unit weight of Specimen AB5 was larger. It is likely that, during the testing of specimens AB3 and AB4 in the as-compacted condition, some densification occurred. On the other hand, Specimen AB5 was tested only in the saturated condition. Accordingly, the densities of specimens AB3, AB4, and AB5 may have been similar when tested in the saturated state, although AB3 and AB4 were initially compacted to lower densities.

Moduli of Specimen AB6 are shown in Figure 4.13. As a result of the ten day "drying" procedure described earlier, the water content decreased from 5.5 percent to 2.9 percent. Thus, Specimen AB6 "dry" is included to compare the dry and saturated conditions. Interestingly, the results for the tests in the saturated condition are similar to those for Specimen AB2. These data are summarized in Figure 4.14 for comparative purposes.

4.3.3 Test Results - Aggregate Subbase

The aggregate subbase (ASB) contains large portions of gravel and rock (material coarser than the 4.75 mm [No.4] sieve). Because of the required specimen size, it was impossible to compact the material in the laboratory. Accordingly, the scalp-and-replace method of ASTM procedure D698-78, Method D *(American Society for Testing and Materials, 1989)* was used in the preparation of two specimens, SB1 and SB2. The scalp-and-replace method requires removal of all material larger than 19 mm with replacement by

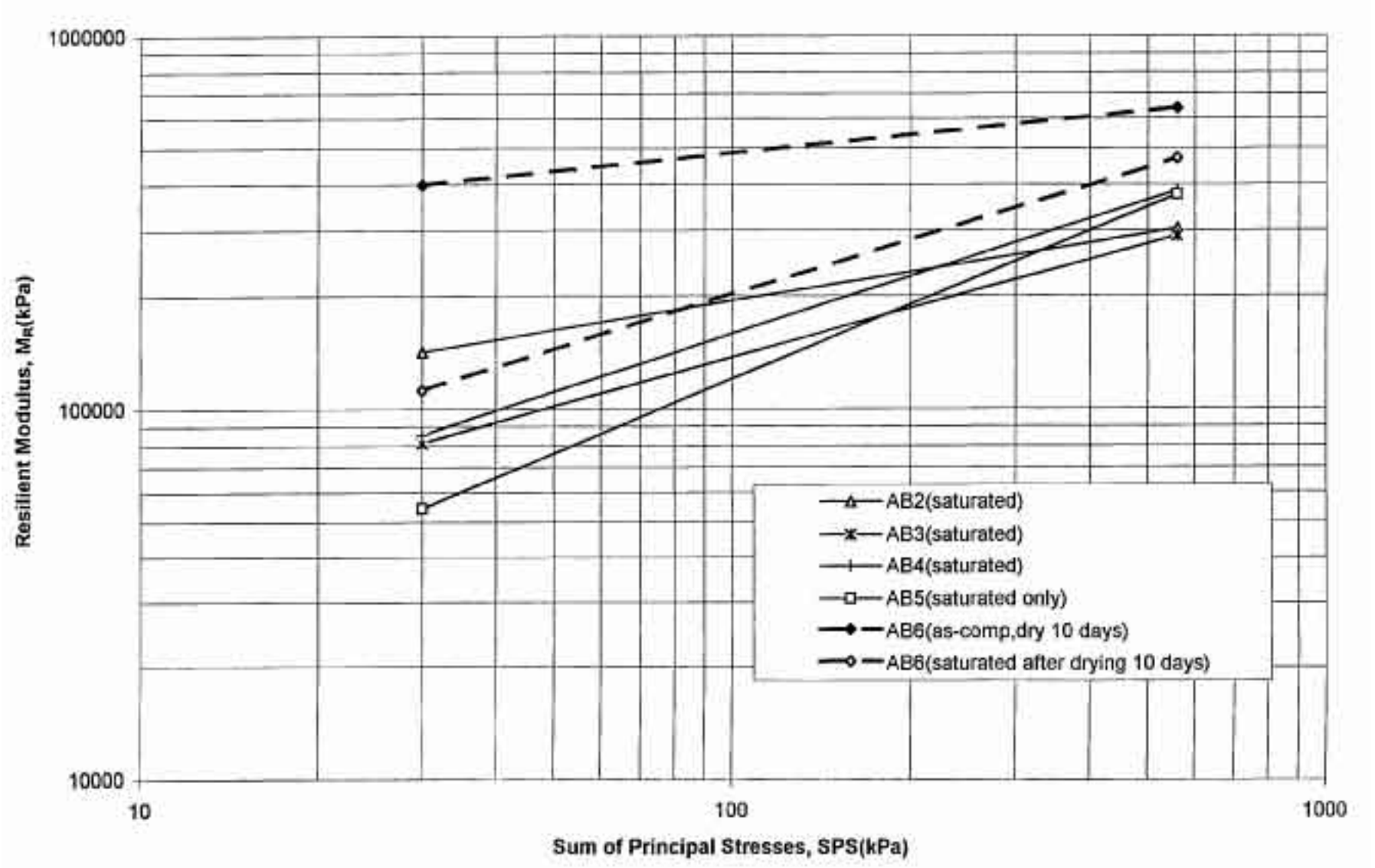

Figure 4.14 Comparison of Triaxial Test Results, Aggregate Base

an equal weight of 4.75 mm to 19 mm material. The specimens were compacted to a dry density of 2.43 g/cc and 7.5 percent water content. Both specimens were tested in saturated states. Specimen SB1 was first tested in the as-compacted state; however, those data were not considered reliable due to an omission in its testing.

Moduli of saturated Specimens SB1 and SB2 are shown in Figures 4.15 and 4.16, respectively. The moduli of Specimen SB1 are larger than those of Specimen SB2 because Specimen SB1 was tested in the as-compacted condition prior to saturation (presumably resulting in additional densification). Comparison of these data with those in Figures 4.9 through 4.13 indicate that the moduli of the saturated subbase are somewhat smaller than those of the aggregate base.

4.4 K-MOLD DETERMINATION OF THE ELASTIC AND SHEAR PROPERTIES

The Division of Roads and Transport Technology (DRTT) of the Council for Scientific and Industrial Research (CSIR) has developed an easy to use triaxial compression testing rig, termed the K-mold *(Semmelink, 1994, and Semmelink and De Beer, 1993)*. This device, a schematic diagram of which is shown in Figure 4.17, can be used to measure the elastic and shear properties of treated or untreated roadbuilding materials.

The K-mold has many advantages, both as a routine design tool as well as a research tool. It is far more productive than the conventional triaxial test in that it only requires one specimen instead of a family of similarly prepared specimens to determine the Mohr-Coloumb envelope. Furthermore, all the elastic and shear properties can be determined for each specimen. It also uses standard size density samples (for example, CBR mold size) instead of the larger sizes

required for conventional triaxial testing. Because all the data is determined from one specimen, the measured properties can also be related to the actual

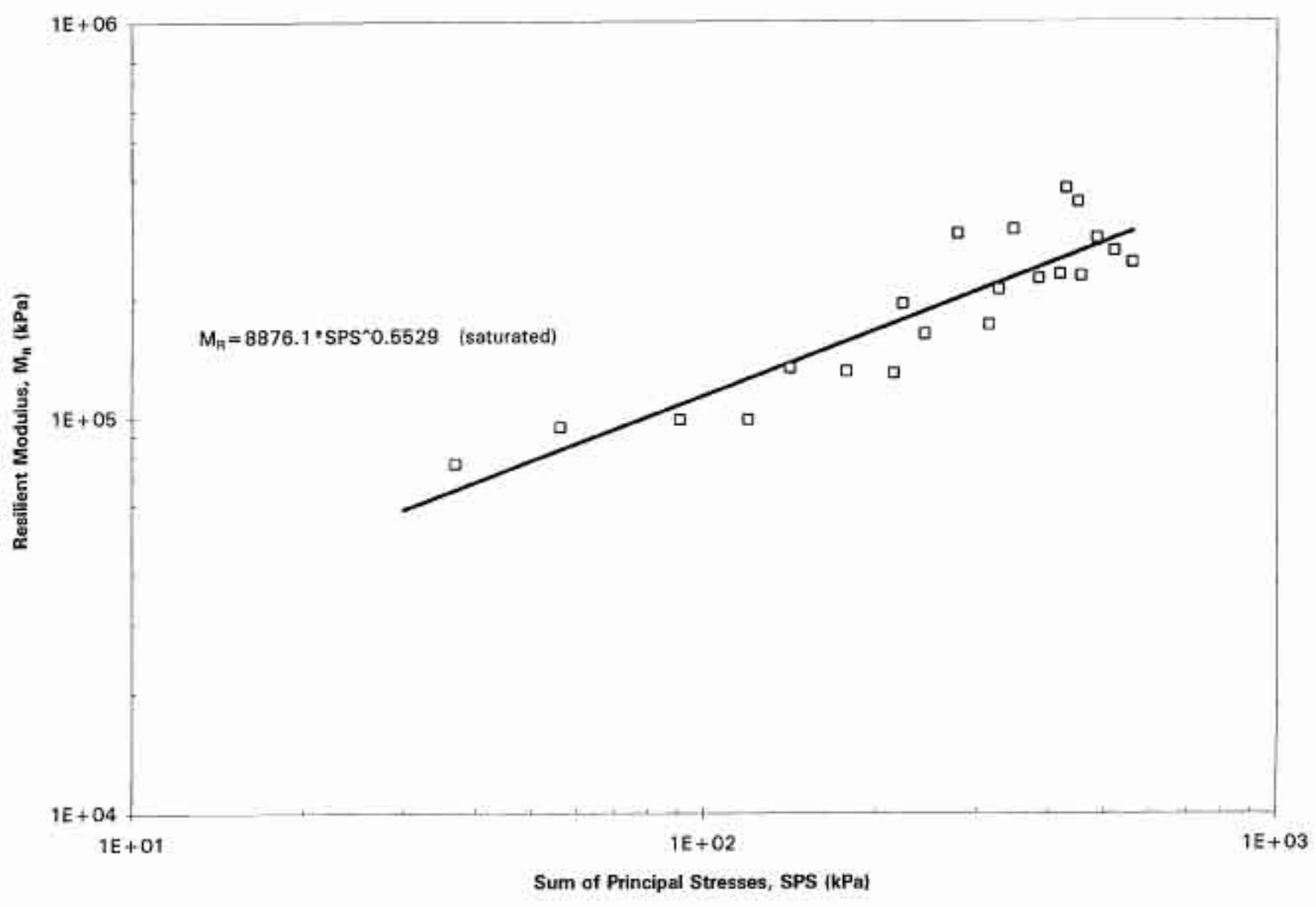

Figure 4.15 Resilient Modulus Test Results of SB1 Specimen (Saturated)

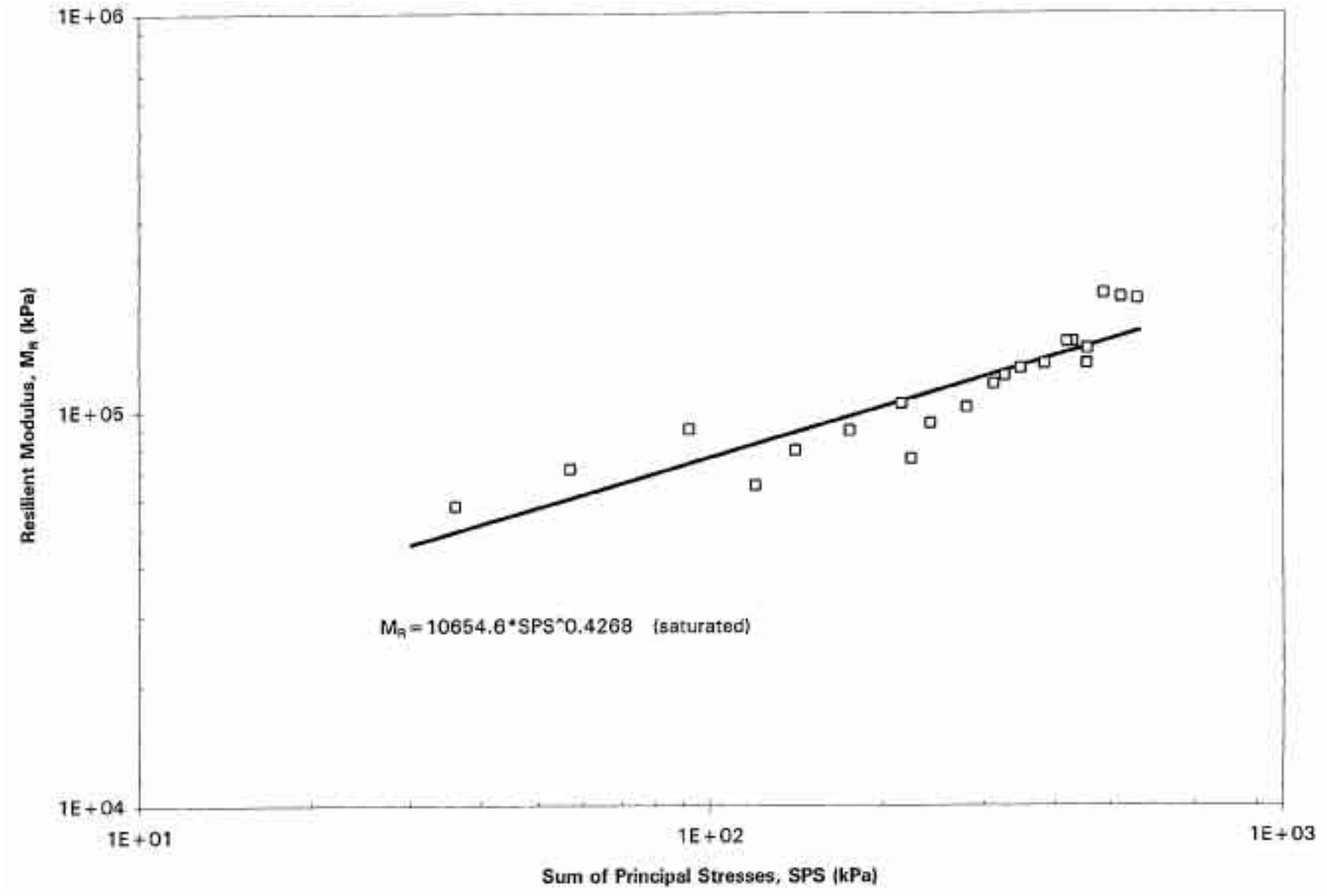

Figure 4.16 Resilient Modulus Test Results of SB2 Specimen (Saturated)

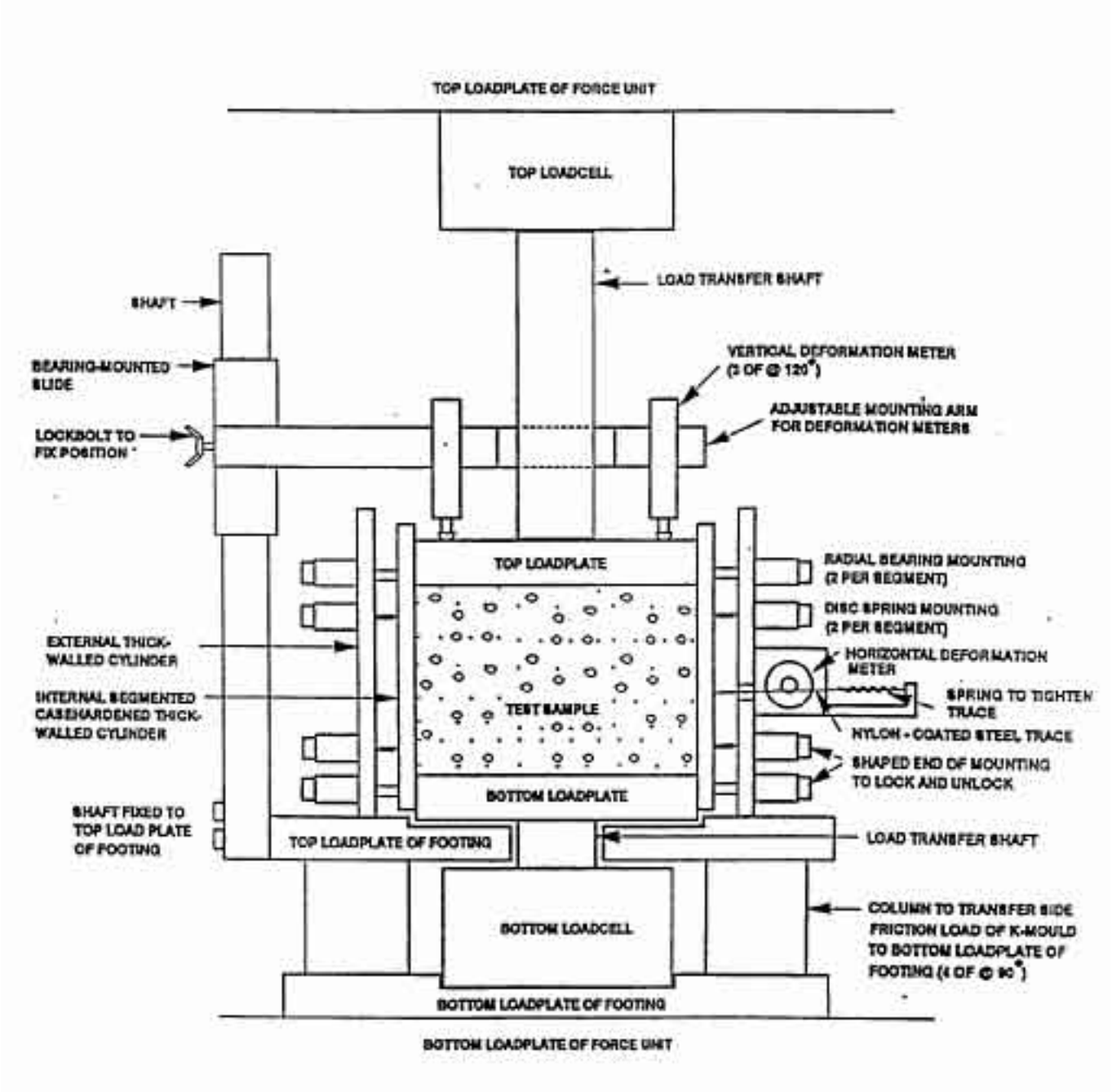

Figure 4.17 Schematic of K-mold Apparatus

specimen conditions (that is, dry density, water content, etc.). Total testing time is also reduced because fewer specimens are required and each is easier to prepare and handle. It also does not require a sophisticated pressure cell.

Although prior research has not directly compared the K-mold test with the conventional triaxial test, a limited comparison was made with back-calculated elastic moduli from HVS experiments. Material samples from the different layers from some HVS sites were compacted to the same density and air-dried to approximately the same water content as the field measurements, after which the samples were tested with the K-mold. In general good agreement was found between K-mold measured elastic moduli and the back-calculated elastic moduli from the HVS pavements *(Semmelink, 1994)*.

Using the K-mold, it is possible to determine the requisite properties of a material at a given density and water content using a single specimen. This results from the fact that the horizontal stress, s_3, changes continuously as the vertical stress, s_1, varies during loading and unloading according to the particular material's response. Unlike most other triaxial compression tests, a pressure vessel is not used.

The mean vertical load (that is, at both top and bottom of the specimen) is used to determine s_1, the mean vertical deformation (that is, at three vertical deformation meters) is used to determine e_1, and the expansion of the specimen circumference is used to determine e_3. Disc springs, which have been calibrated against e_3, are used to measure the horizontal stress, s_3. From these continuous measurements, it is possible to determine, at any given instant, fundamental properties such as E (elastic moduli), c (cohesion), f (internal friction), and v (Poisson's ratio) using standard theories.

Research with the K-mold has shown that both the "loading" and "unloading" phases of the load cycle are actually divided into two separate sub-phases, namely, a rigid or consolidation sub-phase and a dynamic or shear sub-phase. In both loading and unloading phases, the rigid or consolidation sub-phase occurs first because of the material's inherent resistance to change with changing conditions. The E, c, and f values for each of the four sub-phases are determined separately, and v is determined separately for the loading and unloading phases.

For this investigation, two K-mold tests were performed by the CSIR staff on materials from both the subbase and subgrade layers. The materials were tested at approximately the same dry densities and moisture contents as measured in situ by a nuclear moisture/density gage.

An example of the output from the K-mold can be seen in Figure 4.18. The figure shows the materials response in terms of the stress and strain (s_1 and e_1) relationships for the load and unload phases of the load cycle. The average stiffness of the material is calculated as the average stiffness which occurred during the load and the unload phases (that is, the secant modulus, E_{sec}). A summary of the test results for the subbase and subgrade materials is shown in Table 4.4. The average subbase stiffness is thus 103 MPa (14,000 psi), and the average subgrade stiffness is 21 MPa (3,050 psi).

It should be stressed that E_{sec} is the average modulus for both the load and unload phases of the loading cycle and that more accurate response modelling is possible by measuring the tangential slope of the stress/strain diagram at any instant. Comparison with other methods should be viewed in this light and will be discussed further in the final report.

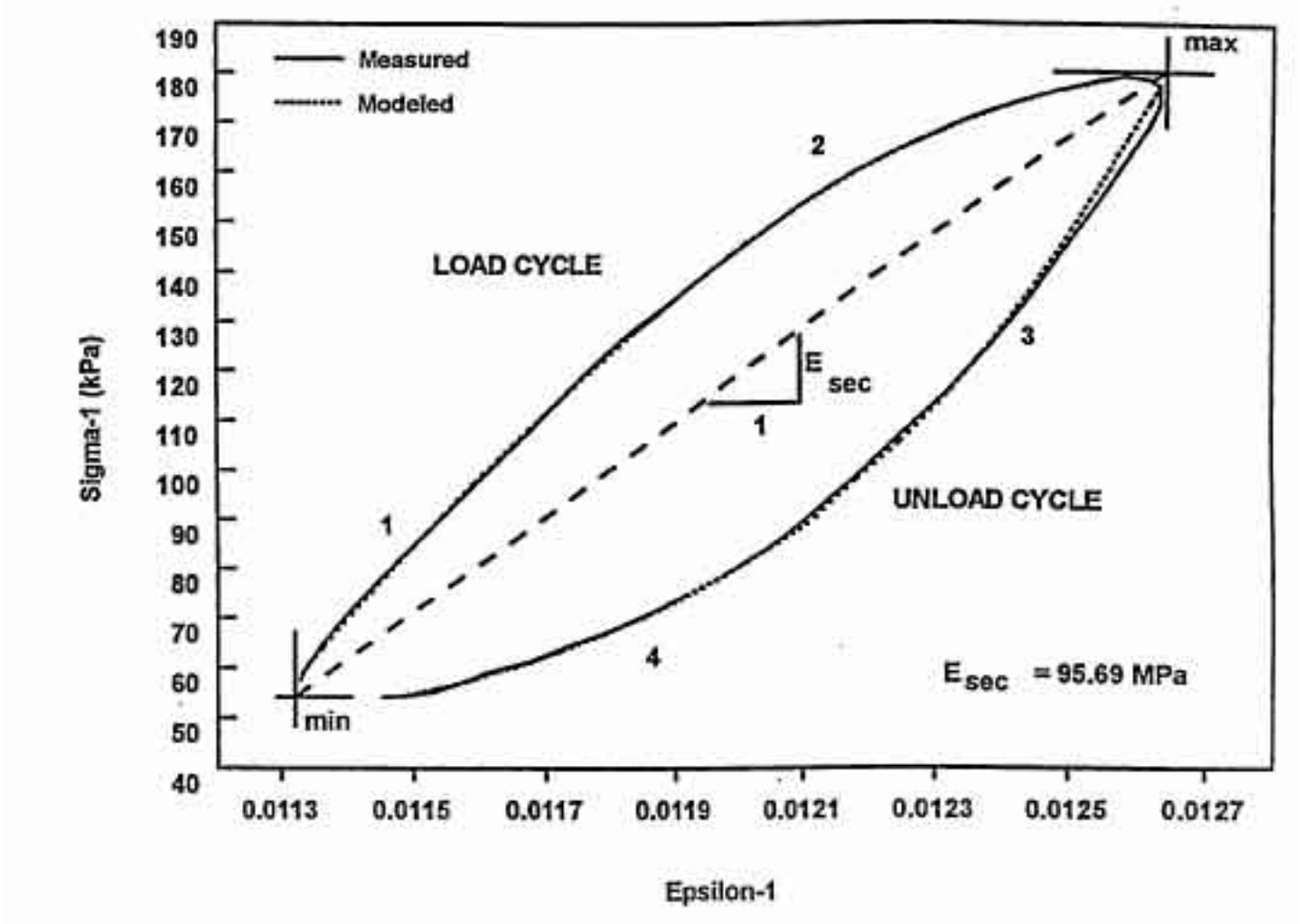

Figure 4.18 Example of Output from the K-mold

Table 4.4 K-Mold Results

Parameter	Specimen 1	Specimen 2	Average
Aggregate Subbase			
Water Content (%)	8.5	8.5	8.5
Dry Density (kg/m3)*	2,159.4	2,166.1	2,162.8
Stiffness (MPa)	109.5	95.7	102.6
Subgrade			
Moisture Content (%)	19.8	19.8	19.8
Dry Density (kg/m^3)*	1,678.9	1,705.7	1,692.3
Stiffness (MPa)	19.9	22.0	21.0

*Dry Density = Average %SD x Solid Density (kg/m^3)

Solid Density = RSD x 1000 (kg/m^3)

RSD = ((100 - P-4.75)/100) x BRD+4.75 + (P-4.75/100) x BRD-4.75

where RSD = relative solid density of the material, P-4.75 = percentage of the material smaller than 4.75 mm, BRD+4.75 = bulk relative density of fraction larger than to 4.75 mm, and BRD-4.75 = bulk relative density of fraction smaller than 4.75 mm

4.5 ESTIMATION OF RESILIENT MODULI FROM R-VALUES

Resilient moduli (M_R) of the subgrade, subbase, and base layers were estimated from R-value testing using correlation charts developed by van Til et al. as part of NCHRP 128 *(van Til et al., 1972)*. They were also estimated using the following equation *(Huang, 1993)*:

$$M_R\,(psi) = 1155 + 555 \bullet R\text{-}value \qquad (4\text{-}5)$$

M_R estimates using Equation 4-5 are consistently larger than those estimated using the NCHRP charts (Table 4.5). For the subgrade, estimates from the chart fall within a much narrower and lower range than do those from the equation. As with the subgrade, estimates for the subbase and base fall into two distinct ranges, with those from the equation being much larger.

4.6 DYNAMIC CONE PENETROMETER ANALYSIS

A full Dynamic Cone Penetrometer (DCP) analysis *(De Beer, 1991)* was undertaken on the test pavement prior to the construction of the asphalt concrete surface. Results of this investigation are covered in full in Appendix E. In this section, only the determinations of effective elastic moduli (E_{eff}), as determined by the DCP, are reported to permit comparisons with stiffness moduli determined by the other testing methods reported in this chapter.

For DCP data to be evaluated and implemented, the penetration rates should be related to known soil parameters. Primarily the penetration data is used to determine standard DCP parameters which can be correlated to soil parameters such as the California Bearing Ratio (CBR), the unconfined compressive strength (UCS), and the effective elastic moduli (E_{eff}).

Table 4.5 Results of R-values

Layer	Sample Number	R-value	Modulus (Chart) (MPa)	Modulus (Equation) (MPa)
Subgrade	1	28	41	115
	2	4	17	23
	3	7	19	35
	4	30	42	122
	5	16	26	69
	Average	**17**	**29**	**73**
	Standard Deviation	**12**	**12**	**45**
Aggregate Subbase	1	75	124	295
	2	72	117	283
	3	82	193	322
	4	55	93	218
	5	67	110	264
	Average	**70**	**128**	**276**
	Standard Deviation	**10**	**38**	**39**
Aggregate Base	1	82	193	322
	2	78	183	306
	3	83	200	325
	Average	**81**	**192**	**318**
	Standard Deviation	**3**	**9**	**10**

Two series of four DCP tests were conducted, one directly after construction of the base and another ten days after construction of the base. The locations were on the transverse centerline of the sections and evenly spaced in the longitudinal direction (Figure 4.1). Results are summarized in Table 4.6. Because the DCP software uses pre-determined empirically based data to calculate E_{eff} values, accuracy depends on material type and the

Table 4.6 Summary of Effective Moduli from DCP Analysis

Layer	DCP Test Number				Average
	1	2	3	4	
	E_{eff} (MPa) just after construction of base				
Base	160	149	202	284	199
Subbase	391	116	211	197	229
Subgrade	171	43	56	49	80
	E_{eff} (MPa) 10 days after construction of base				
Base	727	482	429	493	533
Subbase	305	230	296		305
Subgrade	51	69	43	55	55

in-situ moisture and density conditions. Therefore, the moduli reported in Table 4.6 are subject to further analysis and interpretation.

From an evaluation of the data it is noted that:

? the base and subbase gained significant structural strength from just after construction to 10 days after construction, as shown by the smaller effective stiffness values for the first series of tests as compared to the second;

? the calculated E_{eff} of the subgrade was not greatly affected by changes in strength of the upper layers;

? in terms of the structural bearing capacity, the subgrade is significantly weaker than the upper layers, as shown by its much smaller stiffness; and

? the stiffness varies by location possibly as a result of localized variability in material quality, grading, compaction effort, and water content.

4.7 ELASTIC SURFACE DEFLECTION ANALYSIS

High coverage deflection testing was carried out on various pavement structural layers during and after construction. On each of four separate occasions, measurements were taken every 3.05 m (10 ft) along each of five rows (four where the K-rail obstructed a fifth) running the 61 m (200 ft) length of the test area. Deflections were measured using a Dynatest 8081 Heavy Weight Deflectometer (HWD).

A summary of the various HWD runs is presented in Table 4.7 based on the following measurements:

- at the surface of subbase (ASB) prior to the construction of the base (AB) layer,
- at the surface of base immediately after the construction of the base layer,(AB layer - 1st run),
- at the surface of base 17 days after the construction of the base layer (AB layer - 2nd run), and
- at the surface of asphalt concrete (AC) one day after construction of the AC layer.

Table 4.7 Average Normalized Surface Deflections

HWD Runs	Structure at time of test	Surface Deflection (mm)	One Standard Deviation	Coefficient of Variation (%)
Run 1	ASB layer	2.149	0.92	43
Run 2	AB layer (1st run)	1.773	0.68	38
Run 3	AB layer (2nd run)	0.879	0.28	32
Run 4	AC layer	0.306	0.07	23

Although analyses were performed on both the drained and undrained pavement structures, no significant difference was detected between the two sets of surface deflections. While a positive effect on surface deflections would be expected with the addition of 75 mm (3 in) of ATPB to even a moderately thick structural section, there would also be a positive effect with the addition of the same thickness of good quality aggregate base. Thus, relative differences between the effects of these two layers would be difficult to evaluate in comparatively thick sections, like those constructed for the test sections. Variability of the deflections measured at the surface of the subbase (due to high levels of precipitation immediately prior to testing) further complicate the issue.

The increase in structural capacity of the pavement with the addition of layers is clearly illustrated in Table 4.7. The average elastic surface deflections decreased from approximately 2.1 mm measured on the ASB layer to 0.3 mm on the AC layer. Table 4.7 also shows the variability, as measured by the standard deviation encountered during initial testing, and the subsequent consistent and uniform response after the application of the AC layer.

Although the base course met Caltrans specifications regarding density, gradation, and quality, it was difficult to measure deflections on its surface immediately following construction. At that time, measured deflections averaged 1.77 mm, twice the average of 0.88 mm measured 17 days after construction. This effect is likely due to differences in water content, but it is not clear how much may also have been due to sensor penetration into the surface during the early tests.

Moduli were determined by back-calculation using the program ELMOD. Results of these calculations are summarized in Table 4.8. Variation in moduli along the four rows are

shown in Figure 4.19-4.21 for the asphalt concrete, base/subbase, and subgrade, respectively. It should be noted that the deflections measured on the asphalt concrete were taken the morning after that layer was placed. Because the asphalt concrete was very fresh, and probably still warm from construction, the back-calculated moduli for that layer are substantially lower than those measured for beams and cores taken several months later.

Table 4.8 Stiffness Moduli from Back-Calculations of HWD Deflection Data

Measure	Modulus - MPa (ksi)		
	Subgrade	Base/Subbase	Asphalt Concrete
Tests at Surface of Asphalt Concrete			
Average	132.1 (19.2)	284.9 (41.4)	3,230.5 (468.9)
Standard Deviation	22.2 (3.3)	73.0 (10.7)	903.9 (133.1)
80th Percentile	113.4 (16.4)	223.6 (32.4)	2,471.2 (357.1)
Tests at Surface of Base (Test No 1)			
Average	111.5 (16.2)	104.9 (15.2)	-
Standard Deviation	48.0 (7.0)	53.9 (7.9)	-
80th Percentile	71.2 (10.3)	59.6 (8.6)	-
Tests at Surface of Base (Test No 2)			
Average	116.0 (16.8)	241.7 (35.1)	-
Standard Deviation	23.3 (3.4)	101.3 (14.7)	-
80th Percentile	96.4 (14.0)	156.9 (22.7)	-
Tests at Surface of Subbase			
	Subgrade	Subbase	
Average	111.4 (16.1)	82.4 (11.9)	-
Standard Deviation	38.5 (5.6)	71.2 (10.3)	-
80th Percentile	79.0 (11.5)	22.6 (3.3)	-

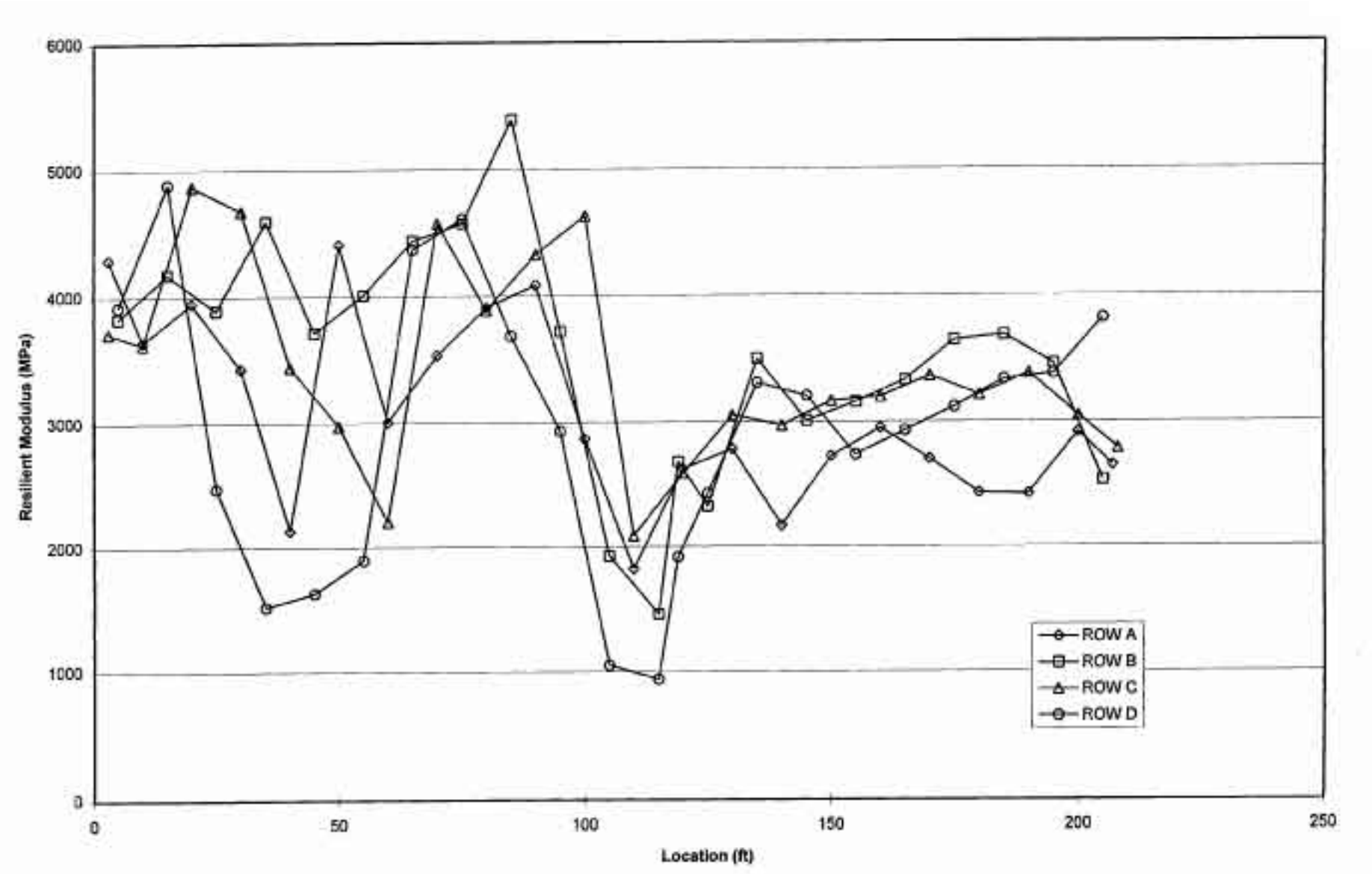

Figure 4.19 Back-Calculated Asphalt Concrete Moduli

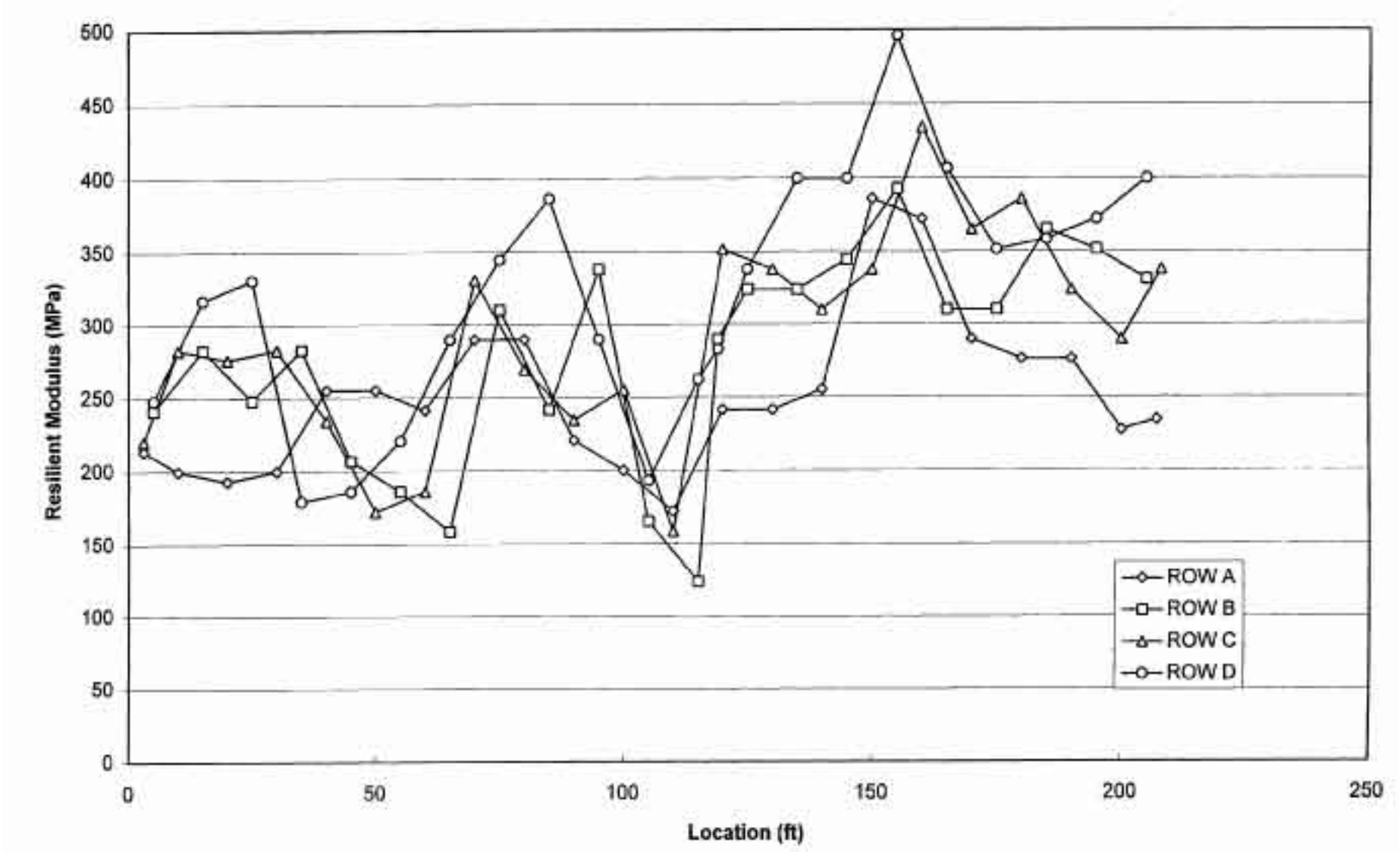

Figure 4.20 Back-Calculated Base/Subbase Moduli

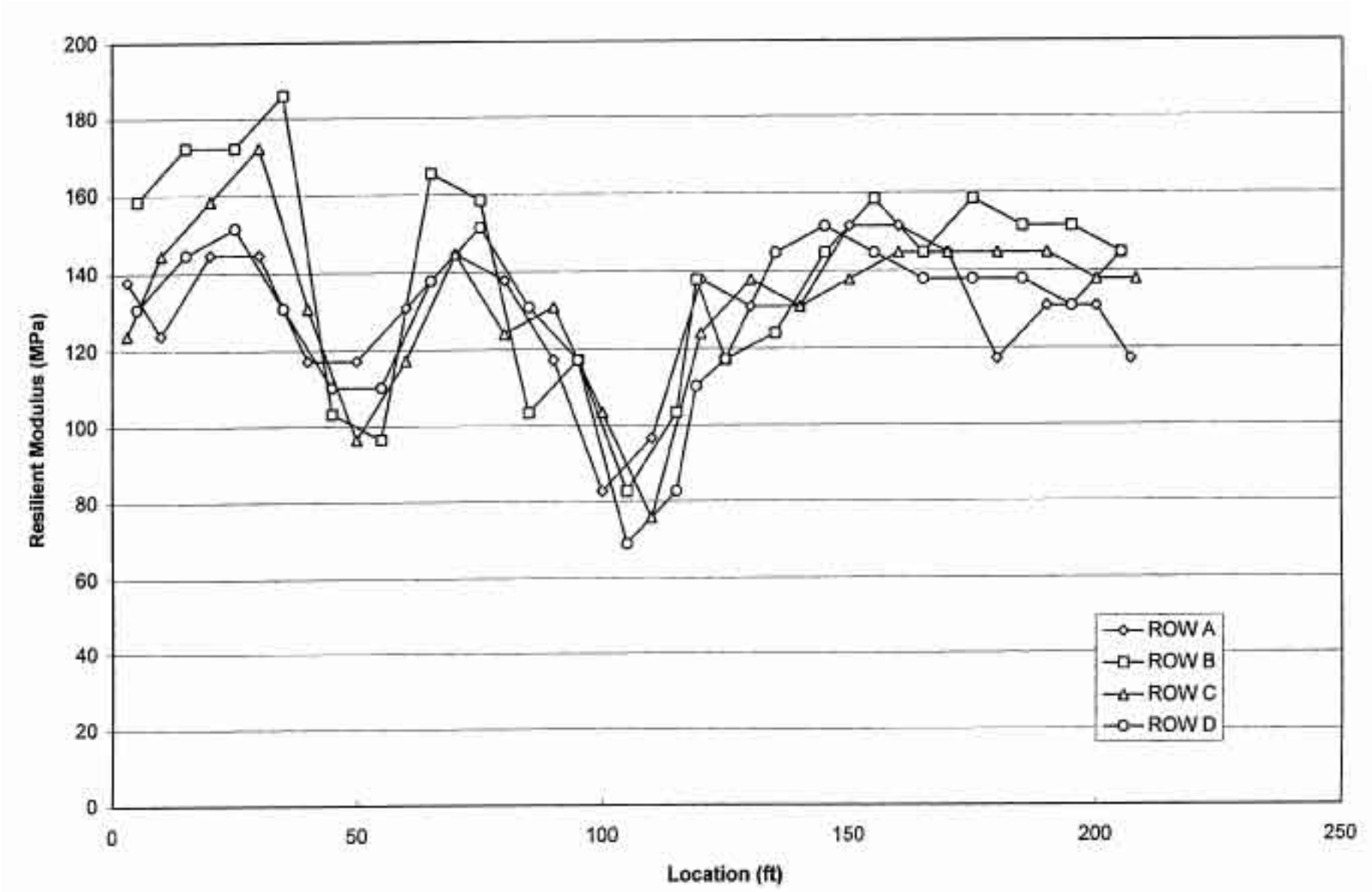

Figure 4.21 Back-Calculated Subgrade Moduli

Contour plots of the variation in moduli are shown in Figures 4.22-4.24. The program SYSTAT was used to obtain these plots.

4.8 MODULI COMPARISONS

The various methods used to determine moduli of the unbound materials produced wide ranges of estimated values. Sampling condition and specimen preparation greatly affect results of laboratory compacted and tested specimens. In addition, each laboratory and field test has its own set of stress-strain states. Variation of in-situ moisture conditions, compaction, and material quality influence stiffness estimates from DCP and deflection tests.

Any comparison of moduli estimated by various methods should bear in mind the specimen preparation on in-situ condition of the material, strain levels, and the method used to arrive at the estimate, i.e. back-calculation, direct measurement, correlation equations, etc. The comparison presented in the following sections suggest that these considerations should be noted when using estimates from any method.

4.8.1 Subgrade

Estimations of elastic subgrade moduli from all tests are shown in Figure 4.25. The subgrade modulus estimated from the R-value, K-mold, DCP, and HWD was the single value obtainable from each of the tests under its standard stress-strain and frequency conditions.

Subgrade moduli from the triaxial test, which is performed over a range of stress states, were estimated at the stress state expected near the subgrade surface (predicted using elastic layer theory). The assumed surface loading was that imposed by the HVS with dual tires, 689 kPa (100 psi) pressure, and a 100 kN (22,500 lb) load.

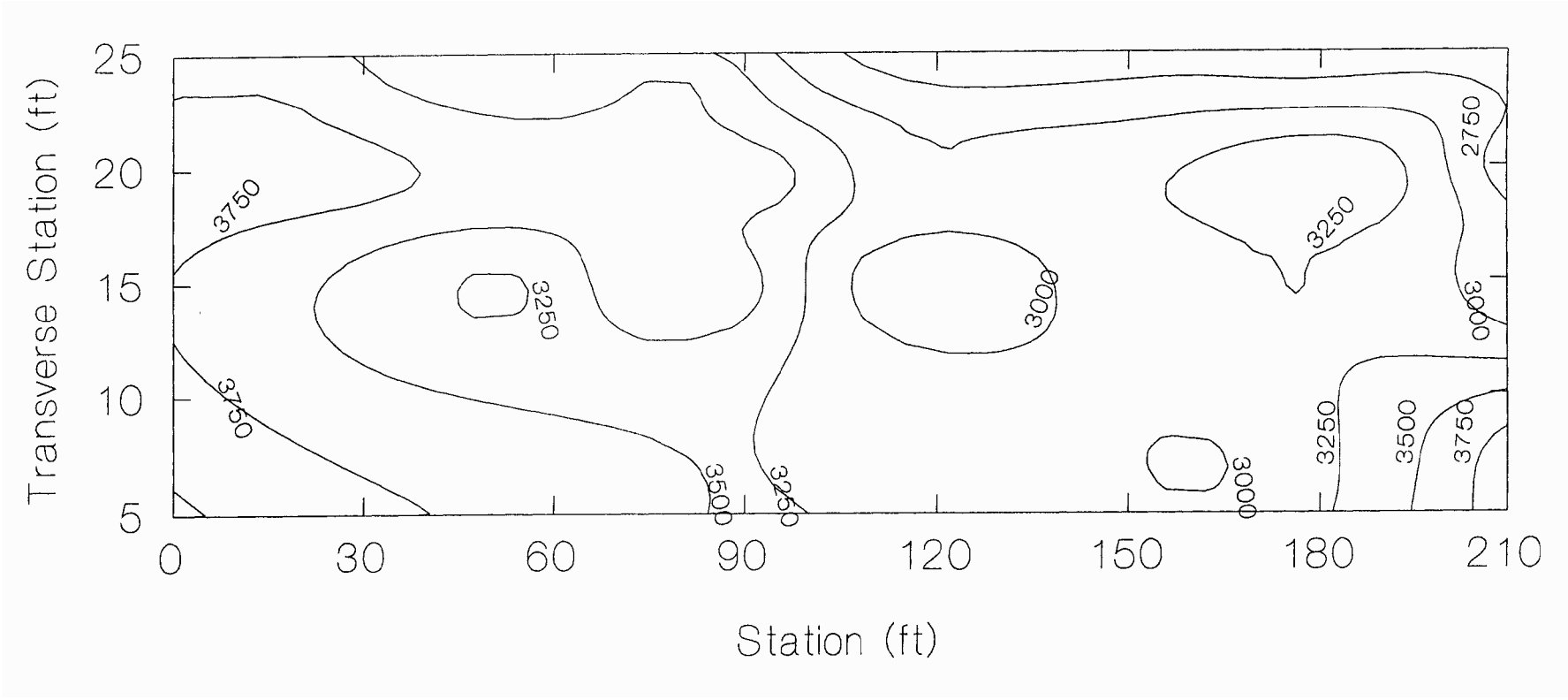

Figure 4.22 Contour Map of Asphalt Concrete Moduli Within Test Sections

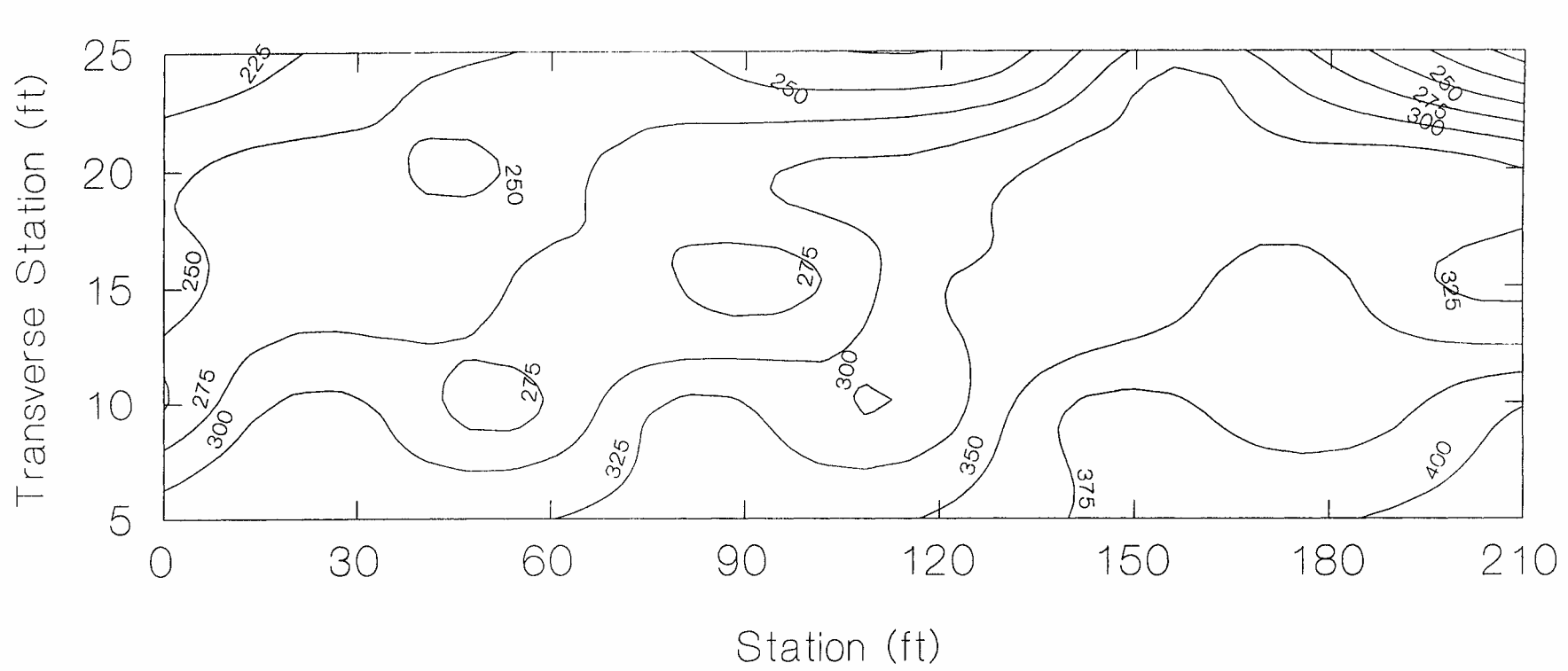

Figure 4.23 Contour Map of Base/Subbase Moduli Within Test Sections

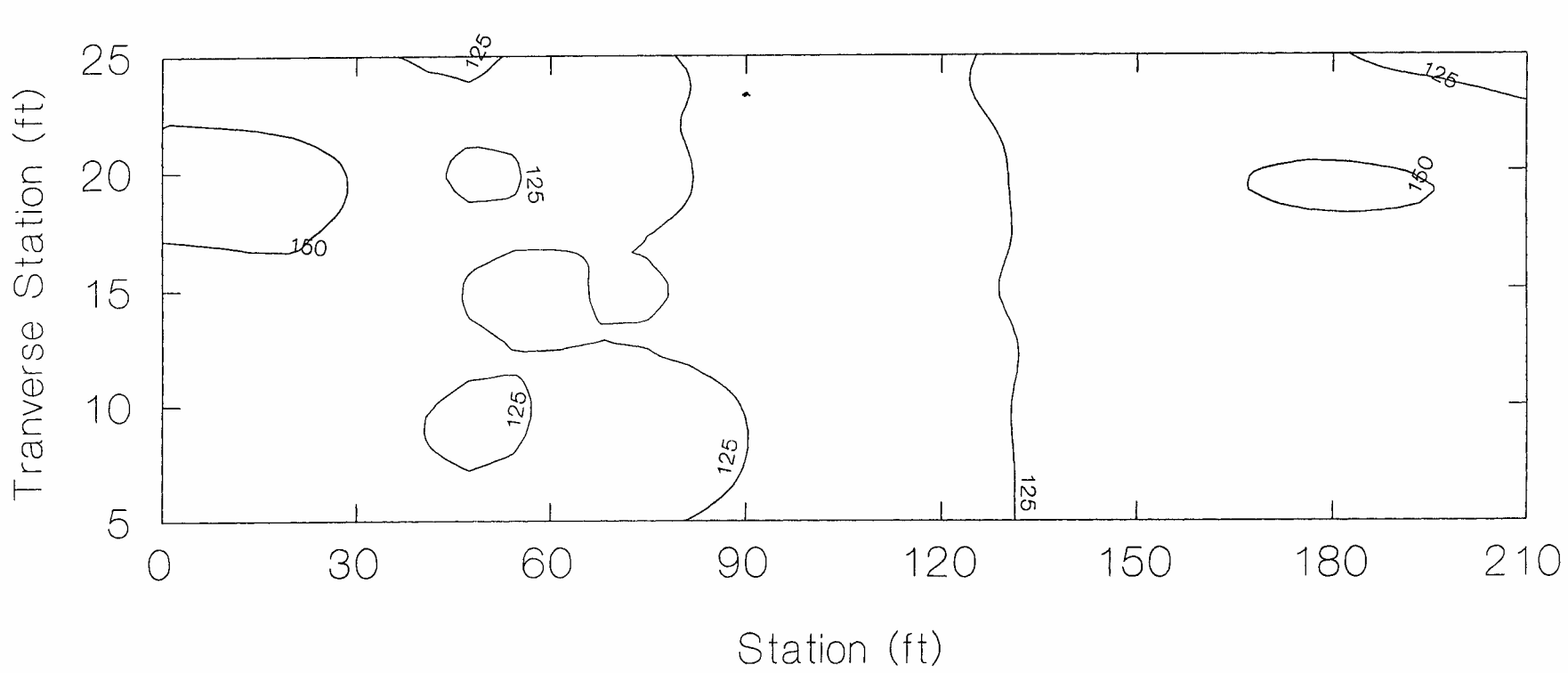

Figure 4.24 Contour Map of Subgrade Moduli Within Test Sections

The sensitivity of resilient modulus estimates for the laboratory methods (triaxial, bender element) to as-compacted density, degree of soaking and water content (w) can be seen in Figure 4.25. Similarly the in-situ test methods (DCP, HWD) indicate some variance in stiffness across the sections. The most variation in estimated M_R is exhibited by the bender element test, and the values found using the equation based on R-values.

Moduli estimated from DCP are generally lower than those found using the other test methods. The K-mold values are the lowest.

4.8.2 Subbase

The subbase moduli from triaxial tests, shown in Figure 4-26, were estimated at the mid-layer stress state calculated using elastic layer theory. The assumed surface loading was the same as that used to estimate subgrade moduli from triaxial testing.

The moduli estimated from HWD, K-mold and triaxial testing are within similar ranges, especially considering that the triaxial specimens were saturated. On the other hand, the K-mold specimens were compacted to lower densities, testing are considerably higher, as are those estimated using the R-value equation. It should be remembered that the DCP and R-value correlations use empirically derived equations which may not have an extensive data base.

4.8.3 Base

There is considerable variation in aggregate base moduli determined by the different methods (Figure 4.27). The base moduli estimated from triaxial tests were calculated following the same method used for the subbase.

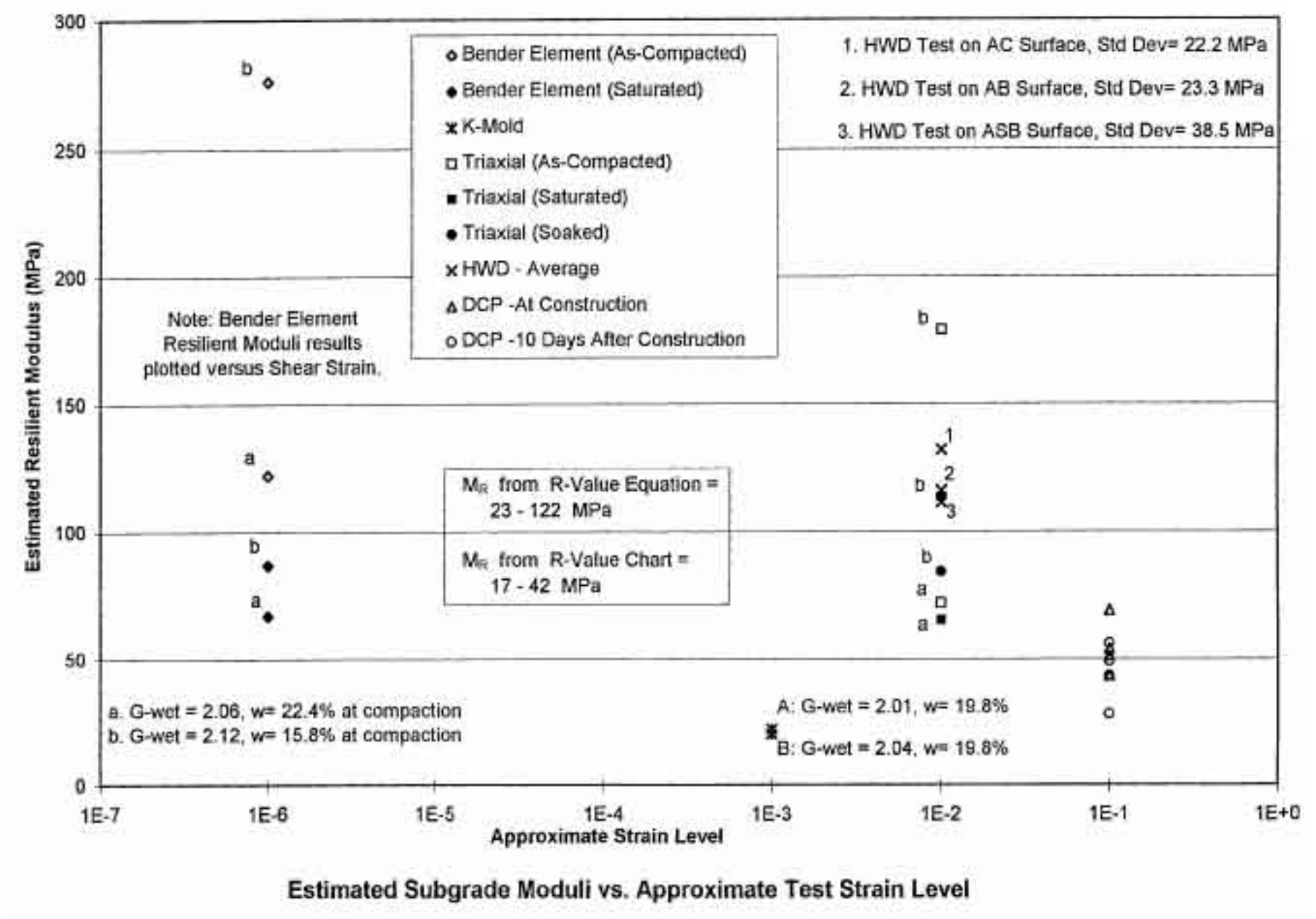

Figure 4.25 Method Comparison of Estimated Subgrade Moduli

Moduli back-calculated from deflections (which considered the sub-base and base to be one layer) vary widely between the two sets of measurements made after construction. The results immediately after compaction of the base average about 100 MPa, while those obtained 17 days later, and those obtained after placement of the asphalt concrete layers, indicate an average modulus of about 260 MPa. A similar change is observed for moduli estimated from DCP tests at compaction of the base and 10 days later. The moduli estimated from the DCP results are considerably higher than any other estimates.

Moduli determined from the R-value equation are larger than all but the DCP estimates, averaging about 320 MPa.

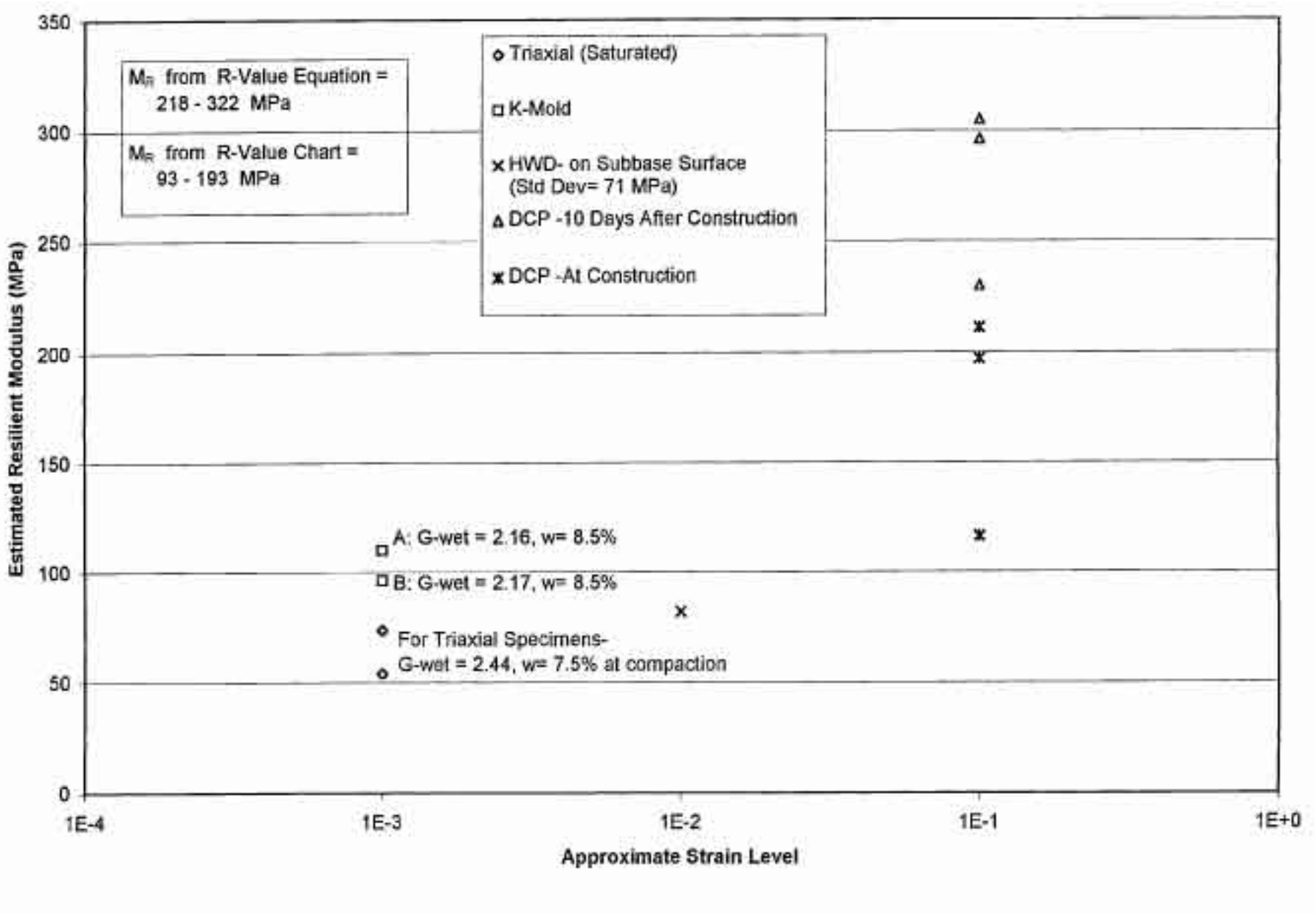

Figure 4.26 Method Comparison of Estimated Aggregate Subbase Moduli

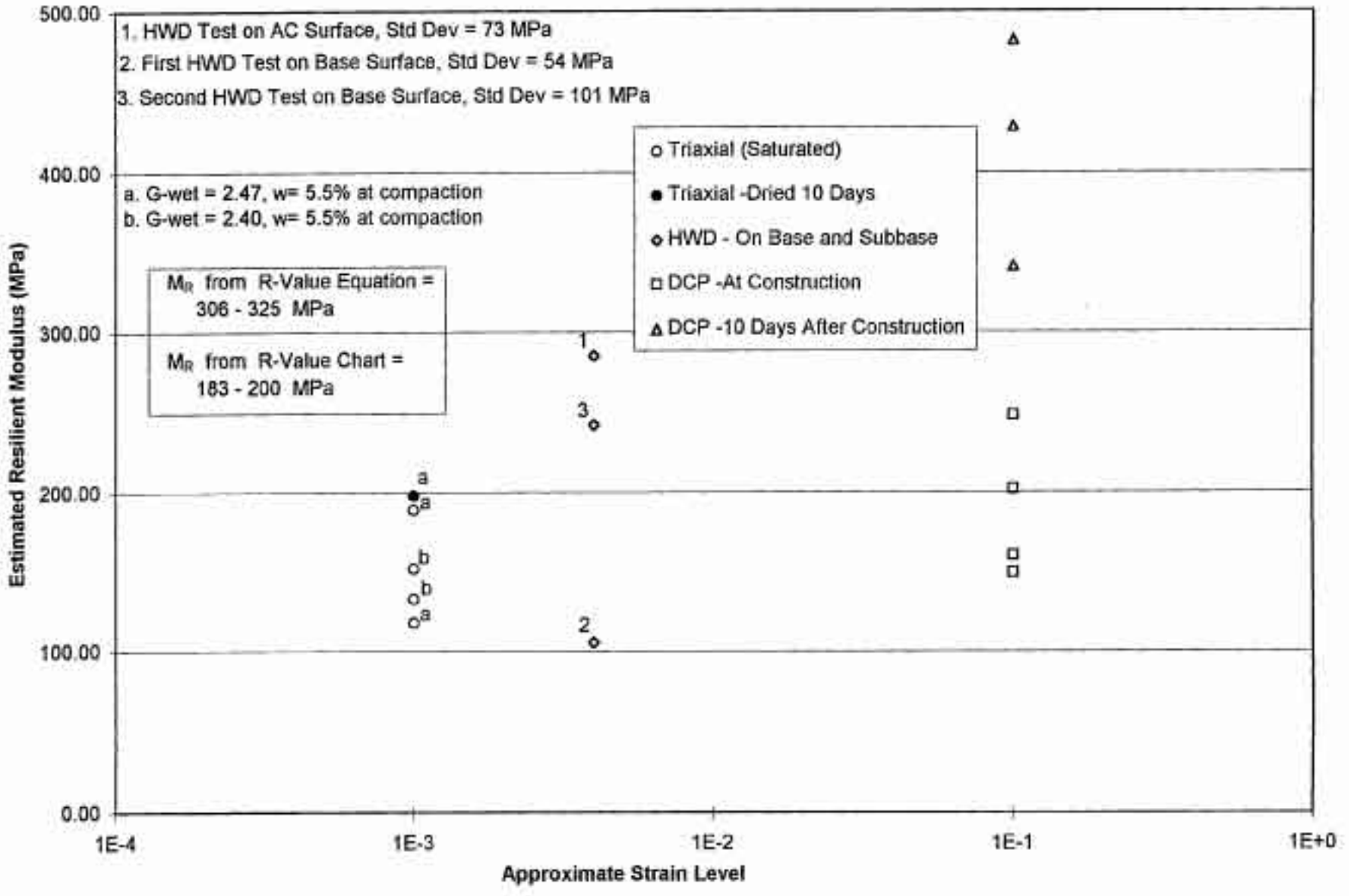

Figure 4.27 Method Comparison of Estimated Aggregate Base Moduli

CHAPTER 5

MATERIALS CHARACTERIZATION:

ASPHALT CONCRETE

5.1 INTRODUCTION

The asphalt concrete mix used in the test sections has been characterized in the laboratory by a number of different procedures. The results of these tests are described in Chapter 2 and in this chapter.

Stabilometer test results have been presented in Chapter 2. Stabilometer results indicate that the mix is stable (Stabilometer "S" value of 46). Unfortunately, the stabilometer test, in use in California since the 1930's, does not permit predictions of the amount of permanent deformation which might be anticipated under traffic. Accordingly, the repetitive simple shear test at constant height (RSST-CH), developed by SHRP Project A-003A, has also been utilized in evaluating the asphalt concrete mix. This test provides results which can be used to estimate rutting through empirical correlations *(Sousa et al., 1994)* and can, therefore, be considered a performance prediction test.

Also in the performance prediction category is the flexural fatigue test developed in the SHRP A-003A program. Fatigue testing and subsequent analysis can be used to predict cracking in the HVS test pavements. Results obtained thus far are included in this chapter; they provide the basis for estimates, described in Chapter 6, of repetitions to cause cracking in both the drained (ATPB) and undrained (AB) test sections.

An important part of the CAL/APT program is the joint laboratory program between

Caltrans and UCB. Included herein are results of the initial cooperative effort in using the simple shear device to evaluate both stiffness and permanent deformation performance. The project also provides an opportunity for Caltrans to evaluate the SuperPave mix design methodology. Results of the Level I mix evaluation procedure are described herein.

5.2 SHRP LEVEL I MIX EVALUATION

The SHRP Level I mix evaluation procedure was performed on samples of the virgin aggregate and the uncompacted asphalt concrete mix obtained at the time of construction. Mix samples were obtained from both lifts. The bottom lift material was taken from the east lane at about station 0 + 30 (ft) which is approximately the location of HVS test site 501RF. The top material was taken from the east lane at about station 1 + 75 (ft), which is approximately the same location as HVS test site 500RF.

5.2.1 Aggregate Characteristics

Results of aggregate testing, including only the SuperPave aggregate consensus properties, are summarized in Table 5.1 *(McGennis et al., 1994)*. Measurements of sand equivalent, coarse aggregate angularity, fine aggregate angularity, and flat or elongated particles in the coarse aggregate indicate that the aggregate meets SuperPave recommended specifications for these properties.

5.2.2 Mix Characteristics

Extracted gradations, plotted together with SHRP control points on Figure 5.1, met

Table 5.1 Aggregate and Mix Properties for the Cal/APT Field Mix

Test/Property	*Result*	*Specification*
Specific Gravity of Fine Aggregate (CT)	2.71	-
Specific Gravity of Fine Aggregate (AASHTO T 84)	2.62	-
Specific Gravity of Coarse Aggregate (AASHTO T 85 and Caltrans)	2.67	-
Sand Equivalent Test (AASHTO T 176)	64.00	40 minimum
Coarse Aggregate Angularity (CT 205)	98.00	50 or 75[a]
Fine Aggregate Angularity (ASTM C 1252)	45.00	40
Flat or Elongated particles in Coarse Aggregate (ASTM D 4791)	0.00	10 maximum
		-
Top Lift		
Hveem Stability	46.00	-
Extracted asphalt content (by weight of aggregate)	5.20	-
Gyratory Results:		
%Gmm at Ninitial (Ni=7)	87.70	89 maximum
%Gmm at Ndesign (Nd=86)	97.40	96
%Gmm at Nmax (Nmax=134)	98.70	98 maximum
%Air Voids at Ndesign (Nd=86)	2.60	4
%VMA at Ndesign	11.40	13 minimum
%VFA at Ndesign	77.20	65-75
%Dust/Asphalt Ratio	1.40	0.6-1.2
Bottom Lift		
Hveem Stability	46.00	-
Extracted asphalt content (by weight of aggregate)	4.80	-
%Gmm at Ninitial (Ni=7)	86.50	89 maximum
%Gmm at Ndesign (Nd=86)	96.10	96
%Gmm at Nmax (Nmax=134)	97.40	98 maximum
%Air Voids at Ndesign (Nd=86)	3.90	4
%VMA at Ndesign	12.10	13 minimum
%VFA at Ndesign	67.80	65-75
%Dust/Asphalt Ratio	1.34	0.6-1.2

a: The specification is 75 for a depth of less than 100 mm and 50 for a depth of more than 100 mm.

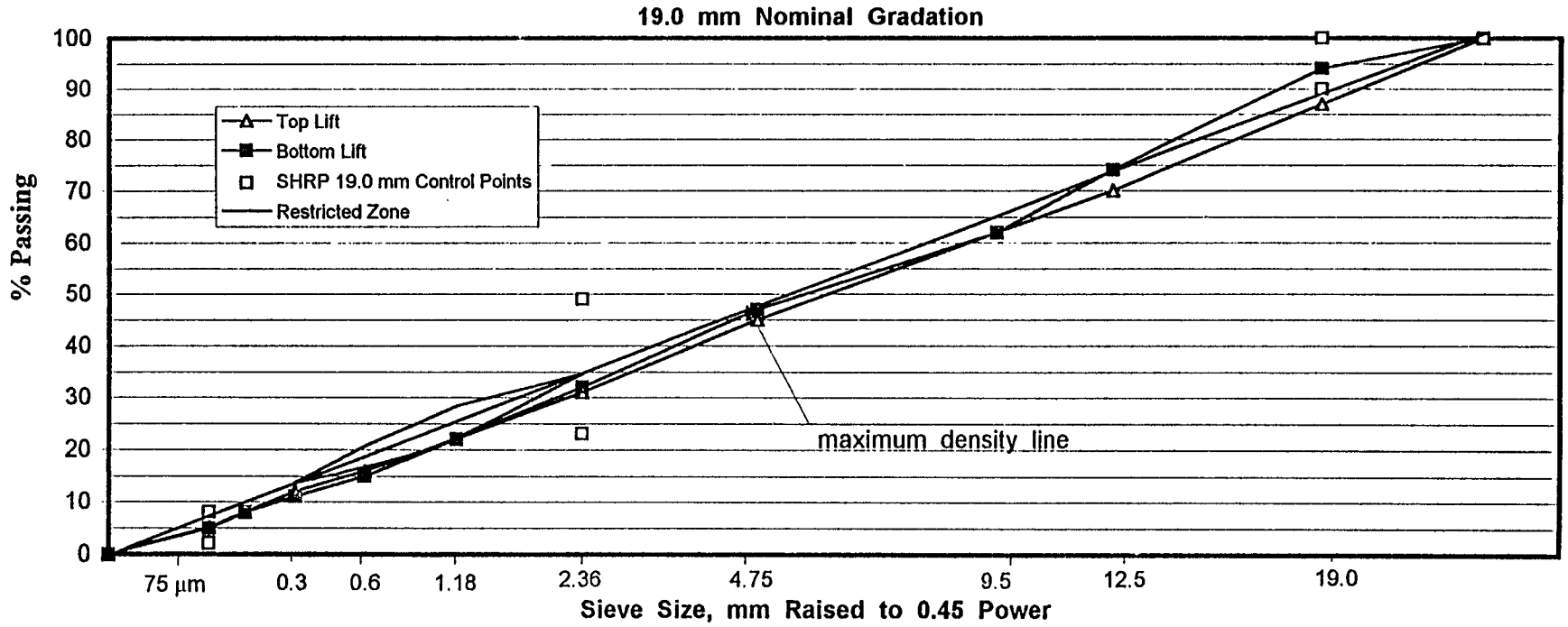

Figure 5.1 Comparison of Extracted Gradation with SHRP SuperPave Control Limits

Caltrans gradation specifications. The sample from the bottom lift also met the gradation requirements of SuperPave, but the top lift failed to meet SuperPave requirements for the 19 mm sieve size. Both gradations passed below the SHRP restricted zone. In general, the sampled aggregate gradations satisfied nearly all of both the Caltrans and SuperPave gradation specifications.

The extracted asphalt contents were 5.2 percent and 4.8 percent by weight of aggregate for the top and the bottom lift samples tested by TransLab (locations shown in Table 2.8) respectively. The mix design asphalt content range was 4.6 to 4.9 percent (Table 2.8). These results indicate that the asphalt content was higher than that recommended by the mix design at some locations in the test pavements. The dust/asphalt ratio, which is a ratio between the percentage of fines (passing the 0.075 mm sieve) and the effective asphalt content (by weight of total mix), exceeded the upper limit of SuperPave's recommended range.

Although not a part of the SuperPave design procedure, Stabilometer “S” value tests were performed on remolded mix obtained from the test sections. Six specimens were tested (three from each lift). Stability values, averaging 46 for each lift, indicated a stable mix.

In the SuperPave Level I procedure, gyratory compaction plays a key role in selection of the design binder content. Accordingly, the SHRP gyratory compactor was used to evaluate the mixes placed in the test sections. Six specimens (three from each lift) were compacted at a temperature of 135°C (275°F), the compaction temperature determined by the viscosity-temperature curves. The gyratory compaction curves are shown in Figure 5.2. This figure shows the relationship between the %Gmm, the ratio between the specimen specific gravity and the maximum theoretical specific gravity, and the number of gyrations.

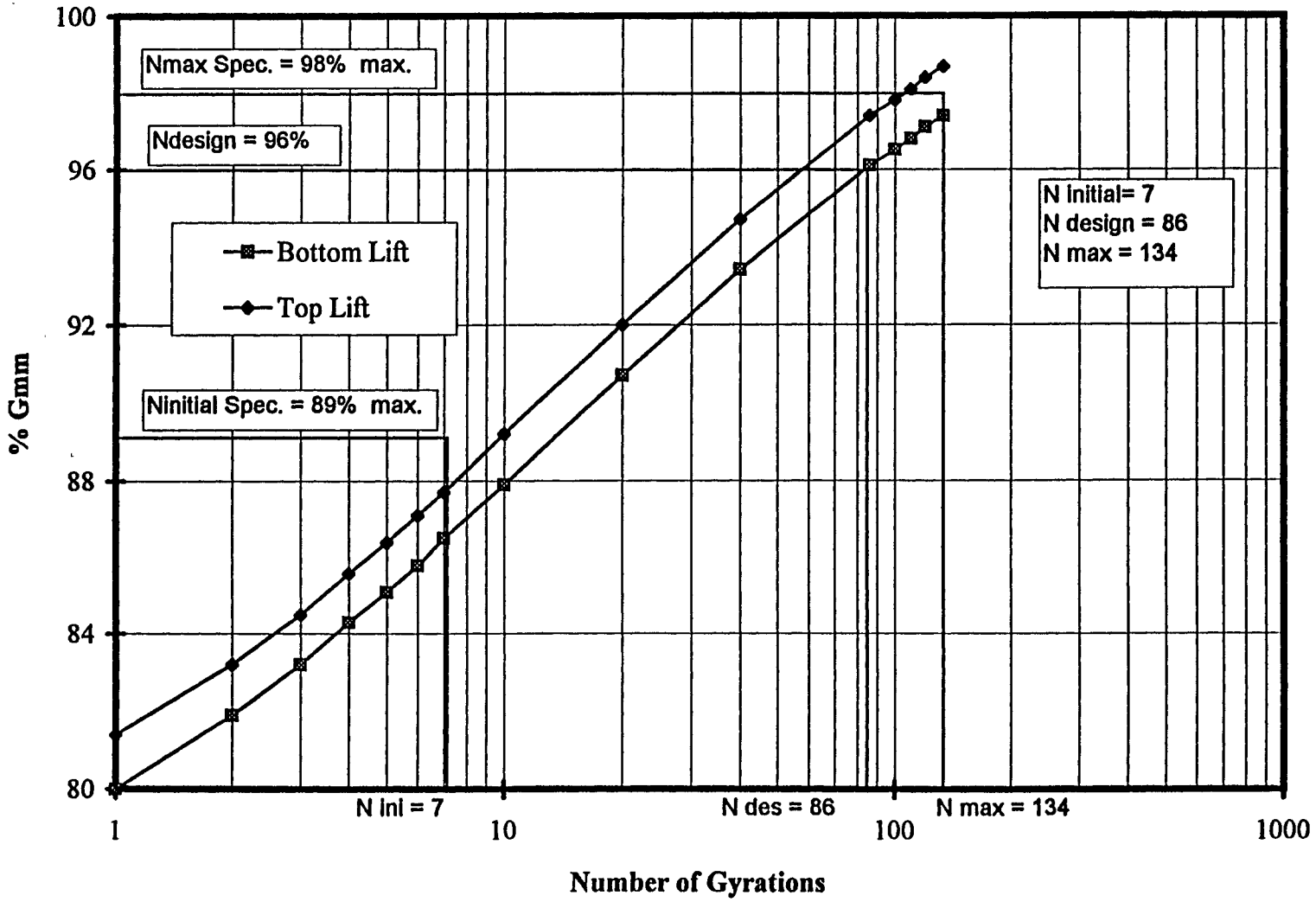

Figure 5.2 Gyratory Compaction Curves, Test Section Mix

The design number of gyrations (N_{design}) is a function of climate and traffic level. The initial number of gyrations ($N_{initial}$) and the maximum number of gyrations (N_{max}) are determined in accordance with the following relationships:

$$\text{Log}(N_{max}) = 1.10 \ \text{Log}(N_{design}) \quad (5\text{-}1)$$

$$\text{Log}(N_{initial}) = 0.45 \ \text{Log}(N_{design}) \quad (5\text{-}2)$$

For a TI of 9 (upper limit of 1.3 million ESALs) and an air temperature of 27°C, the numbers of gyrations were determined to be 7 for $N_{initial}$, 86 for N_{design}, and 134 for N_{max}, as shown in Table 5.1.

Figure 5.2 shows that the densification rates for mixes from both top and bottom lifts were similar (comparable slopes). However, the mix from the top lift had a larger density than the mix from the bottom lift. Since both mixes have essentially the same aggregate, it is likely that the larger asphalt content of the mix from the top lift resulted in increased densification. The larger asphalt content for the top lift sample, taken at approximately the location of HVS site 500RF, may have been an exception since the extracted asphalt content from a composite top lift sample tested by the Contra Costa County materials lab was within the range recommended by the District 4 mix design (Table 2.8).

At an N_{design} of 86 gyrations, the %Gmm values were 96.1 percent and 97.4 percent for the bottom and top lifts, respectively. The SuperPave recommended design value is 96 percent. Therefore only the bottom lift met this criterion. The initial number of gyrations ($N_{initial}$) was 7. At this value of $N_{initial}$, the %Gmm values were 86.5 percent and 87.7 percent for the bottom and top lifts, respectively. The SuperPave recommended design value is 89 percent maximum: both values were below 89 percent.

The voids in the mineral aggregate (VMA) were 12.1 percent and 11.4 percent for the bottom and top lifts, respectively. These values are below the SHRP minimum VMA criterion of

13 percent. The voids filled with asphalt (VFA) were 67.8 percent and 77.2 percent for the bottom and top lifts, respectively. The recommended VFA range is 65 to 75. This shows that only the bottom lift met this criterion.

Thus it should be noted that this mix, although meeting Caltrans requirements, did not meet all of the SHRP SuperPave Level I design criteria.

5.3 SHRP A-003A MIX EVALUATION PROCEDURES

Mix evaluation procedures developed during the SHRP A-003A project included tests to measure mix stiffness *(Tayebali, Tsai, and Monismith, 1994b)*, fatigue response *(Tayebali et al., 1994a)*, and permanent deformation characteristics *(Sousa et al., 1994)*. As compared to the performance related information presented in the previous section, results of these tests permit prediction of the number of load repetitions to produce prescribed levels of fatigue cracking and rutting.

Results from flexural fatigue tests (including stiffness determinations), RSST-CH tests for permanent deformation, and frequency sweep tests for stiffness determination are summarized in this section. Shear and flexural stiffness, fatigue, and permanent deformation tests were performed by UCB; stiffness and permanent deformation tests were also performed by Caltrans.

5.3.1 Flexural Fatigue Tests

Controlled-strain flexural fatigue tests were performed on both laboratory compacted specimens and specimens cut or cored from the transition zone between the test sections. The laboratory compacted specimens were tested at 20°C (19° ± 1°C), and the field compacted specimens, at 20°C and 28°C. The field compacted specimens were obtained from both lifts while the laboratory specimens were compacted by rolling wheel compaction over a range in air-void contents to cover the range anticipated in the field sections. Fatigue tests were performed at a loading frequency of 10 Hz on beams which were 6.35 cm (2.5 in) wide by 5.08 cm (2.0 in) deep by 38.1 cm (15.0 in) in length following established procedures *(Tayebali et al., 1994a)*. Test results are summarized in Tables 5.2 and 5.3, and plots of strain versus cycles to failure (defined as the number of repetitions corresponding to 50 percent reduction in stiffness) are shown in Figures 5.3 and 5.4. Results for fatigue response of the field compacted specimens are bracketed by the data obtained for the laboratory specimens at larger strain levels as seen in Figure 5.3. At smaller strain levels the laboratory compacted specimens had somewhat longer fatigue lives.

Results of these tests, ie. flexural stiffness and fatigue versus tensile strain relations, have been used to predict fatigue response of the HVS test sections (Chapter 6).

5.3.2 Stiffness Determination

Asphalt Concrete. Stiffness measurements were performed on both laboratory and field compacted specimens by UCB and field compacted specimens by Caltrans.

Tests performed by UCB included 1) flexural stiffness measurements at 20°C on both

Table 5.2 Fatigue Test Results for Laboratory Compacted Beams, 20° C

Specimen	Field or Lab Compacted	Test Temperature (C)	Air-Void Content (%)	Nf	Strain	Phase Angle	Stiffness (kPa)	Accumulated Energy (MPa)	Regression Nf = k1 exp (k2)		
AC1A	lab	20	3.2	374,005	1.98E-4	19.0	1.140E+7	35.5			
AC14A	lab	20	2.8	100,814	2.99E-4	20.9	1.062E+7	22.4			
AC1B	lab	20	3.5	81,405	3.00E-4	20.3	1.066E+7	18.0			
AC14B	lab	20	3.2	21,747	4.05E-4	20.9	1.053E+7	8.6	**k1**	**k2**	**R^2**
		average	***3.2***			***20.3***	***1.080E+7***		1.174E-09	-3.927	0.983
AC8A	lab	20	6.5	432,986	1.96E-4	21.4	8.023E+6	29.3			
AC6A	lab	20	6.6	148,991	1.99E-4	20.3	8.734E+6	11.2			
AC8B	lab	20	6.2	20,328	4.01E-4	22.3	8.103E+6	6.4			
AC6B	lab	20	6.6	22,624	4.01E-4	22.0	8.283E+6	7.0	**k1**	**k2**	**R^2**
		average	***6.5***			***21.5***	***8.286E+6***		2.642E-08	-3.505	0.922
AC3B	lab	20	6.9	376,341	1.97E-4	21.4	8.135E+6	27.4			
AC3A	lab	20	7.4	365,399	1.98E-4	22.1	7.870E+6	24.8			
AC9B	lab	20	6.7	82,592	2.97E-4	21.4	8.112E+6	13.9			
AC12A	lab	20	7.7	7,731	4.03E-4	23.3	7.085E+6	2.2			
AC15A	lab	20	7.1	22,739	4.04E-4	22.5	7.100E+6	6.3	**k1**	**k2**	**R^2**
		average	***7.2***			***22.1***	***7.661E+6***		2.843E-12	-4.628	0.938
AC13A	lab	20	8.9	321,826	1.97E-4	22.1	7.494E+6	21.9			
AC5B	lab	20	9.5	220,825	2.01E-4	23.5	5.871E+6	12.1			
AC13B	lab	20	8.7	16,938	3.99E-4	23.5	6.974E+6	4.4			
AC5A	lab	20	9.7	8,714	4.05E-4	23.4	5.933E+6	2.1	**k1**	**k2**	**R^2**
		average	***9.2***			***23.1***	***6.568E+6***		1.309E-11	-4.407	0.978

Table 5.3 Fatigue Test Results for Field Compacted Beams, 20°C and 28°C

Specimen	Field or Lab Compacted	Test Temperature (C)	Air-Void Content (%)	Nf	Strain	Phase Angle	Stiffness (kPa)	Accumulated Energy (MPa)	Regression Nf = k1 exp (k2)		
tsac-f	field-top	20	6.3	199,999	1.97E-4	23.2	7.488E+6	14.1			
tsac-e	field-top	20	6.5	176,365	1.99E-4	22.4	7.640E+6	12.6			
tsac-d	field-top	20	6.6	13,781	3.99E-4	24.3	7.374E+6	4.3			
tsac-c	field-top	20	6.3	20,414	4.03E-4	23.7	7.588E+6	6.3	**k1**	**k2**	**R^2**
		average	***6.4***			***23.4***	***7.523E+6***		4.061E-08	-3.420	0.984
bsac-d	field-bottom	20	3.7	198,522	1.98E-4	23.2	9.689E+6	18.5			
bsac-e	field-bottom	20	3.7	218,772	1.99E-4	24.1	9.349E+6	21.2			
bsac-f	field-bottom	20	4.6	19,116	4.00E-4	25.1	9.386E+6	7.5			
bsac-g	field-bottom	20	3.2	20,629	4.01E-4	24.3	7.906E+6	6.9	**k1**	**k2**	**R^2**
		average	***3.8***			***24.2***	***9.083E+6***		8.364E-08	-3.348	0.998
tsac-k	field-top	28	7.0	297,330	1.98E-4	36.7	4.328E+6	16.9			
tsac-i	field-top	28	7.1	185,911	1.99E-4	33.4	4.851E+6	11.3			
tsac-h	field-top	28	7.2	22,658	3.98E-4	37.1	4.066E+6	4.9			
tsac-j	field-top	28	6.9	22,743	4.00E-4	36.2	4.256E+6	5.1			
tsac-;	field-top	28	7.2	21,396	4.00E-4	35.5	4.584E+6	5.0	**k1**	**k2**	**R^2**
		average	***7.1***			***35.8***	***4.417E+6***		7.559E-08	-3.374	0.985
bsac-n	field-bottom	28	4.2	430,229	1.97E-4	33.9	5.860E+6	32.0			
bsac-m	field-bottom	28	3.6	516,196	1.98E-4	33.7	6.380E+6	41.4			
bsac-i	field-bottom	28	3.9	413,826	1.99E-4	35.7	6.020E+6	33.0			
bsac-h	field-bottom	28	3.5	22,882	4.00E-4	37.7	5.570E+6	7.0			
bsac-l	field-bottom	28	4.1	16,709	4.00E-4	36.2	5.750E+6	5.2			
bsac-k	field-bottom	28	3.8	27,319	4.01E-4	38.3	5.350E+6	8.2	**k1**	**k2**	**R^2**
		average	***3.9***			***35.9***	***5.822E+6***		5.401E-11	-4.299	0.989

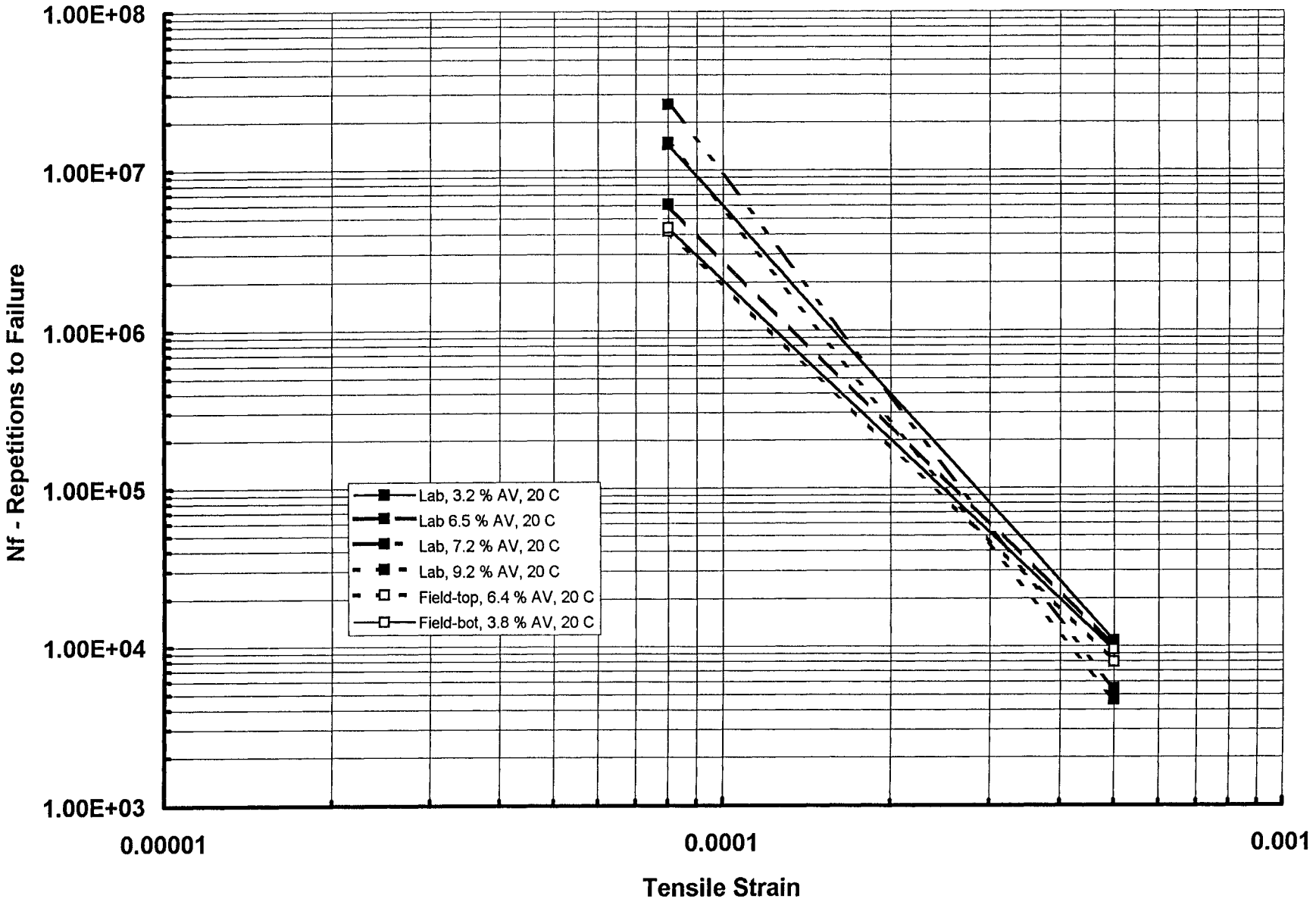

Figure 5.3 Fatigue Life Versus Tensile Strain, Summary of All Flexural Fatigue Tests, 20° C

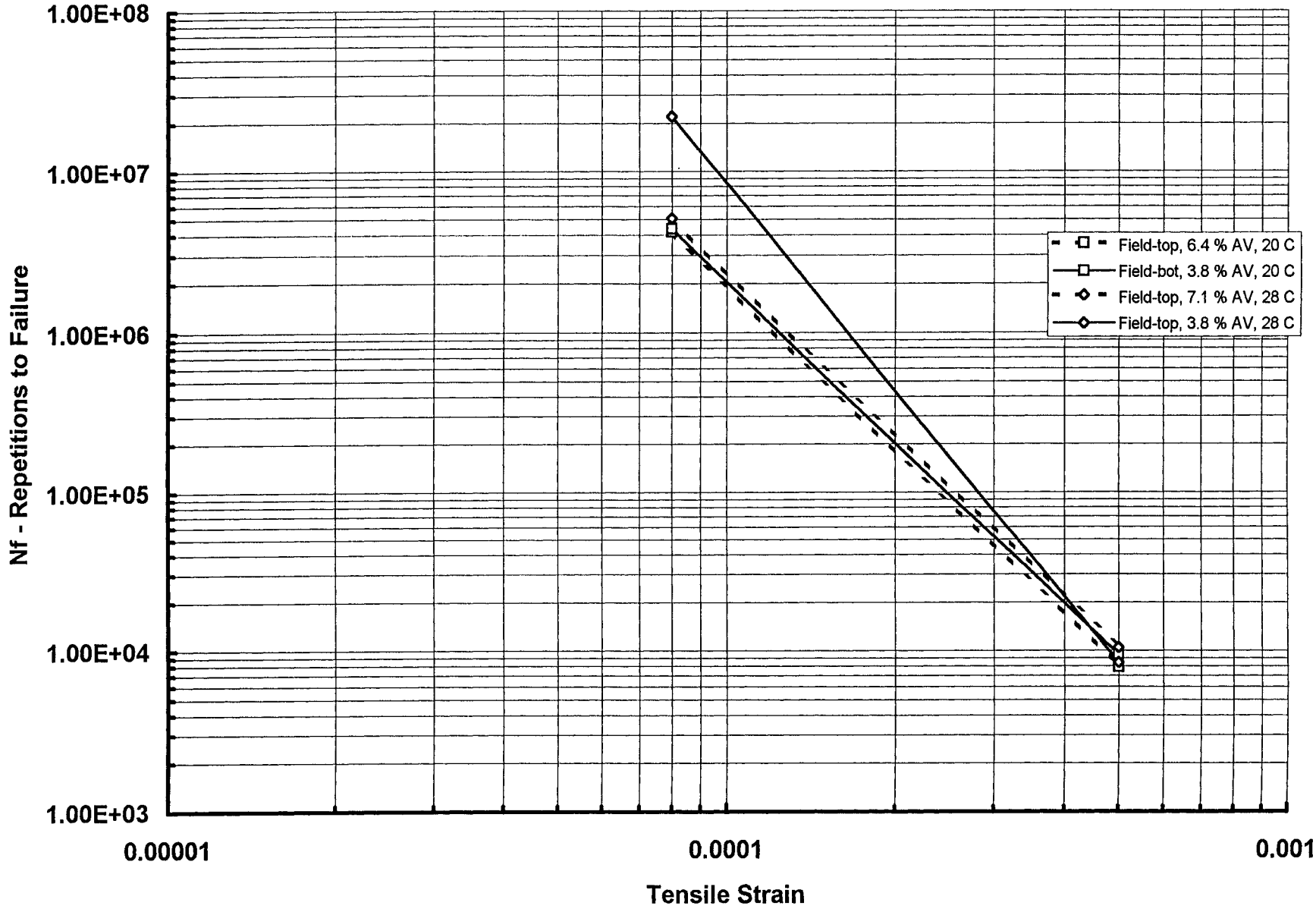

Figure 5.4 Fatigue Life Versus Tensile Strain, Comparison of Field Beam Tests, 20° C and 28° C

laboratory and field compacted specimens and at 28°C on field compacted specimens, all at 10 Hz frequency, and 2) shear frequency sweep tests on both laboratory and field compacted specimens at 20°C. Caltrans performed shear frequency sweep tests at 20°C on field compacted specimens.

Results of the UCB flexural stiffness tests are summarized in Tables 5.2 and 5.3, and Figure 5.5. It should be noted that, at 20°C, the field compacted specimens exhibit flexural stiffnesses about 5 to 10 percent less than the specimens prepared by rolling wheel compaction in the laboratory. Part of this difference might be due to differences in binder hardening between the field and laboratory compacted specimens. In this instance the laboratory specimens were prepared using the field mix after it had been reheated in a forced draft oven for about 90 to 120 minutes to bring it to the desired compaction temperature.

UCB and Caltrans TransLab shear stiffness measurements at 20°C are shown in Table 5.4. The shear stiffness and phase angle can be converted to comparable flexural values using the following regression equations developed in SHRP A-003A research *(McGennis et al., 1994)*:

$$S_0 = 1.178\ (G_0)^{1.015} \exp(0.010VFB) \tag{5-3}$$

$$\sin f_{S_0} = 1.15\ (\sin f_{G_0})^{0.892} \tag{5-4}$$

where S_0 = initial flexural stiffness in psi, G_0 = initial shear stiffness in psi, VFB= percent voids filled with bitumen, f_{S_0} = initial flexural phase angle in degrees, and f_{G_0} = initial shear phase angle in degrees.

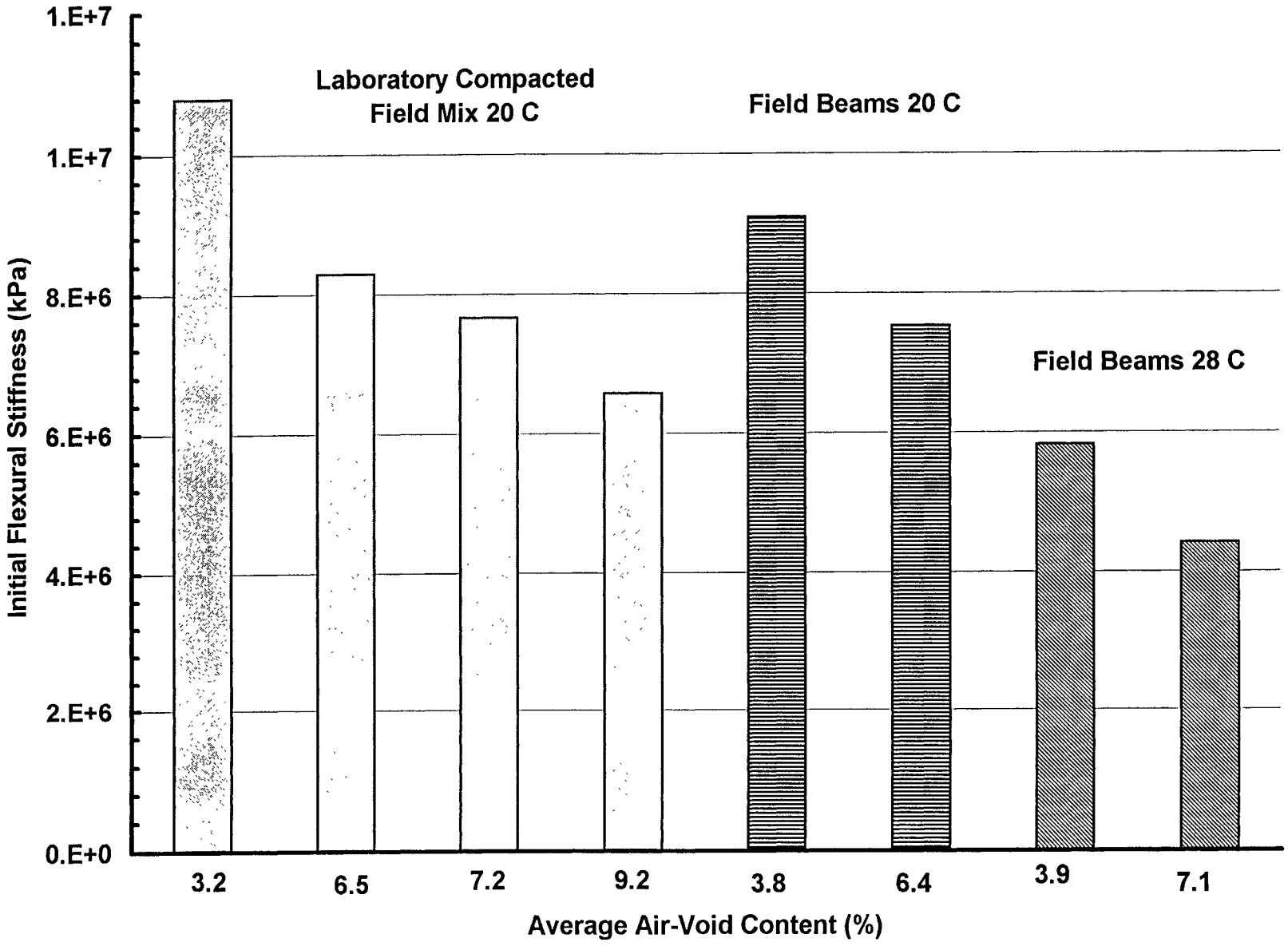

Figure 5.5 Stiffness Results, Averages of All Flexural Tests

Table 5.4 Caltrans and UCB Shear Frequency Sweep Results for Laboratory and Field Compacted Specimens, 20° C

UC-Berkeley Frequency Sweeps

Specimen	Air-Void Content (%)	Frequency Hz	Complex Shear Modulus (kPa)	Shear Phase Angle (none)
AC 34-2	3.1	10	2.17E+06	23.5
Lab compacted field mix		5	1.82E+06	27.5
		2	1.40E+06	33.2
		1	1.08E+06	38.2
		0.5	8.23E+05	43.5
		0.2	5.66E+05	49.9
		0.1	3.67E+05	54.2
		0.05	2.45E+05	56.5
		0.02	1.40E+05	57.1
		0.01	9.18E+04	55.4
AC38-1	4.4	10	1.91E+06	24.0
Lab compacted field mix		5	1.61E+06	27.2
		2	1.24E+06	33.1
		1	9.70E+05	38.4
		0.5	7.29E+05	44.4
		0.2	4.56E+05	52.7
		0.1	3.02E+05	58.4
		0.05	1.85E+05	62.7
		0.02	9.70E+04	64.1
		0.01	5.62E+04	63.0
SAC8B	4.2	10	1.80E+06	20.7
Site core bottom lift		5	1.55E+06	23.5
		2	1.21E+06	28.7
		1	9.46E+05	33.5
		0 5	7.23E+05	39.5
		0.2	4.60E+05	47.6
		0.1	2.98E+05	53.0
		0.05	1.80E+05	57.6
		0.02	8.96E+04	58.4
		0.01	5.26E+04	57.3
SAC2T	6.5	10	1.93E+06	23.2
Site core top lift		5	1.62E+06	27.0
		2	1.22E+06	33.3
		1	9.29E+05	39.2
		0.5	6.85E+05	45.4
		0.2	4.20E+05	53.7
		0.1	2.72E+05	59.4
		0.05	1.67E+05	63.3
		0.02	8.39E+04	64 8
		0.01	5.23E+04	65.4
SAC8T	7 5	10	1.81E+06	17.6
Site core top lift		5	1.59E+06	19.9
Temperature = 23 C		2	1.27E+06	25.0
		1	1.03E+06	29.5
		0 5	8.10E+05	34.7
		0.2	5.35E+05	42.9
		0.1	3.58E+05	49.9
		0.05	2.16E+05	55.2
		0.02	1.03E+05	59.7
		0.01	5.62E+04	59.0
SAC12B	4.0	10	1.52E+06	23.8
Site core bottom lift		5	1.28E+06	27.5
Temperature = 25 C		2	9.49E+05	33.9
		1	7.15E+05	40.0
		0 5	5.13E+05	46.1
		0.2	3.02E+05	53.6
		0.1	1.88E+05	57.8
		0.05	1.12E+05	58.9
		0.02	5.64E+04	56.4
		0.01	3.62E+04	52.2
AC39-3	6.9	10	2.00E+06	19.7
Lab compacted field mix		5	1.72E+06	22.8
		2	1.34E+06	28.3
		1	1.06E+06	33.4
		0.5	8.05E+05	38.7
		0.2	5.11E+05	46.2
		0.1	3.33E+05	52.7
		0.05	2.01E+05	57.3
		0.02	9.97E+04	58.5
		0.01	5.61E+04	57.8
AC39-2	7 7	10	2.82E+06	27.9
Lab compacted field mix		5	2.40E+06	31.9
		2	1.82E+06	37.3
		1	1.39E+06	42.2
		0.5	1.05E+06	48.1
		0.2	6.53E+05	56.4
		0.1	4.15E+05	62.2
		0.05	2.60E+05	66.0
		0.02	1.28E+05	66.6
		0.01	7.56E+04	65.0

TransLab Frequency Sweeps

Specimen	Air-Void Content (%)	Frequency Hz	Complex Shear Modulus (kPa)	Shear Phase Angle (none)
SAC7B	4.1	10	1.92E+06	25.8
Site core bottom lift		5	1.67E+06	28.5
		2	1.20E+06	36.8
		1	9.58E+05	42.6
		0.5	7.36E+05	49.6
		0.2	4.68E+05	57.9
		0.1	3.24E+05	63.8
		0.05	2.15E+05	67.8
		0.02	1.22E+05	70.6
		0.01	8.31E+04	70.1
SAC7T	7.4	10	1.66E+06	26.7
Site core top lift		5	1.44E+06	37.8
		2	9.99E+05	36.8
		1	7.52E+05	42.7
		0.5	5.36E+05	49.6
		0.2	3.07E+05	57.9
		0.1	2.01E+05	63.8
		0.05	1.21E+05	67.8
		0.02	6.25E+04	70.6
		0.01	4.26E+04	70.1

A summary of the stiffness measurements at 10 Hz is contained in Table 5.5. It can be seen that the UCB and Caltrans flexural stiffnesses estimated using Equation 5-3 tend to be smaller than those measured in the flexural beam test, and both the UCB and Caltrans flexural phase angles estimated from Equation 5-4 are larger than those from the flexural test.

The field core shear stiffnesses measured by Caltrans and UCB are similar. The UCB cores had somewhat lower phase angles. The two Caltrans field core tests showed a drop in stiffness with increased air-void content, which was not matched by the UCB results.

Asphalt Treated Permeable Base. (NOTE: the following test results and analysis were completed after the draft interim report was written).

Four specimens were compacted in the laboratory of asphalt treated permeable base (ATPB) material collected from the drained pavement structure during construction. The specimens were 100 mm (4 in.) in diameter and approximately 200 mm (8 in.) in height. The specimens were tested for resilient modulus (M_R) after compaction. The M_R results are included herein.

The specimens were then subjected to several sequences of water conditioning and repetitive loading to evaluate permanent deformation. Those results will be included in a later report.

The specimens were prepared following AASHTO T274-82 (*AASHTO, 1986*). Prior to compaction, the ATPB mix, split mold, rod and cover plate were heated in a forced-draft oven at 80° C (175° F) for 1.5 to 2 hours. A rubber membrane was placed inside the split mold before it went into the oven.

The mix was compacted in six lifts, with each lift vibrated with an air hammer for 90

Table 5.5 Summary of Average Stiffness Measurements, 10 Hz Frequency

Laboratory	UCB	UCB	UCB	UCB	UCB	UCB	UCB	UCB	TransLab	TransLab
Test Mode	Beam	Beam	Beam	Beam	Shear	Shear	Shear	Shear	Shear	Shear
Method of Compaction *	Laboratory	Laboratory	Laboratory	Laboratory	Laboratory	Laboratory	Field(bottom lift)	Field(top lift)	Field(bottom lift)	Field(top lift)
Temperature (C)	20	20	20	20	20	20	20	20	20	20
Average Air-Void Content (%)	3.2	6.5	7.2	9.2	3.75	7.3	4.2	6.5	4.1	7.4
Average VFB (%)					75	60	72	63	73	60
Average Initial Complex Modulus (GPa)										
flexural	10.8	8.29	7.66	6.57						
shear					2.04	2.41	1.80	1.93	1.92	1.66
flexural estimated from shear (eqtn 5-3)					5.14	5.23	4.41	4.32	4.74	3.59
Average Phase angle (degrees)										
flexural	20.3	21.5	22.1	23.1						
shear					23.8	23.8	20.7	23.2	25.8	26.7
flexural estimated from shear (eqtn 5-4)					30.7	30.8	27.1	30.1	33.2	34.3

* Rolling wheel used for laboratory compaction

seconds. It was found that aggregate degradation occurred if the vibration time was extended much beyond 90 seconds.

The specimen was then allowed to sit overnight, and removed from the split mold the next day. Air-void content was measured using parafilm.

To insure a uniform surface for load application, gravel, 2 to 5 mm in diameter was used to fill the voids at the top of the specimen. The specimen was then placed into the triaxial apparatus, and the pre-conditioning and loading sequences included in AASHTO Test Method 274-82 (*AASHTO, 1986*) for granular materials were performed. The loading sequence is shown in Table 5.6. All tests were performed at about 19° C (65° F).

The air-void contents for the four specimens were very similar (Figure 5.6). The resilient modulus versus sum of the principal stresses (SPS) relations, of the form:

$$M_R = a\ SPS^b \tag{5-5}$$

where MR is the resilient modulus
SPS is the sum of the principal stresses, and
a, b are regression coefficients,

have slopes of approximately zero. This indicates that the modulus-SPS relation of the ATPB is similar to that of a bound material, rather than an unbound granular material.

There is a great deal of variance in the moduli between the four specimens. The average moduli from the test sequence were: 836 MPa (121 ksi), 1,428 MPa (207 ksi), 1,925 MPa (279 ksi), and 1,068 MPa (155 ksi), for specimens 1 through 4, respectively.

Table 5.6 Loading Sequences Used in ATPB Resilient Modulus Test

Confining Pressure		Deviator Stress	
psi	kPa	psi	kPa
10	69	12	82.8
10	69	20	138
10	69	30	207
15	103.5	16	110.4
15	103.5	30	207
15	103.5	45	310.5
20	138	20	138
20	138	40	276
20	138	60	414
30	207	30	207
30	207	60	414
20	138	40	276
10	69	20	138
5	34.5	12	82.8
5	34.5	20	138
5	34.5	12	82.8
10	69	20	138
20	138	40	276
30	207	60	414
30	207	30	207
20	138	60	414
20	138	40	276
20	138	20	138
15	103.5	45	310.5
15	103.5	30	207
15	103.5	16	110.4
10	69	30	207
10	69	20	138
10	69	12	82.8

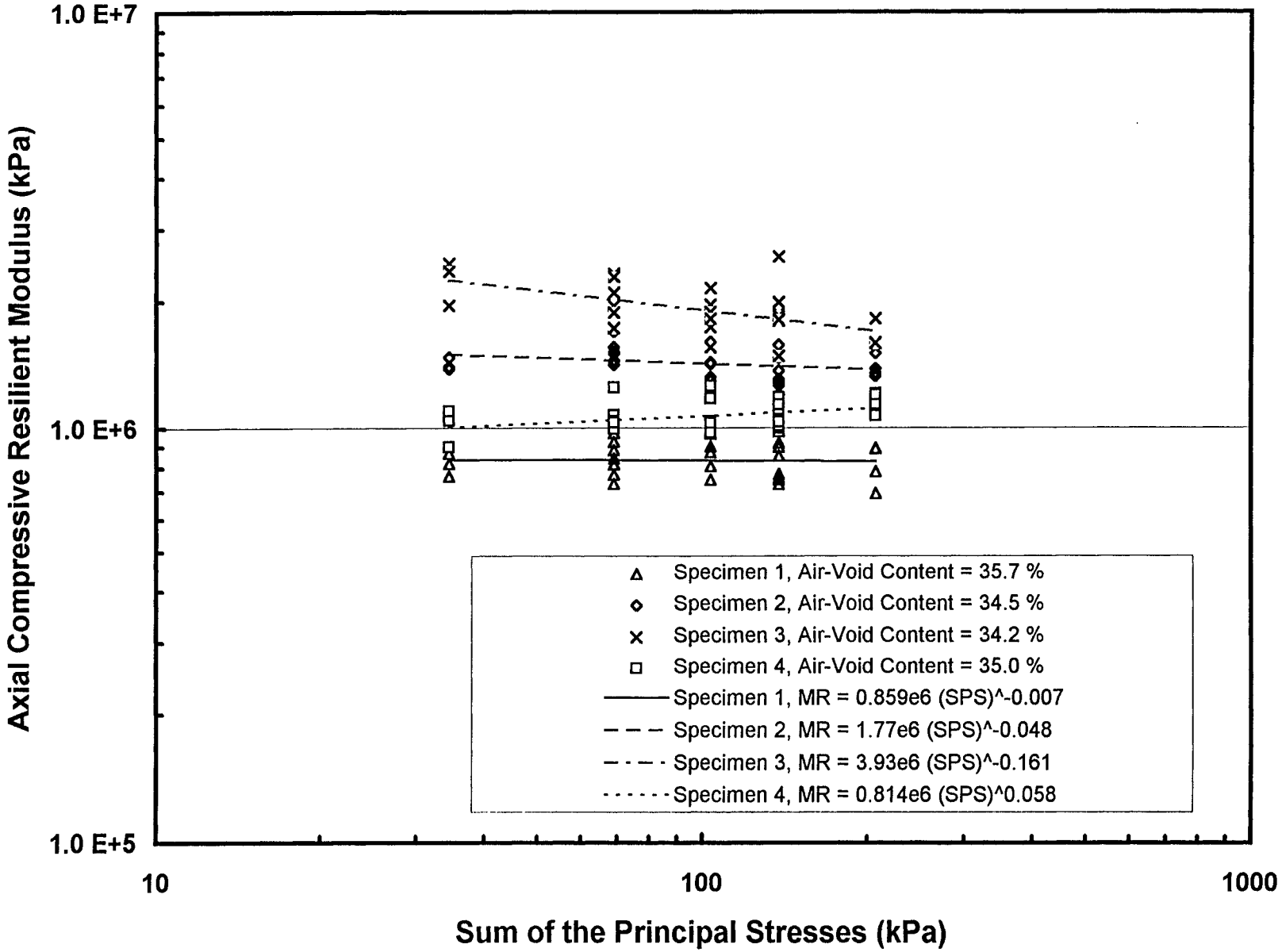

Figure 5.6 Summary Plot of Asphalt Treated Permeable Base (ATPB) Resilient Modulus Test Results, As-Compacted State

5.3.3 Simple Shear Tests - Permanent Deformation

Repetitive simple shear tests at constant height (RSST-CH) were performed on the asphalt concrete at both UCB and Caltrans. The initial tests were conducted at a temperature of 21°C (69°F), a temperature which appeared to be representative of in-situ conditions at the time the tests were conducted. Subsequent to those tests the pavement temperature increased substantially due to hot weather. Additional tests were performed at higher temperatures, the results of which are reported herein.

The shear tests applied a haversine-shaped shear stress of 68.9 kPa (10 psi) to 150 mm (6 in.) diameter by 50.8 mm (2 in.) cylindrical specimens. Loading was applied for 0.1 sec, and the time interval between load applications was 0.6 sec. Each specimen was subjected to at least 5,000 stress repetitions. Results of the Caltrans tests, in terms of repetitions to percent permanent shear strains, are summarized in Table 5.7 and Figure 5.7. Results of the UCB tests are summarized in Table 5.8 and Figures 5.8 and 5.9. The shear strains at which results were evaluated are very small compared to those typically used for mix design or performance evaluation testing. The low temperatures used for testing resulted in very small strains. Extrapolation to larger strains was not considered useful.

In the SHRP A-003A program, a relationship between rut depth and permanent shear strain was established from finite element analyses. This relation is:

$$Rut\ \ Depth = k\ \ (permanent\ \ shear\ \ strain\ \ \ RSST - CH) \qquad (5\text{-}6)$$

where k = approximately 10 for rut depth in inches, or 254 for rut depth in mm. It should be noted that the parameter k is dependent on layer thickness and the values shown above correspond to thicker layers of asphalt concrete.

Table 5.7 Summary of Caltrans Repetitive Simple Shear Test at Constant Height Results

Mix	Specimen	Lift	Test Temperature (C)	Shear to Compaction Direction	Repetitive Shear Stress (kPa)	Air-Void Content (%)	RSST-CH reps to Permanent Shear Strain 0.10%	0.25%	0.50%	1.0%	2.0%	5.0%
Field Mix												
Lab Compact	AC1-4	top	21	varied	68.9	3.0	5,770	35,467				
	AC10B	top	21	varied	68.9	4.2	3,096	17,648				
	average					***3.6***	***4,433***	***26,557***				
	AC1-5	top	21	varied	68.9	6.5	1,319	6,477	23,409			
	AC1-1	top	21	varied	68.9	6.7	367	1,256	3,756	12,953		
	average					***6.6***	***843***	***3,866***	***13,583***			
Field Cores												
	SAC3B	bottom	21	varied	68.9	3.4	5,823	48,841				
	average					***3.4***	***5,823***	***48,841***				
	SAC3T	top	21	varied	68.9	6.2	473	1,830	9,734			
	SAC9T	top	21	varied	68.9	6.7	287	1,743				
	average					***6.5***	***380***	***1,787***				

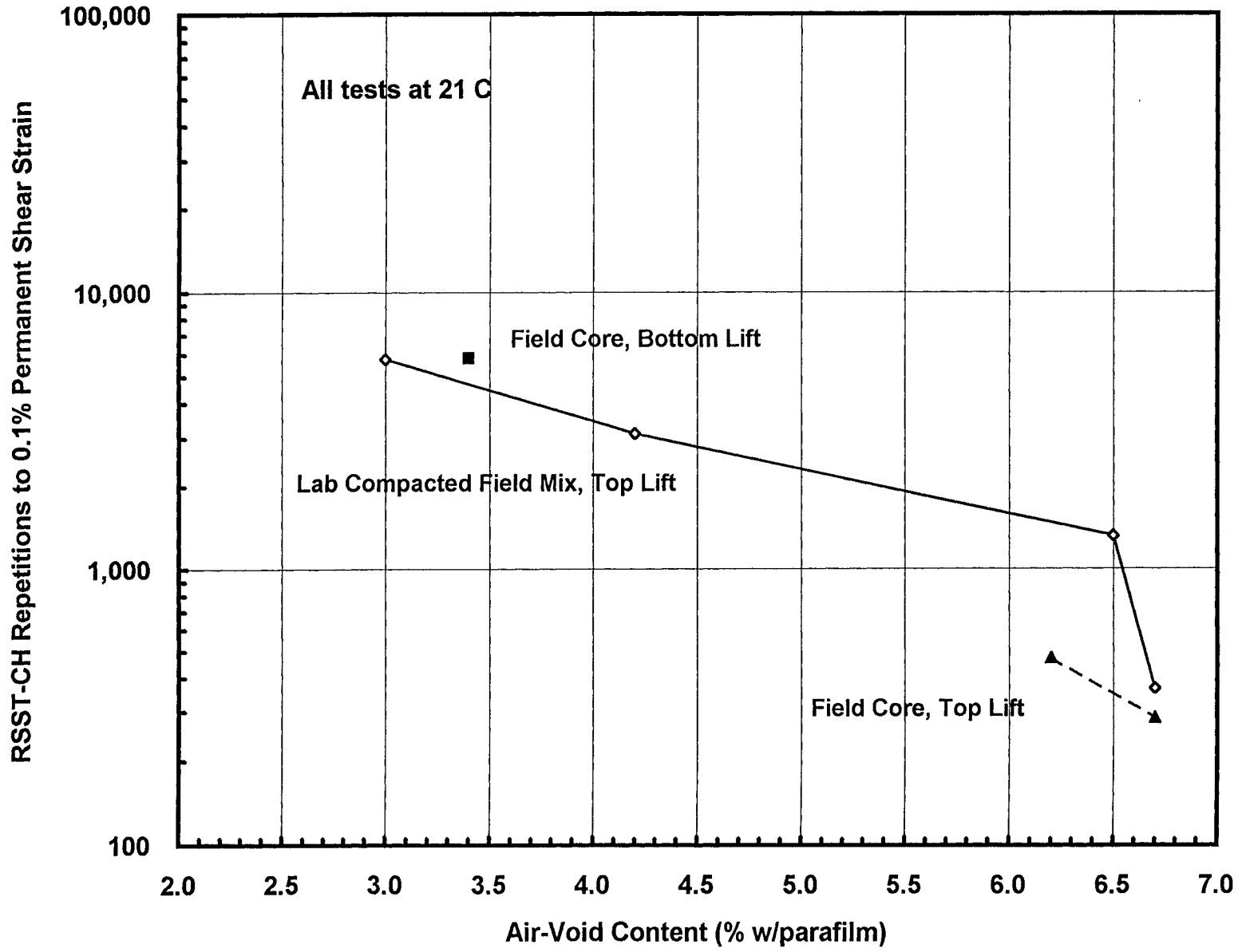

Figure 5.7 RSST-CH Repetitions to 0.1 Percent Permanent Shear Strain, Summary of Caltrans Results

Table 5.8 Summary of UC-Berkeley Repetitive Simple Shear Test at Constant Height Results

Mix	Specimen	Lift	Test Temperature (C)	Repetitive Shear Stress (kPa)	Specimen Orientation Relative to Compaction	Air-Void Content (%)	RSST-CH reps to Permanent Shear Strain 0.10%	0.25%	0.50%	1.0%	2.0%	5.0%
Field Mix Lab Compact	AC1-1	top	21	68.9	varied	3 0	47,242	473,909				
	AC2-1	top	21	68.9	varied	5.0	7,361	83,577				
	average					***4.0***	***27,302***	***278,743***				
	AC3-1	top	21	68.9	varied	7 2	7,501	71,344				
	AC6-1	top	21	68.9	varied	7.4	6,370	40,671				
	AC9-1	top	21	68.9	varied	7.4	2,893	50,002				
	AC8-1	top	21	68.9	varied	7 5	1,522	13,001	48,953			
	average					***7.4***	***4,572***	***43,755***				
	AC18-2	top	29	68.9	perpindicular	2.4	400	6,902				
	AC18-3	top	29	68.9	perpindicular	2.6	510	13,708				
	AC19-1	top	29	68.9	perpindicular	3.6	212	2,247				
	average					***2.9***	***374***	***7,619***				
	AC19-3	top	29	68.9	perpindicular	5.2	454	16,062				
	AC27-1	top	29	68.9	perpindicular	6.0	301	5,714				
	average					***5.6***	***378***	***10,888***				
	AC22-2	bottom	29	68.9	perpindicular	3.5	765					
	AC22-3	bottom	29	68.9	perpindicular	3.9	4,082	51,112				
	AC22-1	bottom	29	68.9	perpindicular	4.3	506	12,001				
	average					***3.9***	***1,784***	***31,557***				
	AC23-3	bottom	29	68.9	perpindicular	5.9	231	2,924	42,131			
	AC23-1	bottom	29	68.9	perpindicular	6.6	152	1,014	6,001			
	AC23-2	bottom	29	68.9	perpindicular	7.2	214	4,000	90,880			
	average					***6.6***	***199***	***2,646***	***46,337***			
	AC35-2	top	29	90.7	perpindicular	5.5	279	2,366	75,141			
	AC35-1	top	29	90.7	perpindicular	5.7	325	3,843	75,804			
	AC33-3	top	29	90.7	perpindicular	6.1	200	1,347	19,499			
	average					***5.8***	***268***	***2,519***	***56,815***			
	AC29-1	top	29	90.7 long load	perpindicular	4 4	44	394	2,976			
	AC37-2	top	29	90.7 long load	perpindicular	5.1	38	258	1,660	13,019	89,930	
	average					***4.8***	***41***	***326***	***2,318***			
Field Cores	SAC5t	top	21	68.9	varied	4 0	1,146	9,001	75,226			
	SAC12t	top	21	68 9	varied	5.8	630	4,902	112,303			
	SAC11t	top	21	68.9	varied	6 8	633	6,502	53,249			
	average					***5.5***	***803***	***6,802***	***80,259***			
	SAC18t	top	29	68 9	varied	4.6	93	789	4,561	53,786		
	SAC19t	top	29	68.9	varied	5.4	39	253	1,078	3,758	38,364	
	average					***5.0***	***66***	***521***	***2,820***	***28,772***		
	SAC5b	bottom	21	68.9	perpindicular	3.3	656	50,107				
	SAC2b	bottom	21	68.9	perpindicular	3 7	972	9,750	103,657			
	average					***3.5***	***814***	***29,929***				
	SAC19b	bottom	29	68.9	perpindicular	3.1	52	395	4,173			
	SAC17b	bottom	29	68.9	perpindicular	3.2	141	1,647	19,238			
	SAC20b	bottom	29	68.9	perpindicular	4.0	47	501	15,962			
	average					***3.4***	***80***	***848***	***13,124***			
	SAC25t	top	29	90 7	perpindicular	4.9	36	162	639	3,290	38,800	
	SAC24t	top	29	90.7	perpindicular	5.0	33	144	588	2,998	83,837	
	average					***5.0***	***35***	***153***	***614***	***3,144***	***61,319***	
	SAC26t	top	29	90.7 long load	perpindicular	4 0	10	50	166	783	5,294	83,336
	SAC28t	top	29	90.7 long load	perpindicular	4 6	15	77	300	1,477	8,420	109,655
	average					***4.3***	***13***	***64***	***233***	***1,130***	***6,857***	***96,496***

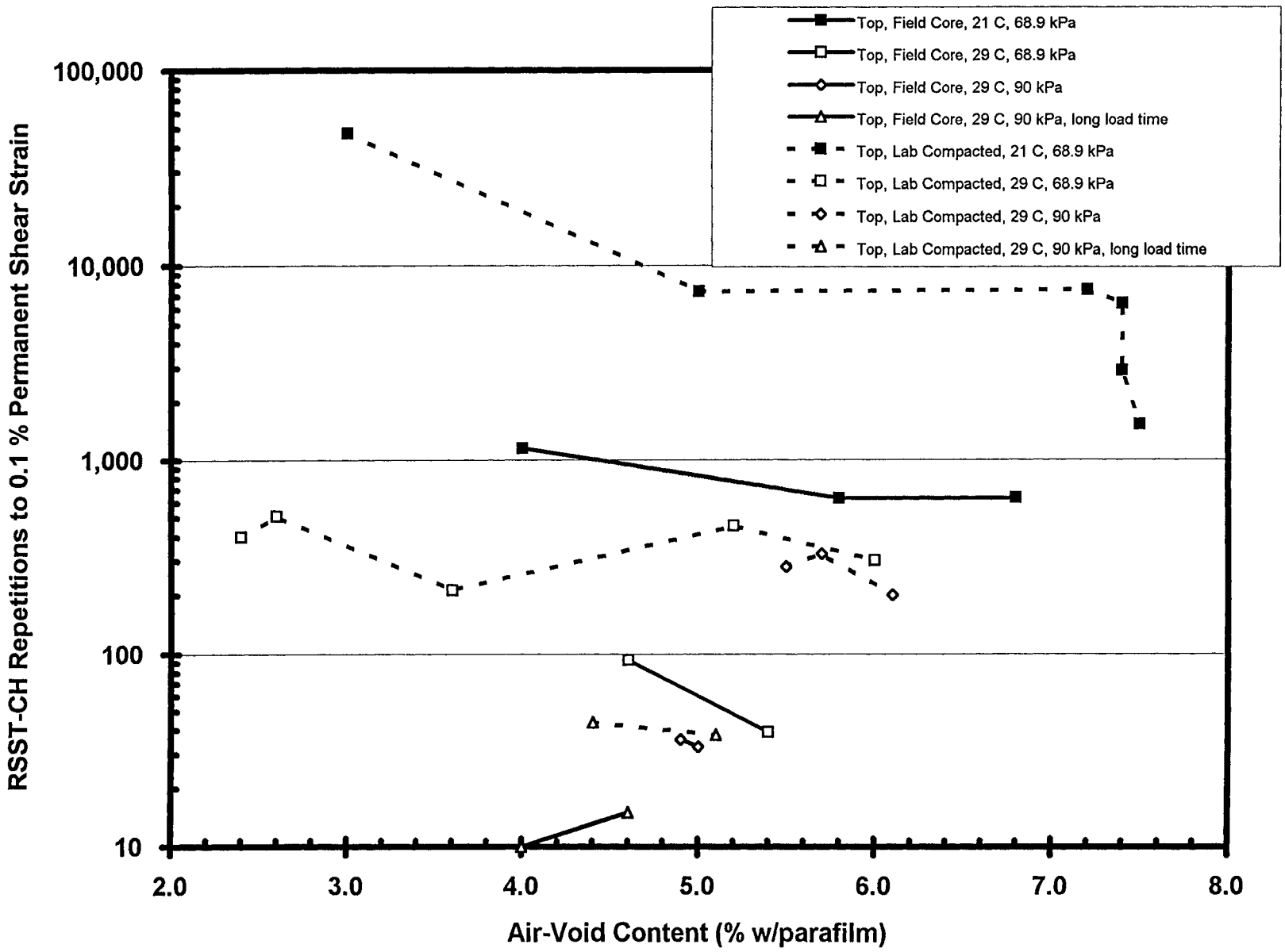

Figure 5.8 RSST-CH Repetitions to 0.1 Percent Permanent Shear Strain, Summary of UCB Results, Top Lift

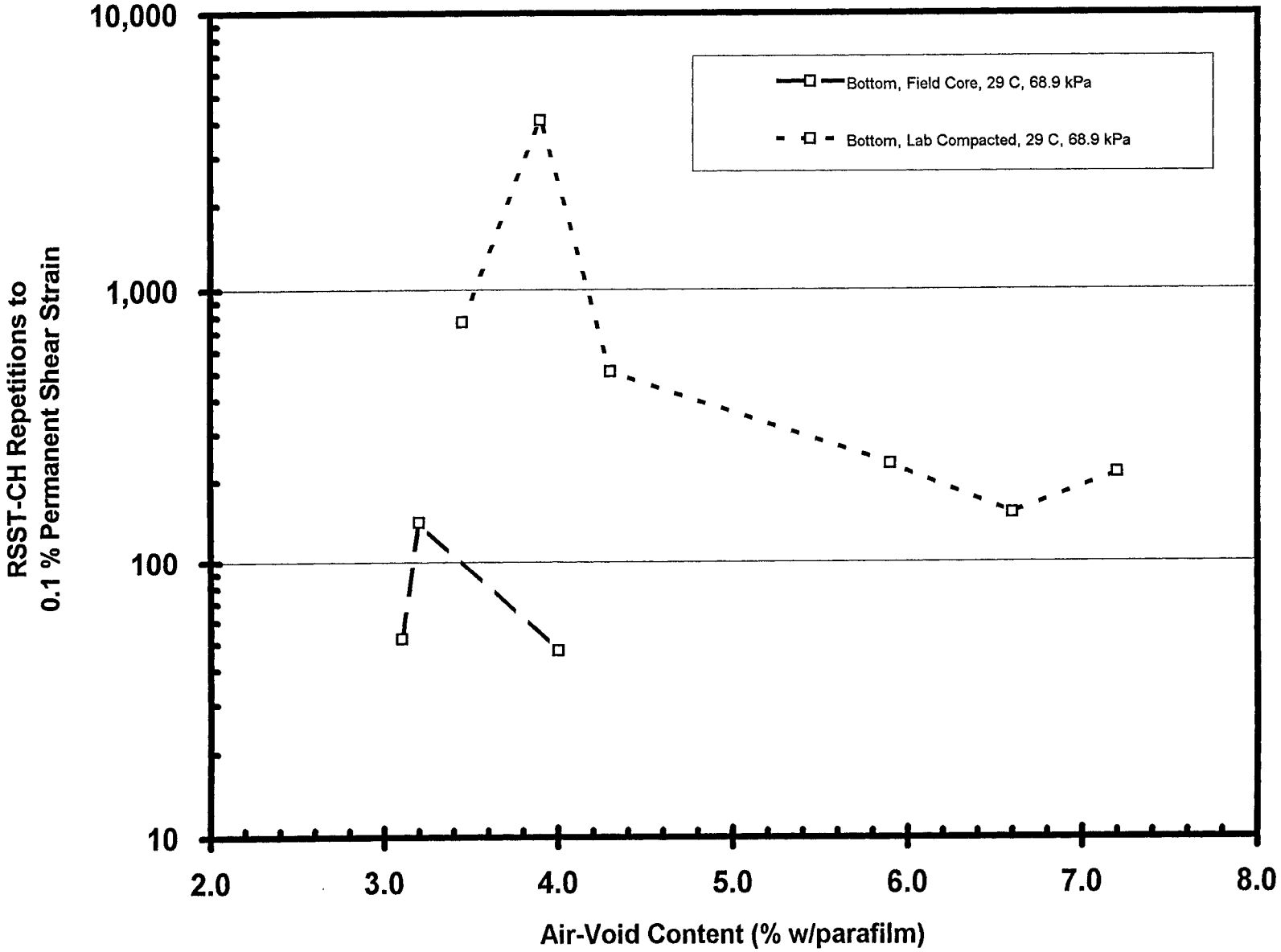

Figure 5.9 RSST-CH Repetitions to 0.1 Percent Permanent Shear Strain, Summary of UCB Results, Bottom Lift

A shift factor for translating RSST-CH repetitions to equivalent single axle load (ESAL) repetitions in the field was also developed as part of the SHRP A-003A program (*Sousa et al*., 1994). Using equation 5-5 and the transfer function the mix was estimated to have very good rutting resistance.

However, the transfer function is based on wheel loads, traffic speeds, and uni-directional trafficking of trucks in the field. They are not directly applicable for predicting rutting in the asphalt concrete under the over-loaded wheel, slow traffic speed and bi-directional trafficking being used for the HVS trafficking in this experiment to produce fatigue cracking.

It is of interest to evaluate the effects of higher temperatures, heavier loads, and slow trafficking associated with these HVS tests through laboratory testing. The results of additional RSST-CH testing to simulate these conditions, at least on a naive basis, are presented herein. The results should not be used with the SHRP A-003A statistical transfer function to predict ESALS to a given rut depth.

In addition to the tests at 21°C (69°F), UCB also conducted a few tests at 29°C and 68.9 kPa shear stress, the temperature at a 50 mm (2 in.) depth representative of the hotter periods occurring later in the HVS testing. These results are shown in Table 5.8 and Figures 5.8 and 5.9. Some laboratory studies have suggested that there may be an orientation of aggregate in the horizontal plane in the direction of compaction. Hence the cores tested at 29°C (84°F) were tested in shear in a direction normal to the direction of compaction, presumably the direction in which shear movements would occur in the wheelpaths.

It can be seen in Figure 5.8 that increasing the test temperature from 21°C to 29°C significantly reduced the number of load repetitions to a 0.1 percent permanent shear strain. This indicates that the higher temperatures occurring later at the HVS test site 500RF could result in

an increase in rutting in the asphalt concrete.

Investigation of Effects of HVS Loading and Traffic Speed. To evaluate the effect of the overloaded HVS wheel, the shear stress applied in the RSST-CH was increased, and additional tests were performed at 29°C. The larger shear stress, 90 kPa, was based on measurement of the contact areas of the HVS wheel at 40 and 100 kN, and calculation of the resulting approximate contact stresses. A 40 kN half-axle load is an ESAL. The approximate contact stress ratio assumed to be of the contact stresses was then used to increase the shear stress in the RSST-CH.

The larger shear stress resulted in a decrease in the number of RSST-CH repetitions to a 0.1 percent permanent shear strain, as can be seen in Figure 5.8. The effect of increasing the shear stress did not appear to be as important as the change in temperature from 21° to 29°C.

The 0.1 s loading time typically used for the RSST-CH is approximately based on the influence time for a standard axle load passing over an element in the asphalt concrete at about 40 kph (25 mph). The HVS wheel operates at approximately 8 kph (5 mph). To simplistically evaluate the effect of a longer shear loading time, RSST-CH results were also obtained using a 0.5 s loading time, 90 kPa shear stress, and 29°C test temperature.

The RSST-CH rest period was increased from 0.6 s to 2.5 s. A 3.0 s rest period was initially used, however, it was found that there was no additional recovery after 2.5 s.

The longer loading time resulted in a further reduction in the number of load repetitions to a 0.1 percent permanent shear strain, as can be seen in Figure 5.8.

The results of this simplistic evaluation indicate that significant increases in rutting can be expected under the HVS loading conditions that occurred later on at the 500RF site, as compared to loads and traffic speeds expected in the field. The results also indicate the need to

control the test temperature when overloading is used to accelerate fatigue damage, if rutting of the asphalt concrete is to be minimized.

Comparison of Field Cores and Laboratory Compacted Specimens. The RSST-CH results for comparable specimens tested by Caltrans and UCB are shown in Figure 5.10. In general, the Caltrans tests indicated less resistance to permanent shear deformation than did the UCB tests. A possible cause for the differences will require further investigation, using more tightly controlled specimens than can be obtained from compacted field mix or field cores. An effort of this type is currently underway. It should be noted that all laboratory compacted specimens were prepared at UCB.

Comparison of Field Cores and Laboratory Compacted Specimens. For nearly all the specimens tested using the RSST-CH, the permanent deformation resistance of laboratory compacted specimens was greater than that of field cores with similar air-void contents, as can be seen in Figures 5.7, 5.8, and 5.9. Although there may be some difference imparted by the two compaction methods, field rollers and laboratory rolling wheel, it is considered likely that differences in aging played a major role. The field mix used to prepare specimens in the laboratory was re-heated for compaction for 1.5 to 2.0 hours at the field compaction temperature.

This additional heating resulted in increased mix stiffness to the mix as was shown in Figure 5.5. At higher temperatures, where RSST-CH results are typically used for mix design and performance evaluation, the relative contribution of the increased asphalt stiffness

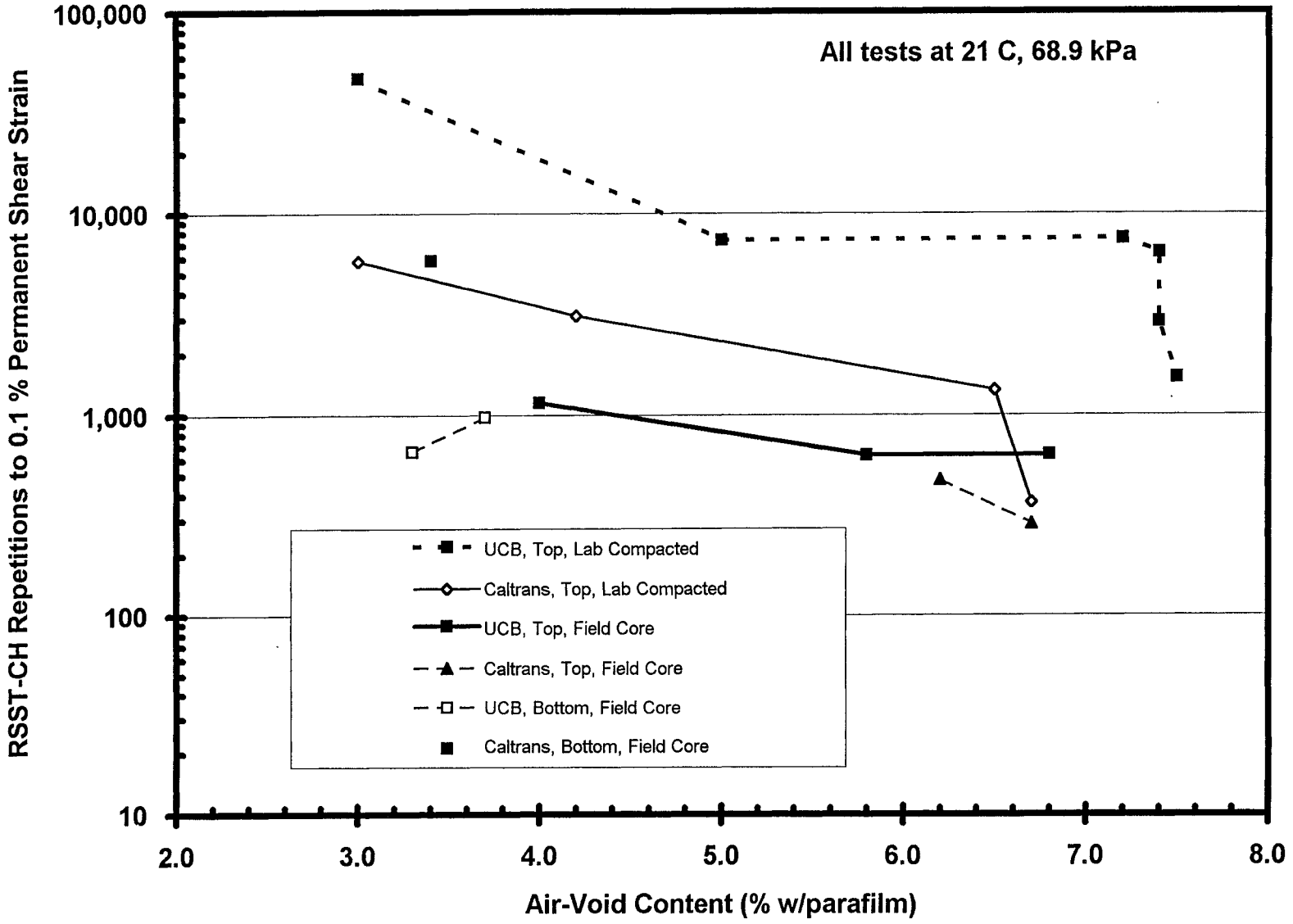

Figure 5.10 RSST-CH Repetitions to 0.1 Percent Permanent Shear Strain, Comparison of Caltrans and UCB Results, 21°C

is probably not significant. However, at the low test temperatures used for this project the contribution of increased asphalt stiffness from the additional oven heating may make a major contribution to the difference in performance between field cores and laboratory compacted specimens.

CHAPTER 6

PAVEMENT PERFORMANCE PREDICTION

6.1 INTRODUCTION

The use of mechanistic-empirical methods to predict fatigue cracking and rutting resulting from permanent deformations in the untreated materials of the pavement structure has been investigated by various researchers throughout the world over the past 30 years. From initial understanding of the critical mechanisms responsible for these distresses has come development of pavement response calculation methods and statistical transfer functions to relate calculated responses (strains) to observed pavement performance.

While the effects of mix variables on fatigue performance could be evaluated through laboratory testing the process required a large number of specimens and was relatively time consuming and at times standard fatigue relationships would be used to assess response. With the development of an improved methodology to evaluate fatigue response in the SHRP A-003A project (*Tayebali et al, 1994*), the time required to perform the requisite tests was reduced substantially. Thus it is possible, particularly for mixes containing modified binders and/or other than conventional aggregate gradings, to use fatigue testing as a part of the mix and pavement design process. Moreover, the use of the HVS permits calibration of the fatigue performance of mixes in specific prototype pavement structures and therefore provides a rapid means to extend mix design to include this factor.

Rutting at the pavement surface can result from the accumulation of permanent deformation in the underlying material and/or from the asphalt bound layers. The HVS provides an opportunity to quickly assess the effectiveness of current rutting prediction procedures and to extend the prediction capabilities to include newly developed procedures such as those resulting from the SHRP A-003 project for asphalt concrete rutting.

This chapter presents the initial performance estimates for fatigue cracking and rutting based on subgrade strain criteria for the drained and undrained test sections at Richmond Field Station (RFS). Fatigue life estimates were made using layered elastic analysis to determine critical tensile strains in the asphalt concrete layers coupled with transfer functions including models from the SHRP A-003A project *(Tayebali et al., 1994a)* and those used as a part of the Shell International Petroleum Company *(Shell International Petroleum Company, Ltd., 1978)* and the Asphalt Institute *(Transportation Research Board, 1986)* pavement design procedures. Estimates of the service life based on subgrade strain criteria were made using the criteria developed by the Shell International Petroleum Company *(1978)*, the Asphalt Institute, the University of Nottingham, and the CSIR of South Africa *(De Beer, van der Merwe, and Rohde, 1994)*.

6.2 PAVEMENT STRUCTURE

The pavement sections, both drained and undrained, have been described earlier. Essentially the only difference between the sections is the inclusion of an asphalt treated permeable base (ATPB) layer in the drained pavement. As discussed in Chapter 2, the aggregate subbase is not uniform in thickness due to a two percent cross slope. Recall that the asphalt concrete layer was constructed in two lifts and that very good compaction was obtained during

construction, with air-void contents of about 3 to 4 percent and 5.5 to 7.5 percent in the bottom and top lifts, respectively. When cutting and coring laboratory samples from the pavement, a weakness was noted in the bond between the two asphalt concrete lifts. The influence of this factor was evaluated in the modeling.

6.3 MODELING OF PAVEMENT STRUCTURES

The horizontal tensile strain at the bottom of the asphalt concrete layer has been found to be a suitable damage determinant for fatigue, while the vertical compressive strain at the top of the subgrade layer is a determinant for rutting resulting from permanent deformation in the unbound materials. Linear elastic theory was used to calculate these critical strains in the pavement structures. Most of the analyses were performed using the program ELSYM5: however, the CIRCLY program *(Wardle, 1976)* was used to investigate the effect of the bond between lifts of asphalt concrete. ELSYM5 allows only full friction interfaces in the asphalt concrete layers whereas CIRCLY allows either a full friction or a frictionless interface. With CIRCLY, the asphalt concrete layer was modeled as two separate lifts, and the tensile strains were calculated at both the bottom of the top lift and at the bottom of the lower lift providing an indication of the effect of a frictionless interface.

6.3.1 Materials Characteristics

Moduli for all the pavement layers and the mix characteristics of the asphalt materials were selected from information presented earlier. Chapter 4 presents the results of the material characterization for the unbound layers using the following tests: triaxial test, bender element analysis, R-value correlation charts and equations, dynamic cone penetrometer (DCP), heavy

weight deflectometer (HWD) deflection backcalculation, and K-mold data. Asphalt concrete stiffnesses were determined both from deflection backcalculations and from the SHRP A-003A flexural beam test results. Stiffness differences between HWD and fatigue testing reflect in part differences due to loading frequency. The two lifts exhibited differing stiffnesses, the bottom lift being stiffer due to a smaller air-void content. Moduli for the ATPB were assumed based on earlier studies at UCB since the actual moduli had not yet been evaluated in the laboratory[1].

The materials testing program provided wide ranges of moduli for each layer, as shown in Table 6.1. In an attempt to model all likely situations, combinations from the wide ranges of moduli were examined resulting in a large number of cases. To reduce the number of cases to be analyzed, unrealistic moduli combinations were eliminated by the following methods:

- The ratios between the aggregate subbase and the aggregate base moduli were limited using the method from the Shell Research Design Procedure *(Shell International Petroleum Company, Ltd., 1978)* as an approximate guide. That is, the stiffness of the untreated base is assumed to be a function of the subgrade stiffness where:

$$E_{base} = k \bullet E_{subgrade}$$

and

$$k = 0.2\ h_{base}^{0.45} \quad (h_{base}\ \textit{in millimeters}) \tag{6-2}$$

[1]Subsequent to the completion of the analyses descibed herein, moduli of the ATPB have been determined (Chapter 5) to be in the range 800 to 2000 MPa which are higher than the assumed values shown in Table 6.1.

Table 6.1 Material Characteristics of Pavement Layers

DRAINED PAVEMENT					
		Elastic Modulus (psi)			
Pavement Layer	Thickness (mm)	Minimum	Middle Values	Maximum	Poisson's Ratio
Asphalt concrete top lift	61		8268		0.35
Asphalt concrete bottom lift	76		10335		0.35
Asphalt treated permeable base (ATPB)	76	689		1034	0.4
Aggregate base and subbase	310 401 488	103	138 190 242 293	448	0.35
Subgrade	Semi-infinite	17	69	234	0.45
UNDRAINED PAVEMENT					
		Elastic Modulus (MPa)			
Pavement Layer	Thickness (mm)	Minimum	Middle values	Maximum	Poisson's ratio
Asphalt concrete top lift	61		8268		0.35
Asphalt concrete bottom lift	76		10335		0.35
Aggregate base	274	172	365	448	0.35
Aggregate subbase[1]	127 218 305	103	242	345	0.35
Subgrade	Semi-infinite	17	69	234	0.45

[1]The thickness of the aggregate subbase at the test sections is as follows: 5.0 in (125 mm) at 500RF, 8.6 in (215 mm) at 501RF, 8.6 in (215 mm) at 502RF and 12.0 in (300 mm) at 503RF.

The method specifies that k should remain within the range 2 to 4. In this evaluation, k ranged between 2.6 and 3.5.

ELSYM5 can only model five layers. Therefore for the drained pavement, the aggregate base and subbase were combined and modeled as one layer. The moduli for the combined layer were limited by the stiffness relationship between the combined layer and the subgrade discussed above. The specific cases used in the ELSYM5 analyses are given in Table 6.2. Poisson's ratios, assumed for all the pavement layers, are summarized in Table 6.1.

6.3.2 Fatigue Models

Four models to predict fatigue performance were evaluated. The models were all developed at different times and in different situations. The only model which is specific to the actual test section is the SHRP laboratory (fatigue beam test) model. Each model has varying degrees of dependency on tensile strain and on mix characteristics which will, therefore, result in different predicted fatigue lives.

Typical highway pavements have larger fatigue lives (N_{field}) than predicted by either laboratory testing or mechanistic analysis (N_{lab}), due to such factors as crack progression, traffic wander, and intermittent loading. Therefore, a shift factor (SF) must be applied in order to more accurately predict the actual field fatigue life as follows:

$$SF = \frac{N_{field}}{N_{lab}} \tag{6-3}$$

Table 6.2 Summary of Moduli Cases for ELSYM5 Analysis for Drained and Undrained Pavements

Drained Cases					
Case	Top AC modulus (MPa)	Bottom AC modulus (MPa)	Asphalt Treated Permeable Base Modulus (MPa)	Combined Aggregate Base / Aggregate Sub Base Modulus (MPa)	Sub Grade Modulus (MPa)
1	8268	10335	689	103	17
2	8268	10335	689	103	69
3	8268	10335	689	138	234
4	8268	10335	689	189	69
5	8268	10335	689	241	69
6	8268	10335	689	293	234
7	8268	10335	689	448	234
8	8268	10335	1034	103	17
9	8268	10335	1034	103	69
10	8268	10335	1034	138	234
11	8268	10335	1034	189	69
12	8268	10335	1034	241	69
13	8268	10335	1034	293	234
14	8268	10335	1034	448	234
Undrained Cases					
Case	Top AC modulus (MPa)	Bottom AC modulus (MPa)	Aggregate Base modulus (MPa)	Aggregate Sub Base Modulus (MPa)	Sub Grade Modulus (MPa)
1	8268	10335	172	103	17
2	8268	10335	172	103	69
3	8268	10335	172	103	234
4	8268	10335	172	241	69
5	8268	10335	172	345	234
6	8268	10335	365	103	17
7	8268	10335	448	103	69
8	8268	10335	448	103	234
9	8268	10335	448	241	69
10	8268	10335	448	345	234

SHRP A-003A laboratory testing method (fatigue beam test). These site specific equations, given in Table 6.3, were developed from samples taken from the actual test section and tested using the third-point, controlled-strain, flexural beam test as specified by SHRP A-003A *(Tayebali et al., 1994a)*. The specimens were tested at 20°C (68°F) which was about the temperature at the bottom of the layer when the HVS tests began. Effects of higher temperatures on the fatigue life will be evaluated as HVS testing proceeds.

A shift factor of 13 was used to determine the field fatigue life from the laboratory determined fatigue lives *(Tayebali et al., 1994a)*. Whether or not this shift factor is adequate for converting laboratory data to pavement response in the HVS test section will be validated when the first CAL/APT HVS test is completed.

The SHRP A-003A procedure presents a way in which to combine actual mix properties as determined in the laboratory with mechanistic pavement analysis to obtain a site specific prediction of pavement behavior.

SHRP surrogate model. The SHRP Project A-003A *(Tayebali et al., 1994a)* surrogate model was developed from tests on 44 mixes with conventional binders. Laboratory testing was used to develop the equation which is shown in Table 6.3.

A shift factor of 13 is suggested for this expression, although for actual design purposes, an initial shift factor of 10 is recommended. For in-situ pavement analysis, temperature distributions through a temperature equivalence factor are included in the SHRP A-003A analyses with flexural beam results or the surrogate model. Temperature distributions were not included herein because of special conditions at the RFS test sections.

Table 6.3 Summary of Fatigue Models and Shift Factors

DESIGN METHOD	SHIFT FACTOR	LEGEND
SHRP A-003A LABORATORY TESTING METHOD		N_f = fatigue life
Top lift (air-voids=6.8%): $Nf = 4.06 \times 10^{-8} \times e_t^{-3.348}$ Bottom lift (air-voids=3.7%): $Nf = 8.36 \times 10^{-8} \times e_t^{-3.420}$	13	e_t = initial strain
SHRP A-OO3A SURROGATE EQUATION		VFB=% voids filled with asphalt
$N_f = 2.738 * 10^5 \exp^{0.077VFB} (e_t)^{-3.624} (S_0")^{-2.720}$	10 - 13	S_0"=initial loss stiffness (psi)
ASPHALT INSTITUTE		
$\log N_f = A[15.947-3.291 \log(e_t/10^{-6}) - 0.854 \log(Smix/10^3)]$ To incorporate effects of the mix, multiply N_f by $A = 10^M$ $M = 4.84 \left(\frac{V_V}{V_V - V_B} - 0.69 \right)$	13	= S_{mix} sin f S_{mix}= flexural mix stiffness (psi)
SHELL METHOD		
$N_f = [e_t \times 0.278 \times (p \times S_{mix} \times \sin f / C)^{0.57}]^{1/0.77(m-1)}$ $Y_f = C \times N_f^m$	10 to 20	f =flexural phase angle
SOUTH AFRICAN MECHANISTIC DESIGN METHOD		
	0.0413 x d	V_V =volume voids
CAL/APT PHASE 1 STUDY		V_B =volume asphalt
	0.01 - 1.3	Y_f = total dissipated energy C,m = mix constants d = layer thickness, mm

Asphalt Institute fatigue equation. This model was originally developed by Finn et al. as part of the National Cooperative Highway Research Program (NCHRP) Project 1-10B *(Transportation Research Board, 1986)* from laboratory fatigue data obtained from controlled stress tests on dense-graded mixes. The equations are shifted for the desired percent cracking in the wheel path based on observations from the AASHO Road Test. The equation used in this study (Table 6.3) includes a recommended shift factor of 13 for 10 percent or less cracking in the wheel path for asphalt concrete layers greater than 100 mm (4 in) thick.

The Asphalt Institute incorporated the influence of mix composition by multiplying the NCHRP 1-10 equation for N_f by a factor, A, which is determined from laboratory data. The equations to calculate A are given in Table 6.3.

Shell method for fatigue. The Shell method was developed by the Shell International Petroleum Company *(1978)* in The Netherlands. It is based on laboratory controlled strain bending tests on several mix types and incorporates temperature extremes to enable the method to be used world-wide. The equation is given in Table 6.3.

The recommended shift factor is in the range of 10 to 20. For this investigation a shift factor of 13 was selected, being within the range recommended by Shell and recommended by the other design methods discussed in this paper.

6.3.3 Unbound Layers Permanent Deformation (Rutting) Models

Four models were used to predict permanent deformation, all by the technique of limiting the subgrade strain. The subgrade strain criteria is based on limiting the permanent deformation of the unbound layer manifested the surface of the pavement. The models were all developed at different times and in different situations. None of the models are specific to the actual test

sections. The models are shown in Table 6.4. Each model has different values for the coefficients incorporated into the equation. Therefore, each model will predict different rutting lives for the same vertical compressive strain.

Table 6.4 Summary of Permanent Deformation Models

DESIGN METHOD	LEGEND
ASPHALT INSTITUTE SUBGRADE RUTTING EQUATION	N = rutting life e_z = vertical compressive strain
$N = (1.05 \times 10^{-2} / e_z)^{1/0.223}$	
SHELL SUBGRADE RUTTING EQUATION	
$N = (2.8 \times 10^{-2} / e_z)^{1/0.25}$	
NOTTINGHAM SUBGRADE RUTTING EQUATION	
$N = (1.126 \times 10^{-6}) / e_z^{3.571}$	
SOUTH AFRICAN SUBGRADE RUTTING EQUATION	
$N = 10 \wedge ((3.395 - \log e_z \times 10^{-6})/0.0872)$	

Asphalt Institute criteria. The Asphalt Institute criteria were initially developed by Chevron for pavements containing asphalt emulsion treated bases. These criteria were developed from pavements designed according to the State of California procedure, and the prediction is for a rut depth of 19 mm (0.75 in).

This equation will result in smaller rutting lives than the Shell equation, probably because pavements designed according to the State of California procedure will have less permanent deformation than the AASHO Road Test sections used to develop the Shell criteria *(Shook, 1982)*.

Shell criteria. The Shell criteria for subgrade rutting were developed from analyses of the AASHO Road Test data. The output from the equation is for a rut depth of 19 mm (0.75 in).

Nottingham criteria. These criteria were developed in the United Kingdom for pavements designed under the guidelines of Road Note 29 (*1970*) and for a rut depth of 19 mm (0.75 in).

South African criteria. The South African criteria for permanent deformation in the subgrade is used for, and was developed from, tests on South African pavements (*De Beer et al, 1994*). Different equations are used for lightly trafficked roads and for major roads and freeways: they are associated with specific rut depths for each road category. The equation used in these analyses is for a 12 mm rut (0.5 in). These criteria have been verified with data obtained from tests on lightly cemented pavements. This study has also indicated that these criteria are independent of the depth to the top of the subgrade.

6.3.4 Location and Magnitude of Critical Tensile Strains

From ELSYM5 (full friction between layers) the maximum tensile strain was found to occur at the bottom of the asphalt concrete layer. However, large principal tensile strains were noticed near the surface of the asphalt concrete layer, and this could indicate the possibility of surface cracking. An investigation into surface cracking is beyond the scope of this report: however, crack development under the HVS loading will continue to be monitored.

The average tensile strains calculated for the 432 ELSYM5 cases (as given in Table 6.2) are summarized in Table 6.5. The table shows the effects of each variable and presents the average strain obtained for each particular variable for both the drained and undrained pavements at the bottom lift of the asphalt concrete layer.

The results summarized in Table 6.5 indicate that tensile strains in the undrained pavement are larger than those for the drained pavement, as a result of inclusion of the ATPB layer in the drained pavement.

Critical location of tensile strain and bonding between the asphalt concrete layers. The ELSYM5 full friction analyses gave consistently larger tensile strains at the bottom of the bottom lift than at the bottom of the top lift for both pavement structures. The strain at the bottom of the bottom lift is expected to be the largest since the two lifts and the underlying layers are modeled as having full friction interfaces, and, therefore, strains will be transferred through the layer interface.

Some cases were also calculated using CIRCLY to investigate the effects of the weak bond between the two lifts of asphalt concrete. As a check, the results for the CIRCLY full friction analyses compare well with the ELSYM5 results. The maximum difference between the two results is 25%. An important result from the CIRCLY analyses is that, in every case analyzed, a frictionless interface between the two asphalt concrete lifts results in the critical location for the maximum tensile strain being found at the bottom of the top lift as opposed to the bottom of the bottom lift. Although the bond between the lifts is weak, some friction will be present, and it is likely that this interface cannot be considered to be fully frictionless. Therefore, even though a substantial increase in the maximum strain is found between the full friction and frictionless cases, the effect on the actual pavement of the weak bonding is not considered to be as substantial as the analyses show.

Table 6.5 Summary of Average ELSYM5 Strains and Predicted Fatigue Lives

Drained		Bottom of Bottom AC Layer - Elsym Tensile Strains	Asphalt Institute - Nf	SHRP Laboratory Fatigue Beam - Nf	SHRP Surrogate - Nf	Shell - Nf
Load (kN)						
	40	080E-06	7.59E+07	6.65E+07	4.18E+08	7.21E+06
	80	139E-06	1.30E+07	1.11E+07	6.03E+07	1.10E+06
	100	167E-06	7.28E+06	6.13E+06	3.18E+07	5.90E+05
Subbase Thickness						
(mm)	127	130E-06	3.10E+07	2.70E+07	1.64E+08	2.86E+06
	218	128E-06	3.22E+07	2.80E+07	1.71E+08	2.98E+06
	305	127E-06	3.30E+07	2.88E+07	1.75E+08	3.06E+06
ATPB Moduli (MPa)						
	690	134E-06	2.74E+07	2.38E+07	1.43E+08	2.50E+06
	1034	122E-06	3.67E+07	3.20E+07	1.97E+08	3.43E+06
AB/ASB Combined						
Moduli (MPa)	103	156E-06	1.60E+07	1.37E+07	7.85E+07	1.40E+06
	138	129E-06	2.72E+07	2.35E+07	1.40E+08	2.47E+06
	190	130E-06	2.71E+07	2.35E+07	1.40E+08	2.47E+06
	242	122E-06	3.22E+07	2.80E+07	1.69E+08	2.96E+06
	293	109E-06	4.48E+07	3.91E+07	2.42E+08	4.20E+06
	448	098E-06	6.12E+07	5.38E+07	3.41E+08	5.86E+06
Subgrade						
Moduli (MPa)	17	165E-06	1.32E+07	1.13E+07	6.38E+07	1.15E+06
	69	133E-06	2.60E+07	2.26E+07	1.34E+08	2.36E+06
	234	112E-06	4.44E+07	3.88E+07	2.41E+08	4.17E+06

Undrained		Bottom of Bottom AC Layer - Elsym Tensile Strains	Asphalt Institute - Nf	SHRP Laboratory Fatigue Beam - Nf	SHRP Surrogate Flexural - Nf	Shell - Nf
Load (kN)						
	40	091E-06	4.98E+07	4.33E+07	2.63E+08	4.59E+06
	80	158E-06	8.36E+06	7.06E+06	3.69E+07	6.83E+05
	100	190E-06	4.59E+06	3.84E+06	1.91E+07	3.60E+05
Subbase Thickness						
(mm)	127	148E-06	2.04E+07	1.76E+07	1.03E+08	1.83E+06
	218	146E-06	2.09E+07	1.81E+07	1.06E+08	1.88E+06
	305	145E-06	2.14E+07	1.85E+07	1.09E+08	1.92E+06
AB Moduli (MPa)						
	172	166E-06	1.28E+07	1.10E+07	6.15E+07	1.11E+06
	365	151E-06	1.62E+07	1.39E+07	7.93E+07	1.42E+06
	448	121E-06	3.22E+07	2.80E+07	1.69E+08	2.96E+06
ASB Moduli (MPa)						
	103	153E-06	1.80E+07	1.55E+07	9.00E+07	1.60E+06
	242	142E-06	2.23E+07	1.93E+07	1.14E+08	2.01E+06
	345	130E-06	2.83E+07	2.45E+07	1.47E+08	2.58E+06
Subgrade						
Moduli (MPa)	17	170E-06	1.22E+07	1.05E+07	5.87E+07	1.06E+06
	69	146E-06	2.07E+07	1.79E+07	1.05E+08	1.85E+06
	234	135E-06	2.55E+07	2.21E+07	1.32E+08	2.31E+06

Effects of increases in moduli and load. The strains predicted by ELSYM5 followed expected trends. An increase in the moduli for all situations analyzed resulted in a decrease in the tensile strain, to varying degrees. In addition, the tensile strain also increased with an increase in load.

Effects of thickness of the aggregate subbase. The thickness of the aggregate subbase does not substantially influence the tensile strains at the bottom of the asphalt concrete layer for either the drained or undrained pavements. As thickness of the aggregate subbase increases, the strains marginally decrease.

6.3.5 Magnitude of Vertical Compressive Strain

A summary of the average vertical compressive strains calculated for the ELSYM5 cases is given in Table 6.6. This table isolates the effects of each variable and gives the average strains obtained for each particular variable for both pavement structures. The compressive strains are marginally larger for the undrained pavement than the drained pavement, again as a result of the inclusion of the ATPB layer in the drained pavement. The ELSYM5 and CIRCLY strains compare well, the maximum difference between the calculations is 25%. Apparent discrepancies in expected trends in average strain in Table 6.6 are due to the influence of moduli for particularities in the unbound layers. Also, some of the moduli cases used to calculate the average for each variable did not incorporate the full moduli ranges. Table 6.3 gives the moduli cases.

Bonding between the asphalt concrete lifts. The analyses show that the effect of a frictionless interface between the two asphalt concrete lifts is to produce a larger vertical

Table 6.6 Average ELSYM5 Subgrade Strains and Rutting Predictions

Drained Section	ELSYM5 Strain in Top of Subgrade	Shell	Chevron / Asphalt Institute	Nottingham	South African
Load (kN)					
40	198E-06	4.05E+09	8.04E+08	1.38E+08	2.28E+16
80	384E-06	4.61E+08	7.66E+07	1.87E+07	6.28E+14
100	438E-06	1.89E+08	2.61E+07	8.84E+06	4.97E+12
Subbase Thickness (mm)					
127.0	413E-06	6.59E+08	1.14E+08	2.56E+07	4.51E+14
218.0	352E-06	1.29E+09	2.42E+08	4.65E+07	3.16E+15
305.0	331E-06	1.89E+09	3.72E+08	6.50E+07	1.12E+16
ATPB Moduli (MPa)					
689	364E-06	1.39E+09	2.67E+08	4.92E+07	6.38E+15
1034	350E-06	1.54E+09	3.00E+08	5.40E+07	8.70E+15
AB/ASB Combined Moduli (MPa)[1]					
103	618E-06	5.64E+07	7.15E+06	2.87E+06	4.18E+11
138	167E-06	3.53E+09	6.94E+08	1.21E+08	1.93E+16
189	385E-06	1.29E+08	1.71E+07	6.34E+06	1.56E+12
241	371E-06	1.54E+08	2.08E+07	7.38E+06	2.67E+12
293	176E-06	2.99E+09	5.79E+08	1.05E+08	1.33E+16
448	171E-06	3.42E+09	6.74E+08	1.18E+08	2.07E+16
Subgrade Moduli (MPa)					
17	837E-06	5.22E+06	4.64E+05	3.63E+05	1.32E+08
69	385E-06	1.30E+08	1.72E+07	6.37E+06	1.69E+12
234	172E-06	3.31E+09	6.49E+08	1.15E+08	1.78E+16

Undrained Section	ELSYM Strain in Top of Subgrade	Shell	Chevron / Asphalt Institute	Nottingham	South African
Load (kN)					
40	213E-06	4.00E+09	8.02E+08	1.35E+08	2.89E+16
80	417E-06	2.62E+08	3.77E+07	1.19E+07	1.15E+13
100	518E-06	1.10E+08	1.43E+07	5.46E+06	9.50E+11
Subbase Thickness (mm)					
127.0	440E-06	6.58E+08	1.15E+08	2.53E+07	5.39E+14
218.0	379E-06	1.29E+09	2.44E+08	4.62E+07	3.92E+15
305.0	329E-06	2.42E+09	4.95E+08	8.09E+07	2.44E+16
AB Moduli (MPa)[1]					
172	406E-06	1.23E+09	2.35E+08	4.39E+07	5.03E+15
365	748E-06	7.84E+06	7.30E+05	5.22E+05	4.15E+08
448	261E-06	2.10E+09	4.17E+08	7.20E+07	1.78E+16
ASB Moduli (MPa)					
103	453E-06	1.42E+09	2.82E+08	4.85E+07	1.20E+16
241	376E-06	1.49E+08	2.02E+07	7.17E+06	2.92E+12
345	177E-06	2.88E+09	5.56E+08	1.01E+08	1.21E+16
Subgrade Moduli (MPa)					
17	806E-06	6.24E+06	5.69E+05	4.24E+05	2.56E+08
69	384E-06	1.38E+08	1.85E+07	6.68E+06	2.33E+12
234	170E-06	3.50E+09	6.93E+08	1.20E+08	2.41E+16

1. Disparities in strains due to moduli cases considered

compressive strain at the top of the subgrade than for full friction. As noted earlier, the bond between the two asphalt concrete lifts probably lies somewhere between these two extremes. Therefore, the actual compressive strains should be within the ranges calculated.

Effects of increases in moduli and load. The subgrade vertical compressive strain also followed expected trends. An increase in load causes an increase in vertical compressive strain. An increase in modulus causes a decrease in compressive strain in all cases, but the magnitude of the increase is dependent on the moduli in the other layers.

Increasing the ATPB moduli causes negligible decreases in subgrade strain. The increases in moduli in the aggregate base and subbase also result in small decreases in the strain. This decrease is negligible for the drained pavement and more noticeable, although still small, in the undrained pavement. An increase in subgrade modulus also causes a decrease in the compressive strain.

Effects of thickness of the aggregate subbase. An increase in the subbase thickness causes a decrease in the vertical compressive strain.

6.3.6 Fatigue Life Estimates

The predicted fatigue results from the ELSYM5 and CIRCLY analyses are illustrated in Figure 6.1 for the SHRP laboratory (fatigue beam test) and the Asphalt Institute equation. These equations were selected for demonstration purposes, using all fatigue models would generate too much data to be illustrated on a single graph. In all cases illustrated, the full friction case predicts the largest fatigue life, and the frictionless case is the shortest. The actual interface between the two lifts of asphalt concrete is neither full friction nor frictionless, and, therefore, the actual fatigue life is probably between these predictions.

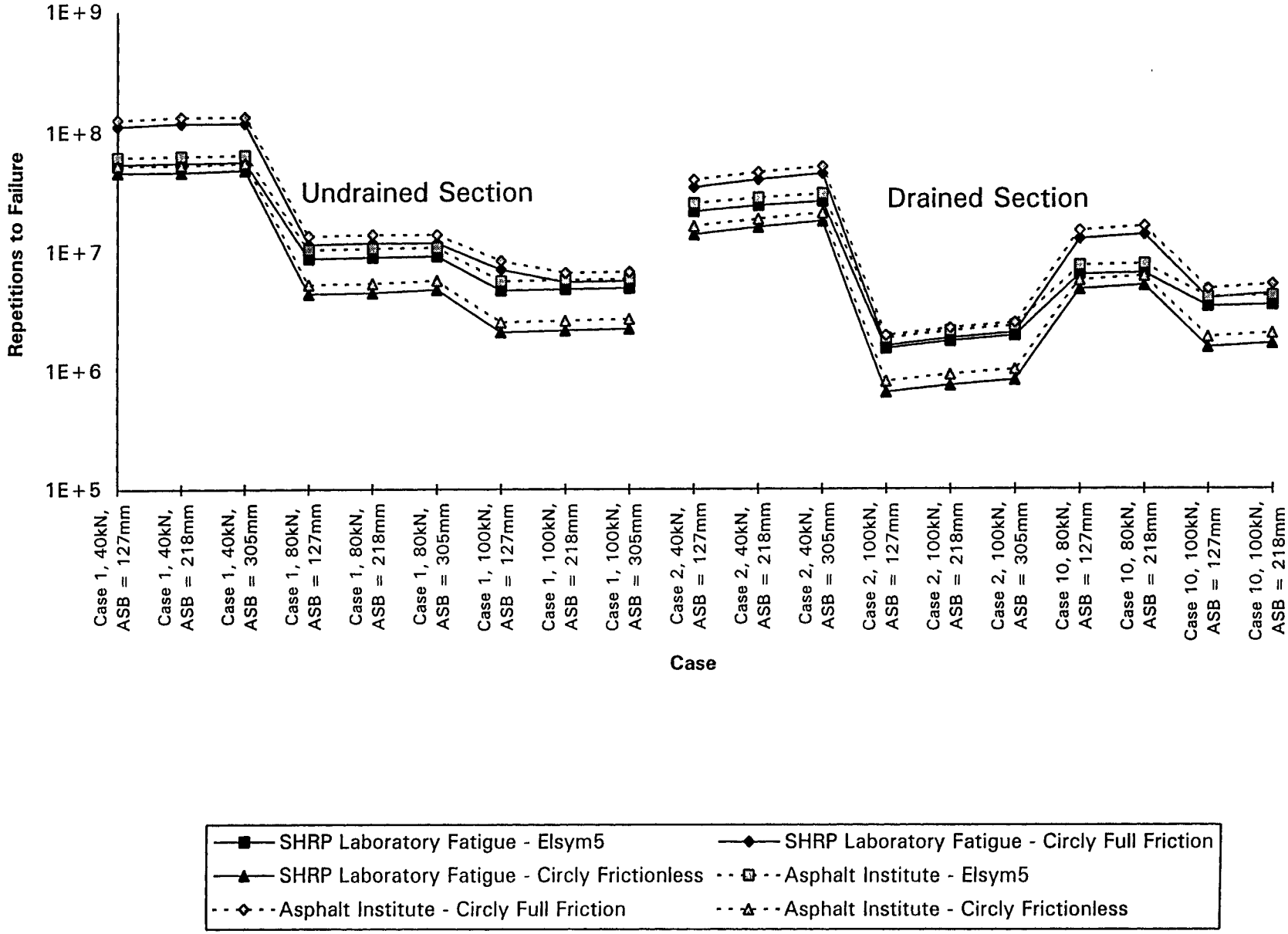

Figure 6.1 Comparison of the Effect of CIRCLY and ELSYM5 Strains on Fatigue Life Predictions

The fatigue lives predicted for these pavement structures are only evaluated for the maximum principal tensile strain which is always found at the bottom of the bottom lift in the ELSYM5 analyses. Summaries of the fatigue lives are given in Table 6.5 where each variable is isolated, and the average fatigue life is given for each variable for the drained and undrained pavement and for each model. Again, the apparent discrepancies in the expected trends in the predicted fatigue lives are due the combination of moduli cases. The remaining number of 100 kN load repetitions to failure of the test sections after the 40 kN and 80 kN loading, calculated using the linear sum of cycle ratios procedure *(Miner, 1945)*, are shown in Figures 6.2 and 6.3 for the drained sections and Figures 6.4 and 6.5 for the undrained sections.

Comparison of predicted fatigue lives between the models. In all cases, the SHRP surrogate model predicts the largest fatigue life. This fatigue life ranges from approximately 5 to 25 times the next largest fatigue life which is predicted by the Asphalt Institute model. The Shell predicts the smallest fatigue life for all cases. The fatigue equation based on laboratory tests predicts a fatigue life similar to that of the Asphalt Institute model. It should be noted that a SHRP A-003A study on shift factors found that the Asphalt Institute model predicted smaller fatigue lives than the SHRP surrogate model. The same trend was observed in this evaluation.

Effects of moduli. The undrained pavement appears to be more susceptible than the drained pavementto changes in the moduli of all the pavement layers. This is most likely due to the increased stiffness of the drained pavement structure with the inclusion of the ATPB layer.

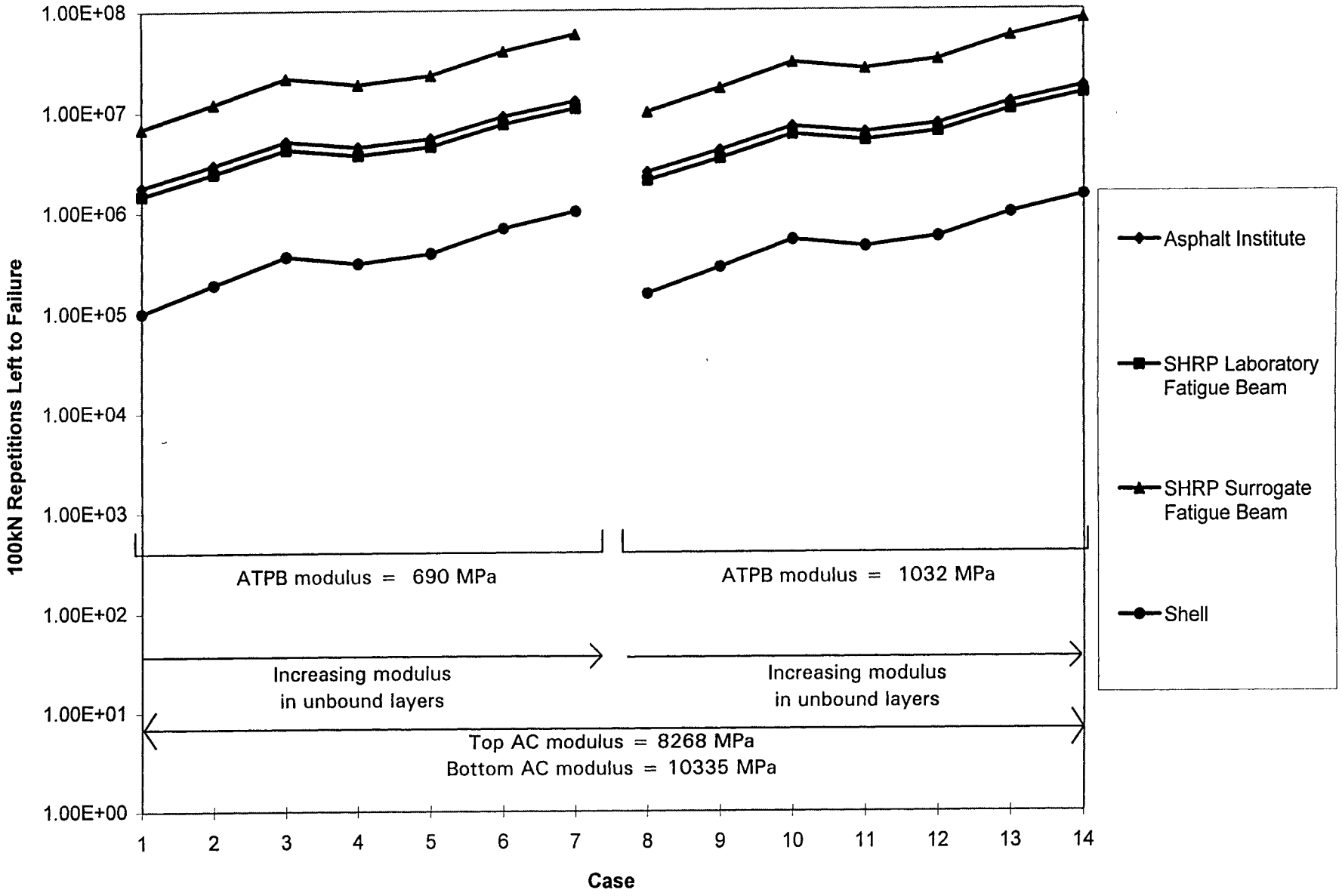

Figure 6.2 Remaining 100 kN Load Repetitions to Fatigue Failure, Drained Section 500RF, Subbase Thickness of 127 mm

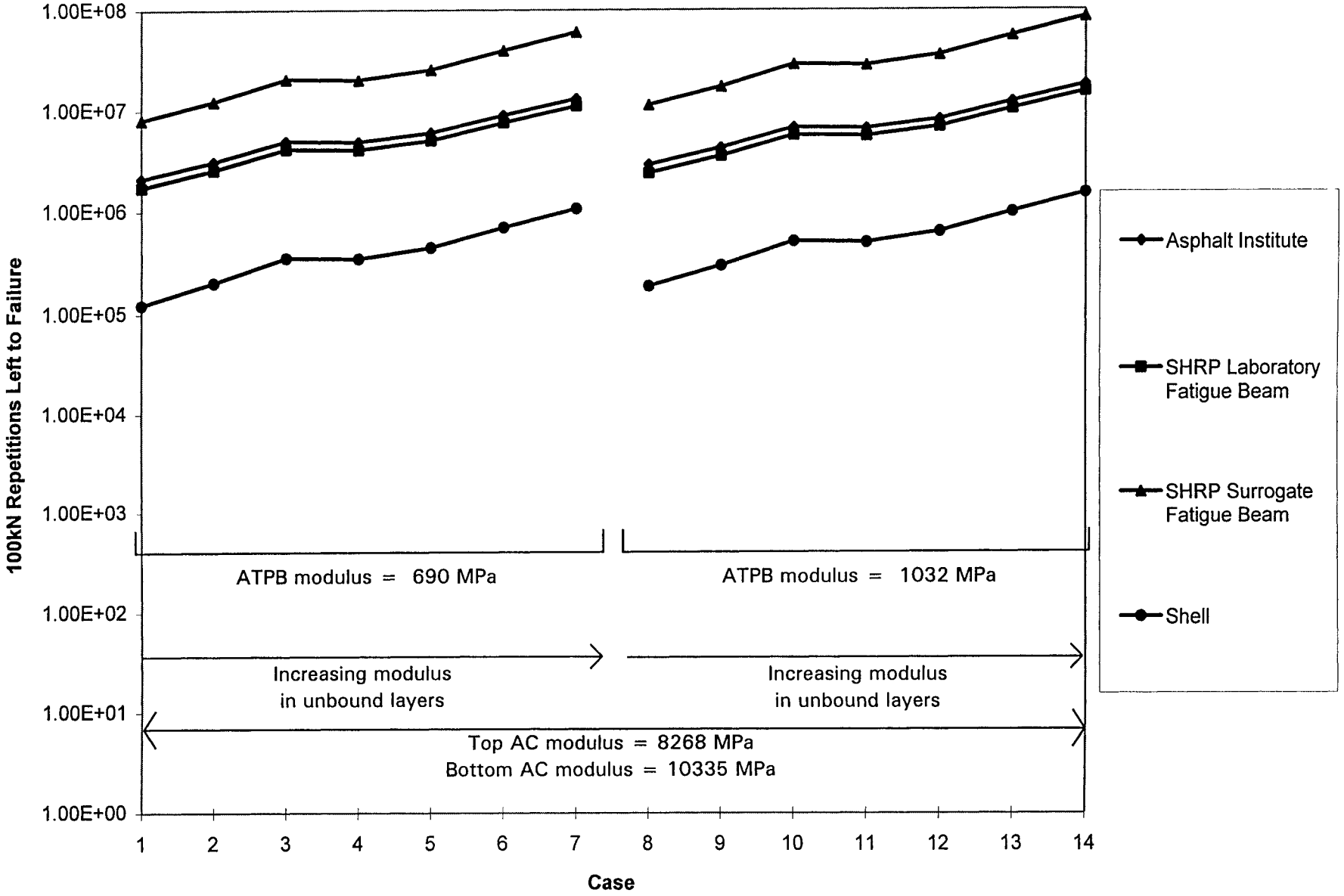

Figure 6.3 Remaining 100 kN Load Repetitions to Fatigue Failure, Drained Section 502CT, Subbase Thickness of 218 mm

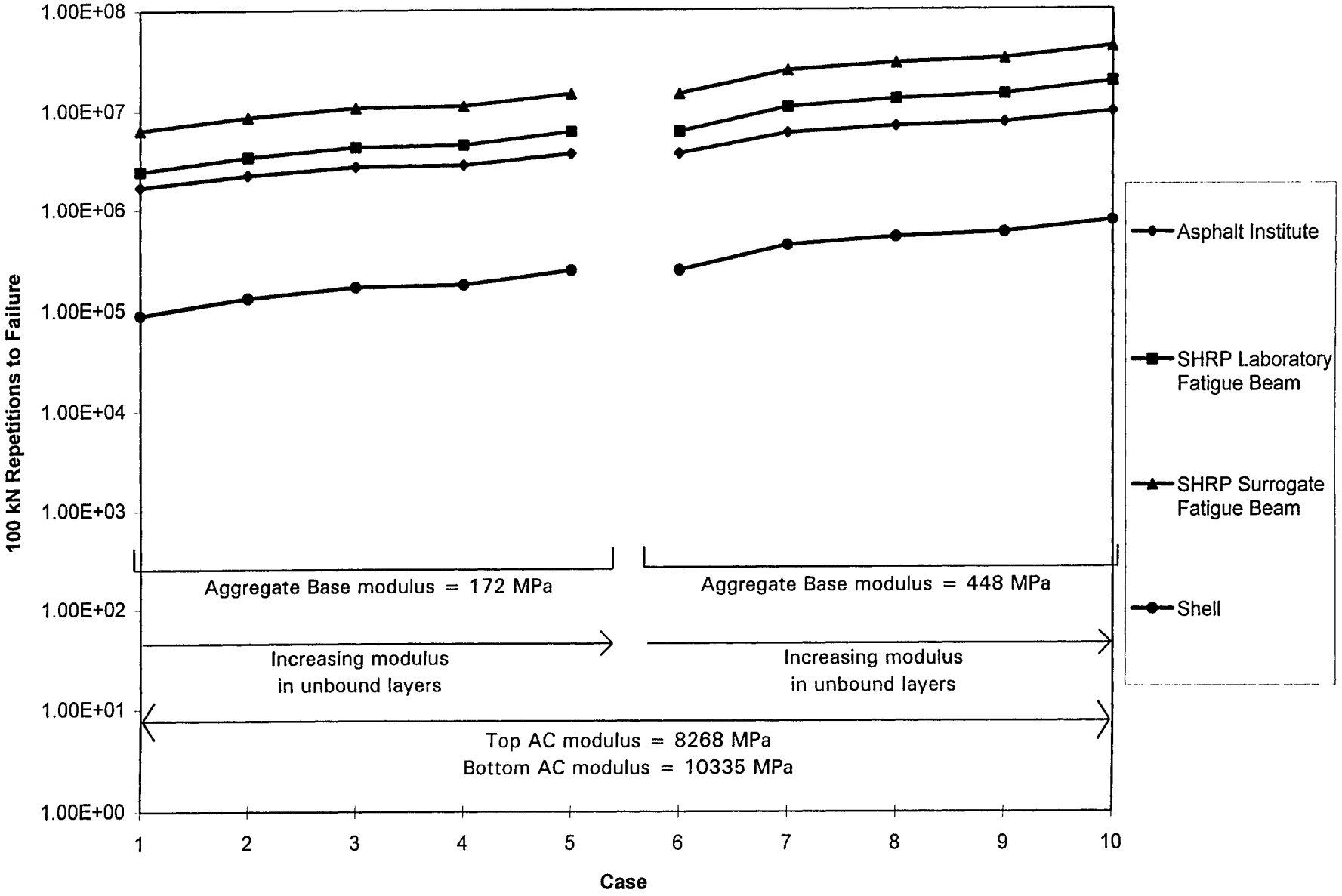

Figure 6.4 Remaining 100 kN Load Repetitions to Fatigue Failure, Undrained Section 501RF, Subbase Thickness of 218 mm

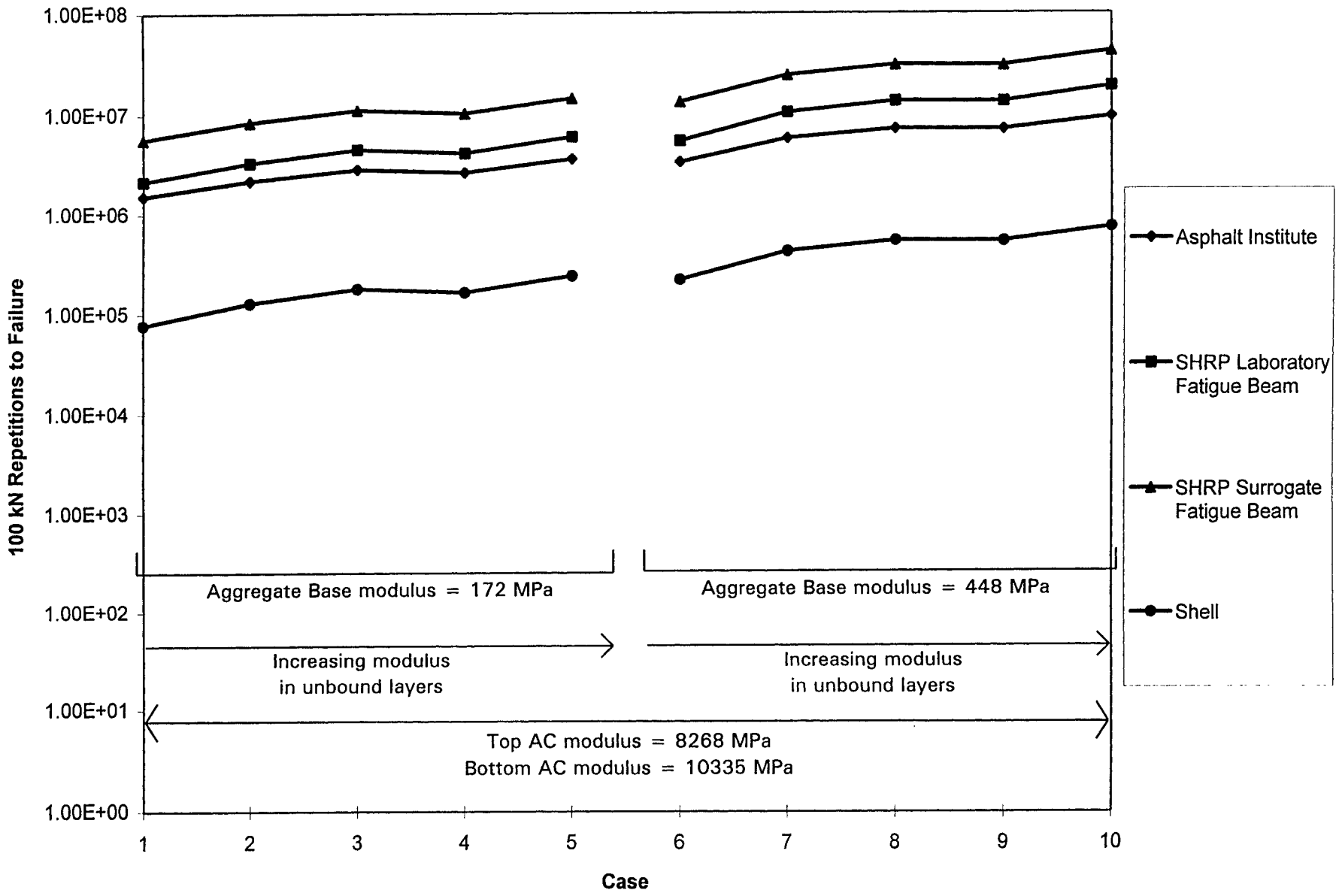

Figure 6.5 Remaining 100 kN Load Repetitions to Fatigue Failure, Undrained Section 503RF, Subbase Thickness of 305 mm

Effects of moduli of unbound layers. In both pavement structures an increase in the moduli of the unbound layers results in an increase in fatigue life. However, the increase in the fatigue life is small relative to the other factors analyzed.

The drained pavement does not appear to be influenced by changes in the combined modulus of the aggregate base and subbase layers. The performance of the undrained pavement is, however, significantly influenced by changes in the moduli of the unbound layers: for example, an increase in the stiffness of the aggregate base results in an increase in the fatigue life.

An increase in the subgrade modulus also increases the fatigue life for both pavement structures although this increase is, again, comparatively small.

Effects of modulus changes in the ATPB layer. The differences between the two moduli assumed for the ATPB layer did not have a substantial effect on fatigue life. Further investigation is necessary to fully understand the influence which the ATPB layer has on the structural capacity of a pavement. In addition, the effects of water on the stiffness of the ATPB and its influence on fatigue should be evaluated. This influence will be evaluated in the laboratory and possibly in future HVS test sections.

Effects of thickness of the subbase. For both pavement structures the thickness of the aggregate subbase has a relatively small effect on the fatigue lives predicted for each modulus case. This is illustrated in Table 6.5 and by comparing Figures 6.2 and 6.3, 6.4 and 6.5.

Effects of increased load and the relative damage. In all cases analyzed in this study, an increase in load causes a decrease in fatigue life. This is illustrated by comparing Figures 6.6, 6.7, and 6.8 for the drained pavement representing section 500RF, and for Figures 6.9, 6.10, and 6.11 for the undrained pavement representing section 501RF. For both pavement structures the

fatigue life under a 40 kN load is approximately five times the fatigue life under an 80 kN load and approximately 10 times the fatigue life under a 100 kN load. In other words, the 100 kN load does 10 times more damage than the 40 kN load. This gives a coefficient of n of approximately 2.5 for the following load equivalency factor equation:

$$Relative\ \ damage = (axle\ \ load\ /\ ESAL\ \ load\ )^{n} \qquad (6\text{-}4)$$

Caltrans typically uses a factor of 4.2 *(California Department of Transportation, 1987)*, which in this situation would overestimate the damaging effect of the 100 kN half-axle load. The reduced damaging effect of the load may be due to the strength of the pavement and the thickness of the asphalt concrete layer. It must be emphasized, however, that this coefficient has been developed from the models discussed in this paper and can only be validated after further extensive HVS testing and analysis.

Comparison of design life and predicted fatigue lives. The test sections were designed for a Caltrans Traffic Index of 9 which corresponds to 0.798 to 1.2 million ESALS. All the fatigue life predictions exceed this design criterion, as illustrated in Tables 6.6 and 6.9 for the 40 kN half-axle load, which is equivalent to an ESAL. This is probably due to the good construction (especially of the asphalt concrete).

6.3.7 Effect of Air Voids on Fatigue Performance

The effect of air voids on predicted fatigue lives was evaluated using ELSYM5 and the prediction equations. The asphalt concrete stiffnesses used in these analyses were those

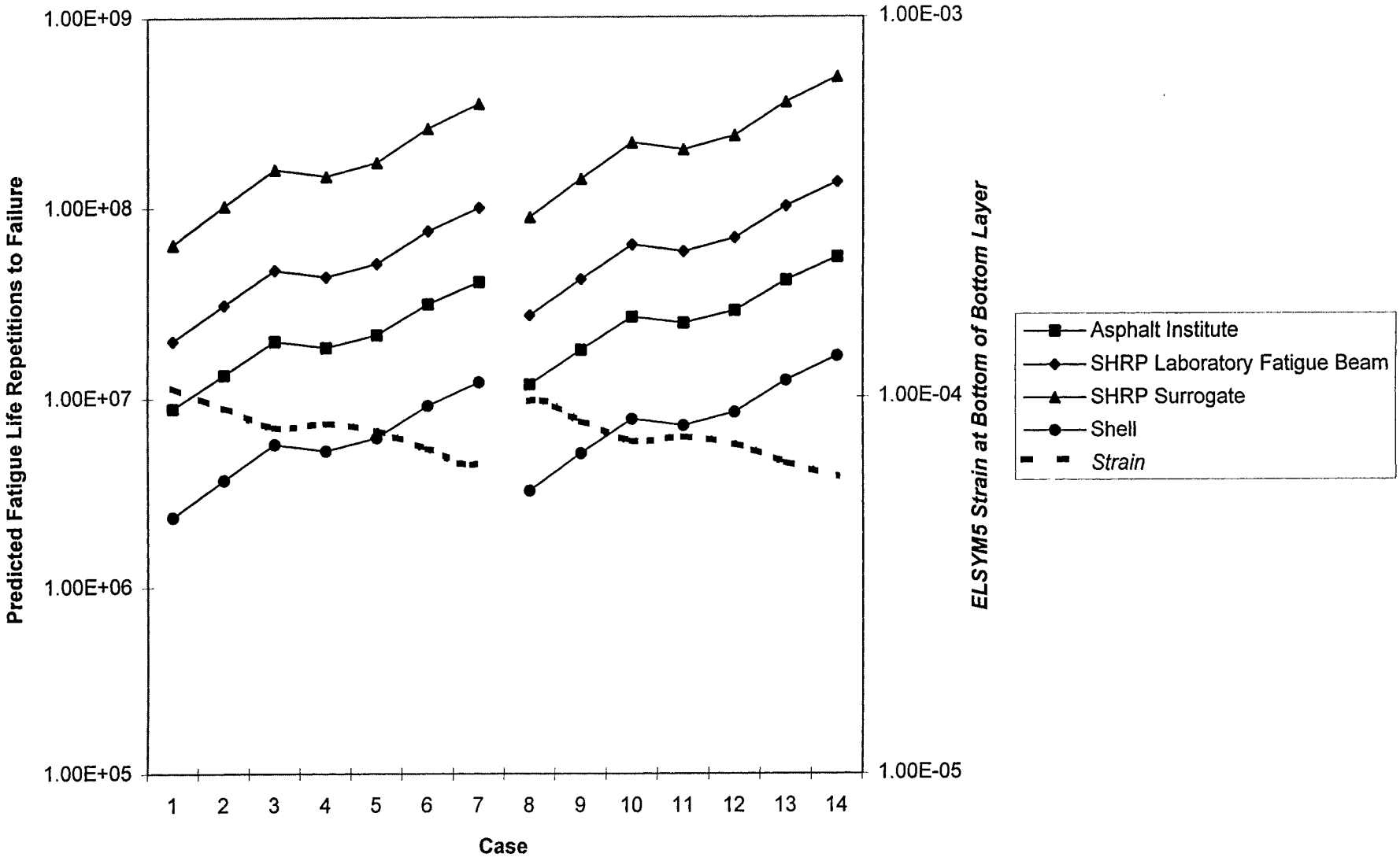

Figure 6.6 ELSYM5 Strains and Resulting Fatigue Life Predictions, Drained Section 500RF, Load of 40 kN and Subbase Thickness of 127 mm

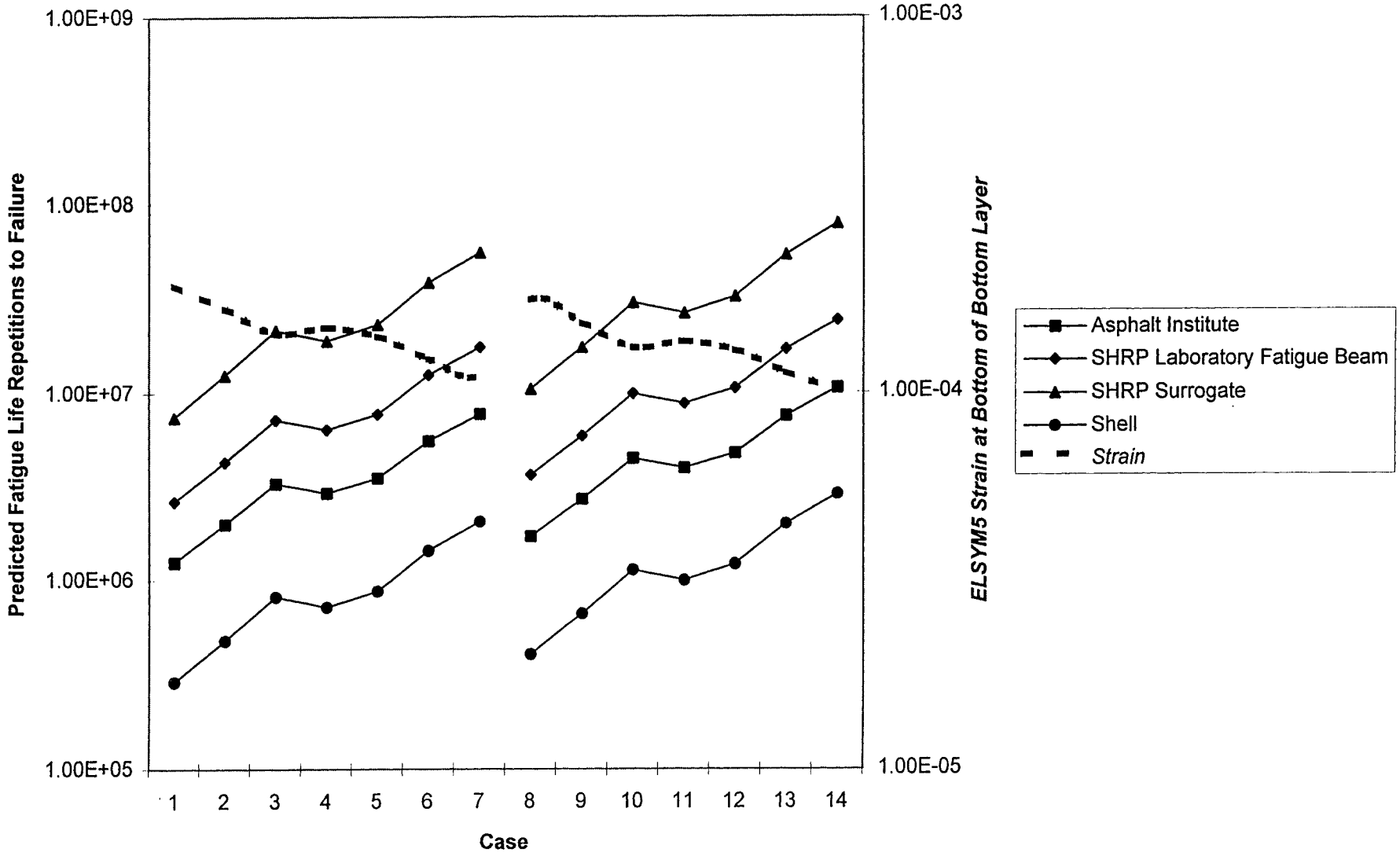

Figure 6.7 ELSYM5 Strains and Resulting Fatigue Life Predictions, Drained Section 500RF, Load of 80 kN and Subbase Thickness of 127 mm

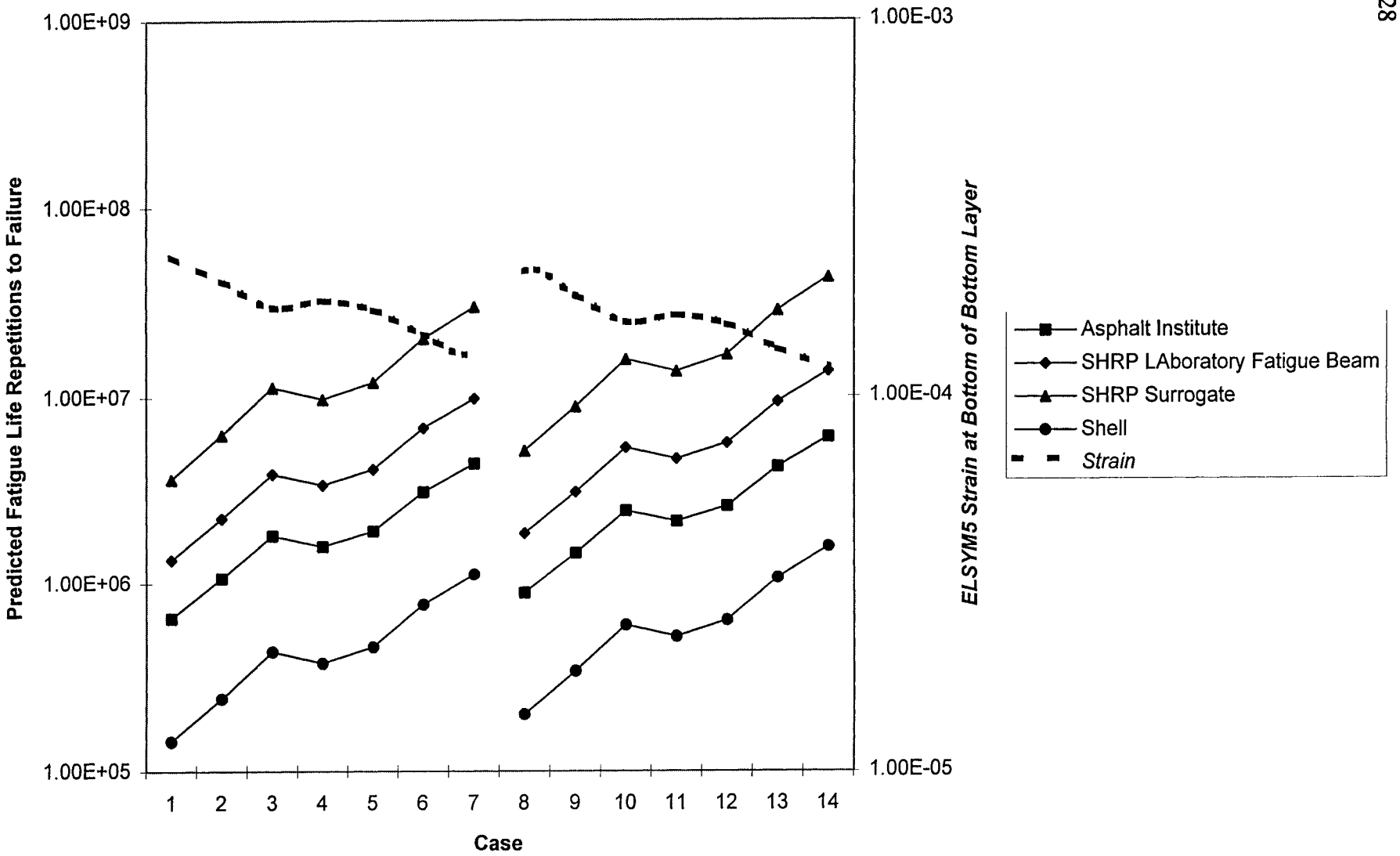

Figure 6.8 ELSYM5 Strains and Resulting Fatigue Life Predictions, Drained Section 500RF, Load of 100 kN and Subbase Thickness of 127 mm

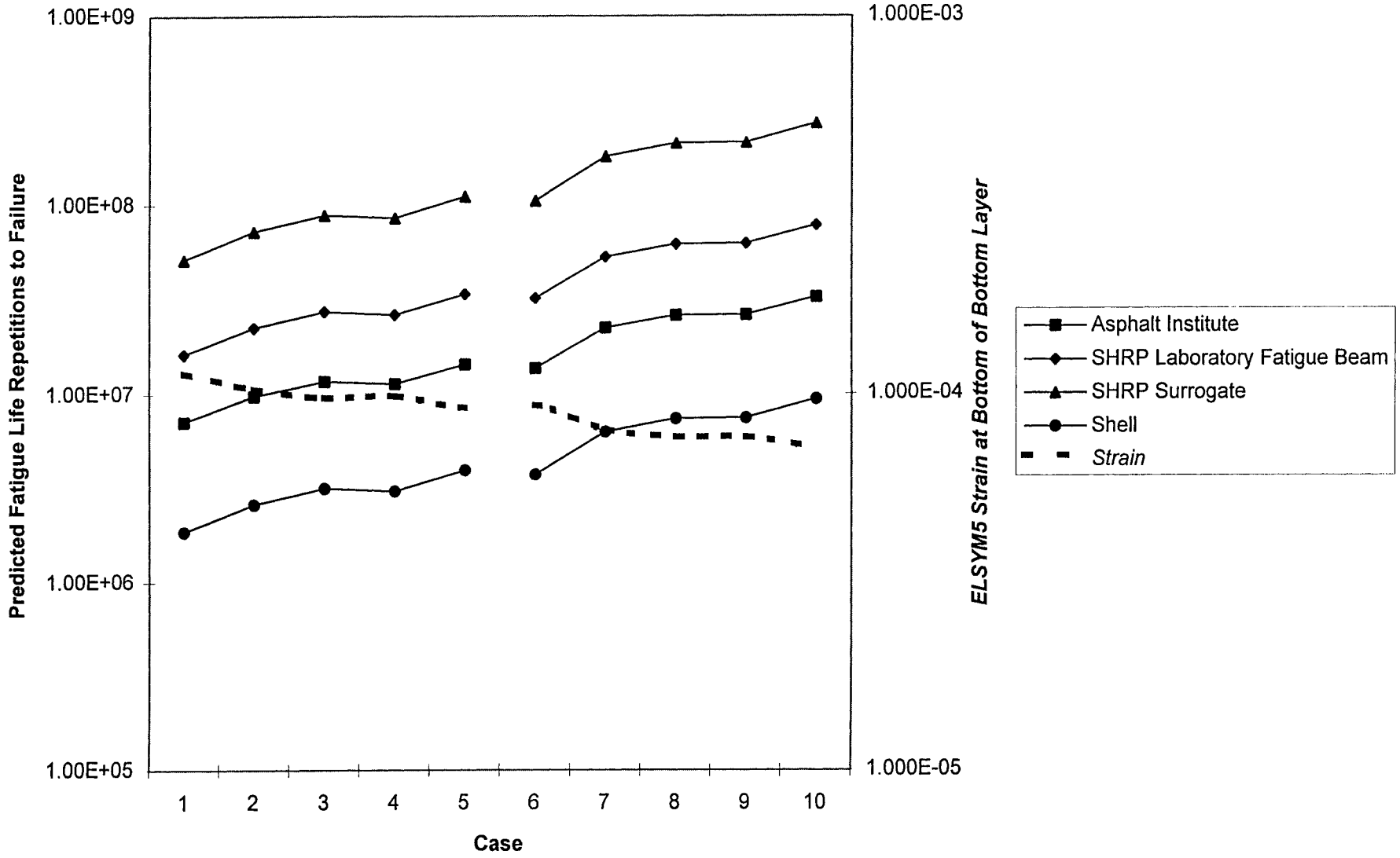

Figure 6.9 ELSYM5 Strains and Resulting Fatigue Life Predictions, Undrained Section 501RF, Load of 40 kN and Subbase Thickness of 218 mm

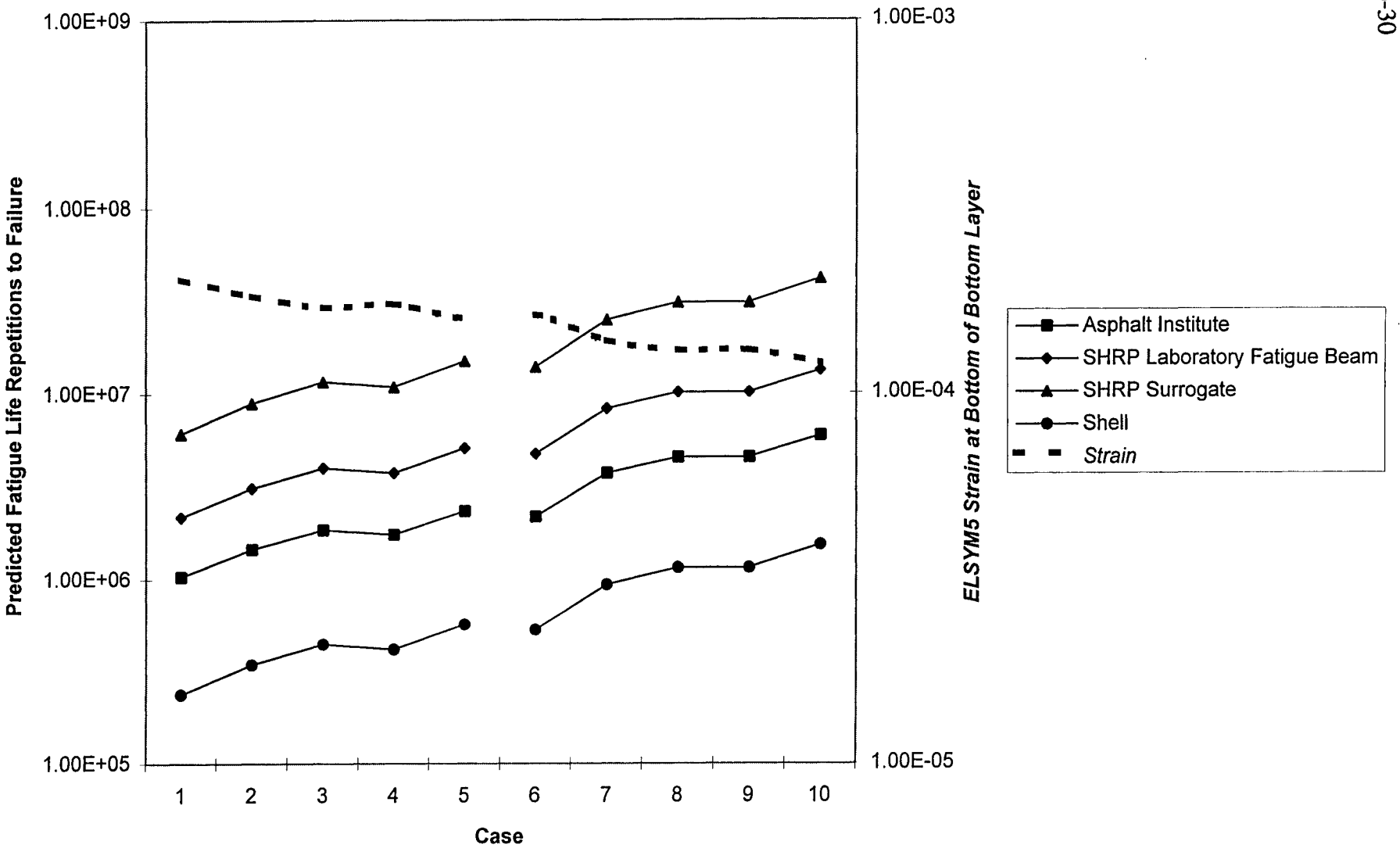

Figure 6.10 ELSYM5 Strains and Resulting Fatigue Life Predictions, Undrained Section 501RF, Load of 80 kN and Subbase Thickness of 218 mm

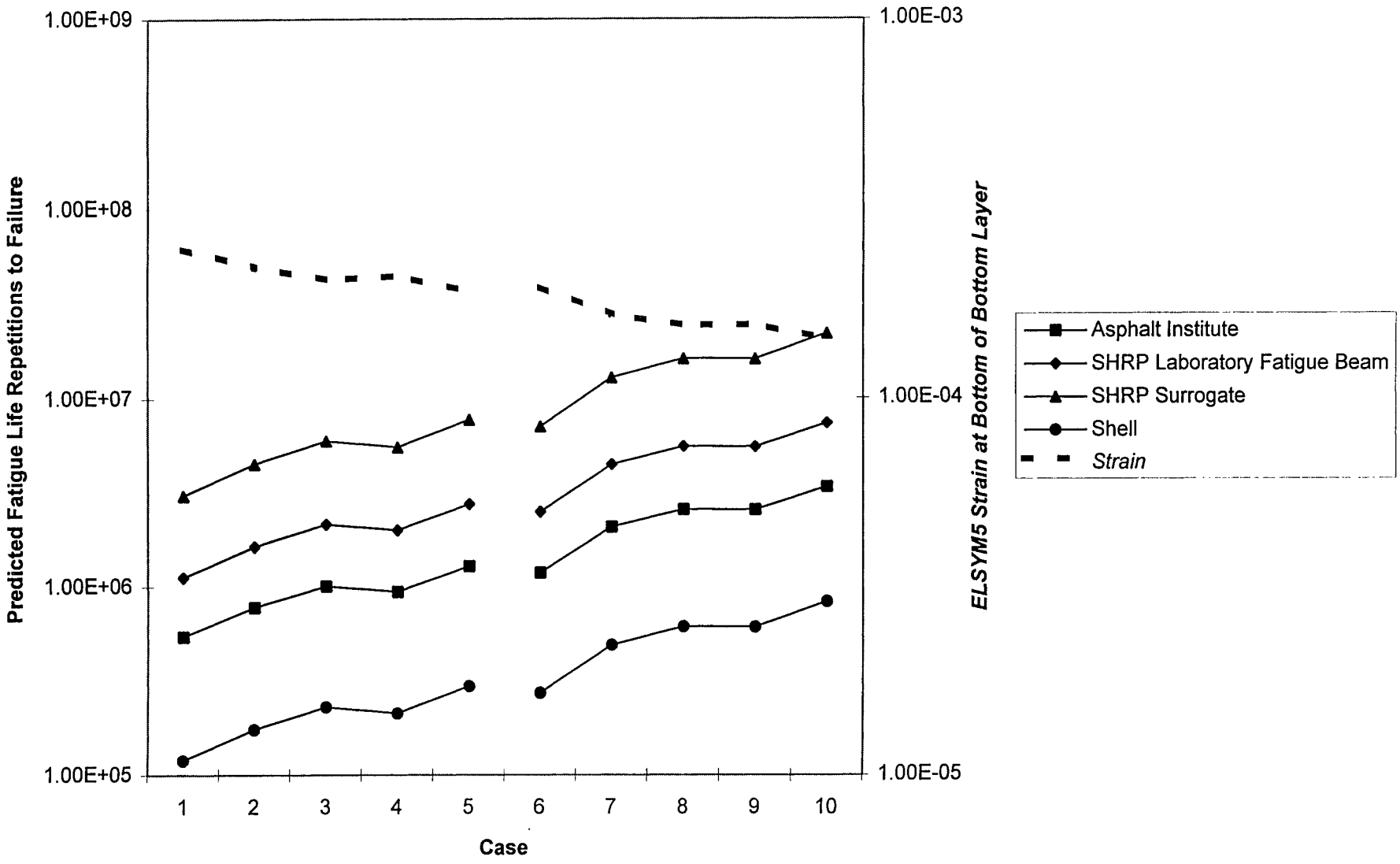

Figure 6.11 ELSYM5 Strains and Resulting Fatigue Life Predictions, Undrained Section 500RF, Load of 100 kN and Subbase Thickness of 218 mm

measured in the flexural beam fatigue test on laboratory compacted specimens at four air void contents, 3.2 percent, 6.5 percent, 7.2 percent, and 9.2 percent. Only one asphalt concrete layer was simulated. The moduli for the remaining layers were the averages used in the previous ELSYM5 analyses. To limit the scope of the analyses, the thickness of the aggregate subbase was kept constant at 218 mm (8.6 in). ELSYM5 analyses were performed at the three load levels, 40 kN, 80 kN and 100 kN. As summarized in Table 6.7, a total of 24 cases was evaluated, 12 for the drained pavement and 12 for the undrained pavement. The tensile strains obtained in these analyses were used to predict fatigue lives using the prediction models.

Results of these analyses are illustrated in Figures 6.12 and 6.13. An increase in air voids results in an increase in strain in all cases, due to the decreased stiffness of the mix. This increase in air voids and increase in strain causes a decrease in the predicted fatigue life in all cases. This follows the trends experienced in the fatigue predictions discussed earlier.

6.4 RUTTING LIFE PREDICTIONS FROM SUBGRADE VERTICAL COMPRESSIVE STRAIN

Rutting predictions were determined using the models discussed previously and the strains determined using the moduli cases outlined in Table 6.2. The temperature at which the moduli were determined is approximately 20°C, the same approximate temperature as the test sections. Results from the ELSYM5 and CIRCLY analyses for the prediction of pavement lives based on subgrade strain criteria are given in Figure 6.14 for the Shell and Asphalt Institute models. The CIRCLY frictionless condition yields the smallest pavement life, and the CIRCLY full friction yields the largest. The actual ranges are within one order

Table 6.7 Cases for ELSYM5 Runs - Comparison of Asphalt Concrete Air Voids and Respective Initial Stiffnesses Using Mean Moduli for Underlying Layers

Drained Section:		case 1	case 2	case 3	case 4	case 5	case 6	case 7	case 8	case 9	case 10	case 11	case 12
	Load (kN)	40	40	40	40	80	80	80	80	100	100	100	100
	ASB thickness	8.6	8.6	8.6	8.6	8.6	8.6	8.6	8.6	8.6	8.6	8.6	8.6
Moduli (MPa)	Subgrade	2245	2245	2245	2245	2245	2245	2245	2245	2245	2245	2245	2245
	ASB	2903	2903	2903	2903	2903	2903	2903	2903	2903	2903	2903	2903
	AB	4354	4354	4354	4354	4354	4354	4354	4354	4354	4354	4354	4354
	ATPB	18142	18142	18142	18142	18142	18142	18142	18142	18142	18142	18142	18142
	AC	227570	174537	161370	138357	227570	174537	161370	138357	227570	174537	161370	138357
	AC Air Voids	3.2%	6.5%	7.2%	0.092	3.2%	6.5%	7.2%	9.2%	3.2%	6.5%	7.2%	9.2%
Undrained Section:		case 1	case 2	case 3	case 4	case 5	case 6	case 7	case 8	case 9	case 10	case 11	case 12
	Load (kN)	40	40	40	40	80	80	80	80	100	100	100	100
	ASB thickness	8.6	8.6	8.6	8.6	8.6	8.6	8.6	8.6	8.6	8.6	8.6	8.6
Moduli (MPa)	SG	2245	2245	2245	2245	2245	2245	2245	2245	2245	2245	2245	2245
	ASB	2903	2903	2903	2903	2903	2903	2903	2903	2903	2903	2903	2903
	AB	4354	4354	4354	4354	4354	4354	4354	4354	4354	4354	4354	4354
	AC	227570	174537	161370	138357	227570	174537	161370	138357	227570	174537	161370	138357
	AC Air Voids	3.2%	6.5%	7.2%	0.092	3.2%	6.5%	7.2%	9.2%	3.2%	6.5%	7.2%	9.2%

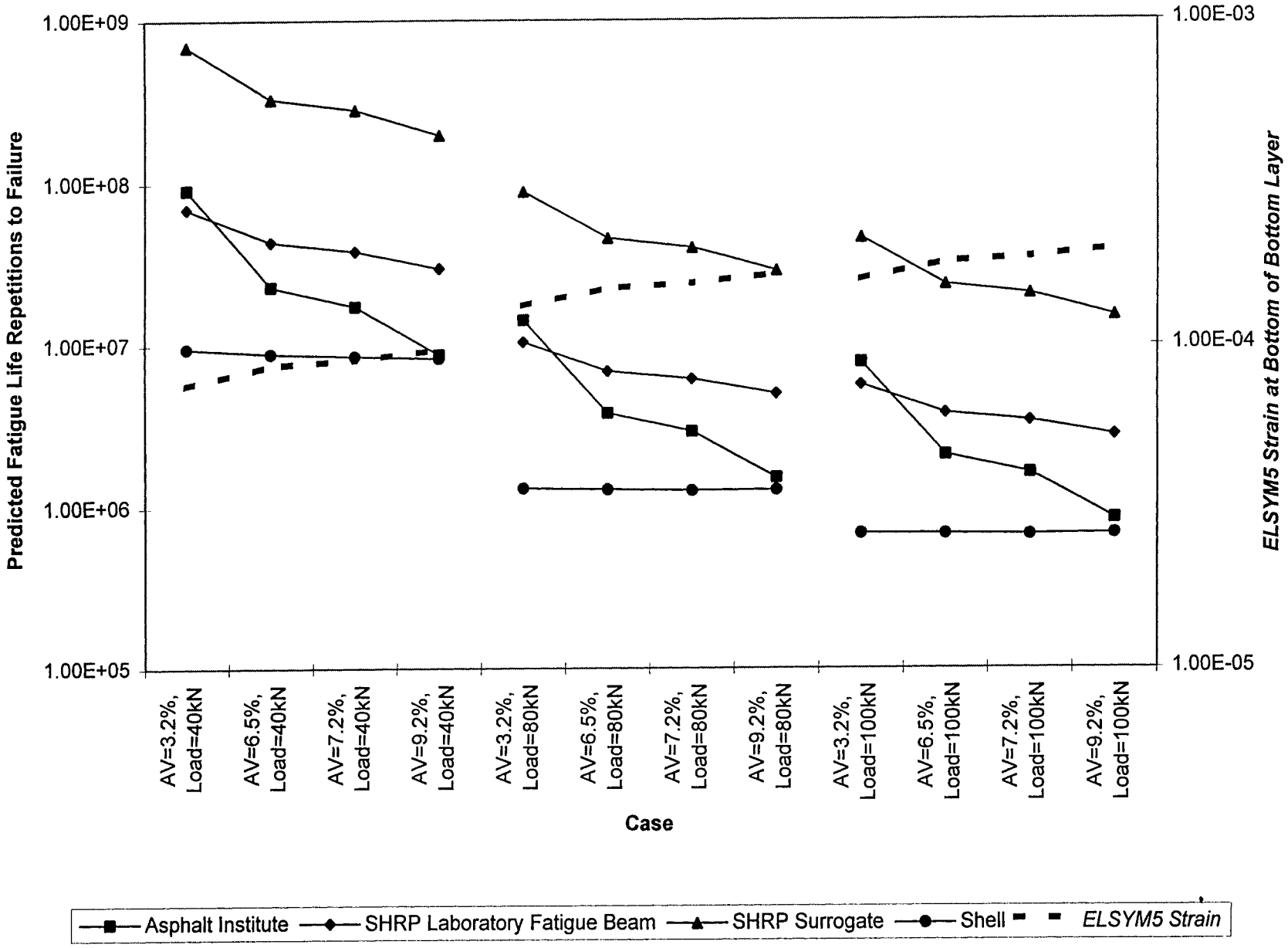

Figure 6.12 Effect of Air-Voids on ELSYM5 Strains and Resulting Fatigue Life Predictions Using Average Moduli Cases Drained Section 501RF, ASB Thickness of 218 mm

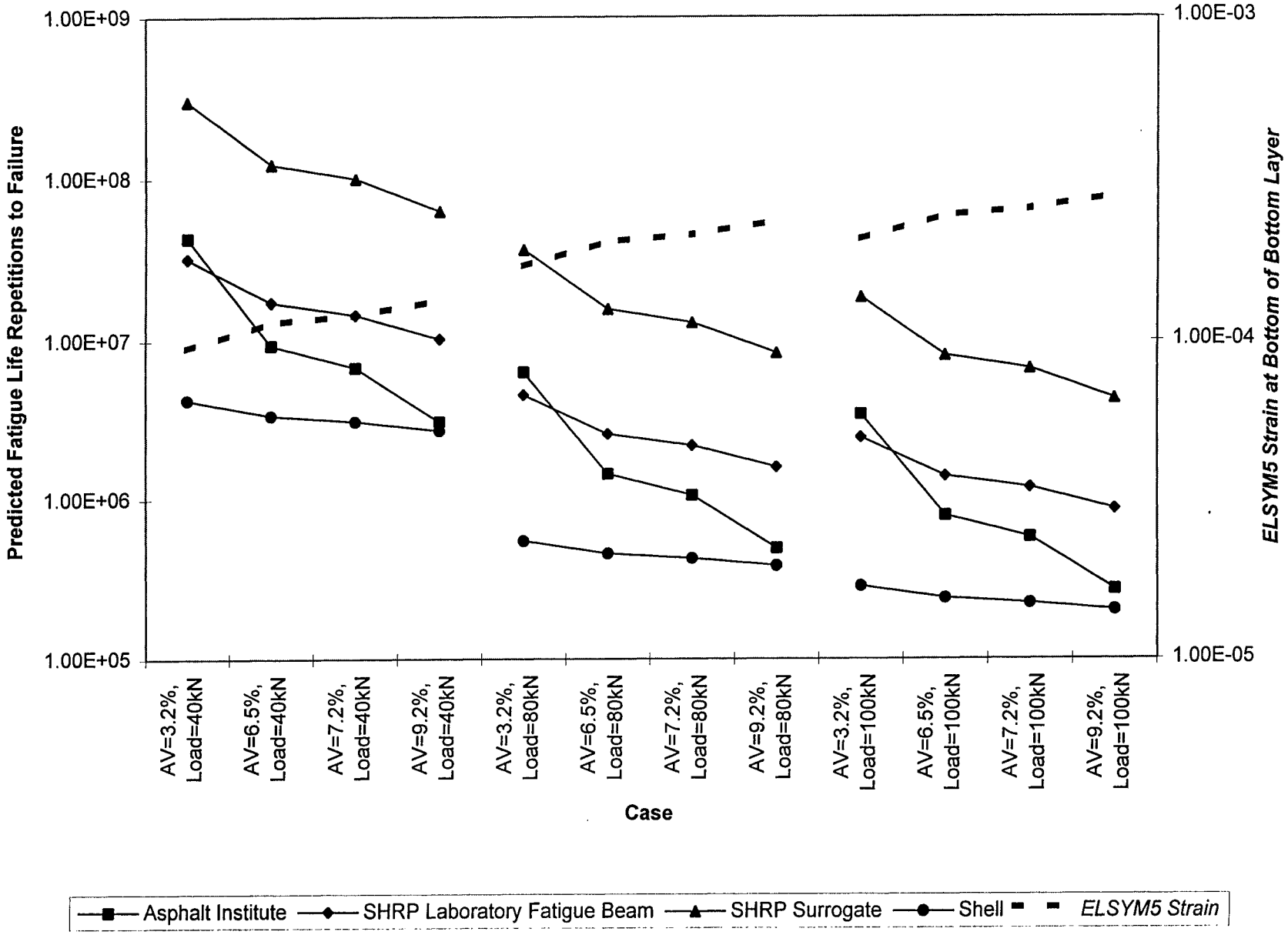

Figure 6.13 Effect of Air-Voids on ELSYM5 Strains and Resulting Fatigue Life Predictions Using Average Moduli Cases Undrained Section 501RF, ASB Thickness of 218 mm

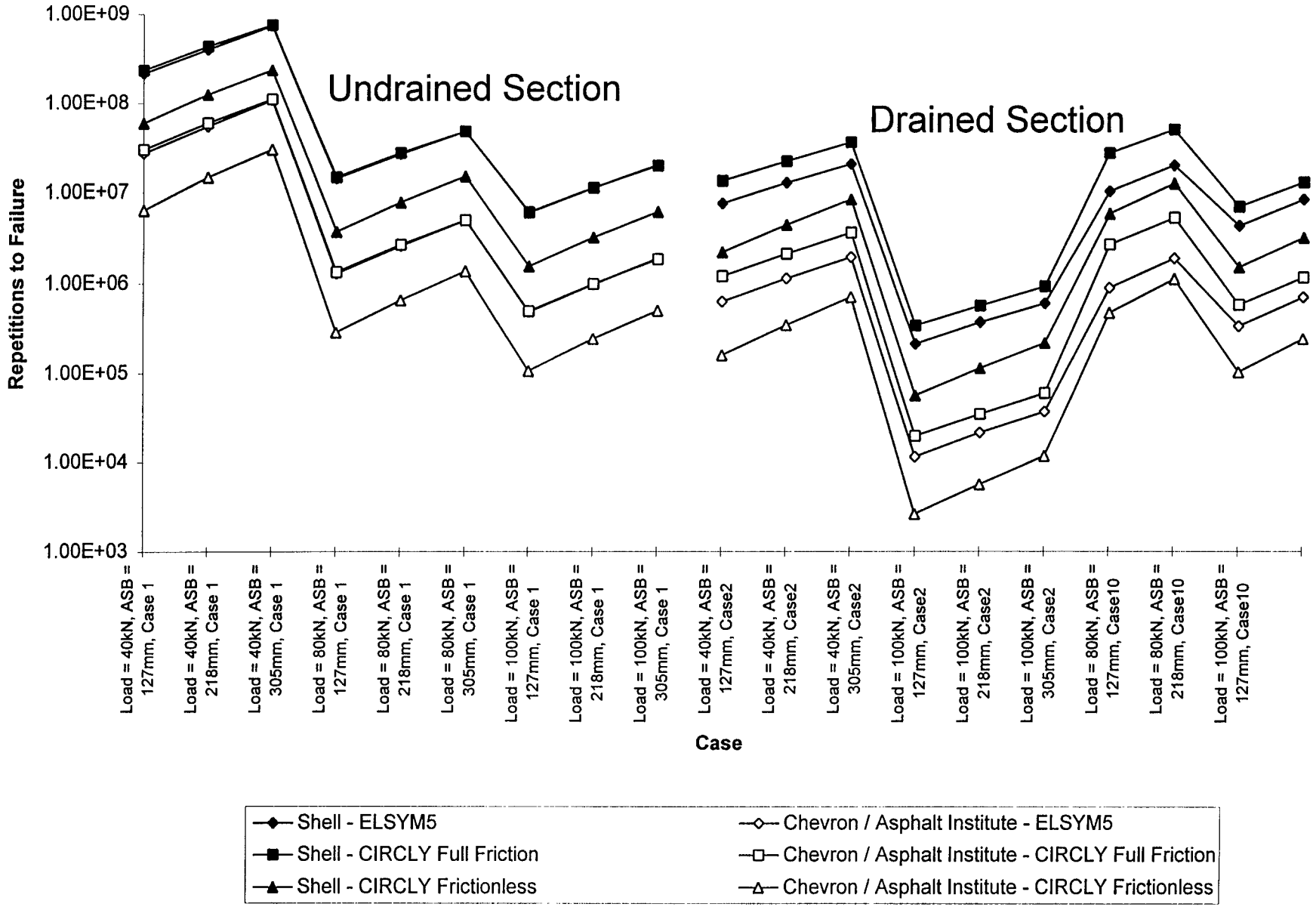

Figure 6.14 Comparison of the Effect of CIRCLY and ELSYM5 Strain Estimates on Rutting Predictions

of magnitude. However, the bond between the two asphalt concrete lifts is not frictionless and most likely not fullfriction either, therefore the predicted subgrade rutting life is probably between the predictions given in the figure. Summaries of the service lives based on limiting subgrade rutting are given in Table 6.6. These lives were calculated from the vertical compressive strain at the top of the subgrade layer. The remaining number of 100 kN load repetitions to failure of the test sections after the 200,000 repetitions of 40 kN and 80 kN repetitions as calculated by the linear sum of cycle ratios procedure *(Miner, 1945)* are illustrated in Figure 6.15 and 6.16 for the drained sections and Figures 6.17 and 6.18 for the undrained sections.

6.4.1 Comparison of Predicted Rutting Lives Among the Models

The Asphalt Institute, Shell, and Nottingham models predict similar trends in the rutting lives. The South African model predicts a wider range of rutting lives than the others.

Effects of moduli. The South African rutting equation is the most sensitive to changes in moduli in comparison with the Asphalt Institute, Shell, and Nottingham models. The rutting predictions between the drained and undrained pavements have similar ranges which is in agreement with the calculated verticle compressive strain, as given in Table 6.6. This agrees with the expectation of comparable service lives from the Caltrans design procedure *(California Department of Transportation, 1987)* for drained and undrained pavements.

For all investigations, an increase in subgrade moduli results in an increase in the predicted rutting life. This effect is especially large in the South African model.

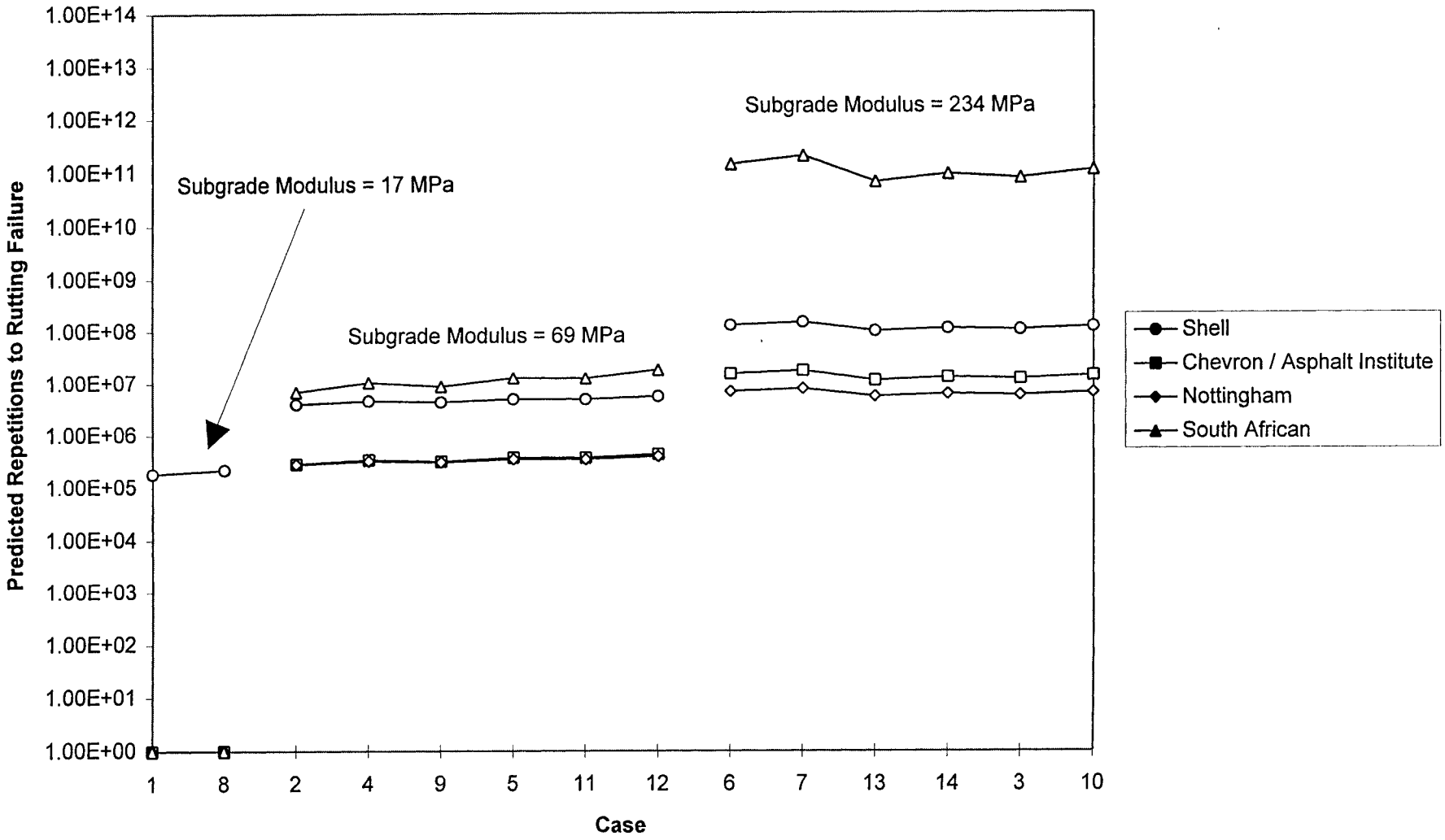

Figure 6.15 Estimate of 100 kN Load Repetitions to Rutting Failure (After 40 kN and 80 kN Repetitions), Drained Section 500RF, Subbase Thickness of 127 mm

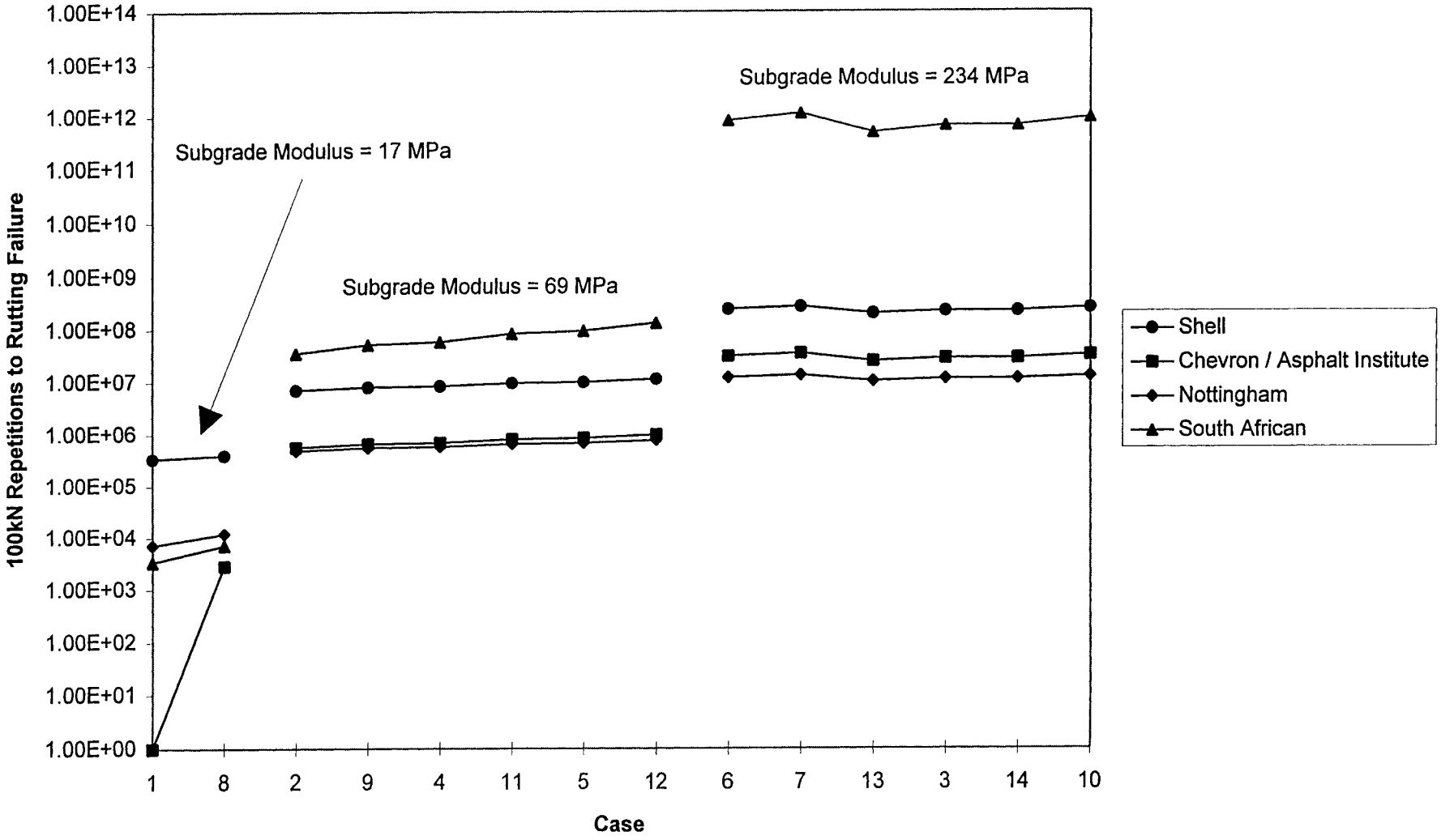

Figure 6.16 Estimate of 100 kN Load Repetitions to Rutting Failure (After 40 kN and 80 kN Repetitions), Drained Section 502RF, Subbase Thickness of 218 mm

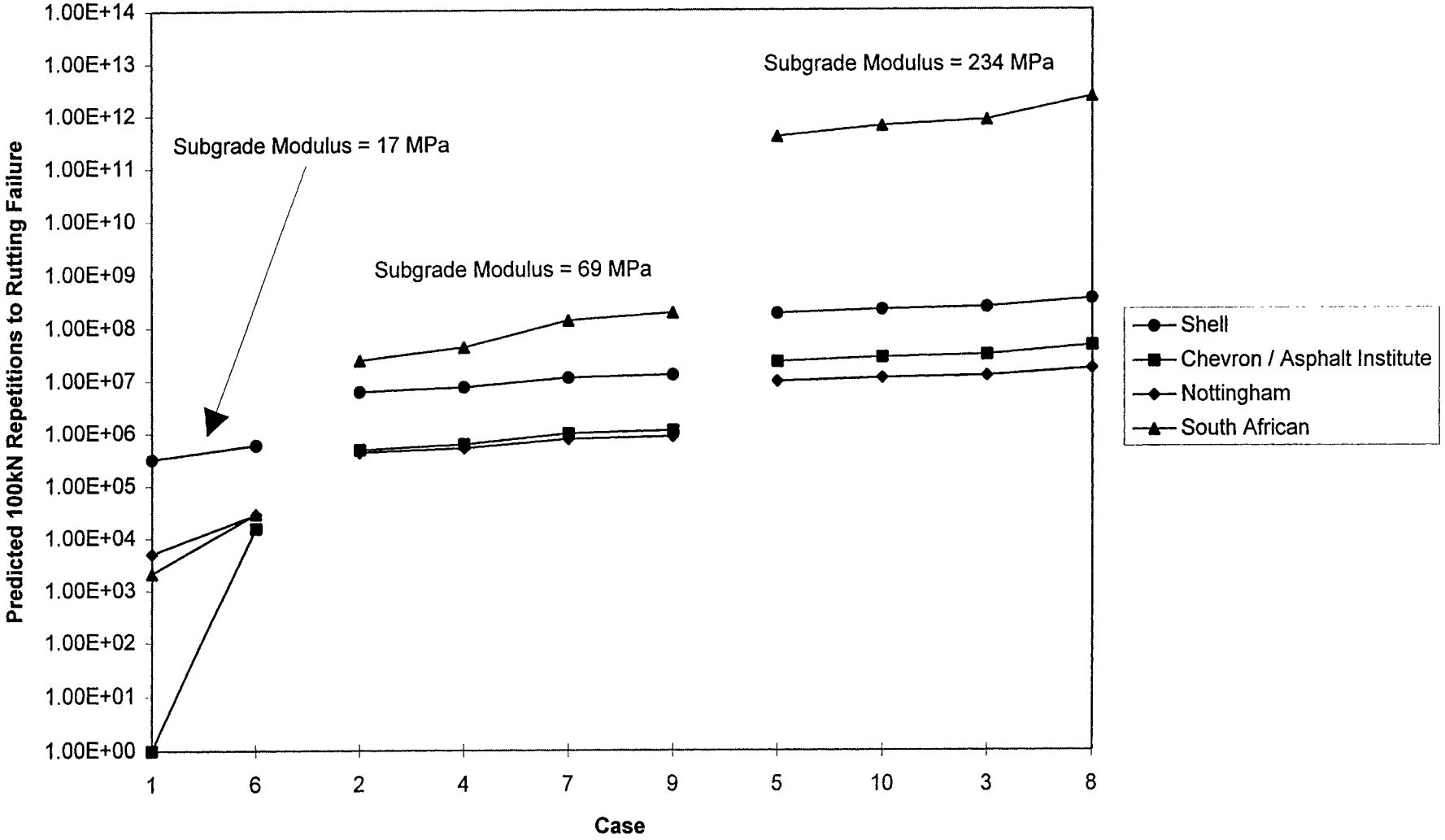

Figure 6.17 Estimate of 100 kN Load Repetitions to Rutting Failure (After 40 kN and 80 kN Repetitions), Undrained Section 501RF, Subbase Thickness of 218 mm

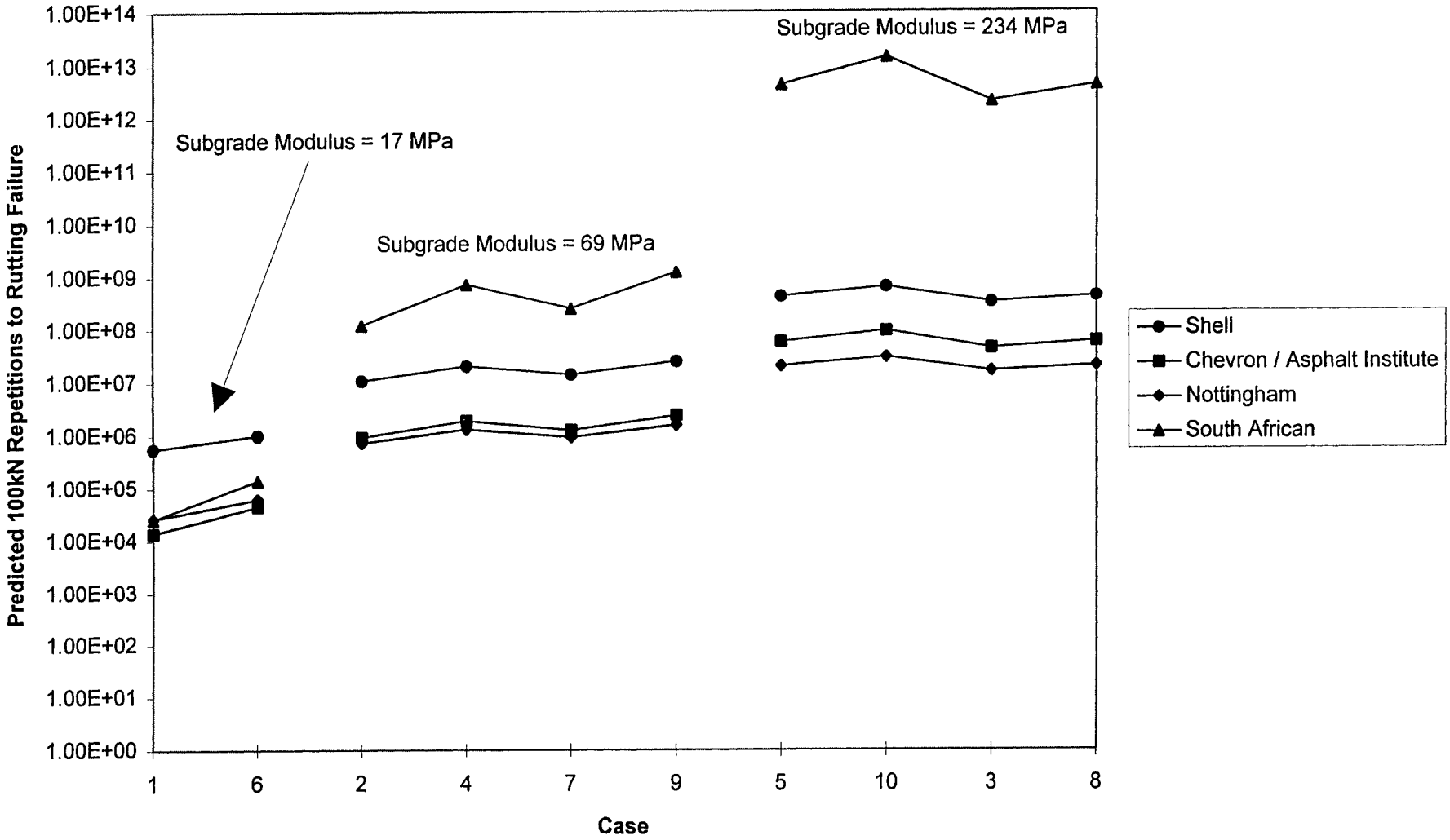

Figure 6.18 Estimate of 100 kN Load Repetitions to Rutting Failure (After 40 kN and 80 kN Repetitions), Undrained Section 503RF, Subbase Thickness of 305 mm

From Table 6.6 the changes in moduli in the unbound layers appear to have a larger effect on the undrained pavement than the drained pavement. This is probably due to the undrained pavement structure being less stiff and therefore the combined modulus of the whole pavement will be more affected by changes in the moduli of the unbound layers.

Increasing the modulus of the ATPB layer in the drained pavement causes a marginal increase in the predicted subgrade rutting life: this can be seen from the results of Table 6.6.

Effect of thickness of the subbase. An increase in the subbase thickness results in an increase in the predicted rutting life. The increase in thickness from 127 mm (5.0 in) to 218 mm (8.6 in) and to 305 mm (12.0 in) results in an approximate doubling in the predicted subgrade rutting life with each increase. As a result, these models predict that the HVS test sections will have varying amounts of subgrade rutting. The first section tested, 500RF, will experience the most subgrade rutting and the last section, 503RF, will experience the least.

Effects of increased load and relative damage. The rutting models are far more sensitive to increases in load than are the fatigue models. An increase in load causes a substantial reduction in the predicted rutting life, although the actual magnitude of the reduction is different with every model. This can be visually seen in Figures 6.19, 6.20, and 6.21 for the drained pavement representing section 500RF, and Figures 6.22, 6.23, and 6.24 for the undrained pavement representing section 501RF.

In a comparison of predicted rutting life under 40 kN and 100 kN loading, the Shell model gives the rutting life under a 40 kN load as approximately 35 times the rutting life African 27,700 times. Using the load equivalency factor equation given in Equation 6.4, the under a 100 kN load, the Asphalt Institute 55 times, the Nottingham 24 times, and the South

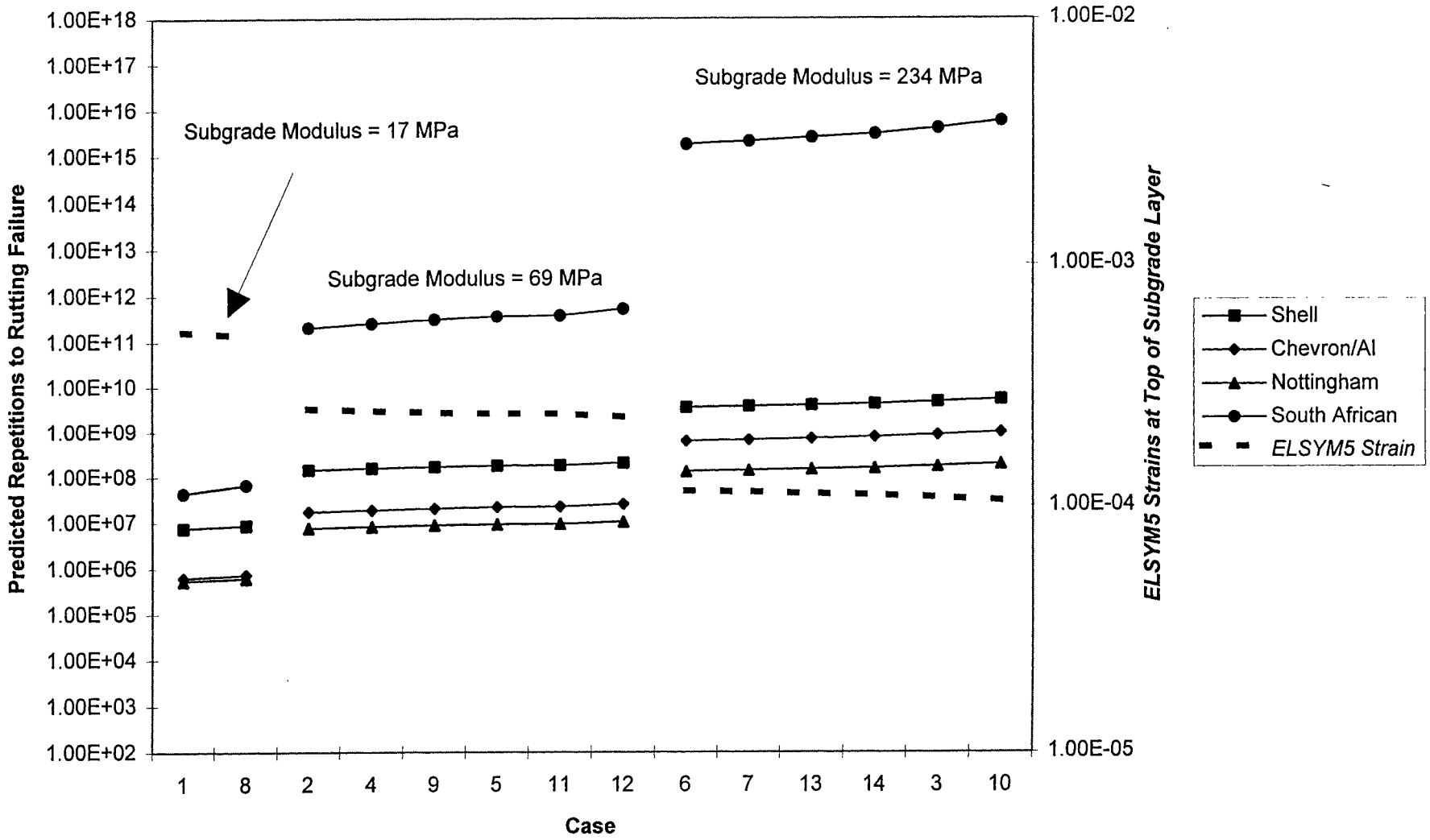

Figure 6.19 Subgrade ELSYM5 Strains and Resulting Rutting Predictions, Drained Section 500RF, Load of 40 kN and Subbase Thickness of 127 mm

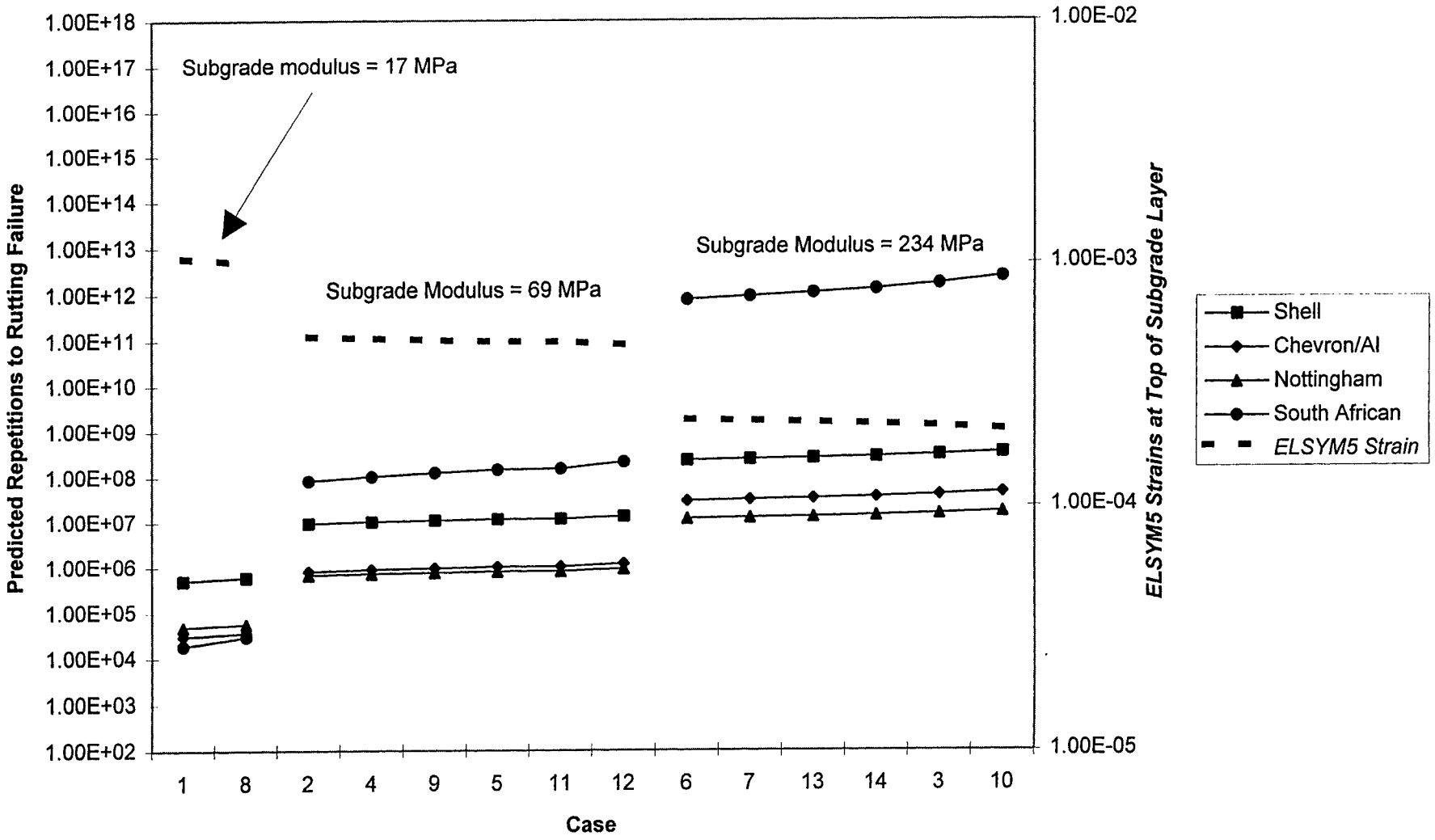

Figure 6.20 Subgrade ELSYM5 Strains and Resulting Rutting Predictions, Drained Section 500RF, Load of 80 kN and Subbase Thickness of 127 mm

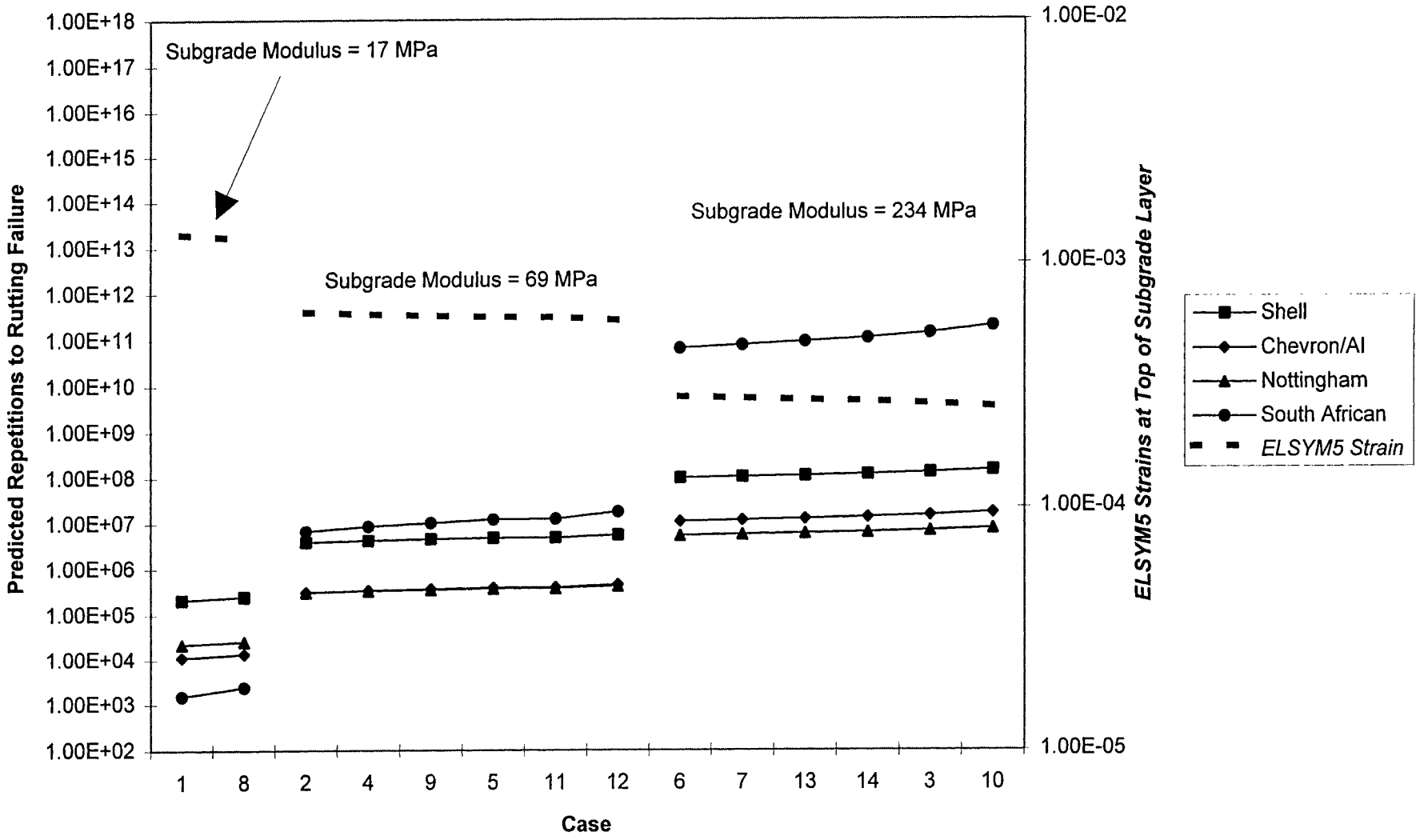

Figure 6.21 Subgrade ELSYM5 Strains and Resulting Rutting Predictions, Drained Section 500RF, Load of 100 kN and Subbase Thickness of 127 mm

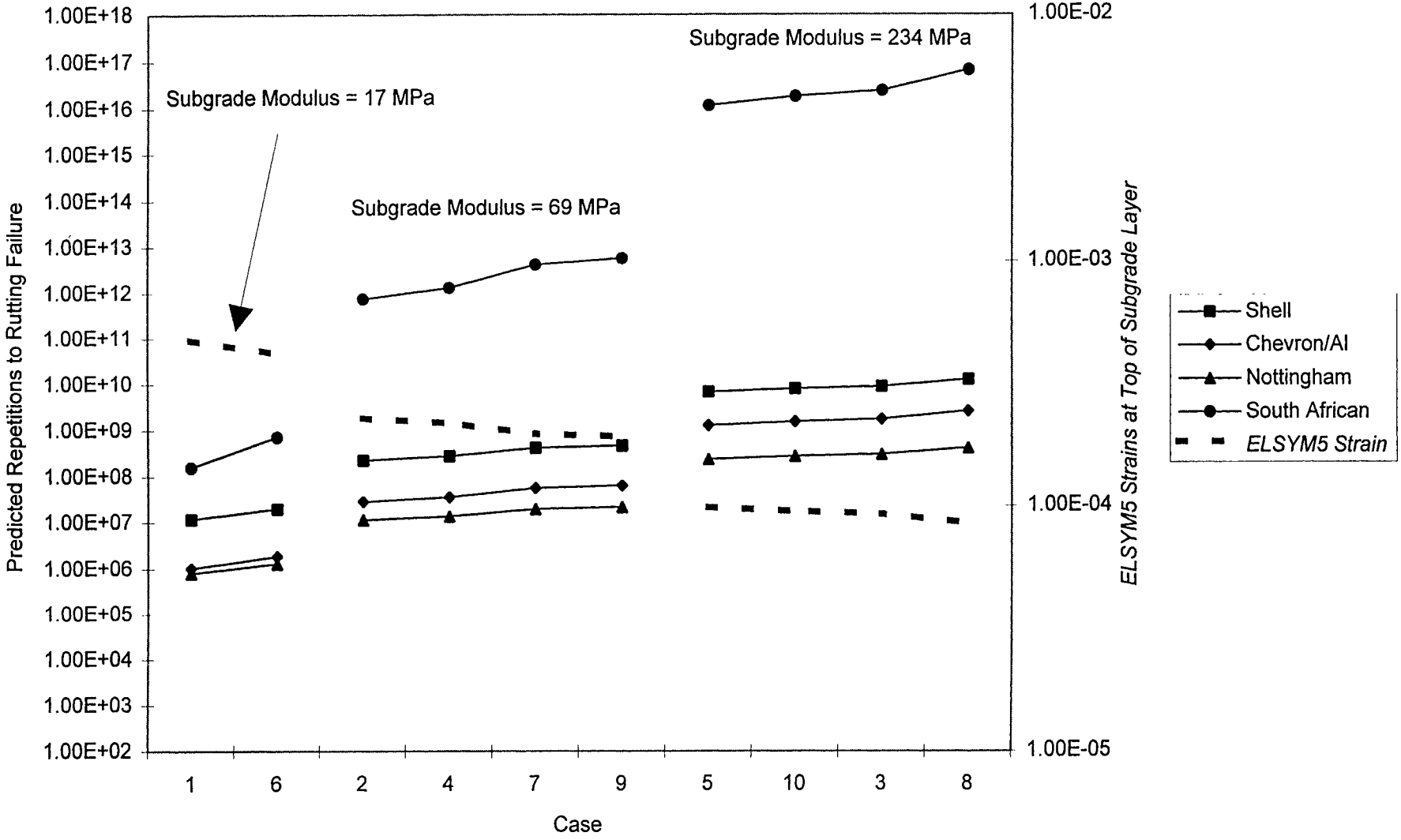

Figure 6.22 Subgrade ELSYM5 Strains and Resulting Rutting Predictions, Undrained Section 501RF, Load of 40 kN and Subbase Thickness of 218 mm

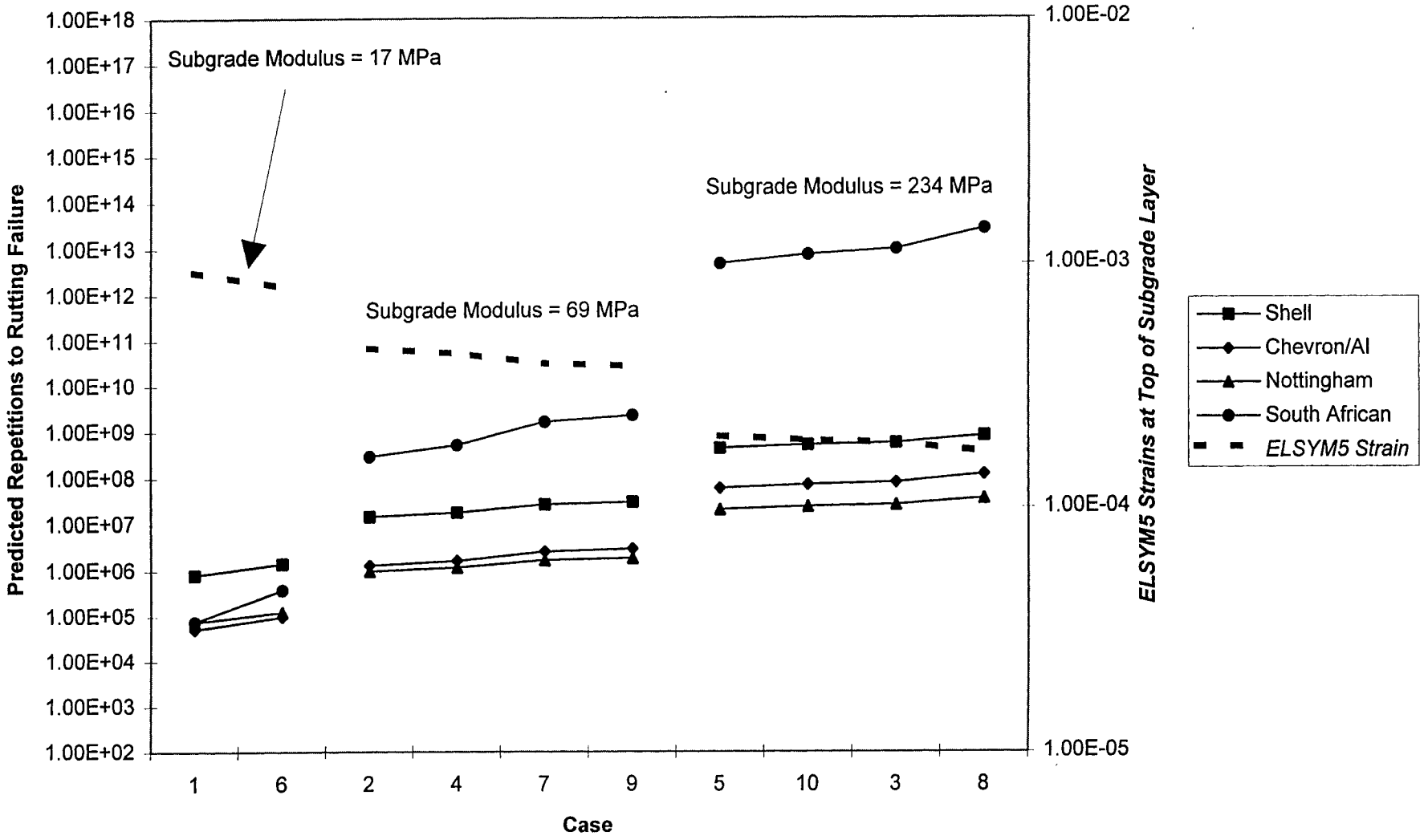

Figure 6.23 Subgrade ELSYM5 Strains and Resulting Rutting Predictions, Undrained Section 501RF, Load of 80 kN and Subbase Thickness of 218 mm

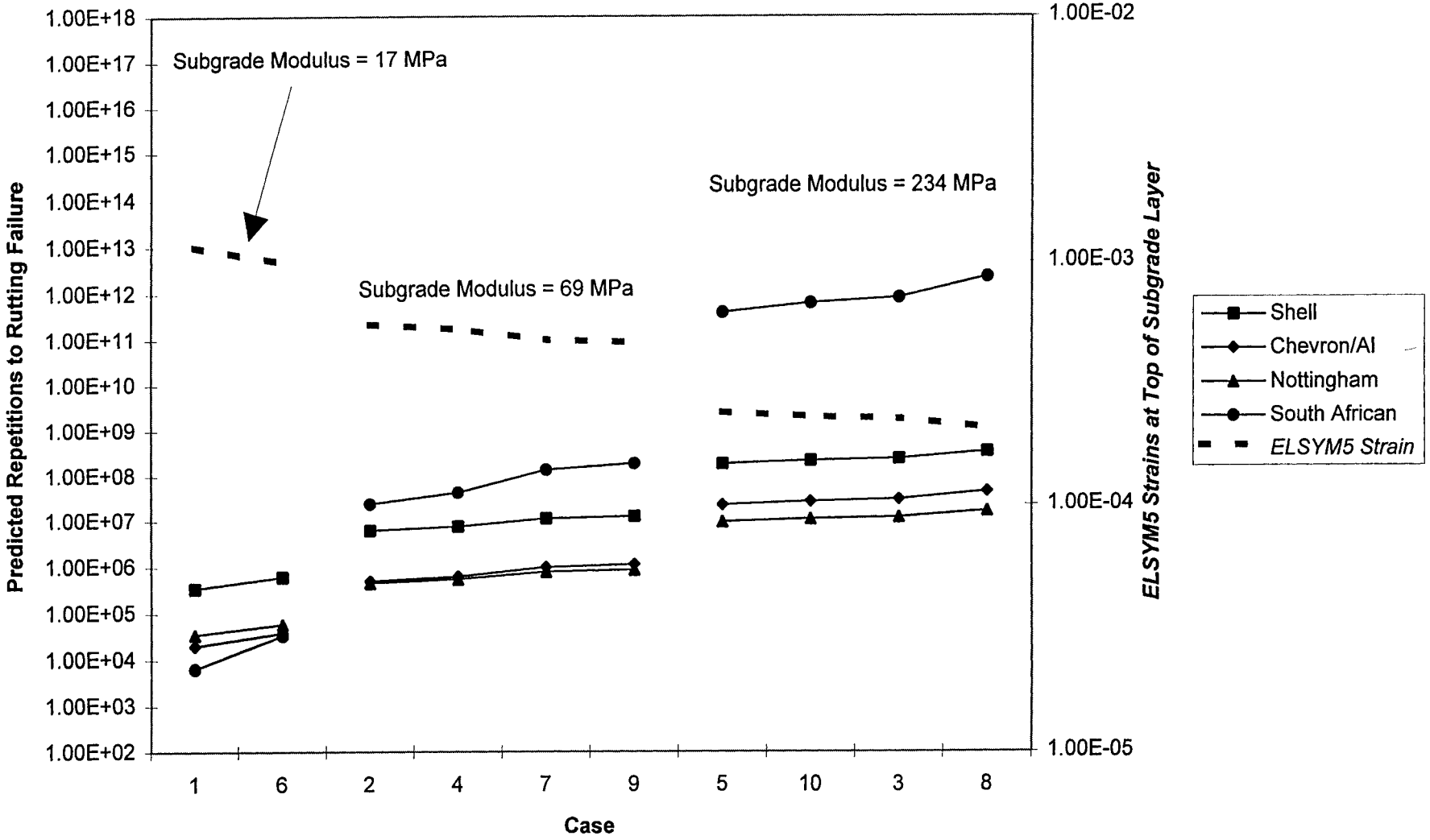

Figure 6.24 Subgrade ELSYM5 Strains and Resulting Rutting Predictions, Undrained Section 501RF, Load of 100 kN and Subbase Thickness of 218 mm

values for n are calculated to be 3.9 for the Shell model, 4.4 for the Asphalt Institute, 3.5 for the Nottingham, and 11.2 for the South African. All but the South African are close to the value of 4.2 used by Caltrans *(California Department of Transportation, 1987)*. This coefficient is theoretical and is not calculated from actual test section results. It must be emphasized again that further extensive HVS testing is necessary to validate the coefficient.

In comparison with the coefficient, n of 2.5, calculated from the predicted fatigue lives, the coefficients from the rutting predictions are much larger. This means that the modeling predicts the increased load to have a much larger effect, and therefore more relative damage, on the rutting performance than the fatigue performance of the pavement.

Comparison of design life and predicted rutting lives. Most of the predicted subgrade rutting lives exceed the criterion for the pavement design life of 0.798 to 1.2 million ESALS. This is illustrated in Figures 6.19 and 6.22 for the 40 kN load, which is equivalent to an ESAL.

CHAPTER 7

SUMMARY

While it is premature to draw many definitive conclusions from Heavy Vehicle Simulator (HVS) Test No. 1, it was considered important to prepare this interim report to summarize the extensive program completed in the 1994-95 period. This report will serve as a reference for future reports describing the results of Test No. 1 as well as other HVS tests in this first test series.

7.1 HVS ACCEPTANCE BY CALTRANS

As noted in Chapter 1, substantial progress was made during the first year of the Phase II portion of the project. During this time, the two HVS units have become operational, and both units were accepted by Caltrans within the time schedule shown in the original proposal. This has been in no small measure due to extraordinary efforts by both the staff of the Council for Scientific and Industrial Research (CSIR) of South Africa and Dynatest Consultants, Inc.

7.2 CONSTRUCTION

7.2.1 Test Section Structural Design and Construction Control

The first test sections, designed in accordance with Caltrans structural design methodology for a traffic index (TI) of 9, were constructed in April, 1995. Construction was in accordance with Caltrans procedures: construction control was performed by the staff of Contra

Costa County, Caltrans District 4, and the University of California at Berkeley (UCB). Pavement components met or exceeded all applicable Caltrans specifications.

7.2.2 Construction Recommendations

A high degree of compaction was achieved in the asphalt concrete surface mix. Better compaction nearly always results in improved fatigue performance and less rutting (if air-void contents are not below approximately 2.5 percent for dense graded mixes).

Experience gained from test-section construction suggests that the following guidelines might be of use for the construction of highway pavements by Caltrans:

- Reduce the length of mix that can be laid down prior to beginning compaction,
- Increase the minimum compaction thickness, especially for placement over cold existing surfaces and during night construction,
- Require simultaneous construction of adjoining lanes where feasible and,
- Install lateral confinement such as curbs or other similar devices prior to mix compaction where possible and economically feasible.

7.3 TECHNOLOGY TRANSFER

UCB staff have been trained by CSIR staff and are currently conducting the HVS test program on the first test section (containing the asphalt treated permeable base [ATPB]). Three work shifts per day are currently providing 24 hours per day, seven days per week operation, amounting to an average of about 17,000 load repetitions per day, including maintenance, data collection, and all other down time. These facets of the technology transfer from the CSIR to California have worked quite well.

7.4 TEMPERATURE CONTROL

This first test has emphasized the importance of temperature control to induce and understand specific distress mechanisms. Based on the experience gained thus far, it is recommended that a temperature control unit for the HVS be available before any more sites are tested. The effects of temperature variation complicate analyses of in-situ behavior as will be demonstrated in the report describing the results of the first test.

7.5 MATERIALS TEST RESULTS

7.5.1 Unbound Materials

Materials tests on the unbound layers have provided moduli which will be used to assess the performance of the test sections using analytically-based procedures. Resilient modulus tests and results of the analyses of the heavy weight deflectometer (HWD) deflection data appear to be in reasonable agreement. Test results obtained from the unbound materials demonstrate the influence of water content and dry density on material stiffness. Test results also provide evidence of the increased understanding of pavement performance obtained from evaluation of unbound materials in-situ and/or in the laboratory at the in-situ water content and density.

7.5.2 SuperPave Evaluation of Asphalt Concrete

The results of the mix test program completed to date indicate that the asphalt concrete used in the test pavement meets the Caltrans specifications for type A asphalt concrete. On the other hand, this mix does not meet all requirements of the SHRP SuperPave Level I procedure. In general, the aggregate meets both Caltrans specifications and the SuperPave consensus

properties. While the mix met the SuperPave gradation criteria, certain of the compaction requirements, the voids-in-the-mineral-aggregate (VMA) criteria, and the dust ratio were not satisfied. Stabilometer data suggest that the mix should be resistant to rutting, and this appeared to be confirmed by the gyratory compaction test results.

7.5.3 Flexural Beam Tests on Asphalt Concrete

Relative to fatigue performance, test results indicated similarity of the two compacted lifts except for effects of the air-voids differential between the two. Beams sawed from the compacted pavement exhibited similar performance characteristics to specimens produced by rolling wheel compaction in the laboratory. It should be noted that the laboratory compacted specimens exhibited slightly larger flexural stiffnesses which resulted from reheating the mix for laboratory compaction.

7.5.4 Stiffness Determinations for Asphalt Concrete

Flexural stiffnesses estimated from complex shear modulus determinations in the simple shear device at UCB and Caltrans were smaller than those measured in flexure while, at the same time, phase angles were larger. Shear stiffnesses measured by Caltrans were similar to those measured by UCB.

7.5.5 Repetitive Simple Shear Tests on Asphalt Concrete

Differences were observed in the simple shear constant height repeated load tests between Caltrans and UCB laboratories. These differences indicate the importance of a cooperative test effort between the two laboratories to insure that both testing units provide comparable results.

Field cores appeared to have greater resistance to permanent shear deformation than did laboratory compacted specimens which may be due in large part to additional oven heating for compaction

Results of the repetitive simple shear tests suggest that little rutting should occur in the test pavement at 21°C (69°F). However, significant rutting under the 100 kN (22,500 lb) load has occurred at higher temperatures experienced in July and August, emphasizing the strong recommendation that temperature control be implemented as soon as possible.

A simplistic evaluation of the effects of increased temperatures, heavier wheel loads and slower trafficking speeds associated with the HVS was performed using the RSST-CH.

Overall, these results emphasize the importance of continuing laboratory tests with the accelerated pavement test program because the laboratory test program is essential in evaluating and interpreting HVS test results. They also emphasize the need for temperature control during HVS testing.

7.6 PERFORMANCE SIMULATIONS

Extensive analyses of the fatigue performance and resulting influences on subgrade strain of both the drained (ATPB) and undrained sections have been conducted. These analyses assumed the pavement to be represented as a multi-layer elastic solid and utilized a series of models for both fatigue and rutting.

The predicted fatigue life is larger for the drained pavement than for the undrained pavement. This is due primarily to the increased stiffness of the ATPB compared to that of the aggregate base it replaces. However, the relative performance of drained and undrained pavements may be different under field conditions especially if severe moisture conditions

reduce the effectiveness of the asphalt treatment. A companion laboratory study is underway to evaluate the effect of the environment on the performance of ATPB. These effects may be evaluated in future HVS test sections as well.

When the first HVS test and analyses are completed, the actual fatigue life will be compared to predicted fatigue lives to validate the models. The SHRP surrogate model simulates a larger fatigue life than the Asphalt Institute, SHRP A-003A (laboratory), and the Shell models. The relative effectiveness of these models will be compared in the final report.

The moduli of the unbound layers and the thickness of the subbase have little effect on the fatigue life of the HVS pavement. Changes in the asphalt concrete moduli have much greater effect. Increasing the dual-tire load from 40 to 100 kN (9,000 to 22,500 lb) results in a decrease in fatigue life: however, the resulting damage is not as large as normally predicted using conventional load equivalency factors. These results provide the first link between laboratory and in-situ performance simulated by the HVS that will be validated after all four sections have been tested by the HVS.

The predicted subgrade rutting life is in the same range for both the drained and undrained pavement structures. The South African model is the most susceptible to changes in the modulus, especially the subgrade modulus. The Asphalt Institute, Shell, and Nottingham models predicted subgrade rutting lives within a one-order-of-magnitude range.

Increases in moduli in any pavement layer result in increases in the predicted subgrade rutting life. However, the degree of the effect varies from layer to layer. An increase in aggregate subbase thickness results in large increases in the subgrade rutting life. Therefore, HVS test section 500RF, which has the thinnest aggregate subbase should, according to predictions, have a smaller rutting life than the other sections to be tested later.

An increase in load from 40 to 100 kN (9,000 to 22,500 lb) causes a much larger reduction in the subgrade rutting life than predicted for the fatigue life.

REFERENCES

American Association of State Highway and Transportation Officials (1986), "Standard Method of Test for Resilient Modulus of Subgrade Soils, Method T 274-82," *AASHTO Methods of Sampling and Testing*, Washington, D. C.

American Association of State Highway and Transportation Officials (1990), *Specifications for Transportation Materials,* AASHTO Designation M145, Washington, D. C.

American Society for Testing and Materials (1989), *Annual Book of ASTM Standards*, Section 4, Volume 04.08, Philadelphia.

Bronstein, M. and J. Sousa (1993), *Automated Testing System V.3.11 Software*, SHRP Equipment Corporation, Walnut Creek, California.

California Department of Transportation (1987), *Highway Design Manual*, Sacramento, January.

California Department of Transportation (1991), *NEWCON90* Computer Program, Version April_30_91.1, Sacramento.

California Department of Transportation (1992a), *California Standard Specifications,* Sacramento, July.

California Department of Transportation (1992b), *Standard Plans*, Sacramento.

De Beer, M. (1991), "Use of the Dynamic Cone Penetrometer (DCP) in the Design of Road Structures," Proceedings of the Tenth Regional Conference for Africa on Soil Mechanics and Foundation Engineering and the Third International Conference on Tropical and Residual Soils, 'Geotechnics in the African Environment,' Volume 1, Maseru, Lesotho, 23-27, September.

De Beer, M., C. J. van der Merwe, and G. T. Rohde (1994), "The Evaluation, Analysis and Rehabilitation Design of Roads," Report No. IR 93/296, Division for Roads and Transport Technology, Council for Scientific and Industrial Research, Pretoria, South Africa.

Dyvik, R. and C. Madshus (1985), "Laboratory Measurements of G_{max} Using Bender Elements," Proceedings, ASCE Convention, Detroit.

Finch, D. M., R. Horonjeff, and H. G. Paula (1966), "Evaluation of Runway Lighting Systems for Effectiveness in Dense Fog," Final Report No. RD-65-58, Institute for Transportation and Traffic Engineering, University of California, Berkeley, January.

Harvey, J. and C. L. Monismith (1994a), "Accelerated Pavement Testing, Phase I, Laboratory Evaluation of Dense-Graded Asphalt Concrete (DGAC) and Asphalt-Rubber Hot Mix Gap-Graded (ARHM-GG)," Final Report for the California Department of Transportation, Institute of Transportation Studies, University of California, Berkeley, January.

Harvey, J. and C. L. Monismith (1994b), "Accelerated Pavement Testing, Phase I, Field and Laboratory Evaluation of Dense-Graded Asphalt Concrete (DGAC) and Asphalt-Rubber Hot Mix Gap-Graded (ARHM-GG), Executive Summary and Recommendations," Final Report for the California Department of Transportation, Institute of Transportation Studies, University of California, Berkeley, January.

Huang, Y.H. (1993), Pavement Analysis and Design, Prentice Hall Inc., New York.

Human, C. (1992), "Time Dependent Property Changes of Freshly Deposited Sands," Ph.D. Thesis, University of California, Berkeley.

McGennis, R., R. Anderson, T. Kennedy, and M. Solaimanian (1994), "SuperPave™ Asphalt Mixture Design and Analysis," National Asphalt Training Center Demonstration Project 101, Federal Highway Administration, Office of Technology Applications, Washington, D. C., and the Asphalt Institute, Lexington, Kentucky, April.

Miner, Milton A., "Cumulative Damage in Fatigue," Transaction, American Society of Mechanical Engineers. Volume 66 (1945).

Monismith, C. L., R. G. Hicks, and F. N. Finn (1994), "Accelerated Performance-Related Tests for Asphalt-Aggregate Mixes and Their Use in Mix Design and Analysis Systems," Report No. SHRP-A-417, Strategic Highway Research Program, National Research Council, Washington, D. C.

Nokes, W. A., P. J. Stolarski, C. L. Monismith, J. T. Harvey, N. Coetzee, and F. C. Rust (1996), "Establishing the Caltrans Accelerated Pavement Testing (CAL/APT) Programs," Paper Offered for Presentation at 1996 Annual Meeting of Transportation Research Board, Washington, D. C., January.

Pouch, G. (1986), "Hydrogeologic Site Assessment of the Engineering Geioscience Well Field at the Richmond Field Station, Contra Costa County, California," Department of Materials Science and Mineral Engineering, University of California, Berkeley.

Rust, C., J. du Plessis, B. Verhaeghe, and J. Grobler (1993), "Heavy Vehicle Simulator Testing of Trial Sections for Caltrans," Report No. DPVT C/255, prepared for the California Department of Transportation by Division of Roads and Transport Technology, Council for Scientific and Industrial Research, South Africa, October.

Seed, H. B., R. Wong, I. Idriss, and K. Tokimatsu (1984), *Moduli and Damping Factors for Dynamic Analyses of Cohesionless Soils*, Earthquake Engineering Research Center Report No. UCB/EERC-84/14, University of California, Berkeley, September.

Semmelink, C.J. (1994), "Recent Research with the DRTT K-Mould on Different Road Building Materials," Report No. COD/94, Department of Transport, South Africa.

Semmelink, C. J. and M. De Beer (1993), "Development of a Dynamic DRTT K-Mould System," Research Report DPVT 216, Division for Roads and Transport Technology, Council for Scientific and Industrial Research, Pretoria, South Africa, July, 1993.

Shell International Petroleum Company, Ltd. (1978), *Shell Pavement Design Manual*, London, England.

Shook, J.F., F.N. Finn, M.W. Witczak, and C.L. Monismith, "Thickness Design of Asphalt PavementsCThe Asphalt Institute Method," Fifth International Conference on the Structural Design of Asphalt Pavements, Volume 1, University of Michigan, 1982.

Sousa, J., J. Deacon, S. Weissman, J. Harvey, C. Monismith, R. Leahy, G. Paulsen, and J. Coplantz (1994), "Permanent Deformation Response of Asphalt-Aggregate Mixes," Strategic Highway Research Program Report No. A-414, National Research Council, Washington, D.C.

Tayebali, A. A., J. A. Deacon, J. S. Coplantz, J. T. Harvey, F. N. Finn, and C. L. Monismith (1994a), "Fatigue Response of Asphalt-Aggregate Mixes: Part I Test Method Selection; Part II Extended Test Program; Part III Mix Design and Analysis," Strategic Highway Research Program Report No. A-404, National Research Council, Washington, D.C.

Tayebali, A. A., B. W. Tsai, and C. L. Monismith (1994b), "Stiffness of Asphalt-Aggregate Mixes," Strategic Highway Research Program Report No. A-388, National Research Council, Washington, D. C.

Transport and Road Research Laboratory, Road Note No. 29, "A Guide to the Structural Design of Pavements for New Roads," Department of the Environment, 3rd Edition, Her Majesty's Stationary Office, London, 1970.

Transportation Research Board (1986), *AASHTO Guide for Design of Pavement Structures*, Volume 3, National Cooperative Highway Research Program, National Research Council, NCHRP Project 20-7 (Tasks 24 and 28), August.

van Til, C. J. et al. (1972), "Evaluation of AASHO Interim Guides for Design of Pavement Structures," National Cooperative Highway Research Council Report No. 128, National Research Council, Washington, D. C.

Viggiani, G. and J. H. Atkinson (1994), "Interpretation of Bender Element Tests," *Geotechnique*, Vol. 45, No. 1.

Wardle, L. J. (1976), *Program CIRCLY - A Computer Program for the Analysis of Multiple Complex Circular Loads on Layered Anisotropic Media: User's Manual*, Geomechanics Computer Program No. 2, CSIRO Division of Applied Geomechanics, Melbourne, Australia.

Weissman, S. (1993), "South Africa Mixes: Constitutive Constants and Finite Element Simulations of the HVS Pavement," Prepared for the University of California by Symplectic Engineering Corporation, Albany, California, November.

Zaman, M., D. H. Chen, and J. Laguros (1994), "Resilient Moduli of Granular Materials," *ASCE Journal of Transportation Engineering*, Vol. 120, No. 6, November-December.

MAY 1995

Test Plan for CALHVS1

Prepared for:
California Department of Transportation

Prepared by:
Dynatest Consulting INC.

University of California, Berkeley

Division of Roads and Transport Technology, CSIR

Dynatest

Roads and Transport Technology

CSIR

ACKNOWLEDGEMENTS

The input of the following people from Caltrans is gratefully acknowledged:

Joe Hannon
Ok-Kee Kim
Bill Nokes
Shakir Shatnawi
Skip Sowko
Phil Stolarski
Jack van Kirk
Gordon Wells

TABLE OF CONTENTS

LIST OF ILLUSTRATIONS

Page

LIST OF TABLES:

LIST OF FIGURES:

1. INTRODUCTION

Accelerated Pavement Testing (APT) of pavements is accepted as an important aid in decision making for road design, material characterization, and pavement behavior analysis world-wide. The California Department of Transportation (Caltrans) has recently bought 2 Heavy Vehicle Simulators (HVSs) from South Africa in order to assist in the Caltrans APT (CAL/APT) program.

The first HVS, CALHVSl is currently stationed at the Richmond Field Station (RFS) on the campus of the University of California, Berkeley (UCB). In collaboration with UCB and the Council for Scientific and Industrial Research (CSIR), CALHVSl is designated to test various experimental pavement sections at the RFS.

The initial tests with CALHVSl are due to start in May 1995, and a suggested test program is needed for structuring the objectives, the test plan and expected output from these initial tests. The test sections on which the first tests will be conducted are already under construction and represent typical pavement structures currently in use throughout California.

As a part of the program, laboratory tests are planned to evaluate the asphalt mix used for initial tests as the surface course, the various components of the pavements underlying the asphalt surfacing, and the overlay mixes to be placed in the constructed pavement sections following load testing to failure (fatigue) of the initially constructed test pavements.

The database developed from the extensive HVS program in South Africa will also be utilized to expand on the data obtained in this test sequence. Included, for example, will be evaluations between laboratory measured parameters and those determined in-situ using Non-Destructive Testing (NDT) of the pavement sections and Dynamic Cone Penetrometer (DCP) measurements of the pavement components.

In this document the objectives for the first series of pavement tests with CALHVSl are explained, together with the suggested test program in order to achieve the set objectives.

This document is a discussion document for use by Caltrans and UCB in developing the final objectives and test program for the initial CALHVSl tests.

2. OBJECTIVES

Although HVS testing has been used successfully on various South African roads over the past 15 years, CALHVSl is the foundation of HVS testing on an international basis. The overall objective of this project is to establish a sound platform for HVS testing in California. It also involves an extensive technology transfer program with the aim of providing Caltrans with complete operational Accelerated Pavement Testing capabilities.

In addition to the overall objectives each series of tests have specific objectives of a more technical motivation. The objectives for the first series of HVS tests are discussed below.

First objective

The first objective is to quantify pavement behavior of test sections at ambient temperature with increased load applications and to verify the existing design methodologies for Asphalt Treated Permeable Base (ATPB) pavements and conventional Asphalt Concrete (AC) pavements (aggregate base course), while preparing a uniform platform on which the overlays will be constructed.

This objective includes:

- the quantification of the effective elastic moduli of the various pavement layers, based on the linear-elastic or quasi linear-elastic approach;
- the quantification of the stress dependence of the pavement layers;
- determination of the failure mechanisms of the various layers, and
- determination of the fatigue lives of the two main pavement structures (the scope of this test does not allow for the development of transfer functions for fatigue of the pavement layers).

Second objective

The second objective of this series of HVS tests is to compare the fatigue performance of Asphalt Rubber Hot Mix gap-graded (ARHM-GG) using type 2 asphalt rubber binder, with that of conventional Asphalt Concrete Dense Graded (DGAC) mixes. This study is in essence a repeat of a similar study conducted in South Africa in 1993 for Caltrans and serves, therefore, as an experiment to validate the findings of the test performed in South Africa.

3. PAVEMENT STRUCTURE AND SECTION LAYOUTS

Figure 1 illustrates the pavement structure of the test sections and the layout of the ATPB and AC sections.

Two pavement structures are being constructed, a conventional undrained Asphalt Concrete (AC) pavement and a drained Asphalt Concrete pavement with a Asphalt Treated Permeable Base (ATPB). The pavement structures and layer thicknesses are shown in Table 1.

The asphalt concrete used for both sections will meet Caltrans specifications for 3/4 in. coarse gradation, Type A material. The mix design for the asphalt concrete will be from the Caltrans District 4 laboratory. The ATPB will meet Caltrans specifications, and the mix design will have been previously approved by Caltrans District 4. The asphalt concrete and ATPB layers will be compacted following Caltrans standard specifications. The asphalt concrete compaction will follow the standard method specification, which for research purposes will also be checked with the nuclear gauge (Caltrans Test 375).

The imported aggregate base will be virgin material meeting Caltrans specifications for Class 2 Aggregate Base. The compacted density must meet standard specifications, as measured using Caltrans Test 231. The existing aggregate subbase has been tested by the Contra Costa County Materials Laboratory and meets Caltrans specifications for Class 2 aggregate subbase. R-value tests were also conducted by the Caltrans District

TABLE 1: PAVEMENT STRUCTURES AND LAYER THICKNESSES

	UNDRAINED ASPHALT CONCRETE PAVEMENT (AC)	DRAINED ASPHALT TREATED PERMEABLE BASE PAVEMENT (ATPB)
Type of layer	Layer thickness	Layer thickness
Asphalt concrete (AC)	137 mm (0.45 ft)	137 mm (0.45 ft)
Asphalt treated permeable base (ATPB)		**76 mm (0.25** ft)
Aggregate base (AB)	**274** mm (0.90 ft)	182 mm (0.60 ft)
Aggregate subbase (ASB)	229 **mm (0.75** ft)	**229 mm (0.75** ft)
Subgrade (SG)	∞	∞

4 laboratory, and showed that the subbase material met the required R-value for the Class 2 specifications. At 152 mm (0.5 ft) below the existing subbase surface (approximately 335 mm (1.1 ft) in total thickness), the subbase layer met the Caltrans standard density specification in both Test Section A and B using Caltrans Test 231. The existing subgrade layer also met the Caltrans standard density specification in both test sections using Caltrans Test 231.

On each of these two pavements two sections will be tested. The test sequence is shown in Figure 2. All four sections will be subjected to accelerated traffic to the point that maintenance or rehabilitation is required. The failure criteria to determine this pavement condition are described in section 5.1.

After the failure of the initial four sections, overlays will be constructed on top of the failed sections (See Figures 2 and 3). Various alternatives are available for the construction of the overlays, these are discussed below and are illustrated in Figures 3a and 3b.

One of the undrained AC sections will be overlaid with a conventional asphalt concrete overlay with a specified thickness. The thickness of this overlay is influenced by the following factors:

- the mode, and degree of failure;
- the elastic surface deflection measured when the failure condition is reached, and
- the design procedure used to determine the overlay thickness, ie, structural adequacy or reflective crack control.

Therefore, the thickness of the overlay can only be determined once the tested section has reached the set failure criteria. The Caltrans TM356 overlay design procedure will be used for this purpose, by applying the Caltrans computer program, "ACREHAB".

The second undrained AC test section will be overlaid with an Asphalt Rubber Hot Mix (ARHM) using type 2 asphalt rubber binder, with a thickness of half of that used for the conventional asphalt concrete overlay. The two ATPB test sections will be overlaid with ARHM with thicknesses of one-third and two-thirds of the conventional Asphalt Concrete overlay, respectively.

The maximum depth for the ARHM layer will be limited to 61 mm (0.20 ft) as recommended in the “Caltrans ARHM-GG Thickness determination guide”.

4. SITE SELECTION

The different sites should be selected and prepared before HVS testing commences (see Figure 4). This preparation includes marking out of the test site and instrument installation. In order to do comparative tests it is of vital importance that all HVS test sites (as shown in Figures 3a & b) meet the necessary requirements regarding uniformity.

These include uniformity in:

- mix designs:
  - gradation
  - asphalt content
  - air void content (compaction)
- materials:
  - aggregate type
- layer thicknesses
- subgrade structural behavior
- structural behavior of the whole pavement system, within each test section

Quality control throughout the construction period is thus of vital importance to ensure that all above requirements are met.

The design tool which is usually used to ensure uniformity in structural behavior of the pavement system as a whole, is elastic surface deflection measurements. The Falling Weight Deflectometer (FWD) will be used for this purpose.

5. TEST PROGRAM

In order to meet the set objectives a carefully designed HVS test plan is necessary. For example, very high accelerated trafficking loads in the beginning of an HVS test, may induce premature shear cracking, which does not simulate real field behavior. Therefore, in order to simulate real field behavior, a lower wheel load will initially be applied to the test section.

Another example is that of temperature variation. An elevated pavement temperature causes a drop in asphalt stiffness values, which in turn causes the pavement to rut at a rate higher than normal. If the objective was to investigate the fatigue cracking behavior

(as a failure mechanism) the application of additional heat should, therefore, be discouraged. The test program is therefore designed around the expected failure mechanism within the boundaries of the set objectives.

5.1 Failure criteria

Three main types of failure mechanisms are probable:

- fatigue cracking;
- permanent deformation; and,
- total accumulated structural damage (monitored by elastic surface deflection).

As it is not entirely certain at this stage which of these three failure mechanisms will be dominant in the behavior of the initial test sections, all possible failure mechanisms will be monitored.

5.1.1 Fatigue cracking

The suggested target failure for cracking of the AC layer in both the drained and undrained (ATPB and AB) pavements is 12 % of the surfacing, as a percentage of length of the wheelpath, based on the South African failure criteria (TRH12). Current Caltrans HA-22 Reconstruction and Restoration program (PMS priority system) cracking criteria may serve as the basis for determining failure.

5.1.2 Permanent surface deformation level

The failure limit for permanent surface deformation (rutting) of the test section will be an average maximum of 10 mrn (0.4 in) permanent surface deformation.

5.1.3 Elastic surface deflection level

The tolerable limit for elastic deflection, based on the 80th percentile, will be determined using a standard wheel load of 40 kN (18 kip axle load) and a tire pressure of 690 kPa (100 psi). The Caltrans Dynaflect as well as the HVS will be used to measure the elastic surface deflections. This deflection is similar to the specified maximum deflection used

in the Caltrans pilot study done in South Africa, and will be used for overlay design using Caltrans TM 356 Test Method.

5.2 Test plan alternatives

In order to meet the set objectives, different test plan alternatives are possible. Because of the nature of the two sections it is difficult to meet both objectives equally well.

The first objective calls for the investigation of the structural behavior of the two different base designs. The ideal basis for an investigation of this nature, is to perform accelerated testing in different moisture regimes in the base layer.

The second objective calls for a uniform platform (in terms of structural behavior) in order to investigate the performance of the different thicknesses of the ARHM and standard AC overlay successfully. Because the four sections are built on two different types of base course (conventional AB and ATPB), which may react very differently to the applied load, the achievement of the second objective may be complicated by this.

Unfortunately , by adding another variable (such as different base moisture conditions) the uniformity necessary to obtain the second objective is lost and the degree of non-uniformity is very difficult to measure.

In order to meet both objectives, within the constraints mentioned above, the following three alternatives are suggested.

The failure criteria for the overlays depend on the structural behavior of the pavement and the design thicknesses. This accelerated test design falls out of the boundaries of this document and will be adequately addressed once information on the pavement structural behavior is available.

Alternative 1

Alternative one involves testing the four test sections at in-situ moisture conditions and ambient temperatures. The procedure is as follows:

- Apply accelerated testing on one drained ATPB and one undrained AC section until the set failure conditions are met. This is done in order to facilitate early comparison between the two pavement types.
- Test the other two sections to failure by applying accelerated testing
- Overlay all four sections with the specified overlays
- Test all four overlay sections to failure by applying accelerated testing

Alternative 2

The proposed procedure for the initial testing on the four constructed test sections is as follows:

- Apply accelerated testing on one drained ATPB section and one undrained AC section under in-situ moisture and temperature conditions.
- Saturate the pavement structures by injecting water into the pavement (sub soil or surface applications) and test the two remaining sections, one drained ATPB section and one undrained AC section under the saturated conditions.
- Overlay all four sections with the specified overlays
- Continue to test all four sections to failure

Alternative 3

The third alternative comprises the construction of only two overlays, and both overlays will be constructed on each of the two different initial pavement structures (drained ATPB and undrained AC pavement structures).

After completion of the HVS testing for the first objective, an AC overlay with a thickness as calculated with the Caltrans TM 356 method will be constructed on one half

of each of the undrained and drained test pavements. An ARHM-GG overlay with a thickness of 50 percent of that of the recommended AC overlay will then be constructed on the other half of each of the drained and undrained test sections. These overlaid test sections will then be subjected to accelerated trafficking to determine the pavement behavior of the ARHM and AC overlays on the different base structures.

Either alternative 1 or alternative 3 is suggested because these are the only quantifyable methods of establishing reasonably uniform support on which to test the overlays. It is suggested that no additional water is introduced to the pavement because it will be difficult to fully understand and measure the moisture under which the pavement will be tested. However, the most important reason for not introducing water into the tests at this stage is that the ATPB section may behave differently than the AC section under different moisture conditions as this is the intent of the design. This will then **result** in a non-uniform support for the overlays, which contradicts the second objective of this study.

5.3 Test program for individual sections

In this section all the relevant data to perform the actual HVS test is detailed. This includes the traffic wheel load, tire pressures, instrumentation layout, measurement schedule and any other relevant data to perform the test as planned.

The tests will begin with a 40 kN wheel load and a tire pressure of 690 kPa. Because of testing a fresh asphalt concrete which has not been subjected to normal environmental aging, nor post construction compaction, a lower test load is suggested. This load (40 kN) will be applied until the end of the "bedding-in" phase is reached. It is envisaged that the end of this phase will be reached after 50 000 load repetitions, after which the pavement response is expected to be constant. However, monitoring of the actual behavior is important to prevent the wheel load being changed before the bedding-in phase is complete, if in fact this phase takes longer than 50 000 load repetitions.

At this point the wheel load should be increased to 80 kN and the tire pressure should remain constant. These conditions should continue until the failure conditions are met.

It is emphasized again that if the pavement behavior (i.e. deflection, layer deformation) is not constant, the testing conditions should not be changed or the effects of the changes cannot be adequately quantified. It is also advisable for only one testing condition to be changed at a time in order to be able to attribute the change in pavement behavior to the change in condition. This test plan should be constantly monitored to ensure the required results are being observed and any changes can be made at any stage which will contribute to better test results.

If the pre-mentioned failure conditions are not met after the application of 200 000 load repetitions, the applied wheel load shall be increased to 100 kN (22.5 kip axle load) to induce failure.

A full set of elastic surface deflections will be taken immediately after a test is terminated. These deflections will be done using the standard 40 kN dual wheel load at the following points:

- center line: points 1 - 16;
- 200mm to the left of the center line: points 1 - 16, and
- 200mm to the right of the center line: points 1 - 16.

This is necessary to adequately ensure the investigation into the uniformity of the platform on which the overlays are going to be built.

The conditions for testing and the taking of measurement readings are detailed below in Table 2. It should be noted that this is a suggested test plan and constant adjustments may be necessary depending on pavement behavior under accelerated trafficking.

TABLE 2: TEST PLAN

HVS TEST NUMBER: 500RF		POSITION: RICHMOND FIELD STATION		STARTING DATE: 3 May 1995		TIRE PRESSURE [kPa]: 690kPa (100psi) TRAFFIC LOAD [kN]: 40. 80,100 kN DUAL WHEEL			
REPETITIONS	LOAD [kN]	TIRE PRESSURE (kPa)	PROFILOMETER POINT[1] 0-16	MDD CL POINT[1] 4,12 Dual wheel loads (kN)	RSD CL POINT[1] 4,6,8,10,12 Dual wheel loads[3] (kN)	RSD 200TS[2] POINT[1] 4,8,12 Dual wheel loads[3] (kN)	RSD 200CS[2] POINT[1] 4,8,12 Dual wheel loads[3] (kN)	TEMPERATURE POINT[1] 4,12 AT DEPTH 0,70,137,and 175mm	MDD DEPTHS & POSITION (mm)
10	40	690	YES	40	40	30,40	30,40	YES	MDD 4: 0 150 411 640 820
10 000	40	690	YES	40	40	40	40	YES	
20 000	40	690	YES	40	40	40	40	YES	
30 000	40	690	YES	40	40	30,40	30,40	YES	MDD 12: 137 411 640 820 1000
40 000	40	690	YES	40	40	40	40	YES	
50 000	40	390	YES	40,60,80	40,60,80	40,60,80	40,60,80	YES	
100 000	40	690	YES	40,60,80	40,60,80	40,60,80	40,60,80	YES	
125 000	40	690	YES	40,80	40,80	40,80	40,80	YES	
150 000	80	690	YES	40,60,80	40,60,80	40,60,80	40,60,80	YES	
175 000	80	690	YES	40,80	40,80	40,80	40,80	YES	
200 000	100	690	YES	40,60,80,100	40,60,80,100	40,60,80,100	40,60,80,100	YES	
225 000	100	690	YES	40,100	40,100	-	-	YES	
250 000	100	690	YES	40,100	40,100	-	-	YES	
50 000 steps to failure	100	690	YES	40,100	40,100	-	-	YES	
Crack initiation	100	690	YES	40,80,100	40,80,100	40,80,100	40,80,100	YES	
Failure	100	690	YES	40,80,100	40,80,100	40,80,100	40,60,100	YES	

NOTES:
- The test is done in the in-situ moisture condition
- The test is done in the ambient temperature condition and temperature measurements should be taken three times daily

LEGEND:
MDD Multidepth deflectometer
RSD Road surface deflectometer

1: Point of measurement on test section
2: 200 TS - 200mm towards one side (traffic side)
200 CS - 200mm towards the other side from the center line
3: Loads for measurements

6. TIME SCALES

In order to do an estimation of the time needed to complete phase one of CALHVSl testing the following assumptions are made:

- Number of traffic repetitions per day: 16 000 (including daily service)
- Number of hours needed to complete a full set of measurements: 8 hours
- Number of hours needed to reposition CALHVSl onto new test site: 4 hours
- Downtime of CALHVS1: 5 %

It must be emphasized that the test plan is flexible and is subject to the actual performance of the test section. It is feasible that the test sections will not fail before 250 000 repetitions. Assuming a total of 250 000 repetitions, the time required to perform 1 HVS test is as follows:

		TOTAL TRAFFICKING DAYS
Time for 250 000 reps	250 000 / 16 000	16
Time for measurements	14 x 8 hours	5
Downtime	5% of 21 days	1
TOTAL:		22

During this first test extensive training will be provided which will influence the above suggested schedule. A 20 % increase in time due to this training adds 5 days to the total. Thus, the total time necessary is calculated at 27 trafficking days per test. Therefore to successfully complete 8 test sections will approximately take 7 months, assuming a 24 hour and seven day a week operation.

It should be noted that this estimate may be influenced by operational factors such as the availability of fuel and staff during weekends, and pavement performance factors such as the influences from construction and the effects of material quality.

7. INSTRUMENTATION AND MONITORING METHODS

The standard instrumentation and monitoring methods available for use during these HVS tests are the following:

- Road surface deflectometer (RSD)
- Multi-depth deflectometer (MDD)
- Laser profilometer
- Thermocouples
- Visual inspections & crack growth monitoring

A brief discussion on the use of the instrumentation and the results obtained is included below.

Road surface defiectometer

The road surface deflectometer measures the elastic surface deflection of a pavement under the action of a wheel load. The RSD is a modification of the Benkelman Beam. The output from the RSD is elastic surface deflection bowls which can be used to:

- characterize pavement behavior;
- backcalculate effective E moduli (stiffness);
- monitor changes in the stiffness of the pavement with time, and
- determine stress dependency of pavement layers (non-linear elastic behavior)

During a test the RSD measuring points on the pavement are clearly marked to ensure that the deflection is measured at the same point each time. An adequate number of RSD

readings should be taken to ensure that the behavior of the whole test section is monitored (Figure 4).

Multi-depth deflectometer

MDDs are installed in a pavement to allow measurement of both elastic deflection and permanent deformation at in-depth positions. A maximum of six modules may be vertically installed, ie. six vertical positions in one MDD may be measured. The minimum vertical distance between each module is 150 mm (6 inches) due to the physical size of each module. The modules are usually placed at layer interfaces or at other critical depths in the pavement structure (see Figure 5).

The outputs from an MDD are influence lines of deflection at the selected depths within the pavement and the permanent deformation of the pavement with time, obtained by the permanent vertical movement of the various pavement layers as measured by the MDD modules.

MDD measurements can be used to:

- characterize the behavior of the whole pavement system;
- monitor changes in the stiffness of the various layers in the pavement with time;
- backcalculate effective E moduli (stiffness) of the various layers;
- determine stress dependency of pavement layers (non-linear elastic behavior), and
- determine the permanent deformation (compression) of all pavement layers

Laser profilometer

The laser profilometer is used to measure the profile of the surface of a test section. This output allows the determination of rut progression. The profilometer traverses the test section and the points of measurement are clearly marked to ensure the same point is always measured. An adequate number of data points should be taken to ensure that the behavior of the whole test section is monitored.

Thermocouples

Thermocouples can be installed in the pavement to measure temperature at selected depths. This allows the monitoring of temperature fluctuations within the test section. In Figure 4 the positions and depths of the thermocouples are shown.

Visual inspection

Regular visual inspection of the test sections allows crack growth and bleeding progression to be monitored. Measuring techniques are available to quantify the crack growth and bleeding progression in terms of percentages of the test section area. These results can be compared to the Caltrans criteria regarding the degree of cracking to warrant maintenance or rehabilitation.

Usually all the above factors are measured at selected load repetitions. The time taken for the readings is obviously dependant on the number of specified readings to be taken. In other words, the larger number of readings required, the longer the test will take. However, it is important to ensure an adequate number of readings are measured to draw representative conclusions.

Trench

After completion of a tests, a trench will be dug across each test section to gain an understanding of the in-situ profile of the pavement. This will aid in understanding the pavement behavior measured during the test. Material samples for testing will also be obtained from the trench.

8. LABORATORY TEST PROGRAM

The laboratory and field testing for this experiment will be a joint effort between the many participating agencies and institutions as shown in Table 3. The report will be written by UC Berkeley and Caltrans.

8.1 Work Plan

The work plan incorporates testing of the materials before construction in the laboratory, as constructed in-situ, and after construction in the laboratory. In-situ testing and pre- and post-construction laboratory testing will provide information regarding the properties of the pavement system materials, and provide data needed to evaluate current Caltrans specifications and design methods (materials and pavement thickness). Mechanistic analysis (linear and non-linear elastic layer analysis as a minimum) will be used to investigate the pavement failure mechanisms and validate analytical procedures for predicting pavement performance based on laboratory testing, such as fatigue life based on maximum tensile strain in the asphalt bound layers and laboratory fatigue curves, subgrade rutting based on the vertical compressive strain at the top of the subgrade, and rutting of the asphalt concrete based on permanent shear strain from repetitive simple shear testing.

Data will be obtained for statistical correlations relating various laboratory test methods with in-situ test methods. Data will also be obtained for statistical correlations relating laboratory predicted performance to accelerated pavement testing performance (transfer functions). These data will later be useful for relating routine pavement analysis, design and specifications based on laboratory testing to in-situ performance. Once the second HVS is available and operating in the field, it will provide additional data for transfer functions relating accelerated pavement testing performance to pavement performance under normal trafficking.

The following testing will be performed:

Subgrade:

borehole logs and location of water table,
classification tests,
R-values,
in-situ densities and water contents,
dynamic cone penetrometer (DCP),
triaxial resilient modulus and permanent deformation testing,
K-mould (CSIR test for resilient modulus and permanent deformation);

Subbase:

classification tests,
sand equivalent test,
R-values,
in-situ densities and water contents,
triaxial modulus and permanent deformation testing,
K-mould ,
Heavy Weight Deflectometer deflection testing on completed subbase layer;

Base:

classification tests,
sand equivalent test,
R-values,
in-situ densities and water contents,
triaxial modulus and permanent deformation testing,
K-mould,
Heavy Weight Deflectometer deflection testing on completed base layer;

Asphalt Treated Permeable Base:

gradation of aggregate,
percentage of crushed particles,
LA Rattler,
cleanness value,
film stripping,
extracted asphalt content,
fatigue beams,
repetitive simple shear test at constant height (RSST-CH);

Asphalt Concrete and ARHM (where applicable):

a From Mix Design on file
- LA Rattler,
- swell,
- moisture vapor susceptibility,
- CKE,
- Caltrans (Hveem) procedure,
- percent crushed particles,
- sand equivalent,
- gradation,
- specific gravities;

a From Plant Just Before Time of Construction
- gradation of aggregate,
- sand equivalent,
- Superpave aggregate tests;

a From Construction Site
- in-place densities,
- swell,
- moisture vapor susceptibility,
- Caltrans (Hveem) procedure,
- extracted asphalt content,
- moisture,
- ASTM D 2041 (maximum specific gravity);

a On Field Cores and Beams
- repetitive simple shear test at constant height (RSST-CH),
- air-void content,
- fatigue beam test and stiffness (beams to be taken at later date);

a On Laboratory Compacted Field Mix
- fatigue beams,
- repetitive simple shear test at constant height (RSST-CH),
- Caltrans (Hveem) Procedure,
- Superpave Level I; testing (gyratory) and analysis.

8.2 Task Assignment and Required Effort

The time required for each item of work described in this plan is stated for continuous work, not an estimate of time to completion of work from the present date. Some tasks, such as fatigue testing, do not require a full-time commitment, but must be regularly monitored.

Much of the in-situ soils testing has been performed already. Construction compliance testing will be completed soon after construction. The deflection testing will be finished soon after construction. The K-mould results should be ready within one month.

For the current scope of the experiment the following specimens, where applicable, are required per mix type (original AC, ATPB, AC overlay, ARHM) :

- minimum 12 specimens for fatigue testing,
- minimum 12 specimens for RSST-CH (3 for ARHM, 3 for AC, 6 for ATPB at different confining stresses), and
- minimum 6 specimens for gyratory tests.

It is anticipated that the UCB laboratory will require approximately 3 weeks to prepare specimens, and 2 week for testing. The remainder of the tests, except triaxial testing have been completed. The tri-axial testing will require some modifications to UCB equipment, but should be completed by the end of June, 1995.

It is anticipated that the Caltrans laboratory will require approximately 1 week for RSST-CH testing, totalling 9 specimens. Additional AC mix aggregate testing to be performed at Caltrans will require approximately 1 week.

Analysis and report writing will each require approximately 2 to 3 weeks of work.

TABLE 3: LABORATORY AND IN-SITU TESTING ASSOCIATED WITH CALHVSI

Aggregate and mix collection	UCB
AB, ASB: R-values, SE, sieve analysis, densities, WC	Contra Costa County Caltrans District 4 UCB
SG: classifications, DCP, R-values, K-mold (ASB also)	UCB Contra Costa County Caltrans District 4 CSIR
SG, ASB, AB: Tri-axial M_R	UCB
Deflection tests, Back-calculation of E_i	Dynatest
Standard AC, ATPB, ARHM tests	Contra Costa County Caltrans District 4
AC, ATPB, ARHM: RSST-CH	UCB Caltrans Translab
AC, ATPB, ARHM: fatigue beams	UCB
AC: SuperPave I (not applicable to ARHM)	UCB Caltrans Translab
Analysis	UCB Caltrans Translab
Report writing	UCB Caltrans Translab

9. UTILIZATION OF THE CSIR DATA BASE

The CSIR developed a database of HVS test results from HVS tests done in the past. This database consists of two parts:

- All the raw data of the standard HVS measurements of elastic deflection (RSD and MDD based) and permanent deformation (profilometer, straight-edge and MDD based) of the pavement structures; and

- a text-based section which consists of all analyzed results contained in reports developed from the HVS tests. The text-based database also includes results of visual assessments, test pits analysis, non-destructive test (NDT) measurements and laboratory tests.

Data can be extracted from these two databases on any of the types of pavement structures on which HVS tests have already been done. This data also includes the data from the initial Caltrans pilot study done in South Africa.

The database may be utilized in the current accelerated pavement testing program, by first extracting data of the Caltrans piiot study and any other HVS tests done on pavements with similar structures and/or similar layers, and then analyzing this data. This analyzed data will then be used together with the data from the current CALHVSl tests to develop an understanding of the behavior of the test section with a wider perspective than the current HVS test sections.

The analysis of the data from the database and current HVS tests, could include the following:

- the determination of effective elastic moduli for different materials in the pavement structure using surface and in-depth elastic deflections;
- determination of the stress dependency (non-linear behavior) of layers and/or pavement structures;
- determination of resistance to permanent deformation of various pavement layers in pavement structures; and
- determination of the fatigue behavior of various pavement structures.

10. BENEFITS

Benefits from this initial test program include the following:

- Evaluation and comparison of the current Caltrans design for pavement structures consisting of asphalt concrete (AC) and untreated aggregate base (AB) and subbase and sections including asphalt treated permeable base (ATPB).

- Feasibility of mechanistic empirical methods to predict performance using layered elastic analysis.

- Evaluation of the fatigue test and simple shear test developed at UCB as part of the SHRP program to predict performance relative to fatigue and permanent deformation. As a corollary to this benefit, the program promotes an opportunity to compare the results of the mix design according to the Caltrans (Hveem) procedure to the suggested mix design procedure from SHRP-A003A based on the simple shear test.

- Evaluation of the SHRP developed equipment and methodologies to predict the performance of both DGAC (dense graded asphalt concrete) and ARHM (asphalt rubber hot-mix, gap-graded) used as overlays. In addition the program promotes

the potential for the development of a procedure for the design of mixes containing modified binders.

11. IMPLEMENTATION

Performance of these and other supplementary test sections will be used to validate present Caltrans design procedures and may result in modifications to the current Caltrans practices in pavement evaluation and design.

12. CONCLUSIONS

In conclusion, the objectives of the first series of CALHVSl tests have been discussed, alternative test plans to meet the set objectives are proposed and guidelines on the instrumentation of the test sections are given.

In addition to this, the laboratory test plan complimenting the CALHVS l tests, and suggestions for utilization of the CSIR HVS database in enhancing the CALHVSl tests are included in this report.

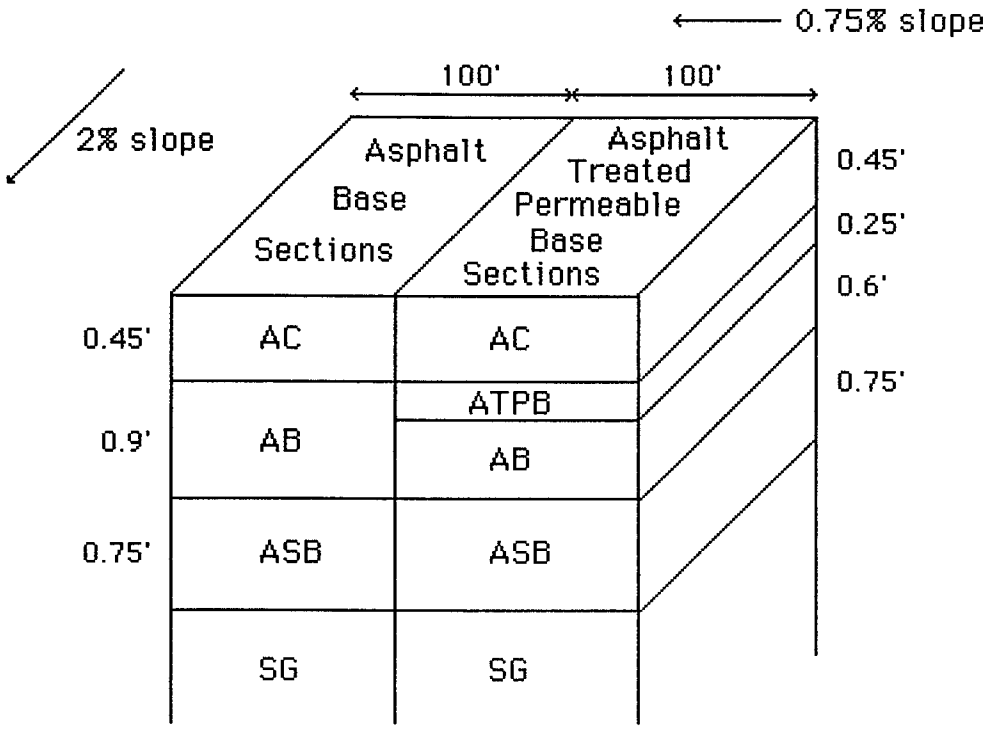

Fig 1: Initial Construction of Sacrificial Pavements

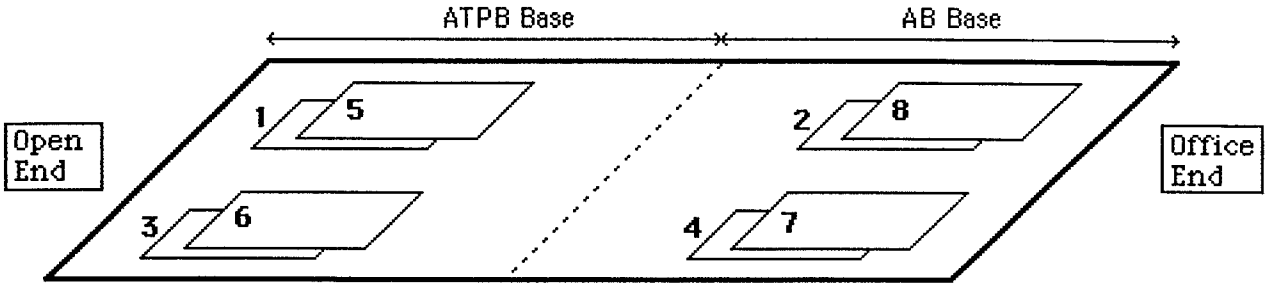

Fig 2: Placement of Test Sections

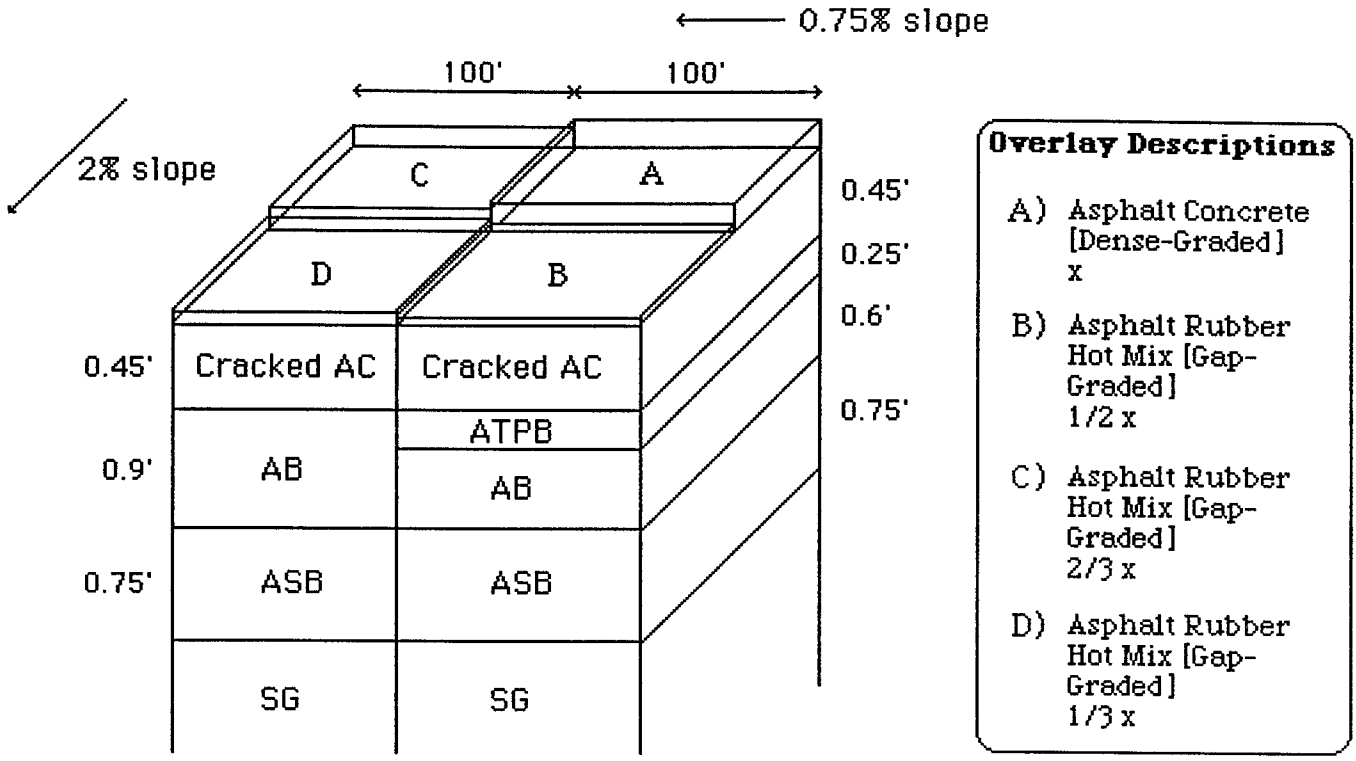

Fig 3a: Construction of Overlays (Alternatives 1 & 2)

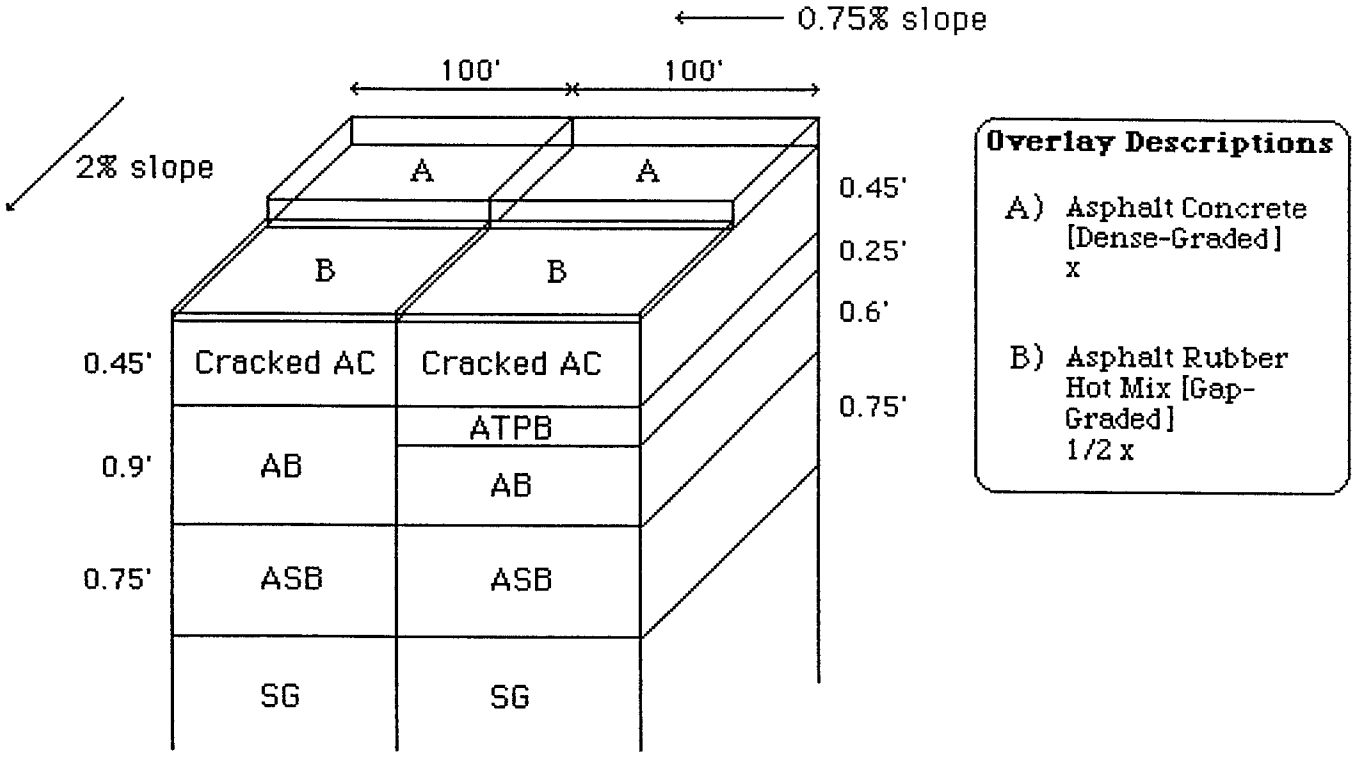

Fig 3b: Construction of Overlays (Alternative 3)

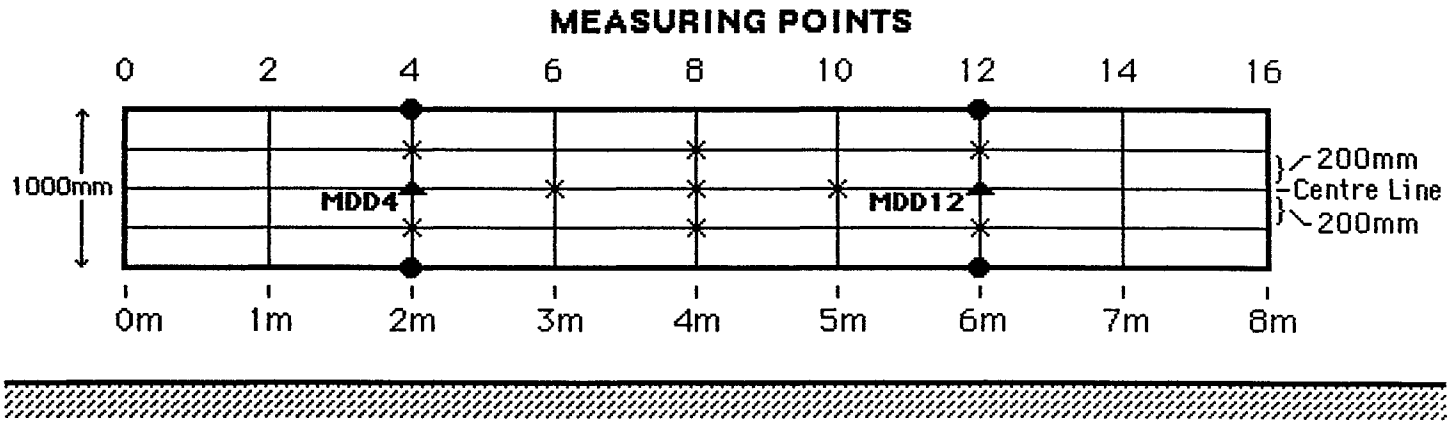

* RSD Deflection
● Measuring Points
Thermocouples
Depths: 0 mm
70 mm
137 mm
175 mm

Fig 4: Layout of a Typical HVS Test Section

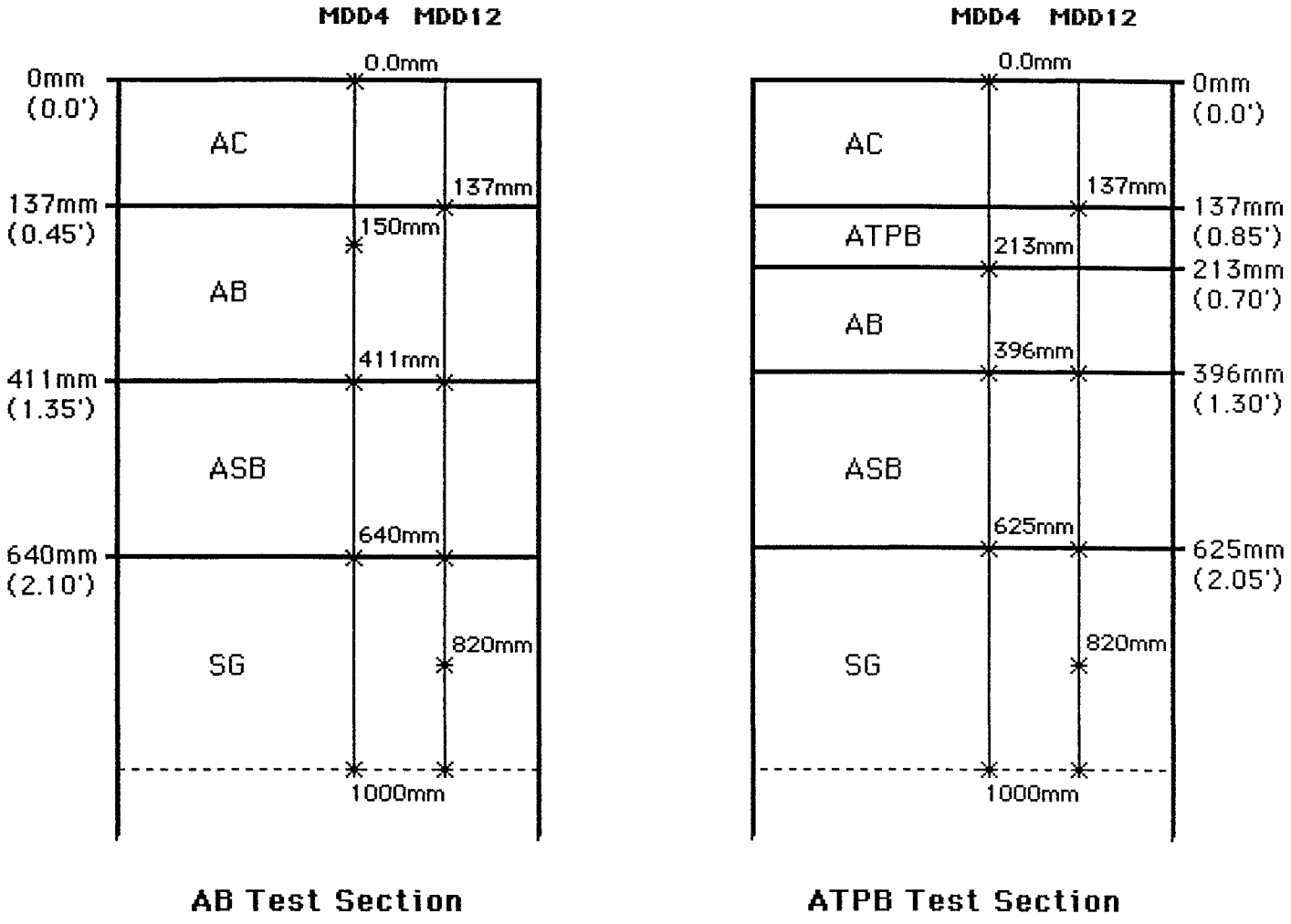

Fig 5: In-Depth Positions of MDD Modules in both Pavement Structures

APPENDIX B

BOREHOLE DATA; BORING LOGS AND DISCUSSION

BOREHOLES

Four boreholes were dug within the HVS test sections prior to placement of the base and asphalt concrete layers. Two boreholes each were located in the drained and undrained pavement sections. The borehole logs are included in this Appendix.

All boreholes were excavated with a hand auger until groundwater was reached. The interface between the subgrade and subbase was somewhat poorly defined for all boreholes, consisting of a zone approximately 50 to 75 mm (2 to 4 in.) thick consisting of a mix of subbase and subgrade material. Once past the subbase, subgrade samples were collected for later testing and moisture content was measured at various depths in each hole. The moisture contents are summarized in Table B.1.

The soil profiles for all of the boreholes were fairly similar. The uppermost layer of the subgrade is a stiff, high plasticity black or gray clay. Below the upper layer, there are repeated layers of stiff brown clay and softer green clay, with inclusions of small white stones approximately 2 to 9 mm in diameter. Once the groundwater table was encountered, at depths between 3.5 and 4.8 m (11.5 and 15.7 ft), excavation was stopped. The boreholes were left open for observation for several days to confirm the location of the groundwater table.

The observations made at the four boreholes are consistent with a line of much deeper boreholes (30 m [100 ft]) in a well field placed by Lawrence Berkeley Laboratory (LBL) parallel to, and approximately 100 m (350 ft) east of the HVS test sections. In their report (Ref Pouch), UC-Berkeley geologists described the area as an alluvial fan/delta on top of older Bay Mud deposits, through which have passed meandering streams. The fluvial deposits consist of alternating layers dominated by clays, with some sands and gravels most likely correlated with wet season flows. The sands and gravels occur as lenses set in a clay matrix.

TABLE B.1: Borehole Data

Borehole	Sample	Depth (m)	Water Content (%)	Liquid Limit	Plastic Limit	Plasticity Index
Hole A1	1	1.0	23.4	54	20	34
	2	1.9	27.0	50	19	31
	3	2.5	22.9	45	17	28
Hole A2	1	1.5	23.9	53	12	41
	2	2.8	20.2	45	16	29
Hole B2	1	0.9	23.1	55	15	40
	2	1.6	20.6	39	12	27

REFERENCES

G. Pouch, "Hydrogeologic Site Assessment of the Engineering Geoscience Well Field at the Richmond Field Station, Contra Costa County, California," Department of Materials Science and Mineral Engineering, University of California, Berkeley, 1986.

PROJECT NUMBER HVS	BORING NUMBER A1 Sheet of
	SOIL BORING LOG

February 22, 1995

Project HVS borings in old Fog building Location 16.5 m North of save

Elevation _____ Drilling Contractor UCB Geotech

Drilling Method and Equipment Pick, shovel, auger

Water Levels _____ Start 10:00 Finish 5:00 Logger _____

Depth Below Surface (m)		Sample			Standard Penetration Test Results	Soil Description	Comments
		interval	# and type	recovery (FT)	6"-6"-6" (N)	Soil name, USCS group symbol, color, moisture content, relative density or consistency, soil structure, mineralogy	Depth of casing, drilling rate, drilling fluid loss, tests and instrumentation
-					pocket pen	Top Existing ASB to .5 m	Bucket 1
-	.5		bag 1				.5m - 1.6m
-			.5-1.9			(.5m) black clay, medium stiff,	Bucket 2
-	.9					moderate plasticity ("dark" Bay Mud)	1.8m - 2.1m
—1						(1.6m) starting grade greener	Bucket 3
-			bag 2			(1.8m) lighter green, greener, with	2.1m - 2.9m
-			1.9-			white flecks (5%?)	Bucket 4
-	1.6		2.5m			(1.9m) water content bag taken	3.4m - 4.1m
-	1.8					(2.1m) green with 15% white rock,	
—2	1.9		bag 3			brown streaks	2.3 m : attempted to
-	2.1		2.5-			(2.15m) change in color, green to	push sample tube
-	2.5		3.15m			brown, black streas in brown, some	~70mm
-						rock, drier, stiffer than green	
-	2.8		bag 4			(2.5m) some green returned; marble	
—3	2.9		3.15-			green-brown. More moisture than	3.8 m : attempted to
-	3.15		3.25m			before.	push sample tube
-	3.4					(2.8m) 90% green again, more moist	~70mm
-	3.5		bag 5			(2.9m) very green, softer, much wetter	
-	3.75		3.25-			(3.25m) brown re-introduced, marbling	
—4	4.1		3.8m			again	
-						(3.4m) much stiffer, increasing brown	
-			bag 6			(less coming up with each augur)	
-			3.8-			(3.5m) pure brown	
-			4.1m			(3.75m) slightly stickier (doesn't want to	
—5						come out of auger)	
-						(3.8m) hit water (water table?)	
-						(4.1m) stop, still wet.	
-							
-							

PROJECT NUMBER HVS	BORING NUMBER A2 Sheet of
SOIL BORING LOG	

February 22, 1995

Project HVS borings in old Fog building Location

Elevation Drilling Contractor UCB Geotech

Drilling Method and Equipment Pick, shovel, auger

Water Levels Start 10:00 Finish 5:00 Logger

Depth Below Surface (m)		Sample			Standard Penetration Test Results	Soil Description	Comments
		interval	# and type	recovery (FT)	6"-6"-6" (N)	Soil name, USCS group symbol, color, moisture content, relative density or consistency, soil structure, mineralogy	Depth of casing, drilling rate, drilling fluid loss, tests and instrumentation
-					pocket pen	Top Existing ASB to .5 m	Bucket 1,2
-	.5		bag 1				1.1m - 1.6m
-			.5-1.5m			(.5m) dark gray, medium stiff, moderate plasticity	Bucket 3
-	.9						1.6m - 2m
—1							Bucket 4
-	1.3		bag 2			(9m) white coarse sand/gravel in green clay, lightweight (limestone) (15%?)	2m - 2.6m
-	1.5		1.5-				Bucket 5
-	1.6		2.8m				3.1m - 3.6m
-						(1.3m) grading light green with depth, less white stuff	
—2	2						
-	2.2		bag 3				
-			2.8-			(1.6m) Grading tan to brown, drier (~PL?)	
-			3.1m				
-	2.8						
—3	3		bag 4			(2m) slightly more moist	
-	3.1		3.1-				
-	3.5		3.7m			(2.2 m) add water, no white stuff	
-	3.7						
-	3.8		bag 5			(2.2 m) tan, drier again	
—4	3.9		3.7-				
-			3.9m			(3m) added water to assist recovery	
-							
-			bag 6			(3.5m) first "free water," with blocks of stiff clay	
-			3.9-4m				
—5							
-						(3.8m) more water, stiff clay (tan), (fractures)	
-							
-							
-							

PROJECT NUMBER HVS	BORING NUMBER B1 Sheet of
SOIL BORING LOG	

February 22, 1995

Project HVS borings in Building 280 Location 46.5 m N of save

Elevation _____ Drilling Contractor UCB Geotech

Drilling Method and Equipment Pick, shovel, auger

Water Levels _____ Start _____ Finish _____ Logger _____

Depth Below Surface (m)		Sample			Standard Penetration Test Results	Soil Description	Comments
		interval	# and type	recovery (FT)	6"-6"-6" (N)	Soil name, USCS group symbol, color, moisture content, relative density or consistency, soil structure, mineralogy	Depth of casing, drilling rate, drilling fluid loss, tests and instrumentation
-						Top Existing ASB	Bucket 1
-	.38					.38 m - 1.09 m	.38m - .785 m
-						Black clay	Bucket 2
-	.785					1.09 m - 1.48 m	.785 m - 1.09 m
—1	1.09		1.12 m			Green clay with small white pebbles	Bucket 3
-	1.12		bag 1			1.48 m - 1.80 m	1.09 m - 1.48 m
-	1.48					Brown clay	Bucket 4
-	1.65		1.65 m			1.80 m - 1.98 m	1.48 m - 1.98
-	1.80		bag 2			Brown/green mix, silty	Bucket 5
—2	1.98					1.98 m - 2.7 m	1.98 m - 2.32 m
-	2.14		2.14 m			Green and gray, silty, flakey	Bucket 6
-	2.32		bag 3			2.7 m - 3 m	2.32 m - 2.7 m
-						Brownish, silty, flakey, stiff clay,	Bucket 7
-	2.7		2.7 m			comes up as shavings, green with tan	2.7 m - 3.1 m
—3			bag 4			staining	Bucket 8
-	3.1		3.1			3 m - 3.95 m	3.1 m - 3.5 m
-	3.5		bag 5			Brownish, clayey, greenish	Bucket 9
-							3.5 m - 3.95 m
-							
—4	3.95						
-	4.2						
-							
-							
-	4.8						
—5							
-							
-							
-							
-							

PROJECT NUMBER HVS	BORING NUMBER B2 Sheet 1 of 1
	SOIL BORING LOG

February 22, 1995

Project HVS borings in Building 280 Location 56.6 m N of save AC

Elevation _____ Drilling Contractor UCB Geotech

Drilling Method and Equipment Pick, shovel, auger

Water Levels _____ Start _____ Finish _____ Logger _____

Depth Below Surface (m)		Sample			Standard Penetration Test Results	Soil Description	Comments
		interval	# and type	recovery (FT)	6"-6"-6" (N)	Soil name, USCS group symbol, color, moisture content, relative density or consistency, soil structure, mineralogy	Depth of casing, drilling rate, drilling fluid loss, tests and instrumentation
-						(.35m) black begins, turned steely dark	Bucket 1
-	.35					grey after 2-3 augurs	.35m - 1m
-	.5					(.5m) Pocket penetrometer: 1.4, 1.3	
-	.6		bag 1			(.6m) Pocket penetrometer: 1.3	
—1	1		.9m			(1m) hit brown and rocky	Bucket 2
-	1.1					(1.1m) turns brown, gravelly, very stiff	1m - 2m
-						(1.5) brown and crumbly	
-			bag 2			(1.7m) very crumbly, still brown,	
-	1.7		1.6m			aggregate w/in	
—2							
-	2.1		bag 3			(2.1m) slightly more moist, less	
-			2.1m			crumbly, brown clay	
-	2.6		bag 4			(2.6m) stiff, brown, crumbly	
-			2.6m				
—3							
-	3.2		bag 5				Bucket 3
-			3.2m				3.4m - 4.2 m
-							
-							
—4							
-	4.2		bag 6			(4.2m) still no water table	
-			4.2m				
-							
-	4.8					(4.8m) large aggregate, sometimes very	
—5						moist but not water table yet	
-							
-							
-							
-							

APPENDIX C

PLANS AND SPECIAL PROVISIONS

FOR CONSTRUCTION OF DRAINED AND UNDRAINED

TEST SECTIONS

AT RICHMOND FIELD STATION

Dynatest

DYNATEST CONSULTING, INC.

Post Office Box 71
Ojai California 93024-0071, U.S.A.
Telephone (805) 646-2230
Fax (805) 640-0345

Pavement Evaluation
and Management
Services

Engineering,
Methodology and
Equipment

INVITATION TO BID

Attached are plans and specifications for the construction of two research pavement test areas and associated work at the University of California Berkeley Richmond Field Station at Richmond, CA. Each test area will be approximately 98.4 ft. X 24.6 ft. You are invited to submit a price proposal to perform this work. It is anticipated that the site will be available for construction activities between 27 February and 14 March, 1995.

Site Inspection:

The site representative is Mr. Ed Diaz (510) 231-9560, who can be contacted for site inspections. Clean copies of the plans and specifications are available from Mr. Diaz.

Bid Due Date:

22 February, 1995
12:00 noon

Submit Bids To:

N.F. Coetzee
Dynatest Consulting, Inc.
P.O. Box 71
209 Bald Street
Ojai, CA 93023

Dynatest, Inc.
209 Bald Street, P.O. Box 71
Ojai, CA 93023
Tel. (805) 646 2230
Fax (805) 640 0345

10 February, 1995

Memorandum

Subject: Site Work for HVS Study Test Job - Description of Test Pads 1 and 2

Intent of Project: The intent of the test pads is to duplicate actual freeway paving so that the tests duplicate as closely as possible the effects of trafficking on in-service pavements.

Site Conditions: The site is located at the University of California at Berkeley Richmond Field Station, at 1353 South 46th Street, Richmond, California. The test pads are to be constructed inside a large pole building (Building 280 also known as the "fog chamber") covered with tin sheets. The nominal width of the building inside the poles is 9 m (29.5 ft), and the nominal length is 99 m (325 ft). There are several roll-up doors along the west side of the building, as shown on the plan.

Office and shops are located at the south end of the building. The height of the building in the test pad area at the south end of the building is approximately 9 m (30 ft), measured from the existing subbase to the rafter. The roof line slopes downward from south to north. At the north end the building is open, and the height of the building is approximately 4.2 m (13.6 ft) from the surface to the rafter.

Access to Field Station is through a gate on Regatta Boulevard at the northwest corner of the field station. Construction traffic shall use a gravel surfaced road between the gate and the test pad area inside the building, approximately 215 m (700 ft) in length.

1. Two test areas shall be constructed according to sections described below. Each section to be 30 m (98.4 ft) in length and approximately 7.5 m (24.6 ft) in width. All work shall conform to the standard plans and specifications of the State of California Department of Transportation, July 1992 editions, except as modified or supplemented by these special provisions.

2. Contractor shall grade and compact existing ASB in sections A, B, and 2-3A. Existing AC surface will be removed and off-hauled between stations 2+00 and 2+17. Existing ASB to be graded to an elevation of 0.91 ft at the point of station 0+20 at 0.3 ft

from face of east pole line, and to be compacted to Caltrans standard specifications for ASB. Excess subbase material shall be spread uniformly on the access road, graded and rolled. Full compensation shall be considered as included in various items of work and no additional payment allowed.

3. Unsuitable material encountered below the existing ASB grade-line shall be excavated and off-hauled as directed by the owner. Unsuitable material is defined as per section 19-2.02 of the standard specifications. Excavated areas shall be replaced with excess ASB, graded and rolled. Full compensation for furnishing all labor, equipment, materials, tools and other costs and items necessary shall be considered included in the unit cost paid for excavation and replacement of unsuitable material below the existing ASB grade-line.

4. Contractor shall furnish and place temporary railing (Type K) on the graded and compacted subbase, along the east and west walls for all of Sections A, B, 2-3A and 2-3B. The total length of temporary railing (K-type) is 158.5 m (520 ft) Temporary railing (Type K) shall be 6.1 m (20 ft) per unit. Temporary railing (Type K) to be placed 0.2 m (0.3 ft) from the existing structural poles on the east side of the building and from the existing structural poles and electrical transformer at Sta 47.5 on the west side of the building, flush with each other to provide smooth curbs along the sides of the building and the abutted rail ends shall bolted as shown on the plan. All temporary railing (Type K) shall be staked from behind to prevent sliding on the subbase as shown on the plan. A lump sum payment shall be made for the temporary railing (Type K), including transportation and placement.

5. Contractor shall furnish and place Class 2 AB. The compacted AB shall maintain the 2 percent cross slope of the ASB layer across the full width of sections A and B, and the 0.75 percent longitudinal slope across the full length of sections A and B.

6. Contractor shall furnish and install drainage system along inside of east side temporary railing (Type K) between stations 0+12 and 2+21.8 following standard plan D99A Type 5.

   a. Drainage cleanout shall be installed at station 2+21.8, and pass to the outside of the temporary railing (Type K) following standard plan D99C Type I Cleanout with Alternative I plastic pipe plug.

   b. Edge drain outlet shall be installed at station 0+12. Outlet shall consist of a 90° elbow at the end of the edge drain, passing through the temporary railing (Type K)

7. All grading shall be done with electronic control (ie laser/cross slope stringline/cross slope).

8. Contractor shall pave ATPB and asphalt concrete with solid extendable screed with electronic cross slope control.

9. Contractor shall pave each ATPB and asphalt concrete layer in two passes, maintaining the 2 percent cross slope of the AB and ASB layers across the full width of sections A and B, and the 0.75 percent longitudinal slope across the full length of sections A and B. The asphalt mat width for any pass shall be not less than 12.05 ft nor more than 12.55 ft.

Compacted lift thicknesses shall be as follows:

a. Section A bottom lift asphalt concrete 0.28 ft, middle lift asphalt concrete 0.18 ft, top lift asphalt concrete 0.17 ft.

b. Section B one lift ATPB 0.25 ft, bottom lift asphalt concrete 0.15 ft, middle lift asphalt concrete 0.18 ft, top lift asphalt concrete 0.17 ft.

10. Contractor shall furnish asphalt concrete meeting Caltrans specifications for 3/4 in. maximum, medium grading, Type A asphalt concrete.

11. Construction inspection and testing shall be performed by Contra Costa County. Compaction testing will be performed using Test Method No. Calif. 231.

12. For ease of construction, material layer thicknesses may vary within the transition zone between Sections A and B, Sta 1+15.2 to 1+21.7.

13. Contractor shall furnish samples of AB, AC and ATPB for lab testing. Contractor shall provide AB 135 kg (300 lbs), AC 365 kg (800 lbs), and ATPB 365 kg (800 lbs) to UC-Berkeley for research testing. Sampling to be performed during construction, as arranged between owner and contractor.

14. The contractor shall make the necessary arrangements to ensure that all paving and rolling equipment is clean of dirt and mud and will not contaminate the AC paving.

15. Full compensation for furnishing all labor equipment, materials, tools and other costs and items necessary for the complete placement of asphalt concrete, asphalt treated permeable base and aggregate base shall be considered included in the unit cost paid for AC, ATPB and AB.

16. Longitudinal joints are to be offset between 0.3 and 0.5 ft from underlying paving joints.

17. Full compensation shall for costs of labor, equipment, material, tools and other costs and items incurred due to delays caused by the owner performing testing other than inspection testing after completion of ASB and AB layers shall be considered included in the unit cost of standby time and no additional payment will be considered. Standby time will be calculated in minimum increments of 0.5 hours. Standby time shall not be paid except between the hours of 7 am and 5 pm, and a maximum of 4 hours standby time shall be paid for any day.

Summaryof bid items

Grade and compact ASB as per item 2 I95
(estimated quantity of excess ASB is ~~159~~),
Lump Sum:

Excavate unsuitable material. as per item 3,
Cost per square yard:

Furnish and place temporary railing
(Type K) as per item 4, (estimated
quantity of railing is 520 ft), Lump Sum:

Furnish and install drainage as per
item 6 (estimated length is 210 ft),
Lump Sum:

Furnish and place AB
(estimated quantity is 325 tons),
Cost per ton:

Furnish and place ATPB
(estimated quantity is 36 tons),
Cost per ton:

Furnish and place AC
(estimated quantity is 215 tons),
Cost per ton:

Standby time as per item 17,
Cost per hour:

HVS Study Test Pads Description

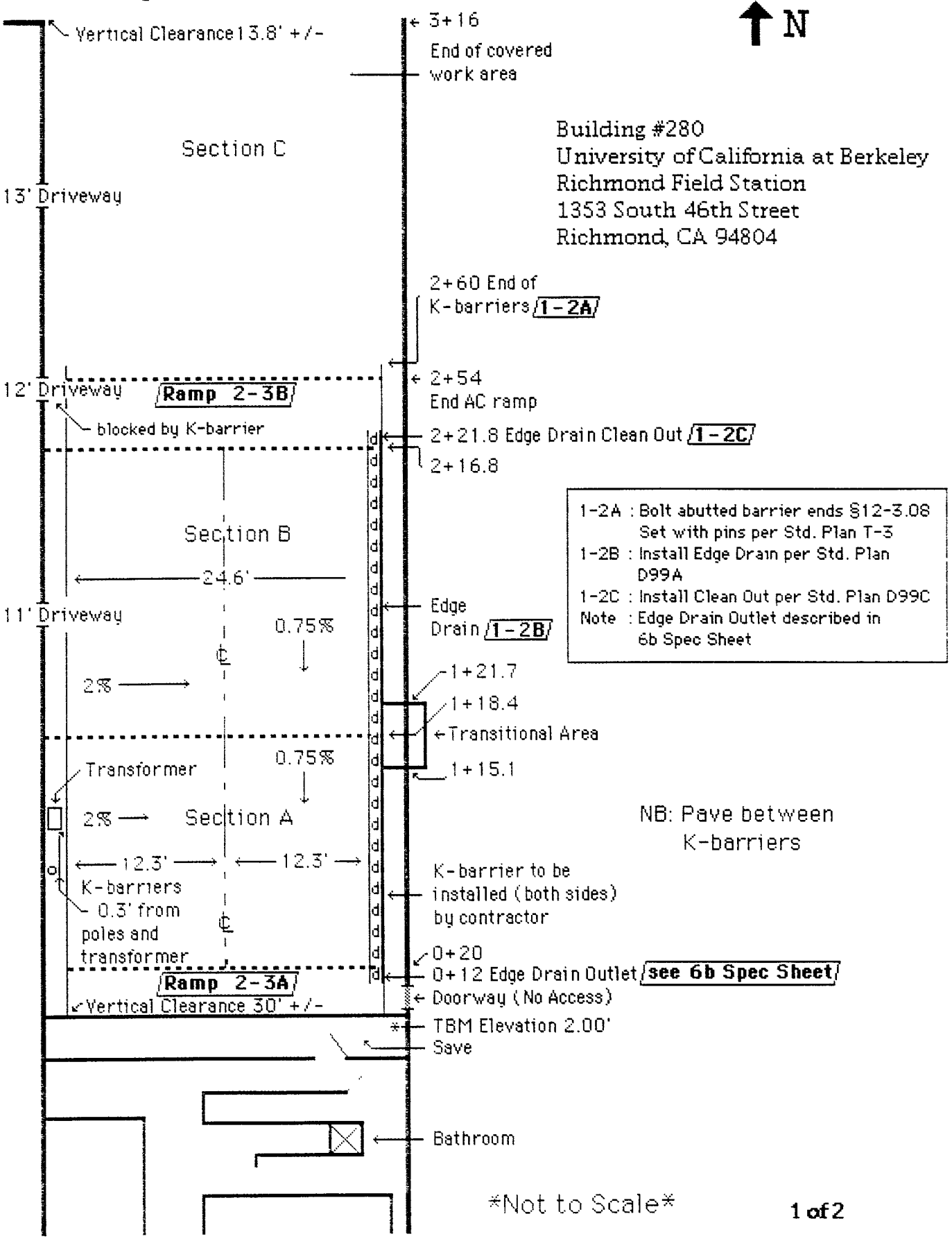

1) Tolerances ASB +/- 0.08
§25-1.05
AB +/- 0.05 §26-1.05
ATPB +/- 0.05 §29-1.05
AC 12' straightedge 0.01-longitude
0.02-transverse
§39-6.03

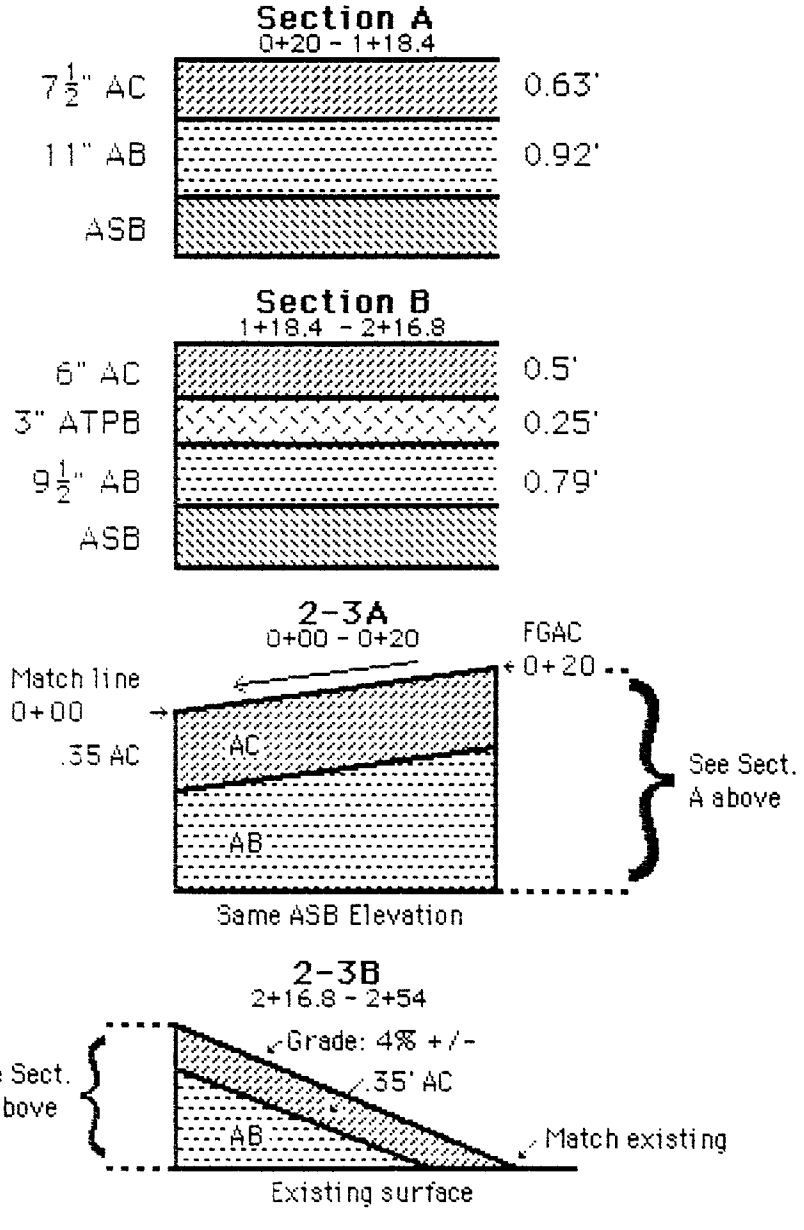

Not to Scale

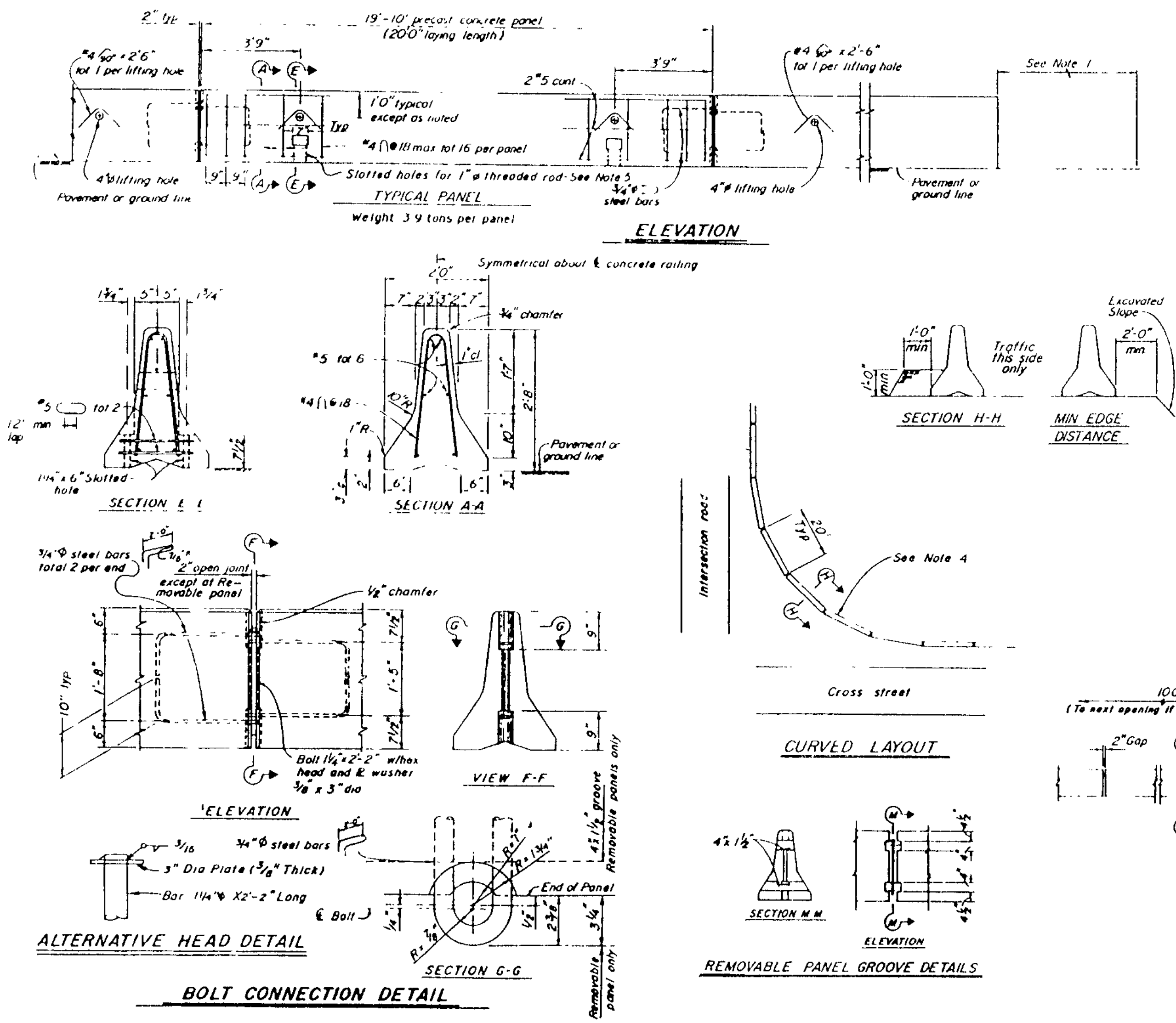

NOTES:

1. For end treatment, layout and crash cushions, where needed, see Project Plans or Special Provisions.
2. All 3½" gaps at removable panels are to be backed at the base with # 8x10" dowel or 1" ø pin each side of joint. See Section K K.
3. Alternative details for lifting the precast concrete panels of the Temporary Railing may be submitted by the Contractor for the Engineer's approval.
4. Where Temporary Railing (Type K) is placed on curves and radii that are too severe to connect panels with bolted joints, the railing is to be backed continuously with earth fill. See Section H-H.
5. Attach units to deck slabs when required by Bridge Plans

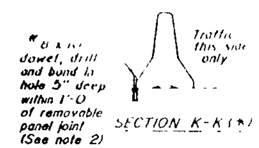

* Section K-K is for PCC pavement. Alternative detail, 1" ø pins 2'-0" long driven in AC or firm soil permitted minimum 1'-6" deep

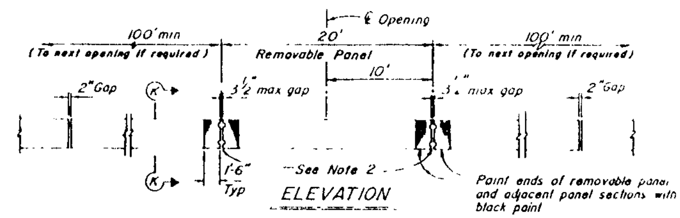

TYPICAL OPENING DETAIL

STATE OF CALIFORNIA
DEPARTMENT OF TRANSPORTATION

TEMPORARY RAILING (TYPE K)

STD. PLAN T3

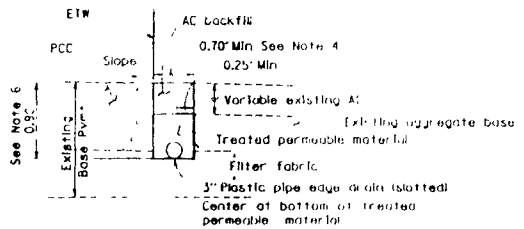

TYPE 1 STRUCTURAL SECTION DRAINAGE SYSTEM
(FOR EXISTING HIGHWAY FACILITY)

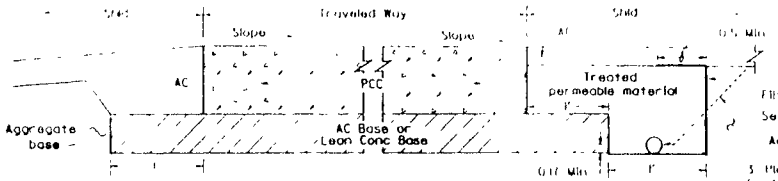

TYPE 2 STRUCTURAL SECTION DRAINAGE SYSTEM
(NEW CONSTRUCTION)

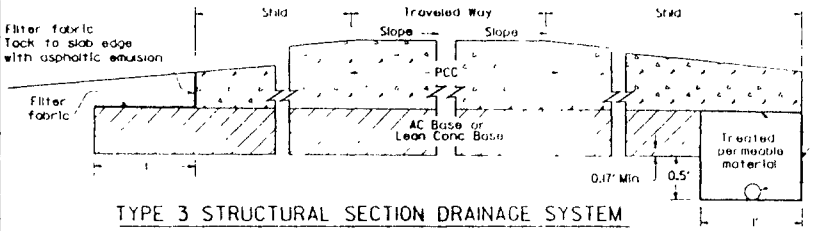

TYPE 3 STRUCTURAL SECTION DRAINAGE SYSTEM
(NEW CONSTRUCTION)

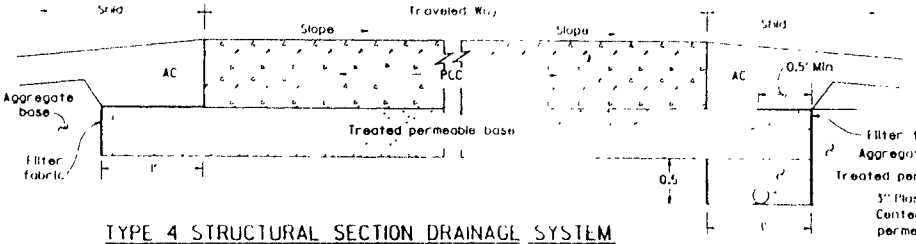

TYPE 4 STRUCTURAL SECTION DRAINAGE SYSTEM
(NEW CONSTRUCTION)

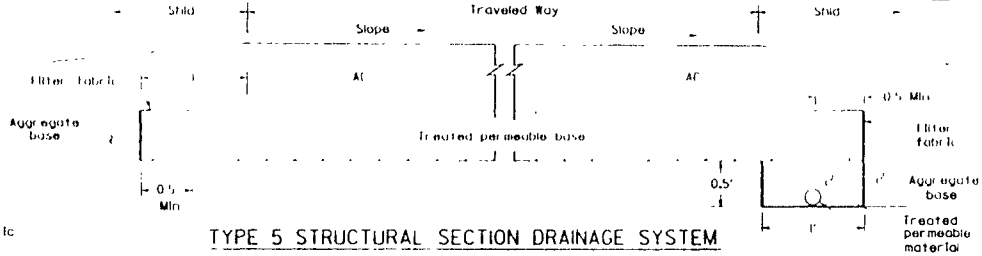

TYPE 5 STRUCTURAL SECTION DRAINAGE SYSTEM
(NEW CONSTRUCTION)

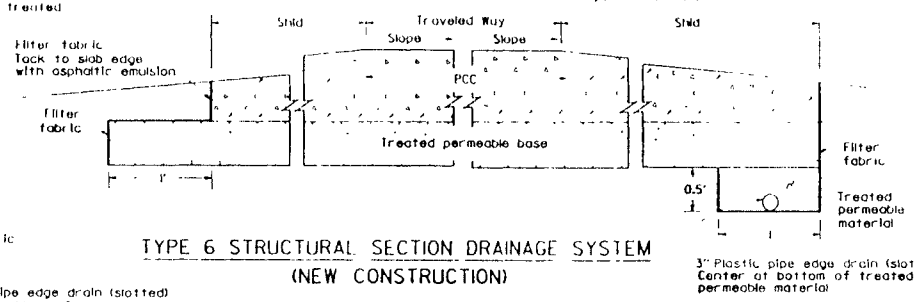

TYPE 6 STRUCTURAL SECTION DRAINAGE SYSTEM
(NEW CONSTRUCTION)

NOTES

1. At the Contractor's option, on new construction, the vertical jointline (including the filter fabric) between the treated permeable material and the shoulder base/subgrade material may be rotated about its midpoint to a slope not flatter than 1:1 as shown by the dashed lines.
2. See the project plans and typical cross sections for pavement structural section details.
3. The plan layout for structural section drainage collector and outlet systems for new portland cement concrete pavement and new asphalt concrete pavement is the same as that shown on Standard Plan D99B.
4. For plastic pipe edge drain diameter larger than 3 inches, the minimum trench width shall be equal to the outside diameter of the plastic pipe plus 4 inches.
5. For plastic pipe edge drain diameters larger than 3 inches, all details for 3" plastic pipe edge drain shall apply.
6. For pavements thicker than 9 inches, the minimum trench depth is 1.00 foot.

DIST	COUNTY	ROUTE	POST MILES TOTAL PROJECT	SHEET NO.	TOTAL SHEETS

Kenneth Y. Mori
REGISTERED CIVIL ENGINEER
July 1, 1992
PLANS APPROVAL DATE

REGISTERED PROFESSIONAL ENGINEER
K Mori
No. 14733
Exp. 3-31-93
CIVIL
STATE OF CALIFORNIA

STATE OF CALIFORNIA
DEPARTMENT OF TRANSPORTATION

STRUCTURAL SECTION DRAINAGE SYSTEM DETAILS

NO SCALE

D99A

STD. PLAN D99A

Dynatest, Inc.
209 Bald Street, P.0. Box 71
Ojai, CA 93023
Tel. (805) 646 2230
Fax (805) 640 0345

Site representatives:
Ed Diaz (510) 231 9513, John Harvey (510) 231 9513
fax (510) 231 9589

7 March, 1995

Ref: PAVEMENT RESEARCH TEST AREAS AT UNIVERSITY OF CALIFORNIA AT BERKELEY, RICHMOND FIELD STATION

Change Order No. 1

Changes to Specifications and Plans **of** 10 **February, 1995** and Previous Changes in Invitation to Bid of 21 February, 1995

2. Contractor shall grade and compact existing ASB in sections A, B and 2-3A. Existing AC surface will be removed and **off-hauled** between stations 2+00 and 2+17. Existing ASB to be graded to an elevation of 1.09 ft at the point of station 0+20 at 0.3 ft from face of east pole line, and to be compacted to Caltrans standard specifications for ASB. Excess subbase material shall **be** spread uniformly on the access road and in the intermediate areas between the building and the access road as directed by the site representative, graded and rolled. Full compensation shall be considered as included in various items of work and no additional payment allowed.

3. Unsuitable material encountered below the existing ASB line shall be excavated and off-hauled as directed **by the owner.** Unsuitable material is defined as per section 19-2.02 of the standard specifications. Excavated areas shall be replaced with excess ASB, graded and compacted. **Full** compensation for furnishing all labor, equipment, materials, tools and other **costs** and items necessary shall be considered included in the unit cost paid for excavation and replacement of unsuitable material below the existing ASB grade-line.

9. Contractor shall spread each ATPB and asphalt concrete layer in two longitudinal sections, maintaining the 2 percent cross slope of the AB and ASB layers across the full width **of sections A and E3,** and the 0.75 percent longitudinal slope across the full length of sections A and B. The asphalt mat width for any spread section shall be not less than 12.05 ft nor more than 12.55 ft.

Compacted lift thicknesses shall be as follows:

a. Section A bottom lift asphalt concrete 0.25 Et, top lift asphalt concrete 0.20 ft.

b. Section B one lift ATPB 0.25 ft, bottom lift asphalt concrete 0.25 ft, top lift asphalt concrete 0.20 ft.

10. Contractor shall furnish asphalt concrete meeting Caltrans specifications for 3/4 in. maximum, coarse grading, Type A asphalt concrete.

Summary of changes to bid items

Grade and compact ASB as per item 2
(estimated quantity of excess ASB is 100 tons),
Lump Sum:

Excavate and replace unsuitable material as per item 3,
Cost per square ft:

Furnish and place AB
(estimated quantity is **250** tons),
Cost per ton:

Furnish and place AC
(estimated quantity is 178 tons),
Cost per ton:

Change Order #1
7 March, 1995

HVS Study Test Pads Description

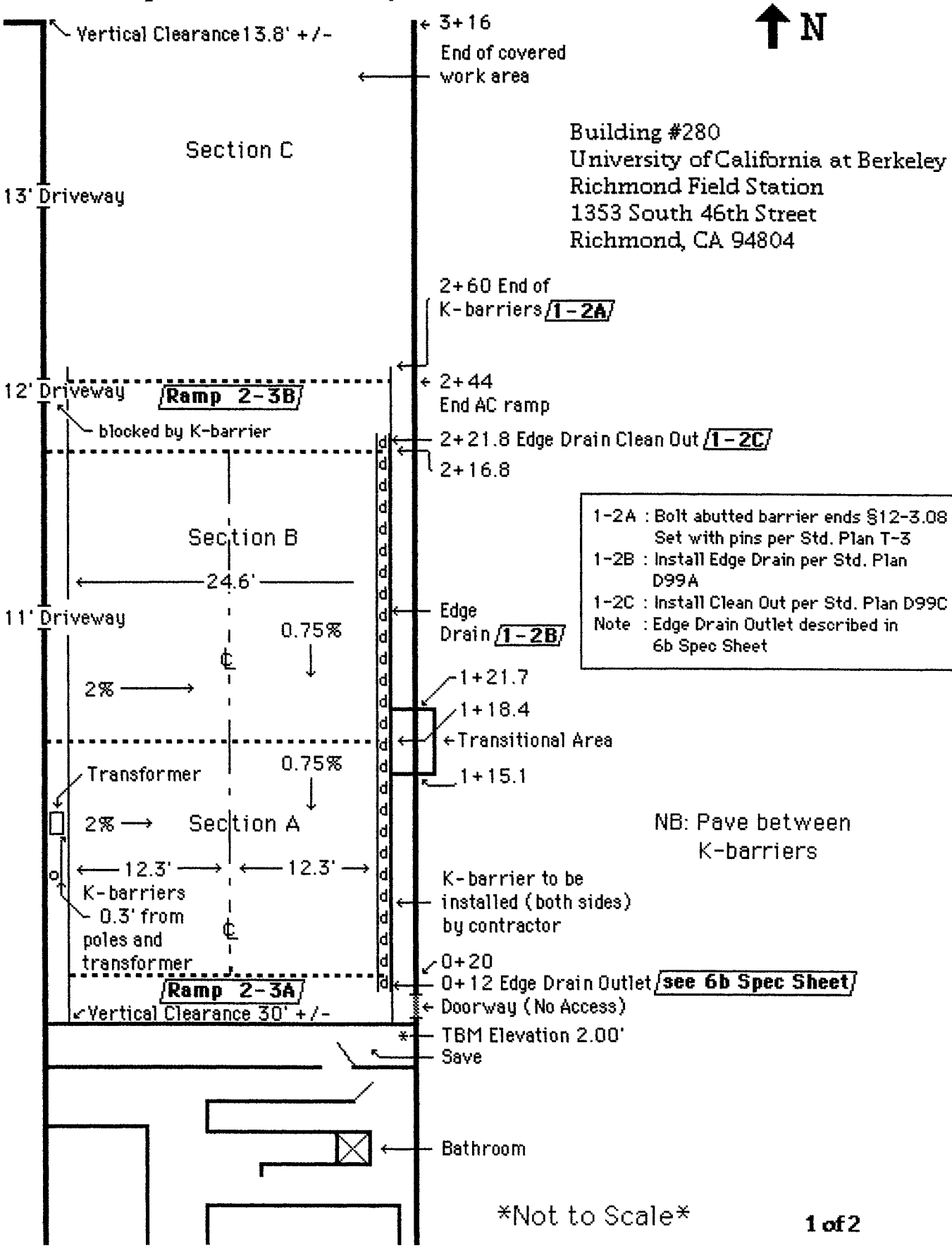

1) Tolerances ASB +/- 0.08
§25-1.05
AB +/- 0.05 §26-1.05
ATPB +/- 0.05 §29-1.05
AC 12' straightedge 0.01-longitude
0.02-transverse
§39-6.03

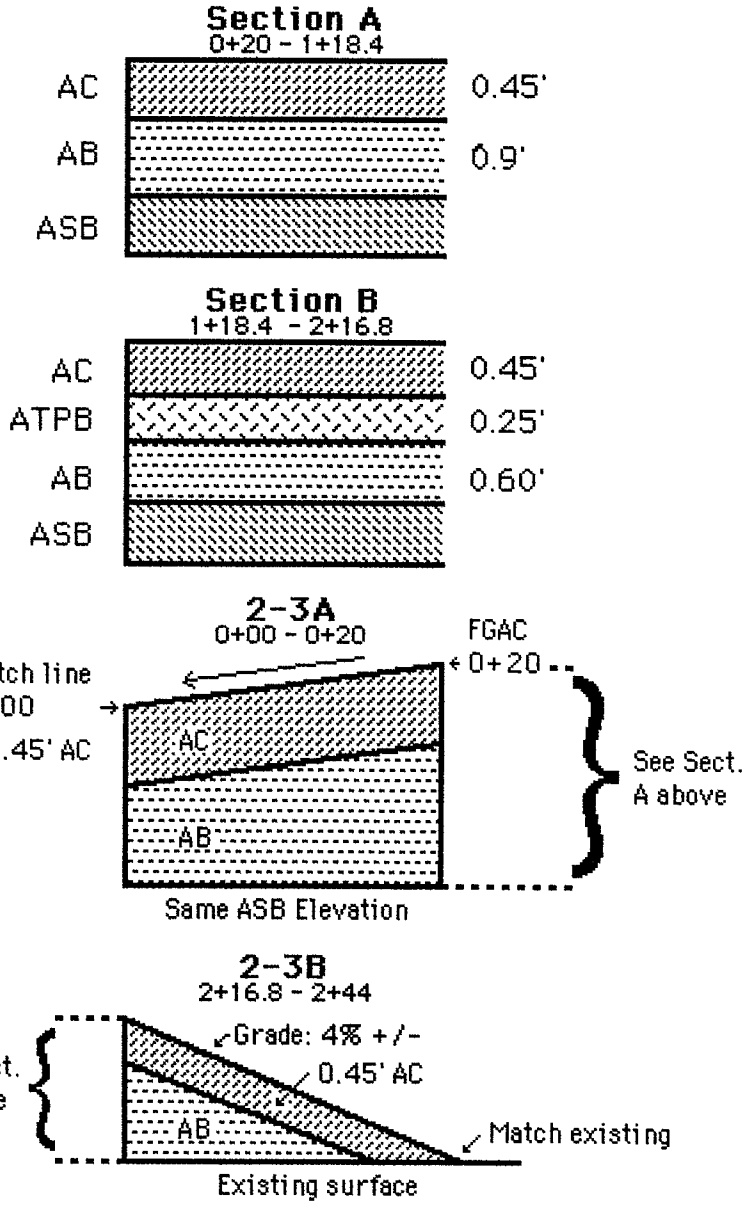

Not to Scale

APPENDIX D

TABLES OF TRIAXIAL COMPRESSION REPEATED LOAD TEST;

ESTIMATION OF RESILIENT MODULUS

Table 2. Resilient Modulus Test Results of Specim AB2.
(wet density=2.47 g/c.c.; moisture content=5.5%)

Confining Stress (kPa)	Nominal Deviator Stress (kPa)	As-compacted			After saturation		
		Actual deviator Stress (kPa)	Sum of Principal Stresses (kPa)	Resilient Modulus (kPa)	Actual deviator Stress (kPa)	Sum of Principal Stresses (kPa)	Resilient Modulus (kPa)
138	14				16.6	430.6	165287
138	35				35.9	449.9	234942
138	69				71.0	485.0	313597
138	104				106.2	520.2	331245
138	138				140.7	554.7	346314
104	14				15.0	327.0	162607
104	35				37.6	349.6	211489
104	69				68.8	380.8	377364
104	104				104.3	416.3	388675
104	138				138.3	450.3	365035
69	14				15.3	222.3	239261
69	35				35.9	242.9	285507
69	69				69.6	276.6	266865
69	104				106.8	313.8	300858
35	14				16.0	121.0	155243
35	35				34.9	139.9	176398
35	69				69.0	174.0	236055
35	104				105.3	210.3	251599
6.9	14				13.8	34.5	174849
6.9	35				35.0	55.7	152736
6.9	69				62.5	83.2	213248
Regression Equations					RM=58867.8*SPS^0.2589		

Table 3. Resilient Modulus Test Results of Specim AB3.
(wet density=2.40 g/c.c.; moisture content=5.5%)

Confining Stress (kPa)	Nominal Deviator Stress (kPa)	As-compacted			After saturation		
		Actual deviator Stress (kPa)	Sum of Principal Stresses (kPa)	Resilient Modulus (kPa)	Actual deviator Stress (kPa)	Sum of Principal Stresses (kPa)	Resilient Modulus (kPa)
138	14				15.0	429.0	288412
138	35				35.7	449.7	229034
138	69				72.3	486.3	257362
138	104				107.0	521.0	284919
138	138				142.8	556.8	281553
104	14				11.9	323.9	295177
104	35				32.7	344.7	275421
104	69				59.4	371.4	252268
104	104				110.1	422.1	274575
104	138				141.9	453.9	269506
69	14				16.0	223.0	167560
69	35				35.9	242.9	198011
69	69				69.0	276.0	208921
69	104				107.8	314.8	217734
35	14				15.7	120.7	142039
35	35				33.3	138.3	124266
35	69				70.7	175.7	176697
35	104				107.6	212.6	173574
6.9	14				15.7	36.4	99388
6.9	35				32.0	52.7	101635
6.9	69				72.0	92.7	145547
Regression Equations					RM=18408.1*SPS^0.4362		

Table4. Resilient Modulus Test Results of Specim AB4.
(wet density=2.40 g/c.c.; moisture content=5.5%)

Confining Stress (kPa)	Nominal Deviator Stress (kPa)	As-compacted			After saturation		
		Actual deviator Stress (kPa)	Sum of Principal Stresses (kPa)	Resilient Modulus (kPa)	Actual deviator Stress (kPa)	Sum of Principal Stresses (kPa)	Resilient Modulus (kPa)
138	14				14.1	428.1	250799
138	35				34.4	448.4	433100
138	69				66.1	480.1	438025
138	104				105.3	519.3	414992
138	138				140.0	554.0	400434
104	14				14.7	326.7	230147
104	35				34.9	346.9	313789
104	69				64.8	376.8	338764
104	104				107.5	419.5	346850
104	138				140.7	452.7	354506
69	14				15.5	222.5	219692
69	35				34.3	241.3	254971
69	69				69.0	276.0	272545
69	104				104.9	311.9	265800
35	14				14.2	119.2	150309
35	35				34.3	139.3	173458
35	69				69.1	174.1	198415
35	104				105.0	210.0	192111
6.9	14				15.3	36.0	101522
6.9	35				35.9	56.6	146090
6.9	69				70.6	91.3	151122
Regression Equations					RM=14856.8*SPS^0.5139		

Table 5. Resilient Modulus Test Results of Specim AB5.
(wet density=2.47 g/c.c.; moisture content=5.5%)

Confining Stress (kPa)	Nominal Deviator Stress (kPa)	As-compacted			After saturation		
		Actual deviator Stress (kPa)	Sum of Principal Stresses (kPa)	Resilient Modulus (kPa)	Actual deviator Stress (kPa)	Sum of Principal Stresses (kPa)	Resilient Modulus (kPa)
138	14				16.1	430.1	253106
138	35				37.8	451.8	467711
138	69				72.8	486.8	400194
138	104				107.8	521.8	426697
138	138				141.5	555.5	418806
104	14				13.5	325.5	187716
104	35				36.3	348.3	302915
104	69				72.6	384.6	305911
104	104				108.1	420.1	319292
104	138				141.0	453.0	299424
69	14				15.1	222.1	209919
69	35				37.5	244.5	224911
69	69				70.9	277.9	214244
69	104				107.9	314.9	229117
35	14				14.8	119.8	144013
35	35				35.0	140.0	149032
35	69				70.6	175.6	150060
35	104				107.3	212.3	165040
6.9	14				14.1	34.8	78307
6.9	35				34.6	55.3	85132
6.9	69				70.6	91.3	89213
Regression Equations					RM=5766.0*SPS^0.6597		

Table 6. Resilient Modulus Test Results of Specim AB6.
(specimen subjected to dried-out for 10 days after compaction in the situation of wet density=2.47 g/c.c., moisture content=5.5%)

Confining Stress (kPa)	Nominal Deviator Stress (kPa)	As-compacted			After saturation		
		Actual deviator Stress (kPa)	Sum of Principal Stresses (kPa)	Resilient Modulus (kPa)	Actual deviator Stress (kPa)	Sum of Principal Stresses (kPa)	Resilient Modulus (kPa)
138	14				15.1	429.1	266219
138	35				34.1	448.1	525454
138	69				70.7	484.7	521258
138	104				107.3	521.3	536549
138	138				142.3	556.3	537115
104	14				11.8	323.8	207185
104	35				36.6	348.6	414280
104	69				70.3	382.3	438520
104	104				107.8	419.8	423707
104	138				142.3	454.3	416875
69	14				13.1	220.1	269158
69	35				35.9	242.9	299171
69	69				69.7	276.7	334752
69	104				106.0	313.0	323765
35	14				13.5	118.5	278130
35	35				36.8	141.8	268389
35	69				72.6	177.6	275987
35	104				107.2	212.2	306023
6.9	14				16.0	36.7	125928
6.9	35				35.2	55.9	176818
6.9	69				75.5	96.2	140121
Regression Equations					RM=21180.8*SPS^0.4896		

Table7. Resilient Modulus Test Results of Specim SB1.
(dry density=2.43 g/c.c.; moisture content=7.5%)

Confining Stress (kPa)	Nominal Deviator Stress (kPa)	As-compacted			After saturation		
		Actual deviator Stress (kPa)	Sum of Principal Stresses (kPa)	Resilient Modulus (kPa)	Actual deviator Stress (kPa)	Sum of Principal Stresses (kPa)	Resilient Modulus (kPa)
138	14				15.0	429.0	376452
138	35				35.7	449.7	347327
138	69				71.3	485.3	282454
138	104				105.5	519.5	262187
138	138				145.0	559.0	245553
104	14				15.0	327.0	209674
104	35				35.0	347.0	296418
104	69				72.0	384.0	222912
104	104				106.6	418.6	229155
104	138				142.9	454.9	226836
69	14				15.3	222.3	193255
69	35				35.9	242.9	162328
69	69				70.6	277.6	289530
69	104				107.6	314.6	170973
35	14				14.7	119.7	98424
35	35				36.8	141.8	133495
35	69				72.8	177.8	130516
35	104				109.7	214.7	129134
6.9	14				16.1	36.8	76202
6.9	35				35.4	56.1	94329
6.9	69				70.3	91.0	98443
Regression Equations					RM=8876.1*SPS^0.5529		

Table 8. Resilient Modulus Test Results of Specim SB2.
(dry density=2.43 g/c.c.; moisture content=7.5%)

Confining Stress (kPa)	Nominal Deviator Stress (kPa)	As-compacted			After saturation		
		Actual deviator Stress (kPa)	Sum of Principal Stresses (kPa)	Resilient Modulus (kPa)	Actual deviator Stress (kPa)	Sum of Principal Stresses (kPa)	Resilient Modulus (kPa)
138	14				14.7	428.7	149687
138	35				38.9	452.9	131405
138	69				71.0	485.0	197668
138	104				105.7	519.7	193547
138	138				140.5	554.5	191720
104	14				14.2	326.2	122474
104	35				35.7	347.7	127982
104	69				70.6	382.6	131341
104	104				106.6	418.6	149282
104	138				142.2	454.2	143332
69	14				16.9	223.9	75317
69	35				35.2	242.2	92750
69	69				73.1	280.1	101750
69	104				105.0	312.0	116621
35	14				15.0	120.0	64713
35	35				35.7	140.7	79345
35	69				70.2	175.2	88873
35	104				110.4	215.4	104306
6.9	14				15.1	35.8	57348
6.9	35				36.2	56.9	71240
6.9	69				71.0	91.7	89700
Regression Equations					RM=10654.6*SPS^04268		

APPENDIX E:

CHARACTERIZATION OF UNBOUND LAYERS OF THE FIRST TEST PAVEMENTS OF THE CAL / APT PROGRAM USING THE DYNAMIC CONE PENETROMETER

INTRODUCTION

The work described in this Appendix was undertaken to characterize the unbound materials used in the first CAL / APT test section pavement and provides additional information to material contained in Chapter 4. In addition, it provides background on the use of the Dynamic Cone Penetrometer (DCP) together with the interpretation of the data obtained with the equipment. This investigation was undertaken to assist in the quantification of the quality, and structural behavior of the subgrade, subbase and aggregate base material using the DCP and to assess its potential applicability as an additional tool for use by Caltrans.

The DCP instrument measures the penetration per blow into a pavement through all the different layers under constant loading. The penetration rate is a function of the in-situ shear strength of the material. The profile in depth thereof gives an indication of the in-situ properties of the materials in each of the pavement layers up to the depth of 800mm. The DCP design approach is in principle similar in principle to the CBR approach in that over-stressing of lower layers is prevented through a balance increase in layer strength from the subgrade up.

The DCP is used to measure the rate of penetration through the various layers of a pavement at in-situ material conditions. Nevertheless, both the CBR and DCP component (layer by layer) analysis methods are empirically based on material shear strength and can only be accurate if used for the evaluation and analysis of pavements similar to those from which they were derived.

OBJECTIVES AND SCOPE

The objectives of this Appendix are to:

- provide background information on the principles of the DCP evaluation and the rehabilitation design method;
- to report on a DCP investigation which was conducted on the HVS test sections pavement at the RFS.
- to report on the analysis done on the DCP data.

Although the analysis may be used to produce design options on new, or rehabilitation strategies on an existing pavement (*1 & 2*), it is not the aim of this investigation. It will, nevertheless produce information useful for understanding the structural behavior of the existing pavement, and together with other design tools such as R value and Elastic Surface Deflection investigations, can produce a sound platform to successfully predict pavement performance.

SOME BACKGROUND ON DCP DEVELOPMENT

Results from more than 58 Heavy Vehicle Simulator (HVS) tests performed on granular base pavements, and approximately 10 HVS tests on stabilized base pavements were used to verify these concepts and to establish remaining expected pavement life versus DCP penetration curves, for pavements with both base types.

The DCP method aims to achieve a balanced pavement design and to optimize utilization of the in-situ pavement material strength. This is done through the design of a pavement capable of carrying the expected future traffic and by comparing the existing pavement DCP properties with that of the design pavement.

The DCP method is however exceptional in that it incorporates an economical and easy-to-use non-destructive test which measures in-situ material properties. Emanating from the work on DCP was the DCP suite of computer analysis programs, designed to facilitate analysis of DCP data. The DCP programs are based on work done by Kleyn (*3*) and subsequent work undertaken by de Beer (*4*). The most important aspect of the latest work is the development of a DCP classification system and determination of the structural capacity (*5*).

To meet the need to successfully analyze and present DCP data in a easy to see, graphical manner, the Division of Roads and Transport Technology (DRTT) of the CSIR developed a PC based computer package (*6*).

BASIC ASSUMPTIONS

In order to understand and interpret the analysis, a basic understanding of the limitations and assumptions of the DCP pavement analysis method is necessary.

Methods using the pavement component analysis approach are based on empirical correlations between material test and expected measurements of an empirically defined material property such as the CBR or DCP measurements to evaluate pavement behavior. Relationships between the measured material property, pavement composition, traffic loading and minimum

cover requirement are used to evaluate the existing pavement, and to determine the structural requirements suitable for a specific traffic loading to design adequate rehabilitation options for the pavement.

ADVANTAGES

In spite of all limitations regarding the use of empirically derived methods, their are a number of considerations which make the DCP method extremely attractive:

- the DCP is an inexpensive portable instrument which can easily be used;
- the method makes the minimum use of laboratory tests which are very often not highly correlated to real field performance, and
- the DCP method is a practical alternative or supplement to deflection measurements as a method of evaluating existing pavements.

The following assumptions are applicable to the DCP empirical design tool:

- the bearing capacity (pavement life) of the pavement in terms of the accumulative traffic loading is a function of the properties of the material measured in the DCP test;
- the thickness of a required overlay is a function of the measured material property of existing pavement layers, as well as the expected future traffic loading;
- acceptable pavement behavior is a function of a tolerable level of the material property measured by the DCP test, and

- the cover requirement of the existing pavement structure is independent of the cover requirement of individual pavement layers within the structure, or the cover requirement of any one layer in the existing pavement is independent of the material properties in other pavement layers.

BASIC CONCEPTS

The DCP consists of a steel rod with a 60° cone fixed to the one end. A 8kg steel hammer which is dropped a vertical distance of 575mm onto an anvil. Figure E1 illustrates a schematic diagram of the DCP tool. The energy released by the drop of the hammer forces the DCP shaft to penetrate into the soil and the penetration is measured at a certain amount of hammer blows. This allows for the calculation of the rate of penetration which is an indication of the shear strength or bearing capacity of layer material with depth.

For DCP data to be evaluated and put to use, the penetration rates should be related to known soil parameters. Primarily the penetration data is used to determine standard DCP parameters which can be related to soil parameters such as, the California Bearing Ratio (CBR), the Unconfined Compressive Strength (UCS) and the effective elastic moduli (Eeff). These relationships were determined from empirical correlations between these soil parameters and DCP data.

DCP Terminology and definitions

The DCP design method makes use of many terms to describe the data, the analysis methodology as well as the output from the analysis. Some of these terms need explanation to ensure good understanding of the design method.

DCP field curve

The DCP field curve is a visual representation of the progress of penetration of the DCP through the pavement as shown in Figure E2.

DCP number (DN)

The DCP number (DN) is defined as the penetration rate of the instrument through a specific pavement layer as measured in *mm per blow*. The DN of a pavement layer is visually represented by the slope of penetration as shown in Figure E3.

The layer-strength diagram

The layer strength diagram is derived from the DCP curve and is a visual representation of the DN in-depth through the pavement structure as shown in Figure E3. DCP penetration has been calibrated against CBR and UCS values.

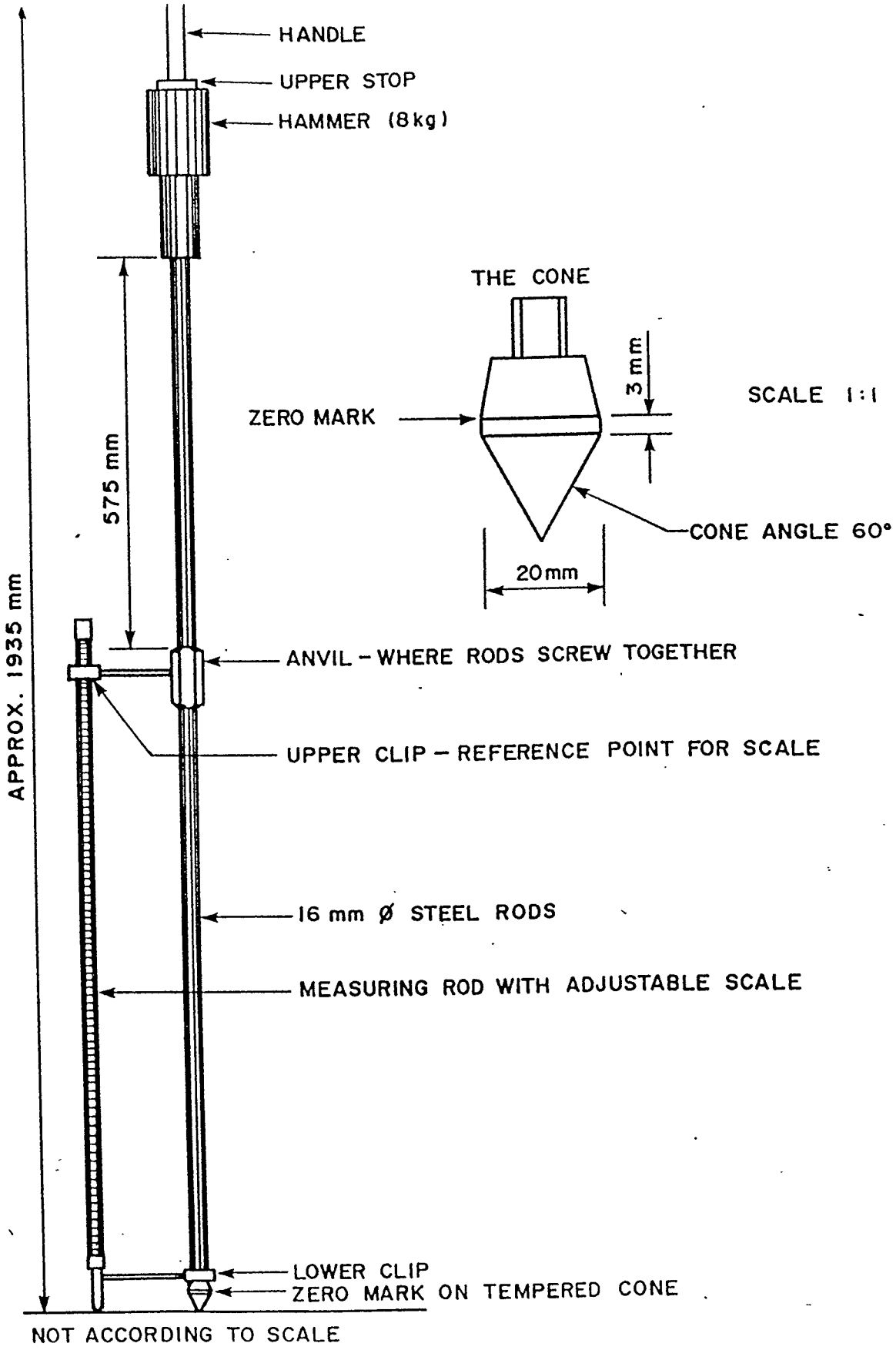

FIGURE E1: SCHEMATIC DIAGRAM OF THE DYNAMIC CONE PENETROMETER

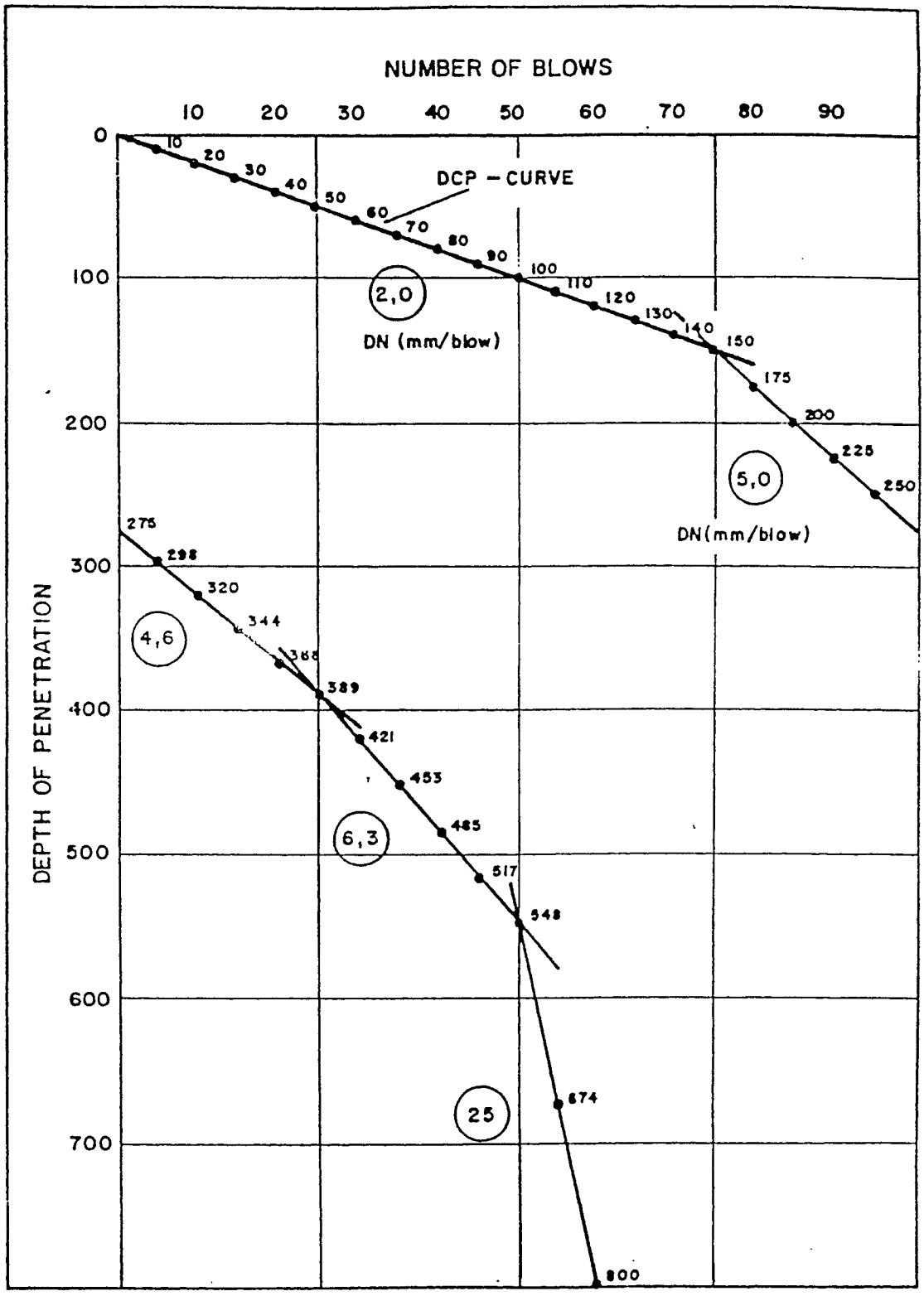

FIGURE E2: EXAMPLE OF A DCP FIELD CURVE

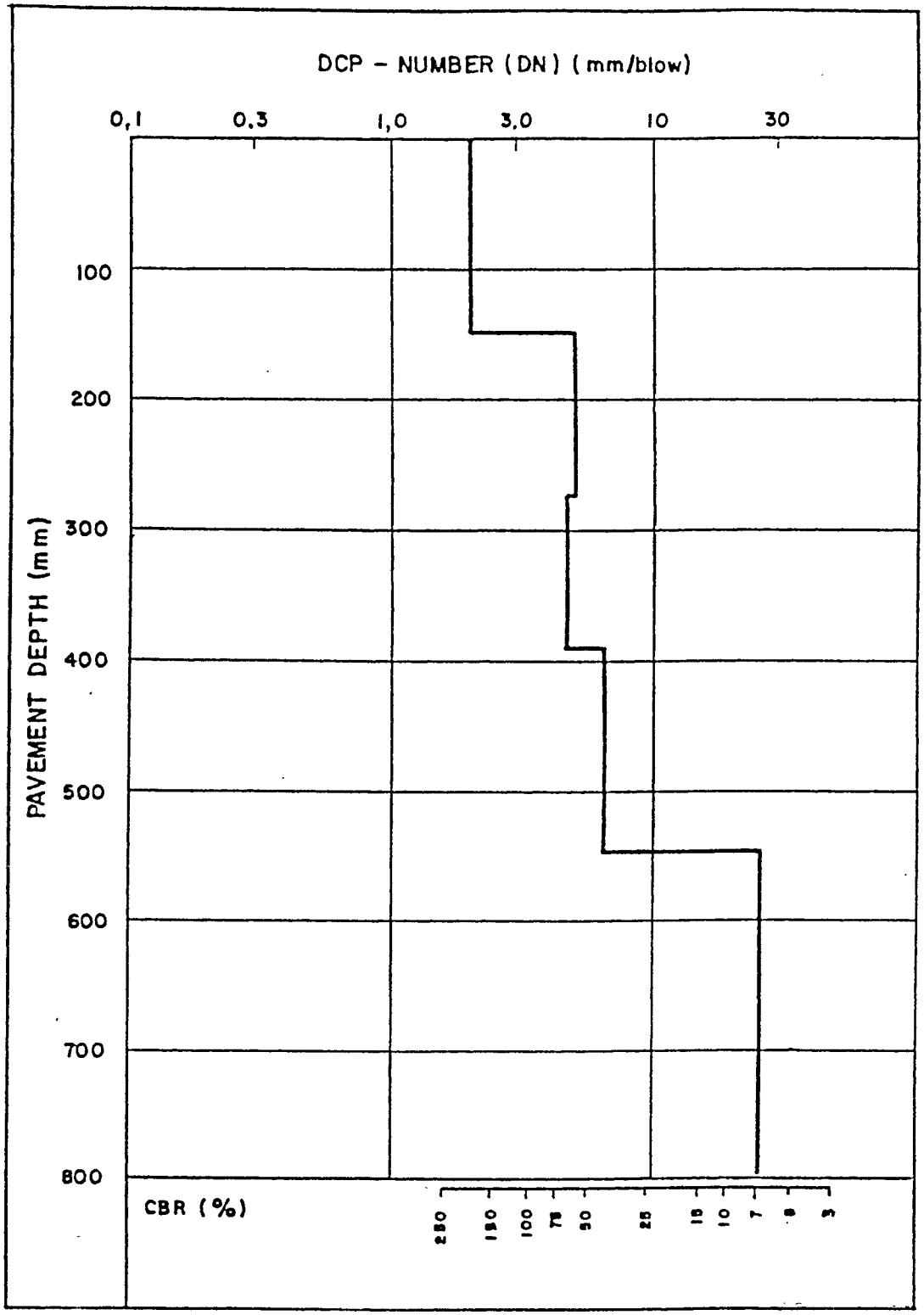

FIGURE E3: AN EXAMPLE OF THE PENETRATION RATE OF THE DCP (DN NUMBER)

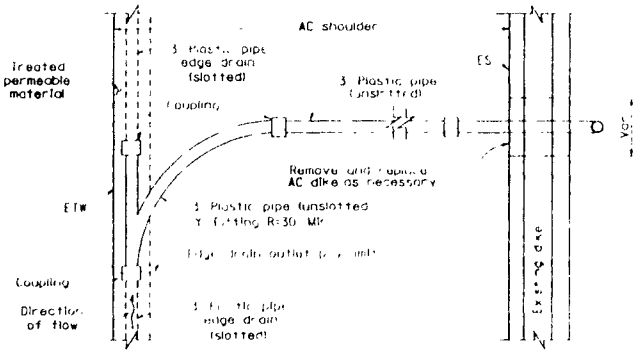

TYPE 1 CLEANOUT
PLAN VIEW
See Note 2

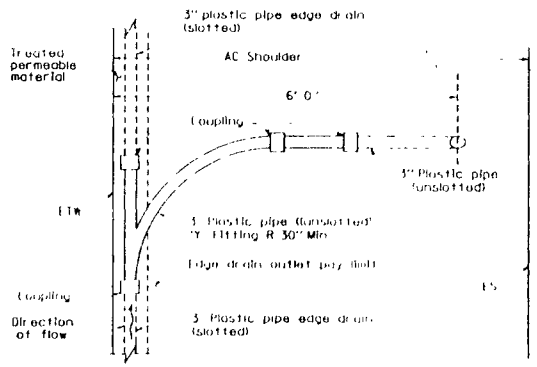

TYPE 2 CLEANOUT
PLAN VIEW
See Note 2

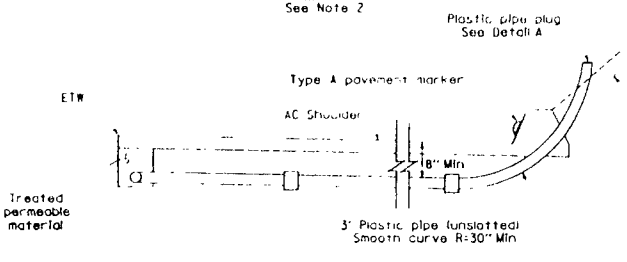

TYPE 1 CLEANOUT
ELEVATION

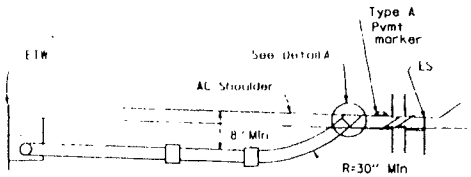

TYPE 2 CLEANOUT
ELEVATION

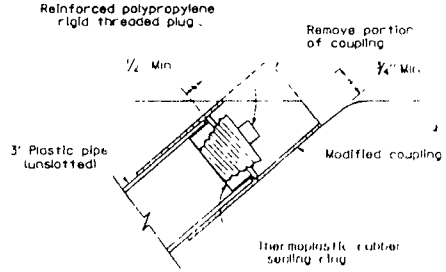

ALTERNATIVE 1

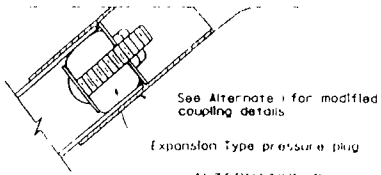

ALTERNATIVE 2

DETAIL A
PLASTIC PIPE PLUG
See Note 3

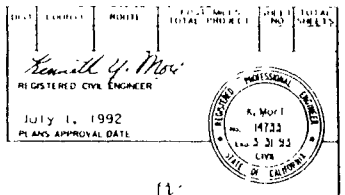

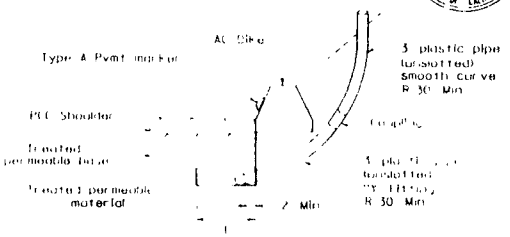

TYPE 3 CLEANOUT/TYPE G VENT
SECTION A-A

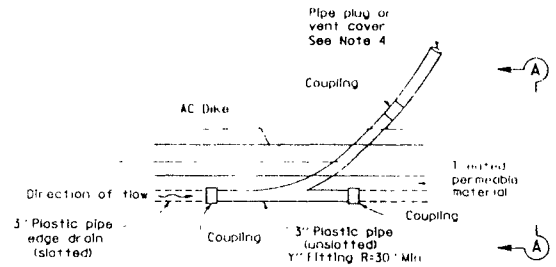

TYPE 3 CLEANOUT/TYPE G VENT
PLAN VIEW
See Note 4

NOTES

1. See project plans for location and type of cleanout or vent installations.
2. The position of slotted plastic pipe and limits of treated permeable material shown are for the Type 1 structural section drainage system shown on Standard Plan D99A.
3. Other types of plugs may be substituted with the Engineer's approval.
4. The Type 3 Cleanout and Type G Vent is for use with Portland Cement Concrete shoulders. The Type 6 structural section drainage system from Standard Plan D99A is shown. Use plastic pipe plug shown in Detail A with Type 3 Cleanouts. Use vent cover shown on Standard Plan D99B with Type G Vents.

STATE OF CALIFORNIA
DEPARTMENT OF TRANSPORTATION

EDGE DRAIN CLEANOUT AND VENT DETAILS

NO SCALE

D99C

STD. PLAN D99C

The DCP structure number

The DCP structure number is the number of DCP blows required to penetrate through a pavement structure or pavement layer. For example, the DSN_{800} of the pavement is the number of blows required to penetrate the pavement to a depth of 800mm.

Pavement strength-balance

The number of DCP blows required to reach a certain depth, expressed as a percentage of the number of DCP blows needed to penetrate the pavement to a depth of 800mm, is defined as the *Balance Number* (BN) at that depth. For example BN_{100} is the number of blows required to reach a depth of 100mm as a percentage of the blows required to reach 800mm in depth. Therefore the balance number represents the percentage of the "DCP strength" of the pavement at a certain depth.

Pavements with a high BN_{100} number (in the order of 80) are considered to be shallow pavements, which means that 80 per cent of the total energy exerted on the pavement causes a penetration of only 100mm. In real terms it means that 80 per cent of the structural strength of the pavement is provided though the top 100mm (see Figure E4)

Pavements with a low BN_{100} number (in the order of 20) are considered to be deep pavements where only 20 per cent of the structural strength is provided through the top 100 mm.

A plot of BN with depth, as shown in Figure E5 gives an indication of the strength-balance of the pavement. The figure contains a series of curves representing balanced pavements with BN_{100} values of 12.5, 15, 20, 30, 40, 50, 60, 70, 80. Note that a BN_{100} of 12,5 is effectively the Boussinesq type homogeneous stratum.

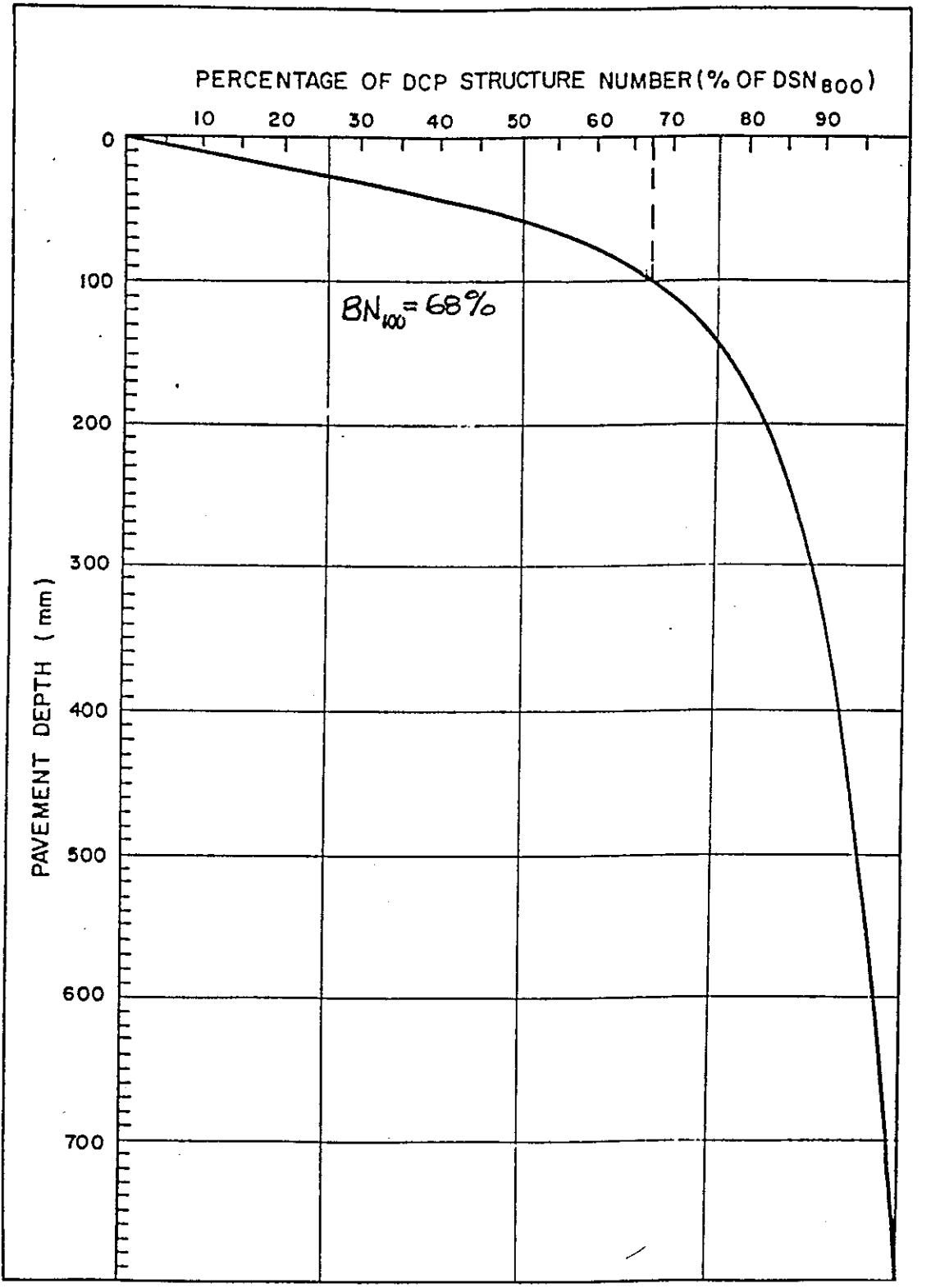

FIGURE E4: A PLOT OF THE BALANCE NUMBER (BN) WITH PAVEMENT DEPTH

Thus a shallow pavement is composed of one or two thin strong and rather rigid upper layers with rapidly diminishing support at depth from the underlying material (such as a cement treated base coarse on top of a poorly compacted natural gravel sub layer). A deep pavement will tend to be composed of a number of rather less rigid layers of relatively equal strength, affording generous support at depth. Examples of this are full depth natural or cemented materials.

Real field data seldom produce such smooth curves as shown if Figure E4. Pavements normally exhibit areas of stress concentrations which cause deviations from the smooth balanced lines. Pavements with a smooth strength-balance curve are considered to be in a state of strength balance.

Pavement strength-balance classification system

Pavement behavior can be described in terms of the strength balance of a pavement. In order to quantify the strength-balance classification of existing pavements, a strength-balance classification system was developed (5), According to this classification system a pavement is classified in terms of a Balance curve (B) which is the strength-balance curve most closely following the measured balance curve of the pavement and the Deviation (A) between the Standard Pavement Balance Curve (SPBC) and the measured curve. Figure E5 gives a collection of SPBCs for B-values ranging between -90 and +90.

During the development of the pavement strength-balance equations, a very handy formulation, describing the relation between the pavement structure number, DSN in percentages, the pavement depth, D in percentages of total depth (total depth being 800mm), and a parameter B, describing the SPBCs, where obtained. According to this formulation, there are, in theory, an

infinite number of SPBCs for pavement structures and this is used as a basis for the pavement strength-balance classification system. The formula is given below:

$$DSN\ (\%) = \frac{D \times [400 \times B + (100 - B)^2}{4 \times B \times D + (100 - B)^2}$$

Where :

= pavement structure number (as a percentage of total blows to penetrate 800 mm)

B = parameter, defining the standard the SPBC

D = pavement depth (as a percentage)

A graphical presentation of this formula is given i Figure E5. If B = 0, the balance is a straight line from DSN = 0% to DSN = 100%. A large value of B indicates a shallow pavement structure. The parameter of B, in theory, varies from - 4 to + 4, which ultimately defines all possible cases of SPBCs.

It is also possible to have negative values of B (B < 0). The SPBCs where B < 0 are a mirror image of the SPBCs where B > 0. Pavements behaving in this manner are considered to be inverted pavements, which means that the top layers are structurally weaker than the bottom layers. A granular base pavement build on bedrock is an example of this type.

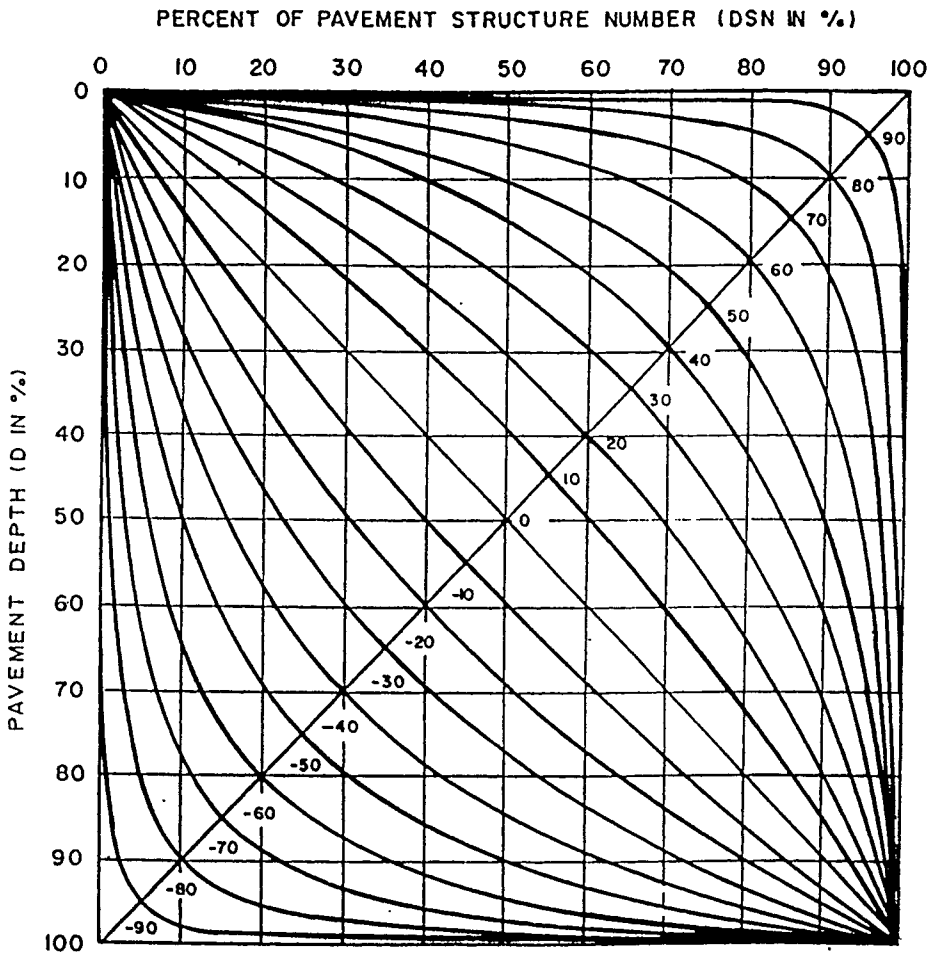

FIGURE E5: A COLLECTION OF SPBCs

(-90 ≤ B ≤ + 90)

A further requirement for a universal classification system is that the state of the balance of the pavement structure has to be quantified because most real pavements are not perfectly balanced. In order to quantify the deviation in the strength-balance of real pavements from standard pavement strength-balance curves (SPBCs), *the deviation (area)* between the best fit SPBC for the data, and the actual data (DSN data) are used for this purpose. In Figure E6 the method for calculating this deviation in terms of the area Ai is illustrated.

Figure E7 also indicates that the best fit SPBC for the given data is where B = 30. The best fit SPBC is then obtained by calculating the total area, A, between the various SPBCs and the true data, and finally selecting the SPBC where this area A is at a minimum (analogy to the least square dimension technique). For a perfectly strength-balanced pavement the area A = 0. This means that the deviation area between the true DCP data and the best fit SPBC of that data is equal to zero.

In summary, the Standard Balance Curve (B) value and the Deviation (A), a pavement can be classified as shown in Table E1 and illustrated in Figure E7.

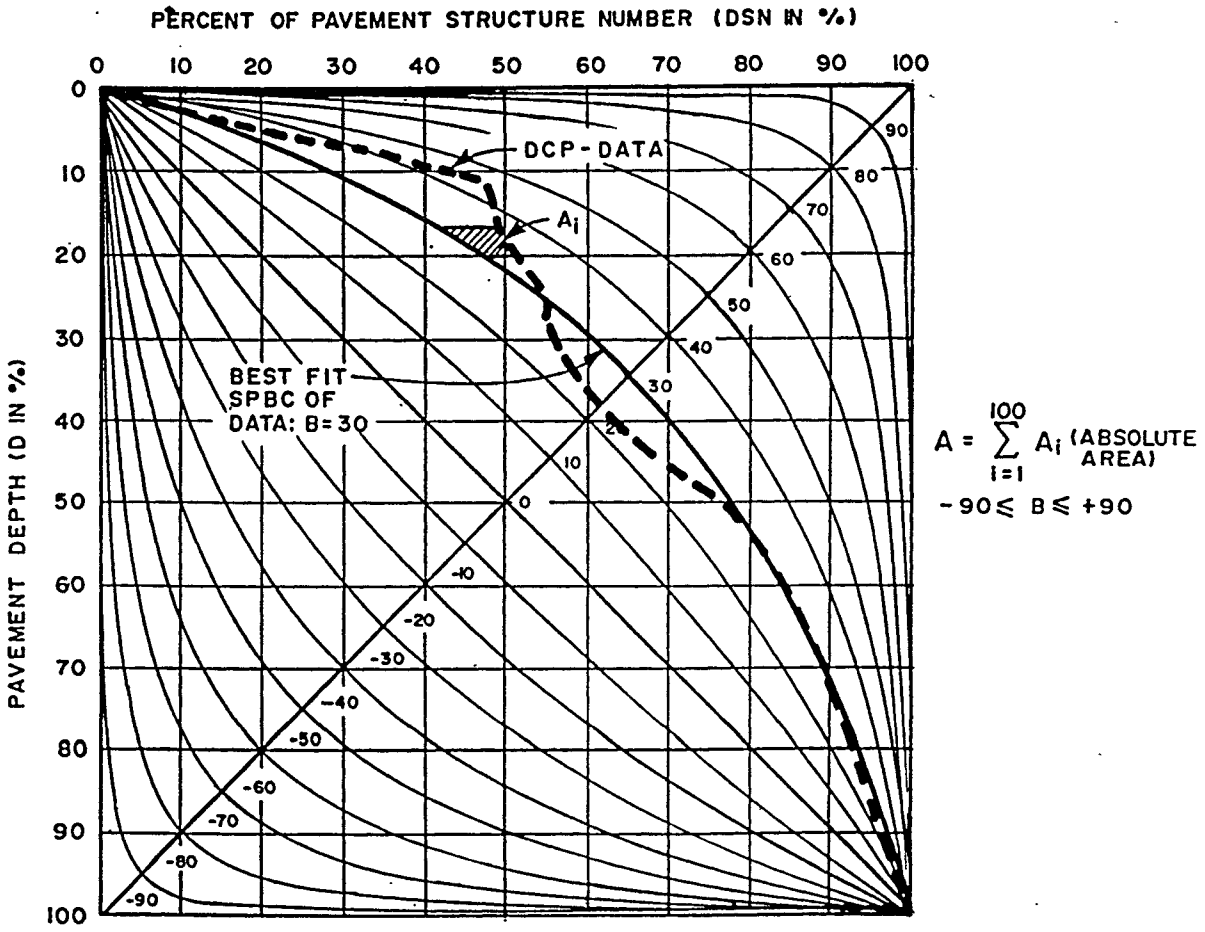

FIGURE E6: ILLUSTRATION OF BEST-FIT SPBC AT B =30

TABLE E1: DEFINITION OF THE NINE DIFFERENT PAVEMENT STRENGTH-BALANCE CATEGORIES

LIMITS FOR PARAMETERS B AND A		DESCRIPTION OF CATEGORY
B $ 40	0 # A # 1200	(I) WELL-BALANCED SHALLOW STRUCTURE (WBS)
B $ 40	1200 < A # 3000	(II) AVERAGELY BALANCED SHALLOW STRUCTURE (ABS)
B > 40	3000 < A	(III) POORLY BALANCED SHALLOW STRUCTURE (PBS)
B # 40 < 40	0 # A # 1200	(IV) WELL-BALANCED DEEP STRUCTURE (WBD)
0 # B < 40	1200 < A # 3000	(V) AVERAGELY BALANCED DEEP STRUCTURE (ABD)
0 # B < 40	3000 < A	(VI) POORLY BALANCED DEEP STRUCTURE (PBD)
B < 0	0 # A # 1200	(VII) WELL-BALANCED INVERTED STRUCTURE (WBI)
B < 0	1200 < A # 3000	(VIII) AVERAGELY BALANCED INVERTED STRUCTURE (ABI)
B < 0	3000 < A	(IX) POORLY BALANCED INVERTED STRUCTURE (PBI)

Computer programs have been developed which automatically process the DCP field measurements, calculate the balance of the pavement and also produce a normalized curve for the deviation (A) from a standard pavement Balance Curve (B) of a pavement in depth (*6*).

DCP data and pavement design parameters

The DCP is used to produce an indication of the in-situ shear strength of the pavement layers. The shear strength is, however not a design parameter normally used in pavement design.

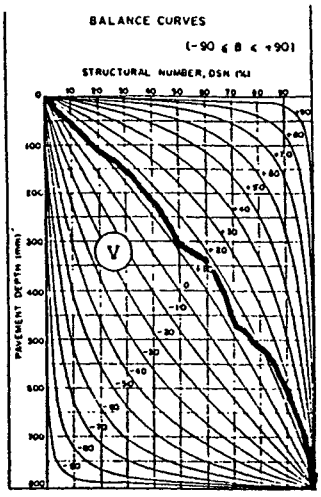

(a) AVERAGELY - BALANCED DEEP (ABD)

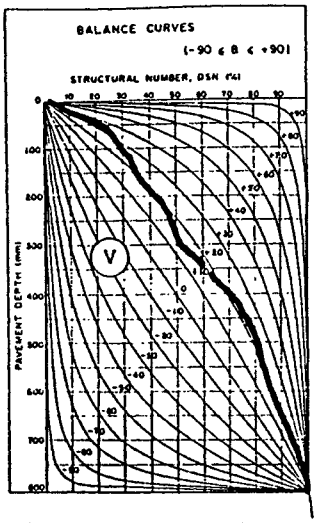

(b) AVERAGELY- BALANCED DEEP (ABD)

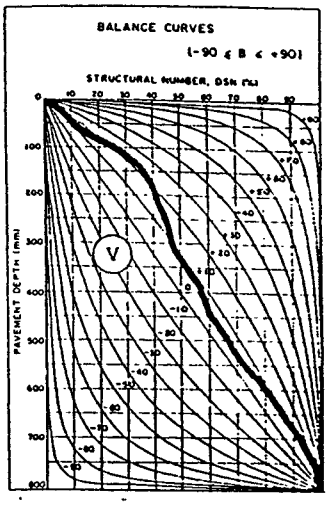

(c) AVERAGELY- BALANCED DEEP (ABD)

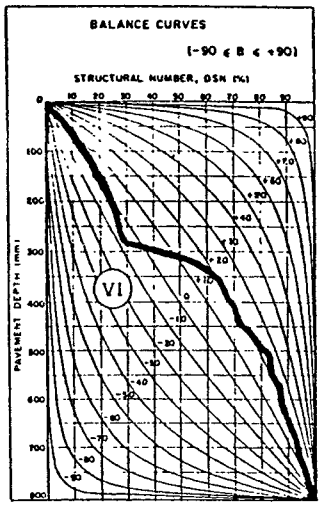

(d) POORLY - BALANCED DEEP (PBD)

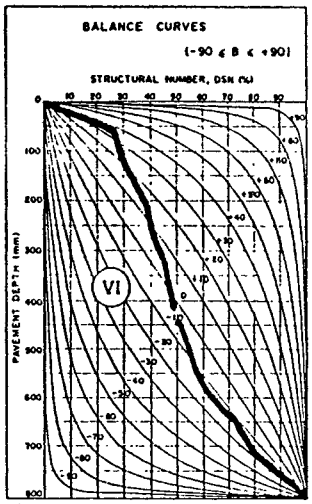

(e) POORLY - BALANCED DEEP (PBD)

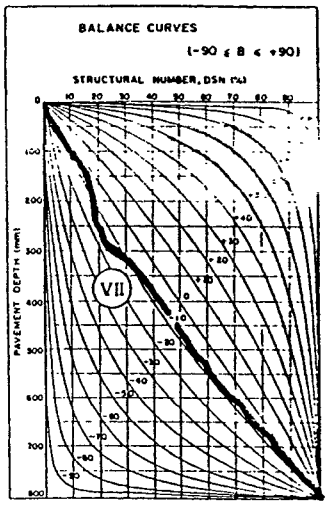

(f) WELL- BALANCED INVERTED (WBI)

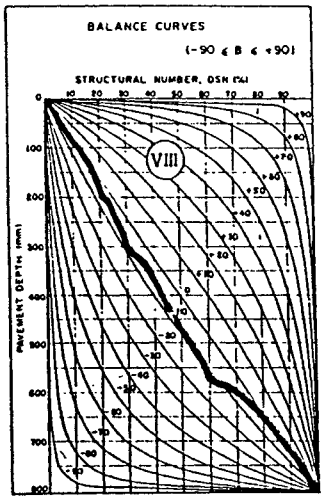

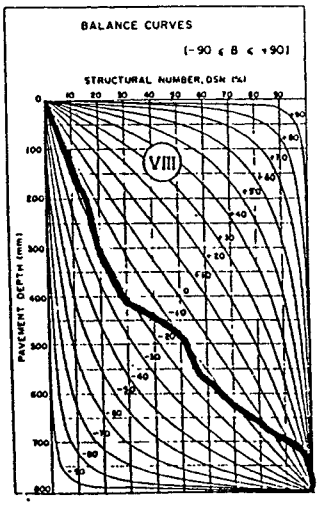

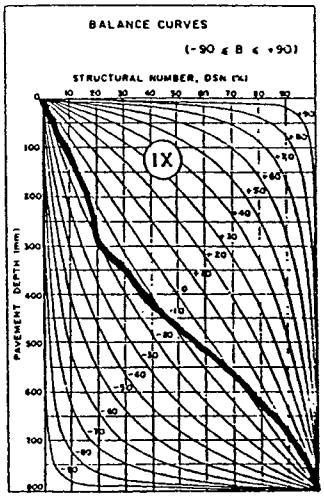

FIGURE E7: A GRAPHICAL PRESENTATION OF THE PAVEMENT STRENGTH-BALANCE CATEGORIES

The common design tools for granular layers are the California Bearing Ratio (CBR), the Unconfined Compressive Strength (UCS), the R value, and the effective layer stiffness (Eeff). It is thus important to relate DCP output to these design parameters.

Correlations have been developed between DCP penetration data and some of these parameters (7). Most of these correlations were developed empirically, and the constraints inherent to the correlations should be kept in mind. The type of material, the in-situ moisture condition, and stress state of the pavement are all examples of limitations regarding the use of empirically derived correlations. Despite all of these constraints, the correlations offer a good indication of the expected values of these various design parameters. The DCP computer package, apart from what was already discussed, also calculates some of these parameters in the following manner:

- CBR values are derived from the following formula:

  IF the average penetration rate (DN) > 2 mm/blow:

  $$\text{then CBR} = 410 \times DN^{(-1.27)}$$

  and if DN $\leq$ 2 mm/blow:

  $$\text{then CBR} = (66{,}66 \times DN^2) - (330 \times DN) + 563.33$$

- UCS values derived from the following formula:

  $$UCS = 15 \times CBR^{0.88}$$

! E-moduli

effective elastic stiffness (E_{eff}) for pavement layers are estimated and given in the formula below. Extensive calibration between in-situ modulus and DCP calculated modulus lead to the following tentative relationship between DCP penetration rate (DN) and Eeff.

Log (Eeff) = 3.04758 - 1.06166 (log (DN))

with n = 86

R^2 = 0.76

STD error of estimate = 0.209

The confidence interval information for Eeff vs DN relationships is given below:

CONFIDENCE INTERVAL	FORMULATION
80 %	Log (Eeff) $\pm$ 0.275
90 %	Log (Eeff) $\pm$ 0.358
95 %	Log (Eeff) $\pm$ 0.421

THE DCP ANALYSIS

Although the DCP may be used to evaluate the complete structure for typical South African pavements (including the AC thin layer) for these first test pavement only the base subbase and subgrade layers were investigated. The pavement was designed using standard Caltrans design procedures (*8*). The design Traffic Index is equal to 9, which translates to a pavement with a bearing capacity of 0.798 to 1.2 million ESALS.

The pavement structure

Two different test sections at RFS were analyzed. The substructures are the same, except for the thickness of the base layer.

The subbase consists of a granular material meeting Caltrans Class 2 aggregate subbase requirements, and varying thickness between 123mm (5") and 294mm (12") primarily due to a 2 percent cross-slope.

The base material met requirements for Caltrans class 2 aggregate base and was 176mm (7.2") in the one test section and 265mm (10.8") in the other. In terms structural analysis using the DCP the various combination of subbase and base thickness were considered equal.

The subgrade, subbase and base were all compacted to Caltrans specifications prior to DCP testing.

DCP Results

DCP tests were conducted twice. The first tests were conducted directly after construction and the second series were conducted 10 days after construction.

Four DCP tests were conducted during each stage. The output results are summarized in Tables E2 and E3.

TABLE E2: Summary of First Set of DCP Data (Just after Construction)

DESIGN PARAMETER	DCP TEST				
	1	2	3	4	AVG
STATION NUMBER	0+25	0+59	1+18.5	1+44.8	
TOTAL NUMBER OF BLOWS	234	89	123	147	148
STRUCTURE CLASSIFICATION	poorly balance inverted	poorly balance deep struct.	poorly balance deep struct	poorly balance deep struct	
CBR					
layer 1	40 %	37 %	53 %	80 %	53 %
layer 2	116 %	27 %	56 %	51 %	63 %
layer 3	43 %	8 %	11 %	9 %	18 %

E_{eff}					
layer 1	160 MPa	149 MPa	202 MPa	284 MPa	199 MPa
layer 2	391 MPa	116 MPa	211 MPa	197 MPa	229 MPa
layer 3	171 MPa	43 MPa	56 MPa	49 MPa	80 MPa

TABLE E3: Summary of Second Set of DCP Data

(10 Days after Construction)

DESIGN PARAMETER	DCP TEST NUMBER				
	1	2	3	4	AVG
STATION NUMBER	1+44.8	1+59	1+18.5	1+44.8	
TOTAL NUMBER OF BLOWS	321	212	224	241	250
STRUCTURE CLASSIFICATION	poorly balance deep struct	poorly balance deep struct.	poorly balance deep struct	poorly balance deep struct.	
CBR					
layer 1	218 %	149 %	130 %	147 %	161 %
layer 2	87 %	62 %	84 %	98 %	83 %
layer 3	10 %	14 %	8 %	11 %	11 %
E_{eff}					
layer 1	727 MPa	482 MPa	429 MPa	493 MPa	533 MPa
layer 2	305 MPa	230 MPa	296 MPa	388 MPa	305 MPa
layer 3	51 MPa	69 MPa	43 MPa	55 MPa	55 MPa

The other design parameter that is of interest is the energy required to penetrate a certain layer. This is recorded in terms of the penetration rate per layer (the DN number) and is measured in mm per blow. A comparison of the penetration rates can be seen in Table E4.

TABLE E4: Summary of Penetration Rates (mm / Blow) (DN Number)

		DCP TEST NUMBER				
	LAYER	1	2	3	4	AVG
1st series	1	6.23	6.65	5.00	3.63	5.38
of	2	2.69	8.46	4.79	5.12	5.27
DCP tests	3	5.86	21.53	16.66	19.16	15.80
2nd series	1	1.50	2.21	2.46	3.05	2.31
of	2	3.39	4.42	3.49	2.18	3.37
DCP tests	3	18.44	13.72	21.25	17.28	17.67

Discussion of results

The first observation is that of variability. The location of the DCP test contributes to the variation of all reported values, as is typical of all in-situ type tests. Possible reasons for this behavior are variability in material quality, layer thicknesses, grading, compaction effort, and moisture content throughout the length of the test pavement.

The second observation regards the influence of water on the aggregate base and subbase

materials. Although all design specifications were met, the base coarse appeared to wet. Construction delays allowed it to dry out before the asphalt concrete was put on. The second set of DCP data was, therefore, taken after the base coarse had dried out. Current Caltrans methods (*8*) do not specify construction moisture contents of granular materials, but the influence of water is clearly illustrated by the DCP investigation. Moisture contents taken just after construction indicated that the base was at or just below optimum moisture content. The minimum amount of water required to obtain the required compaction level is not known.

Total Number of Blows (The DN_{800} Number)

The average number of blows to penetrate 800mm increased from 148 to 250, immediately after construction to 10 days after construction. This represents an increase of 69% in the value of the DN_{800} number. It clearly illustrates the strengthening effect of decreased moisture in granular materials. The shear strength of a granular material decreases dramatically in the presence of water. Although the DN_{800} is not normally used for design purposes it serves as an indication of the total amount of energy required (therefore, the shear strength) for the DCP cone to penetrate 800mm in depth.

Pavement classification

In terms of the DCP classification system the test sections pavement is classified as a deep structure, which indicates that the structural strength of this pavement is caused by a gradual decrease in layer strength.

The classification did not change from the wet to the dry conditions, which indicates that

the drying out of the materials caused a gradual increase in strength throughout the whole pavement structure and the balance of the pavement was unaffected.

The fact that the DCP software classifies the pavement as *poorly balanced* is an indication of the significant difference between the given Standard Pavement Balance Curves (SPBC) and the true DCP data (*5*).

The normal design philosophy is that all pavement layers on top of the subgrade should gradually increase with strength in order to protect the (weak) subgrade and to ensure that the subgrade will be able to carry the loads successfully throughout the design life of the whole structure.

An unbalanced pavement causes stress concentrations and under the effects of traffic loads will force the stronger layer to breakdown in an attempt to keep the pavement in a balanced state. Thus, under loading, all pavements will tend to end-up in a balanced state, with all stress concentrations removed.

CBR values

The average CBR for the base coarse (layer 1) are 53% and 161%, before and after the 10 day drying out period, respectively. According to the South African design specifications a granular base coarse should have a minimum CBR of 80% (*9*).

This result also compares favorably to the R values obtained for the base coarse The R value of 83 (as reported in Chapter 2), indicates that the material has the required structural strength and meets the required criteria (Caltrans standard specifications require the use of granular material with a minimum R value of 78 for a Class 2 aggregate base (*8*))

Stiffness values

The stiffness moduli reported here should be handled with caution. The DCP software uses pre-determined empirically based data to calculate E values as presented in Tables E2 and E3, which has limitations as to the materials types used, the in-situ moisture regime, and in-situ density conditions (*7)*.

Secondly it should be noted that the stiffness values are *in-situ* E values, so called $E_{effective}$, and should, therefore not be directly compared with laboratory results. If an investigation of the stiffness values of the different layers is called for it is suggested that these reported values should be used as seed values in the backcalculation process. Improvements to the calculated E values can be made by applying the relevant confidence intervals as explained earlier.

The penetration rates (DN numbers)

An investigation into the penetration rates (mm/blow) reveals the following (Table E4):

- the wet base coarse caused significant differences in the penetration rates (in the upper layers) of the four tests as presented in the first series of DCP tests ;
- the second series of tests showed that in terms of the shear strength, the pavement section behaves more uniformly (lesser variation in DN values of layers 1 and 2 in comparison with the first series of tests)
- the pavement gained significant structural strength from the wet state to the dryer state, as designated by the lower values of the penetration rates, when

the 1st series of tests is compared to the 2nd series of DCP tests (the average DN number for the base coarse decreased from 5.38mm/blow to 2.31mm/blow);

- the shear strength of the subgrade (layer 3) is virtually unaffected by the moisture regime of the upper layers. The average penetration rates are 15.80mm/blow and 17.67 mm/blow, before and after the 10 day drying out period, and
- in terms of the structural bearing capacity, the subgrade is significantly weaker than the upper layers, as designated by the much higher DN values of the subgrade when compared to the upper layers.

CONCLUSIONS

In this chapter the fundamental background and concepts of the Dynamic Cone Penetrometer (DCP) are explained. Eight complete DCP investigations were performed on the first CAL / APT pavement test sections at RFS.

Caltrans currently uses the R-value test to characterize unbound pavement materials for pavement thickness design. The R-value test is a laboratory test, requiring some effort and time before results can be obtained. As demonstrated in this Chapter, the DCP test provides a rapid and economical method for evaluating constructed unbound materials in-situ that presents several options for implementation. For research it can be used to evaluate in-situ strength and the effects of various construction parameters, as demonstrated herein. In the short-term it may be of use in

construction for comparing design materials properties from laboratory tests to those obtained in-situ, providing much more comprehensive and economical evaluation of large projects than is possible using the R-value test. The DCP has been shown to be of use in providing estimated moduli for mechanistic-empirical design methods. A full investigation into the prediction of the pavement life can be found in Chapter 5.

RECOMMENDATIONS

The influence of moisture on the structural behavior of granular sublayers is illustrated in this investigation. Although the current Caltrans Specification does not call for any control on the moisture content of granular materials, remarkable differences in the structural behavior of the pavement are evident. It is suggested that further research, including measurement of material strength by other methods, should be conducted to investigate the influence of moisture content on DCP measurements.

It is recommended that DCP testing remain a part of the data collection plan for all Cal/APT test sections, at RFS and in the field. This will provide valuable information for further development of the DCP concepts in California.

REFERENCES

1. Jordaan, G.J., Guidelines towards the use of a rehabilitation design method based on Dynamic Cone Penetrometer (DCP) measurements as developed in South Africa, Research Report DPVT 43, DRTT, CSIR, 1989.

2. De Beer, M., van der Merwe, C.J., Rohde, G.T., The evaluation, analysis and rehabilitation design of roads, Report No: IR 93/296, DRTT, CSIR, 1994.

3. Kleyn, E.G., Savage, P.F., The application of the pavement DCP to determine the bearing properties and performance of road pavements, International Symposium on Bearing Capacity of Roads and Airfields, Norway, June 1982.

4. De Beer, M., Use of the Dynamic Cone Penetrometer (DCP) in the design of road structures, Report No: DPVT-187, DRTT, CSIR, 1991.

5. De Beer, M. Kleyn, E.G., Savage, P.F., Towards a Classification System for the Strength Balance for Thin Surfaced Flexible Pavements. Proceedings of the Eight Quintiual Convention of SAICE in co-operation with the 1988 Annual Transportation Convention, University of Pretoria, Pretoria, South Africa, 1988.

6. CICTRAN, Analysis and classification of DCP survey data, Version 3.0, CICTRAN Software, DRTT, CSIR, 1992

7. De Beer, M., Use of the Dynamic Cone Penetrometer (DCP) in the design of Road structures. Proceedings of The Tenth Regional Conference for Africa on Soil Mechanics & Foundation Engineering and the Third International Conference on Tropical & Residual Soils. Geotechnics in the African Environment, Volume 1. Maseru, Lesotho. 23 - 27 September 1991.

8. Caltrans, Newcon90, Pavement Thickness Design Computer program, Version Apr_30_91.1.

9. Committee of State Road Authorities, Structural Design of Interurban and Rural Pavements, TRH 4, Department of Transport, Pretoria, South Africa, 1985